Identification of Genes in Pakistani Families with Inherited Eye Diseases

QUAID-I-AZAM UNIVERSITY

ISLAMABAD

By

RABIA BASHARAT

Department of Biochemistry
Faculty of Biological Sciences
Quaid-i-Azam University

Islamabad, Pakistan

2024

Identification of Genes in Pakistani Families with Inherited Eye Diseases

A thesis submitted in partial fulfillment of the requirements for

the degree of

Doctorate of Philosophy

in

Biochemistry/Molecular Biology

By

RABIA BASHARAT

Department of Biochemistry

Faculty of Biological Sciences

Quaid-i-Azam University

Islamabad, Pakistan

2024

In the name of ALLAH, the most Beneficent and the most Merciful.
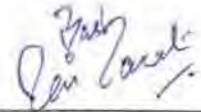
"O my Lord! Increase me in knowledge." (Quran 20:114)

Plagiarism Undertaking

I solemnly declare that research work presented in the PhD thesis, titled **"Identification of Genes in Pakistani Families with Inherited Eye Diseases"** is solely my research work with no significant contribution from any other person. Small contribution/help wherever taken has been duly acknowledged and that complete thesis has been written by me.

I understand the zero-tolerance policy of the HEC and **Quaid-i-Azam University, Islamabad,** towards the plagiarism. Therefore, I as an Author of the above titled thesis declare that no portion of my thesis has been plagiarized and any material used as reference is properly referred/cited.

I undertake that if I am found guilty of any formal plagiarism in the above titled thesis even after award of PhD degree, the University reserves the right to withdraw/revoke my PhD degree and that HEC and the University has the right to publish my name on the HEC/University website on which names of students are placed who submitted plagiarized thesis.

Student/Author Signature:

Ms. Rabia Basharat
Date: *May 27, 2024*

Author's Declaration
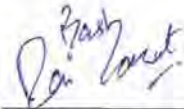
I **Rabia Basharat** hereby state that my PhD thesis, *titled* **"Identification of Genes in Pakistani Families with Inherited Eye Diseases"** is my own work and has not been submitted previously by me for taking any degree from

Department of Biochemistry, Faculty of Biological Sciences, Quaid-i-Azam University, Islamabad, Pakistan.

Or anywhere else in the country/world.

At any time if my statement is found to be incorrect even after my graduation, the University has the right to withdraw my Ph.D degree.

Student/Author Signature:

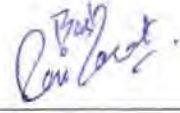**Ms. Rabia Basharat**
Date: *May 27, 2024*

Certificate of Approval

This is to certify that the research work presented in this thesis, entitled: **"Identification of Genes in Pakistani Families with Inherited Eye Diseases"** was conducted by **Ms. Rabia Basharat** under the supervision of Prof. Dr. Muhammad Ansar.

No part of this thesis has been submitted anywhere else for any other degree. This thesis is submitted to the Department of Biochemistry, Faculty of Biological Sciences, Quaid-i-Azam University, Islamabad, Pakistan in partial fulfillment of the requirements for the **Degree of Doctor of Philosophy** in the field of Biochemistry from Department of Biochemistry, Faculty of Biological Sciences, Quaid-i-Azam University, Islamabad, Pakistan.

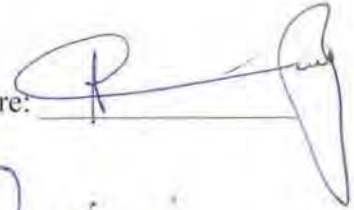**Ms. Rabia Basharat**   Signature: _____

Examination Committee:

1. **External Examiner:**   Signature: _____
   Prof. Dr. Attya Bhatti
   National University of Sciences & Technology
   (NUST) Islamabad
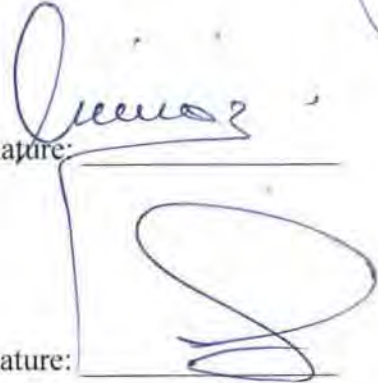
2. **External Examiner:**   Signature: _____
   Dr. Muhammad Ramzan Khan
   Principal Scientific Officer
   National Agricultural Research Center
   Park Road, Islamabad

3. **Supervisor:**   Signature: _____
   Prof. Dr. Muhammad Ansar

4. **Chairperson:**   Signature: _____
   Prof. Dr. Iram Murtaza

Dated: _____May 27, 2024_____

Dedicated

To
My Beloved and Ever Caring

Parents

&

Late Grandparents

ACKNOWLEDGEMENTS

*Words are bound and knowledge is inadequate to praise **Almighty ALLAH**, He is the most beneficent and the most merciful. I have no words to express my gratitude towards Him for blessing us with the wisdom to comprehend knowledge in our surroundings. After Almighty, special praise is for the Holy Prophet **Hazrat Muhammad (PBUH)**, whose personality not only builds the standard of character for the entire world but guided his "Ummah" to seek knowledge from cradle to grave.*

*Special thanks and gratefulness to the families who participated in this research project on voluntary basis. Indeed, without their participation it was impossible for me to carry out this educational research project. I would like to express my deepest sense of gratefulness to praiseworthy **Prof Dr. Muhammad Ansar** for his kind and able guidance, valuable comments, motivating and supportive attitude which provided me a very conducive environment throughout the course of research and studies. I deem it a great honor to have worked under his supervision.*

*I am enormously thankful to **Prof. Dr. Frans Cremers** and **Dr. Susanne Roosing**, Department of Human Genetics, Radboudumc, The Netherlands for providing me lab facilities to conduct a part of my PhD research under International Research Support Initiative Program of Higher Education Commission, Pakistan. It would not be possible to complete my PhD research without their help, support, guidance and collaboration. They have always guided me through the experimental work and complex data analysis.*

*I am extremely obliged and thankful to the **Higher Education Commission, Pakistan** for awarding me scholarship under **Indigenous PhD Fellowships for 5000 Scholars (Phase-II), Batch-IV** and **International Research Support Initiative programs (IRSIP)**. The funds disbursed under aforementioned programs assisted me in carrying out various academic and research activities. This monetary support helped a great deal in completion of my PhD thesis.*

*I am also thankful to **Prof. Dr. Iram Murtaza**, Professor and Chairperson Department of Biochemistry, Faculty of Biological Sciences, QAU, Islamabad for her administrative and academic support during my PhD program.*

*Thanks to all the colleagues in Susanne's lab (Human Genetics, Radboudumc), especially **Suzanne de Bruijn**, **Daan Panneman**, **Kim Rodenburg**, and **Erica Boonen** for their support and company. Special thanks to my friends and housemates especially*

María Rodríguez-Hidalgo, Veronique, Ian Kock and *Arif Aydemir* in Nijmegen, for making my stay enjoyable in The Netherlands.

I would like to extend my gratitude to **Dr. Muhammad Rizwan Alam** for his guidance and appreciation at every step. I am pleased to record my sincerest thanks to my colleagues, seniors and junior from my lab **Ehsan Ullah, Falak Sher, Waleed Khan, Sundus Sajid, Memoona Rasheed, Madiha Amin, Afeefa Jarral, Muhammad Zahid, Irfan Ullah and Samra Akram**. I am very thankful to my hostel mates, **Durre Shehwar, Hajra Fayyaz** and **Saima Barki** as their support, care, guidance and counselling was priceless throughout my PhD journey while I was away from home. I am also thankful to **Muhammad Qadeer** for his timely and cooperative assistance during my lab work. I would also like to acknowledge all office staff members from the Department of Biochemistry, especially to **Mr. Tariq Mahmood** and **Mr. Fayaz** for their cooperation in all official matters during my degree program.

This acknowledgement would be incomplete unless I offer my humble veneration to my loving parents, siblings, and friends, who were all ears to listen to my boring experiment failures and supported me during ups and down of PhD journey. Their love and endless prayers made me able to achieve the success in every sphere of life.

Rabia Basharat

TABLE OF CONTENTS

LIST OF FIGURES

LIST OF TABLES

LIST OF ABBREVIATIONS

A/M	Anophthalmia/Microphthalmia
AAV	Adeno-associated Virus
ABCA1	ATP Binding Cassette Subfamily A Member 1
ABCA4	ATP-binding Cassette, Subfamily A, Member 4
ABCB6	ATP-binding Cassette, Subfamily B, member 6
ACHM	Achromatopsia
ACMG	American College of Medical Genetics and Genomics
ADGRV1	Adhesion G-protein-coupled Receptor V1
AFAP1	Actin Filament Associated Protein 1
AHI1	Abelson Helper Integration Site 1
AIPL1	Encoding Aryl-Hydrocarbon Interacting Protein-Like 1
ALDH1A3	Aldehyde Dehydrogenase 1 Family, Member A3
ALMS	Alstrom Syndrome
AMP	Association for Molecular Pathology
ARHGEF12	*RHO* Guanine Nucleotide Exchange Factor 12
ARL13B	ADP-ribosylation Factor-like GTPase 13B
ARL3	ADP-ribosylation Factor-like GTPase 3
ARL6	ADP-ribosylation Factor-like GTPase 6
ARMC9	Armadillo Repeat-containing Protein 9
ASD	Anterior Segment Dysgenesis
ATOH7	Atonal bHLH Transcription Factor 7
BAM	Binary Alignment Map
BBIP1	BBS Protein Complex-interacting Protein 1
BBS	Bardet-Biedl Syndrome
BBS1	Bardet-biedl Syndrome 1
BBS10	Bardet-biedl Syndrome 10
BBS12	Bardet-biedl Syndrome 12
BBS2	Bardet-biedl Syndrome 2
BBS4	Bardet-biedl Syndrome 4

BBS5	Bardet-biedl Syndrome 5
BBS7	Bardet-biedl Syndrome 7
BEC	Bio-ethical Committee
BEST1	Bestrophin 1
BL	Bilateral
BLAST	Basic Local Alignment Search Tool
BLAT	BLAST-like Alignment Tool
C12ORF57	Chromosome 12 Open Reading Frame 57
C2ORF71	Chromosome 2 Open Reading Frame 71
C8ORF37	Chromosome 8 Open Reading Frame 37
CABP4	Calcium-binding Protein 4
CADD	Combined Annotation Dependent Depletion
CAV1/CAV2	Caveolin 1/ Caveolin 2
CC2D2A	Coiled-coil and C2 Domains-containing Protein 2A
CCT2	Chaperonin Containing T-complex Polypeptide 1, Subunit 2
CDG	Congenital Disorders of Glycosylation
CDH23	Cadherin 23
CDHR1	Cadherin-related Family, Member 1
CDKN2BAS	Cdkn2b Antisense RNA
CDON	Cell Adhesion Molecule-related/downregulated by Oncogenes
CEP104	Centrosomal Protein, 104-kd
CEP164	Centrosomal Protein, 164-kd
CEP290	Centrosomal Protein, 290-kd
CEP41	Centrosomal Protein, 41-kd
CERKL	Ceramide Kinase-like
cGMP	Cyclic Guanosine Monophosphate
CIB2	Calcium- and Integrin-binding Protein 2
CLNs	Neuronal Ceroid Lipofuscinoses
CLRN1	Clarin 1

CLUAP1	Clusterin-associated Protein 1
CNGA1	Cyclic Nucleotide-gated Channel, Alpha-1
CNGA3	Cyclic Nucleotide-gated Channel, Alpha-3
CNGB1	Cyclic Nucleotide-gated Channel, Beta-1
CNVs	Copy Number Variations
COL18A1	Collagen, Type XVIII, Alpha-1
COL4A1	Collagen, Type IV, Alpha-1
COX7B	Cytochrome C Oxidase, Subunit 7B
CRB1	Crumbs Cell Polarity Complex Component 1
CRX	Cone-rod Homeobox-containing Gene
CSNB	Congenital Stationary Night Blindness
CSPP1	Centrosome Spindle Pole-associated Protein 1
CYP1B1	Cytochrome P450, Subfamily I, Polypeptide 1
DMD	Dystrophin
DMSO	Dimethyl Sulfoxide
dsDNA	Double Stranded DNA
DTHD1	Death Domain-containing Protein 1
EDTA	Ethylenediamine Tetraacetic Acid
EEJ	Exon-exon Junction
EJC	Exon Junction Complex
ERG	Electroretinogram
ES	Exome Sequencing
ExAC	Exome Aggregation Consortium
EYS	Eyes Shut Homolog
FAM161A	Family With Sequence Similarity 161, Member A
FBS	Fetal Bovine Serum
FEVR	Familial Exudative Vitreoretinopathies
FNDC3B	Fibronectin Type III Domain-containing Protein 3B
FOXC1	Forkhead Box C1
FOXE3	Forkhead Box E3

FRAS1	Fraser Extracellular Matrix Complex Subunit 1
FVP	Foveal Hypoplasia
GAS7	Growth Arrest-specific 7
GDF6	Growth/differentiation Factor 6
GMDS	GDP-mannose 4,6-dehydratase
GNAT1	Guanine Nucleotide-binding Protein, Alpha-transducing Activity Polypeptide 1
GNB3	Guanine Nucleotide-binding Protein, Beta-3
GPCRs	G- Protein-Coupled Receptors
GPR179	G-Protein-Coupled Receptor 179
GRK1	G-Protein-Coupled Receptor Kinase 1
GRM6	Glutamate Receptor, Metabotropic, 6
GS	Genome Sequencing
GUCY2D	Guanylate Cyclase 2D, Retinal
GWAS	Genome Wide Associated Studies
HARS1	Histidyl-tRNA Synthetase 2
HCCS	Holo-cytochrome C Synthase
HEC	Higher Education Commission
HF	Fill-in Mix High-input
HGMD	Human Gene Mutation Database
HGSNAT	Heparan-alpha-glucosaminide N-acetyltransferase
HM	Hybridization Mix
HTG	High-tension Glaucoma
IEM	Inherited Errors of Metabolism
IFT140	Intraflagellar Transport 140
IFT27	Intraflagellar Transport 27
IMPDH1	IMP Dehydrogenase 1
IMPG2	Interphotoreceptor Matrix Proteoglycan 2
INPP5E	Inositol Polyphosphate-5-phosphatase, 72-KD
IOP	Intraocular Pressure
IQCB1	IQ Motif Containing B1

IQGAP1	IQ Motif-containing GTPase-activating Protein 1
IRDs	Inherited Retinal Dystrophies
JBTS	Joubert Syndrome
JOAG	Juvenile Open Angle Glaucoma
KCNJ13	Potassium Channel, Inwardly Rectifying, Subfamily J, Member 13
KIF26B	Kinesin Family Member 26B
LB	Luria Broth
LCA	Leber Congenital Amaurosis
LCA5	Leberilin LCA5
LE	Left Eye
LRAT	Lecithin Retinol Acyltransferase
LRIT3	Leucine-rich Repeat, Immunoglobulin-like, and Transmembrane Domains-containing Protein 3
LRP6	Low Density Lipoprotein Receptor-related Protein 6
LTBP2	Latent Transforming Growth Factor-beta-binding Protein 2
LZTFL1	Leucine Zipper Transcription Factor-like 1
MAC	Microphthalmia, Anophthalmia and Coloboma
MAF	Minor Allele Frequency
MDB	Membrane Desalting Buffer
MERTK	MER Tyrosine Kinase Proto-oncogene
MICU1	Mitochondrial Calcium Uptake Protein 1
MKKS	MKKS Centrosomal Shuttling Protein
MKS1	MKS Transition Zone Complex Subunit 1
MPS IIIC	Mucopolysaccharidosis Type IIIC
MPSs	Mucopolysaccharidoses
MRI	Magnetic Resonance Imaging
MYO7A	Myosin VIIA
MYOC	Myocilin
NA	Not Applicable
NAA10	N-alpha-acetyltransferase 10, Nata Catalytic Subunit

NCRN	Non-syndromic Congenital Retinal Non-attachment
NDP	Norrin Cystine Knot Growth Factor NDP
NGS	Next Generation Sequencing
NHS	NHS Actin Remodeling Regulator
NLP	No Light Perception
NMD	Non-sense Mediated
NMNAT1	Nicotinamide Nucleotide Adenylyltransferase 1
NR2E3	Nuclear Receptor Subfamily 2, Group E, Member 3
NRL	Neural Retina Leucine Zipper
NTG	Normal-tension Glaucoma
OCT	Optical Coherence Tomography
OFD1	Ofd1 Centriole and Centriolar Satellite Protein
OMIM	Online Mendelian Inheritance in Man
OTX2	Orthodenticle Homeobox 2
PacBio	Pacific Biosciences
PACG	Primary Angle Closure Glaucoma
PAX6	Paired Box Gene 6
pBLAST	Protein BLAST
PBS	Phosphate Buffer Saline
PCDH15	Protocadherin 15
PCG	Primary Congenital Glaucoma
PCR	Polymerase Chain Reaction
PDE6A	Phosphodiesterase 6A
PDE6B	Phosphodiesterase 6B
PDE6D	Phosphodiesterase 6D
PDE6G	Phosphodiesterase 6G
PE	Pseudoexon
PEI	Polycation Polyethylenimine
PHPV	Persistent Hyperplastic Primary Vitreous
PL	Perception of Light
PMM2	Phosphomannomutase 2

POAG	Primary Open Angle Glaucoma
PORCN	Porcupine o-acyltransferase
PRCD	Photoreceptor disc component
PROM1	Prominin 1
PRPF31	Pre-mRNA-processing Factor 31
PRPF8	Pre-mRNA-processing Factor 8
PRPH2	Peripherin 2
PS	Panel Sequencing
PTC	Pre-mature Termination Codon
PTHB1	Parathyroid hormone-responsive b1 gene
PVR	Proliferative Vitreoretinopathies
PXDN	Peroxidasin
QAU	Quaid-I-Azam University
rAAV	Recombinant Adeno-associated Virus
RARB	Retinoic acid receptor, beta
RAX	Retina and anterior neural fold homeobox gene
RBP3	Retinol-binding protein 3
RBP4	Retinol-binding protein 4
RD3	Rd3 regulator of *GUCY2D*
RDH12	Retinol dehydrogenase 12
RDH5	Retinol Dehydrogenase 5
RE	Right Eye
RGCs	Retinal Ganglion Cells
RGR	G protein-coupled Receptor, Retinal
RHO	Rhodopsin
RLBP1	Retinaldehyde-binding Protein 1
ROS	Reactive Oxygen Species
RP	Retinitis Pigmentosa
RP1	Retinitis Pigmentosa 1
RP2	Retinitis Pigmentosa 32
RP22	Retinitis Pigmentosa 22

RP25	Retinitis Pigmentosa 25
RP29	Retinitis Pigmentosa 29
RP32	Retinitis Pigmentosa 32
RPE	Retinal Pigment Epithelium
RPE65	Retinoid Isomerohydrolase RPE65
RPGR	Retinitis Pigmentosa GTPase Regulator
RPGRIP1	Retinitis Pigmentosa GTPase Regulator-interacting Protein
RPGRIP1L	RPGRIL1-like
SAG	S-antigen
SAMtools	Sequence Alignment Map Tools
SCO2	SCO Cytochrome C Oxidase Assembly Protein 2
SDCCAG8	SHH Signaling and Ciliogenesis Regulator SDCCAG8
SEMA4A	Semaphorin 4A
SIFT	Sorting Intolerant From Tolerant
SIX6	Six homeobox 6
SIX6	Six homeobox 6
SLC24A1	Solute Carrier Family 24 (sodium/potassium/calcium exchanger), Member 1
SLN	Senior-Loken Syndrome
smMIPs	single molecule Molecular Inversion Probes
SMOC1	SPARC-related Modular Calcium-binding 1
SMRT	Single Molecule Real Time
SNPs	Single Nucleotide Polymorphisms
snRNP	Small Nuclear Ribonucleoproteins
SNRNP200	Small Nuclear Ribonucleoprotein, 200-kd
SNVs	Single Nucleotide Variants
SOX2	SRY-box 2
SPATA7	Spermatogenesis-associated Protein 7
STRA6	Stimulated by Retinoic Acid 6
SVs	Structural Variants
TEK	TEK Tyrosine Kinase, Endothelial

TENM3	Teneurin Transmembrane Protein 3
TGFBR2	Transforming Growth Factor-beta Receptor, Type II
TMCO1	Transmembrane and Coiled-coil Domains Protein 1
TMEM107	Transmembrane Protein 107
TMEM138	Transmembrane Protein 138
TMEM216	Transmembrane Protein 216
TMEM231	Transmembrane Protein 231
TMEM67	Transmembrane Protein 67
TRIM32	Tripartite Motif-containing Protein 32
TRPM1	Transient Receptor Potential Cation Channel, Subfamily M, Member 1
TSS	Targeted Sanger Sequencing
TTC8	Tetratricopeptide Repeat Domain 8
TULP1	TUB Like Protein 1
TXNRD2	Thioredoxin Reductase 2
USH	Usher Syndrome
USH1C	USH1 Protein Network Component Harmonin
USH1G	USH1 Protein Network Component Sans
USH2A	Usherin
UTR	Untranslated Region
UV	Ultraviolet
VSX2	Visual System Homeobox 2
VUS	Variant of Uncertain Significance
WDPCP	WD Repeat Containing Planar Cell Polarity Effector
WHRN	Whirlin
WNT2B	*Wnt Family Member 2B*
ZNF423	Zinc Finger Protein 423
ZNF513	Zinc Finger Protein 513

ABSTRACT

The development and function of eye in humans is coordinated by well-organized set of events. Several genes play important role in these processes and mutations in these genes can lead to different types of ocular disorders including structural and functional disorders. Anophthalmia, microphthalmia (A/M) and glaucoma are among the defects which arise mostly due to structural abnormalities in the anterior segment of the eye. Inherited retinal dystrophies (IRDs) are among the functional eye disorders which affects retina, the innermost layer of the eye. Genetic and phenotypic overlap makes the diagnosis of these ocular disorders very challenging and frequently require help of comprehensive genomic applications for the accurate diagnosis. Though there are prior studies on ocular disorders from Pakistan, but underlying genes and mutations are still unknown for a large majority of families/patients. Therefore, there is a dire need to expand the genetic spectrum of inherited eye disorders in Pakistan.

In this study, 28 families from different regions of Pakistan were recruited and were divided into four groups based on clinical presentation. Out of 28, 6 families were placed in the glaucoma group (A1-A6) and were subjected to either targeted Sanger sequencing (TSS) or exome sequencing (ES). However, these analyses identified mutation in all six families in *CYP1B1*. The mutation p.(Arg390His) was identified in three families, while in other families one recurrent p.(Pro442Glnfs*15) and two novel mutations p.(Pro118Leu) and p.(Met1?) were identified.

Similarly, TSS of *FOXE3* in eight (FamilyB1-B8) families with A/M phenotype identified p.(Cys240*) variant in three families while a missense p.(Ile97Val) variant was identified in one family. Four families (B3, B4, B5, B8) unsolved with TSS were subjected to genome sequencing (GS) which identified an already known missense variant p.(Asp183His) in *SIX6* gene, a novel 13-bp deletion in *VSX2* and a known 1-bp deletion p.(Cys857Alafs*5) and a novel deep-intronic mutation (c.3609-1307G>A) in *PXDN*. The probable effect p.(Arg1203Serfs*76) and severity of deep-intronic variant was confirmed through minigene splice assay performed in HEK293T cells which showed the activation of a pseudoexon.

Single molecule molecular inversion probes (smMIPs) based panel sequencing was used for the remaining 14 families (Family C1-C11 and Family D1-D3) with different types of IRDs. Two types of smMIPs panels (Retinitis pigmentosa-Leber congenital

amaurosis; RP-LCA) and (Macular degeneration; MD) based panel sequencing was performed in respective families based on their initial diagnosis. Panel based sequencing identified variants in 10 families out of 14 families. In LCA affected family, a known variant p.(Val9Met) was identified in *NMNAT1*. Two known variants p.(Arg482Trp) and p.(Gln301*) in two different families were identified in *TULP1*. The *TULP1* variant p.(Gln301*) was identified in one loop family C7, but the other related loop of the same family has a novel *MERTK* variant p.(Gln146*). A novel *PRPF8* inframe indel p.(Glu2307del) with low penetrance was identified in family C4. In family C5, a hypomorphic allele p.(Ala615Thr) in *HGSNAT* was identified with severe RP and a novel nonsense variant p.(Ser550*) in *PROM1* genetically explained the phenotype of family C6. One previously known canonical splice site variant c.2493-2_2495delinsGGC, p.(?) in *CNGB1* was identified in a family with CSNB. Three already known variants p.(Arg439Trp), p.(Cys319Arg) and p.(Arg436Trp) in *CNGB3* were found in two families achromatopsia (ACHM). The variant p.(Arg439Trp), was identified in homozygous state in affected members of family C10 while heterozygous variants p.(Cys319Arg) and p.(Arg436Trp) were present in trans in the affected members of family C11. Copy number variation (CNV) analysis from smMIPs coverage, identified a novel homozygous deletion in *USH2A* in the family D1 which presented Usher syndrome. The deletion spans the region of 51.47kb covering coding exons 50-58 in the gene. The exact breakpoints were identified (c.9740-5487_11389+5457del) through combination of PCR based genome walking and amplicon based PacBio long-read sequencing.

The four remaining unsolved families (C1, C8, D2 and D3) were screened through GS for the identification of disease causing variant. A novel variant p.(Ala32Profs*55) in *ATOH7* was identified in the family C1 exhibiting congenital blindness. In family D2, a novel COL18A1 indel p.(Pro597Leufs*127) was identified to be associated with Knobloch syndrome, while in the third syndromic IRD family a novel non-coding *NDP* variant c.-208G>A was identified. Regulatory region variants in *NDP* are already known to cause Norrie disease.

The family C8, diagnosed with night blindness and high myopia remained genetically unexplained in this study even after short read GS. Our approach leads us to the

identification of 11 novel variants with a solve rate of 96% in our cohort of diverse inherited eye disorder families.

The work presented here is part of following publications:

- **Basharat, R.,** Rodenburg, K., Rodríguez-Hidalgo, M., Jarral, A., Ullah, E., Corominas, J., Gilissen, C., Zehra, S. T., Hameed, U., Ansar, M., & de Bruijn, S. E. (2023). Combined Single Gene Testing and Genome Sequencing as an Effective Diagnostic Approach for Anophthalmia and Microphthalmia Patients. *Genes*, *14*(8), 1573. https://doi.org/10.3390/genes14081573.

- **Rabia Basharat**, Suzanne E. de Bruijn, Muhammad Zahid, Kim Rodenburg, Rebekkah J. Hitti-Malin, Erica G. M. Boonen, Afeefa Jarral, Arif Mahmood, Sharqa Khalil, Jawaid Ahmed Zai, Ghazanfar Ali, Christian Gilissen, Frans P. M. Cremers, Muhammad Ansar, Daan M. Panneman, Susanne Roosing (2023). Application of NGS to genetically diagnose a diverse range of inherited eye disorders in 15 consanguineous families from Pakistan (*manuscript under preparation*).

- **Rabia Basharat,** Maria Ijaz, Bushra Rao, Muhammad Ansar (2023). CYP1B1; a prevalent cause of PCG in Pakistani families (*manuscript under preparation*).

1.0.INTRODUCTION

Human visual system is an intricate and amazingly complex system, where different types of cells coordinate to perceive visual information about their surroundings and perception of objects' size, shape, color and distance. The light enters from the front of the eye, passes through lens and various sensory cells to reach the back of the eye from where optic nerve takes signals to the brain for interpretation (Figure 1.1). Throughout this process eye is supplied with nutrients through blood vessels and the wastes are properly managed. Many proteins play vital role in the development, function and maintenance of eye structures (Rogers, 2011).

1.1. Anatomy of Human Eye

The human eye has three distinguishing layers. The outer most layer comprises mainly of cornea and sclera. The cornea is 0.5 mm in thickness at the centre while thickness increases at periphery. Being the outermost part it not only protects eye but also transmits and refracts light to lens and retina (the innermost layer of eye) (DelMonte and Kim, 2011). The sclera merges with cornea at limbus and it provides protection and definitive shape to eye. Iris, choroid and the ciliary bodies form the middle part of the eye. The middle part collectively controls the amount of light entering in the eye, maintains the shape of lens, and provides aqueous medium and nutrients to the eye (Willoughby et al., 2010) (Figure 1.2). The innermost layer of the eye is retina which is the most complex layer. This neuronal layer completely lines the inner surface of the eye. The outer epithelial layer of retina is called retinal pigment epithelium (RPE). Majorly, six types of neuronal cells are present in retina (Figure 1.2). The photoreceptor cells facing towards the light entering region of eye, transmits light signal and are of two types; rods and cones. Other cells include bipolar cells, horizontal cells, amacrine cells, ganglion cells and Mullerian glia. These cells collectively form the plexiform which transmits the signal towards the optic nerve (Miller et al., 2005).

1.1.1. Photoreceptors and Phototransduction

Phototransduction is the process through which photoreceptors of the retina converts light signal into electrical signal for signal transmission to brain. Both types of photoreceptors have a light sensitive pigment called opsin which has seven G- protein-coupled receptor (GPCR) transmembrane domains with N-terminus in the extracellular

and C-terminus in the cytoplasmic region of cell membrane. The light signals enter retina, absorbed (at a certain wavelength) by chromophore present in opsin called retinal resulting the conversion of 11-cis retinal to all trans-retinal by photoisomerization. This induces conformational changes in opsin, triggering the signalling cascade which in turn changes the levels of Ca^{2+} and cyclic guanosine monophosphate (cGMP) and disturbs the normal flow of neurotransmitters leading to hyperpolarization (Palczewski, 2014). The signal is then received by bipolar cells and later to ganglion cells, and ultimately reaches in the brain through optic nerve (Arshavsky et al., 2002). Rods receive signal at dim or low light through a specific type of opsin called rhodopsin and provides grey scale images (scotopic vision), whereas cones receive signal at bright light and provide colour images (photopic vision). Therefore, cones are of three types perceiving red, green and blue colours (Shin et al., 2004). These includes L-cones, M-cones and S-cones which express different types of opsins and thus are sensitive to different light wavelengths. L-opsins are sensitive to the light of 560nm, M-opsins are sensitive to 530nm wavelength whereas S-opsins are sensitive to 420nm wavelength (Kolb, 1995).

1.2. Development of Human Eye

The human eye development is a coordinated set of events between cells at embryonic level which starts at 4th week of gestation and the major eye structure formation is completed by 7th week (Mann, 1953). The eye forms as a single field at the centre of developing forebrain during early embryonic development. Later this single field is separated, and two lateral optic pits emerge during neurulation. These optic pits enlarge to form optic vesicles which remain connected to primitive forebrain through optic stalk, which later forms the optic nerve. In the meantime, lens placode originates from the surface ectoderm, fuses with the emerging optic vesicle, leading to the formation of the optic cup. Retina and retinal pigment epithelium originate from this optic cup whereas lens develops from the invagination of the lens placode (Figure 1.3). The detachment of lens from the epithelium surface forms the cornea. The cornea is formed from the cells invading from periocular mesenchyme which is derived from neural crest (Graw, 2010).

1.3. Genetic Eye Disorders

Many genes are known to play their role during early eye development and any disturbance in these processes may lead to varied types of malformations which could result in reduced vision or total vision loss (Ohuchi et al., 2019). There are a significant number of studies which also highlighted the role of environmental factors such as viral infection, alcohol, smoking or drugs causing different types of eye disorders (Lammer et al., 1985; Stromland and Miller, 1993; Stromland, 2004).

1.3.1. Anophthalmia and Microphthalmia

Anophthalmia and microphthalmia (A/M) are ocular defects which occur due to pathological events during early eye development. Microphthalmia is diagnosed when an individual has small eyes, which is based on the measurement of axial length <21mm in adults and <14mm in new-borns (Verma and Fitzpatrick, 2007). In contrast anophthalmia is diagnosed when an individual has either the complete absence of any eye tissue or have remnant eye structures. Frequently anophthalmia and microphthalmia are observed together in patients which led to the use of A/M abbreviation to specify this group of structural eye disorders. The combined prevalence of A/M is one in 10,000 births (Searle et al., 2018). The actual pathophysiological events accountable for A/M are not properly understood yet. Some studies suggest that they arise due to a secondary regression during ocular development (Fitzpatrick and van Heyningen, 2005), but others hypothesize that these are the results of either lens induction failure (Inoue et al., 2007) or disruptions in optical invagination or early differentiation of the retina (Winkler et al., 2000; Loosli et al., 2003; Stigloher et al., 2006). It ranges from unilateral to bilateral and from simplex (non-syndromic) to complex (syndromic) types. A/M are often found with coloboma (a cleft appears due to absence of tissue in inferonasal quadrant of eye) (Gregory-Evans et al., 2004) and anterior segment dysgenesis (ASD), a group of disorders which affect trabecular meshwork, cornea, iris and lens of the eye (Ito and Walter, 2014).

1.3.1.1. Genetics of Anophthalmia and Microphthalmia

Before the identification of A/M-associated genes, a significant number of studies highlighted the role of environmental factors such as viral infection, alcohol, smoking or drugs causing A/M (Stromland and Miller, 1993; Stromland, 2004; Busby et al.,

2005). Chromosomal deletions, duplications and translocations are known to be associated with syndromic A/M (Verma and Fitzpatrick, 2007). To date approximately 150 genes are known to be associated with syndromic and non-syndromic forms of A/M (OMIM, assessed 1st December 2022). Most commonly, pathogenic variants in transcription factors such as (*SOX2, RAX, VSX2, FOXE3*) and in genes encoding signalling pathway proteins are known to cause A/M. Recently alternations in genes involved in retinoic acid metabolism (*ALDH1A3, STRA6, RBP4, RARB*) are also linked with A/M. There are other genes which do not specifically fall in any such category include *ABCB6, FRAS1, NAA10, PORCN, COL4A1, PXDN, SMOC1, COX7B, TENM3, HCCS, C12ORF57* are also reported to be associated with A/M (Plaisancie et al., 2019). Pathogenic variants in *SOX2* with involvement in 10-15% affected individuals are believed to be the most frequently associated gene with A/M. Others A/M associated-genes include *OTX2, RAX, FOXE3* and *PAX6* with 2-5%, 3%, 2.5% and 2% of the cases respectively (Chassaing et al., 2014; Gerth-Kahlert et al., 2013). Prenatal diagnosis of A/M is also difficult even with the experienced ultra-sonographers (Searle et al., 2018; Plaisancie et al., 2019). Therefore, molecular and genetic diagnosis may help in patient management and genetic counselling of the families. Only 20-30% of the patients receives genetic diagnosis, although detection rates are higher in severe bilateral cases (Plaisancie et al., 2019).

1.3.2. Glaucoma

Glaucoma is a heterogeneous group of disorder and has several sub-types which are included under primary and secondary glaucoma. It is characterized mainly by increased intraocular pressure (IOP; normal range 10-22mmHg), megalocornea, cloudy cornea, photophobia and buphthalmos (Tamcelik et al., 2014). Some other features include high myopia, Haab's striae (breaks in Descemet's membrane) and optic nerve head cupping (Ko et al., 2015). These symptoms arise because of some developmental disorder in the trabecular meshwork of the eye which makes Schelmm's canal; the structure which is important for the drainage of aqueous humor (fluid present between lens and cornea). Inadequate outflow of the fluid is responsible for increased IOP thereby increasing the pressure on the optic nerve. The damage in the optic nerve causes irreversible vision loss (Lim et al., 2012).

Primary glaucoma is usually caused by structural birth effects which blocks trabecular meshwork while secondary glaucoma is caused by inflammation, drugs or any external injury or disorder. Among the primary glaucoma, open-angle glaucoma (POAG), primary angle-closure glaucoma (PACG), and primary congenital glaucoma (PCG) are main subtypes, whereas two less common types include normal-tension glaucoma (NTG) and high-tension glaucoma (HTG) (Fernandez-Vega Cueto et al., 2021). The presentation of glaucoma phenotype mainly depends on the angle between junction of cornea and iris (Shown in figure 1.4). In POAG this angle between the junction of cornea and iris is open and it allows the regular flow of aqueous humor but some mechanical strain, older age or thin central corneal thickness causes obstruction in the normal flow of aqueous humor and thus results in the increased IOP (Weinreb et al., 2014). There are forms of POAG (like NTG) where IOP remains normal and it is suggested that such type of glaucoma arises due to decreased cerebrospinal fluid which induces the similar kind of stress on the optic nerve as in the classical glaucoma (Wang et al., 2012). In PACG, the angle between cornea and iris is acute and it causes the blockage of aqueous humor outflow through trabecular meshwork leading to increased IOP eventually resulting in glaucoma (Weinreb et al., 2014). Primary Congenital Glaucoma (PCG) appears within 3 years after birth (Chang et al., 2013). PCG is caused by defects in the anterior chamber angle or due to defective trabecular meshwork (Abu-Amero and Edward, 1993). Glaucoma hence is considered the second leading cause of blindness (first being the cataract) worldwide (Pascolini and Mariotti, 2012) despite of the medications and surgery available.

1.3.2.1. Genetics of Glaucoma

The prevalence of glaucoma varies in different populations with an estimate to affect more than 60 million worldwide (Qassim and Siggs, 2020). It is higher in eastern populations where cousin marriages are common and lowest in the west, ranging from 1 in 1250 (Gencik et al., 1982) to 1 in 30,000 (MacKinnon et al., 2004) respectively. In most cases PCG is inherited in an autosomal recessive manner but in some cases it is also caused by heterozygous variants in *TEK*, following the autosomal dominant pattern of inheritance (Abu-Amero and Edward, 1993). The most frequently reported gene in autosomal recessive PCG is *CYP1B1* (cytochrome p450) which was first identified in 1997 in Turkish and Canadian populations (Stoilov et al., 1998). To date more than 250

mutations in *CYP1B1* are predicted to be the cause of PCG and some other forms of glaucoma (HGMD, 2019). Studies in several populations have shown different percentages of *CYP1B1* mutations in PCG patients but shows that this gene is a major player responsible for PCG worldwide. In a study of Chinese patients, 17.2% cases had *CYP1B1* mutations (Chen et al., 2008), while India shows the involvement of *CYP1B1* in 30% cases (Reddy et al., 2004) which is lower than Brazilian PCG patients (40%) (Stoilov et al., 2002). While Iranian, Arabian and Romany populations have shown the highest number of cases with *CYP1B1* mutations and have reported in 70%, 90% and 100% patients respectively (Plasilova et al. 1999; Bejjani et al. 2000; Chitsazian et al. 2007). *LTBP2* initially reported in Gypsy and Pakistani families (Ali et al., 2009) and latter in Irani families (Narooie-Nejad et al., 2009). The, heterozygous variants in *MYOC,* a gene which is also predicted to be the modifier of *CYP1B1* (Vincent et al., 2002), *TEK* (Souma et al., 2016) and *FOXC1* (Nishimura et al., 1998) are also reported to be associated with PCG.

Other types of glaucoma show more complex pattern of inheritance and genome wide association studies (GWAS) have shown association of several genes. The associated genes are involved in several biological processes including lipid metabolism and membrane biology (*ABCA1, ARHGEF12, CAV1/CAV2*), extracellular matrix (*AFAP1*), cytokine signalling (*CDKN2BAS, FNDC3B, TGFBR2*), fucose and mannose metabolism (*GMDS, PMM2*), ocular development (*FOXC1, SIX6*) and cell division (*CDKN2BAS, GAS7, TMCO1*) (Wiggs and Pasquale, 2017). Recently, *TXNRD2* is also found associated with POAG through GWAS studies (Bailey et al., 2016). *TXNRD2* gene encodes a protein which is required for the reduction of damaging reactive oxygen species (ROS) generated as a result of mitochondrial function. This suggests that oxidative stress may impose damaging effects to ganglion cells whereas reduction of ROS is neuroprotective (Lin and Kuang, 2014).

1.3.3. Non-Syndromic Inherited Retinal Dystrophies

Inherited retinal dystrophies (IRDs) is a vast group of inherited disorders which mainly manifest variable degree of vision loss. These dystrophies appear as a result of dysfunction or cell death of several different types of retinal cells and, therefore cause either the progressive vision loss or non-progressive vision loss depending on the precise nature of degenerative processes. When IRDs are present isolated they are

called non-syndromic IRDs. Predominantly, pigment deposits initially start appearing in the outer part of retina called RPE and later in other parts causing photoreceptors' cell death (Hamel, 2014). The different types of IRDs can be distinguished based on the location of pigmentary lesions.

The central part of the retina is called macula and it surrounds the fovea. This macular region contains the highest number of retinal ganglion cells (RGCs) and is involved in sharp vision. The macular region is approximately 2% of the total retinal area while it contains 30% of the RGCs (Curcio and Allen, 1990). The deposition of pigmentary lesions in the macular region causes the loss of central vision which poses difficulties in face recognition and reading. But if the lesions appear first in the peripheral region of the retina then it affects peripheral vision first and such individuals can read and write with less difficulty but movement at low light levels is more challenging for them (Hamel, 2014). When retinal cells of both periphery and central macula are severely damaged then the dystrophy is called Leber congenital amaurosis (LCA). This is the most severe form of IRDs and the age onset of LCA is as early as few months to one year. The affected individual lost complete vision early in their lifetime. Its prevalence is 1:80,000. The affected individuals mostly have normal intelligence but small number of studies have suggested that 20% individuals sometimes also develop intellectual disabilities (Tsang and Sharma, 2018).

The other types of IRDs include cone-rod dystrophy where cones are more affected causing day vision loss (Haider et al., 2014). Another type of retinal dystrophy in which only cones are affected is called achromatopsia (ACHM) which is characterized by less visual acuity, photophobia and severe colour vision impairment (Perea-Romero et al., 2021). Similarly, when the dysfunction occurs only in rod-photoreceptors or synapses of photoreceptors with bipolar cells then it causes congenital stationary night blindness (CSNB). In CSNB since only rod photoreceptors are affected it causes non-progressive night blindness (Henderson, 2019).

The most prevalent form of IRDs is retinitis pigmentosa (RP), where both rod and cone photoreceptors are affected, and it is characterized by night blindness with a progressive loss of peripheral day vision and eventually complete blindness. It is estimated that worldwide approximately 1.5 million population is affected with RP (Vaidya and Vadiya, 2015). Choroideremia is another type of chorioretinal dystrophy which appears

due to damage in choroid (blood vessels which nourishes retina), RPE or photoreceptors. It is X-linked hence affects males mostly (Kalatzis et al., 2013).

There is another class of IRDs which is specified as vitreoretinopathies. This is not very well-developed class of retinopathies, which include familial exudative vitreoretinopathies (FEVR) and proliferative vitreoretinopathies (PVR). FEVR arises due to failure in retinal blood vessels development leading towards incomplete vascularization of retina and retinal ischemia. This secondarily causes retinal folds, retinal detachment or in severe cases retinal dysplasia (Gilmour, 2015). PVR on the other hand is the consequence of growth defects causing cellular membrane contractions either within the vitreous cavity or on both sides of retinal surfaces, leading towards detachment of retina (Idrees et al., 2019).

1.3.3.1. Genetics of Non-Syndromic Inherited Retinal Dystrophies

IRDs depicts clinical and genetic heterogeneity with autosomal recessive, autosomal dominant and X-linked inheritance patterns. Approximately 341 genes are known to cause different forms of IRDs (Retnet: https://web.sph.uth.edu/RetNet/; assessed 22nd May, 2022). LCA is caused by more than 21 genes, which regulates processes such as photoreceptor morphogenesis (*CRB1, CLUAP1, CRX, PRPH2, GDF6*), phototransduction (*AIPL1, RD3, GUCY2D,*) intra-photoreceptor ciliary transport (*CEP290, IQCB1, LCA5, RPGRIP1, SPATA7, TULP1, IFT140*), signal transduction (*KCNJ13, CABP4*), retinoid cycle (*RDH12, LRAT, RPE65*), coenzyme NAD biosynthesis (*NMNAT1*), retinal differentiation (*OTX2*), outer segment phagocytosis (*MERTK*), guanine synthesis (*IMPDH1*), subcomponent of a chaperon complex (*CCT2*) or other proteins with unknown function (*DTHD1*) (den Hollander et al. 2008; Astuti et al. 2016).

RP is the most prevalent form of IRDs. More than 30 genes are known to cause autosomal dominant form of RP (Retnet: https://web.sph.uth.edu/RetNet/; assessed 22nd May, 2022). But the most frequently associated genes include *RHO* (encodes rhodopsin; an important protein in visual cycle which is activated in photoreceptors by the absorption of light) (Murray et al., 2009), *PRPF31* (a splicing factor which is an important component of U4/U6 and U5 trimer) (Waseem et al., 2007), *PRPH2* (membrane glycoprotein which is located in outer segment of photoreceptors) (Loewen et al., 2001) and *RP1* (a microtubule-associated protein which specifically expressed in

photoreceptors and required for their proper functioning) (Liu et al., 2003). More than 60 genes are known to be associated with autosomal recessive RP (Retnet: https://web.sph.uth.edu/RetNet/; assessed 22nd May, 2022) and most of these genes are responsible for less than 1% cases however some genes like *PDE6A, PDE6B, RP25* and *RPE65* are involved in more then 2-5% of RP cases. Most of the associated genes are involved in either phototransduction (*CNGA1, CNGB1, PDE6A, PDE6B, PDE6G, RHO, SAG*) or retinal metabolism (*ABCA4, LRAT, RBP3, RGR, RLBP1, RPE65*). Some genes are involved in tissue development and maintenance of cellular structures such as (*CRB1, CERKL, EYS, NRL, PROM1, RP1, TTC8, TULP1, USH2A*). Other genes included are either transcription factors (*NR2E3, ZNF513*), transmembrane proteins (*MERTK*) or their functions are not understood yet; loci (*RP22, RP29, RP32)* and genes (*C2ORF71, FAM161A, PRCD, SPATA7*) (Ferrari et al., 2011). It is estimated that 10-15% RP cases are X-linked. The individuals affected with X-linked RP show severe phenotype and early development of the disease. In some cases, milder symptoms appear in female carriers probably because of non-random X-chromosome inactivation (Veltel and Wittinghofer, 2009). The genes responsible for causing X-linked RP includes *OFD1, RP2* and *RPGR*.

CSNB is caused by 3 genes (*GNAT1, PDE6B, RHO*) prevailing in an autosomal dominant pattern, while 12 genes (*CABP4, GNAT1, GNB3, GPR179, GRK1, GRM6, LRIT3, RDH5, SAG, SLC24A1, TRPM1*) are responsible for autosomal recessive CSNB. There are several genes which are associated with multiple phenotypes such as *RHO* is responsible for autosomal dominant CSNB and autosomal dominant RP as well as autosomal recessive RP. Similarly, variants in *ABCA4* cause cone or cone-rod dystrophy as well as macular dystrophies (Retnet: https://web.sph.uth.edu/RetNet/; assessed 22nd May, 2022). The overlapping features in different phenotypes is well explained by the fact that several IRD genes are responsible for different phenotypes.

1.3.4. Syndromic Inherited Retinal Dystrophies

The syndromic IRDs can be broadly divided into two groups; one is inborn errors of metabolism (IEM) and the other group include ciliopathies. IEMs arise due to failures of protein metabolism, carbohydrate metabolism, glycogen storage and fatty acid oxidation. IEMs mostly are associated with neurologic symptoms because of neurodegeneration as a result of metabolic disorders which mainly damages the retinal

cells. As retina is formed from primitive forebrain pouch therefore it is considered as an extension of brain (Ferreira and van Karnebeek, 2019), which may result in the frequent presence of vision loss with cognitive dysfunction in various syndromes. These disorders include mucopolysaccharidoses (MPSs), congenital disorders of glycosylation (CDG), neuronal ceroid lipofuscinoses (CLNs) and peroxisomal disorders (Tatour and Ben-Yosef, 2020).

The other group of syndromic IRDs are ciliopathies. Outer segment of the photoreceptor cells is connected with inner segment proximally through primary cilium. Primary cilia are important sensory structures to gather environmental cues and maintains tissue homeostasis (May-Simera et al., 2017). Therefore, retinal dysfunction is the common consequence observed in ciliopathies along with other abnormalities affecting liver, kidney, skeleton, central nervous system and inner ear. The ciliopathies which are responsible for syndromic IRDs include Joubert syndrome (JBTS) characterized by developmental delay, ataxia, abnormal eye movements, RP and breathing abnormalities (Parisi et al., 2007), Bardet-Biedl syndrome (BBS) which is a combination of skeletal disorders mainly postaxial polydactyly, intellectual disability, renal disease, truncal obesity and hypogonadism along with RP (Forsythe and Beales, 2013), Usher syndrome (USH) which is a combination of hearing loss and RP (Castiglione and Moller, 2022), Alstrom syndrome (ALMS) where affected individuals depicts cone-rod dystrophy along with short stature, hearing loss, truncal obesity, type 2 diabetes, cardiomyopathy, renal, pulmonary and hepatic dysfunction (Marshall et al., 2011) and Senior-Loken syndrome (SLN) which presents LCA or RP retinopathies along with cystic kidney and reduced ability of concentrating (Tsang et al., 2018).

1.3.4.1. Genetics of Syndromic Inherited Retinal Dystrophies

Most of the syndromic IRDs present autosomal recessive pattern of inheritance and are rare but they may appear as autosomal dominant such as Alagille syndrome (OMIM ID: #118450), Dyskeratosis Congenita (OMIM ID: #613990), Revesz syndrome (OMIM ID: #268130) and X-linked such as Alport syndrome (OMIM ID: #3010150), Charcot-Marie-Tooth disease (OMIM ID: #311070) and Norrie disease (OMIM ID: #310600). More than 80 forms of syndromic IRDs are present and most of them are explained with single genes however some show genetic heterogeneity. JBTS, BBS and USH are the three ciliopathies which are among the most genetically heterogeneous

group of syndromic IRDs. The symptomatic heterogeneity is explained by the fact that the protein products of the associated genes are involved in the formation of several types of protein complexes in retina and also in other tissues. Approximately 21 genes are known to cause BBS (*BBS1, BBS2, ARL6, BBS4, BBS5, MKKS, BBS7, TTC8, PTHB1, BBS10, TRIM32, BBS12, MKS1, CEP290, WDPCP, SDCCAG8, LZTFL1, BBIP1, IFT27, IFT74, C8ORF37, CEP164*) and these are involved in intraflagellar transport, maintaining lipid homeostasis and centrosomal functions (Petriman and Lorentzen, 2020). Similarly, 36 genes are known to cause JBTS which are all expressed in primary cilium. All these genes (*INPP5E, TMEM216, TMEM67, TMEM138, TMEM231, TMEM107, AHI1, CEP290, RPGRIP1L, ARL13B, CC2D2A, CEP41, ZNF423, CSPP1, PDE6D, CEP104, MKS1, ARMC9, ARL3*) are responsible for autosomal recessive pattern of inheritance while only one gene (*OFD1*) depicts X-linked inheritance (Tatour and Ben-Yosef, 2020). USH is caused by 11 genes (*MYO7A, USH1C, CDH23, PCDH15, USH1G, CIB2, USH2A, ADGRV1, WHRN, CLRN1, HARS1*) which perform wide range of functions in neurosensory cells of inner ear and retina including cell adhesion, trafficking and scaffolding (El-Amraoui and Petit, 2014).

1.4. Eye Disorders in Pakistan

In populations with higher degree of endogamy the incidence of rare Mendelian diseases are higher, and therefore autosomal recessive inherited disorders are more common. A similar pattern has been observed in Pakistani population and consanguineous families from this region have been utilized to identify underlying genes for many types of inherited eye disorders. The genetic studies on IRDs from Pakistani populations facilitated the identification of eleven novel genes (*AIPL1, BEST1, CC2D2A, CDH23, IMPG2, LCA5, NMNAT1, ZNF513, PCDH15, SEMA4A and SLC24A1*). Additionally, these studies also provided the evidence to associate *CLRN1* and *TTC8* genes with non-syndromic autosomal recessive IRDs which were otherwise known to cause syndromic IRDs (Khan et al., 2014). The study indicating the vision loss burden in Pakistan estimated that 1.12 million Pakistani population is blind and the number is increasing continually since 1990 (Hassan et al., 2019).

A comprehensive account of different congenital ocular defects and their prevalence is not properly reported in Pakistan, but some studies provided information on blindness reports due to cataracts and refractive errors. Single hospital based study from Sindh

indicated that RP is the most prevalent form of IRD in Pakistan with 64% cases, followed by 14.7% Stargardt disease and 6.7% cone dystrophies (Adhi, 2002). *RPE65* and *TULP1* were identified as most frequently mutated genes both with 6.9% among the solved families, in a large cohort of 144 consanguineous Pakistani families affected with RP and collected from different regions of Punjab. The second most frequently mutated genes identified in the same cohort were *PDE6A* and *RP1* in 4.9% solved families (Li et al., 2017). In a study, (Khan et al., 2014) provided an overview of 56 different studies conducted in Pakistan and comprehend the genetic data from 466 Pakistani IRD patients. They found that autosomal recessive RP is the most frequently found IRD in Pakistan with 59% cases and autosomal recessive LCA being second with 19% cases. Autosomal recessive cone-rod dystrophy and autosomal recessive CSNB are at third and fourth numbers with 10% and 9% cases respectively. *AIPL1, CRB1, TULP1, RPGRIP1, RP1, SEMA4A, LCA5* and *PDE6A* are among the most frequently mutated genes collectively reported in the previous Pakistani studies. Similarly, the data collected before 2014 from 22 different studies indicated that USH syndrome account for 36% of the syndromic IRD cases in Pakistan, while BBS account for 33%, JBTS for 10% and SLS for 8%. The most frequently mutated gene collectively in syndromic IRD cases in Pakistan is *CDH23* (Khan et al., 2014). In another study of 26 Pakistani IRD families, single mutation in *RPE65* was found in 5 families (Maranhao et al., 2015). This also indicated that *RPE65* is the frequently mutated gene in Pakistani IRD families.

The major cause of bilateral blindness worldwide second to cataract is glaucoma with the prevalence of 64.3 million (Rulli et al., 2018) and is estimated to reach 111.8 million by 2024 (Tham et al., 2014). Primary congenital glaucoma (PCG) is the type of glaucoma which starts as early as few months to 3 years of age. The most frequently mutated genes in PCG are *CYP1B1* and *LTBP2* with 240 and 26 mutations reported in Human Gene Mutation Database (HGMD) respectively. In a small study of 29 sporadic PCG cases from Pakistan, *GLC3A* locus harbouring *CYP1B1* gene is linked to 17% of cases (Bashir et al., 2014). In a study of 14 Pakistani consanguineous families affected with PCG, 50% families (n=7) were identified with biallelic *CYP1B1* mutations (Rashid et al., 2019). This indicates that *CYP1B1* is also frequently mutated gene in glaucomatous families of Pakistani origin, though there are reports indicating the

involvement of *LTBP2* in PCG (Ali et al., 2009; Rauf et al., 2020). Four consanguineous Pakistani families affected with PCG were reported to have null mutations in *LTBP2* gene (Ali et al., 2009). Another study of PCG families from Pakistan identified three novel *LTBP2* variants (Rauf et al., 2020).

Microphthalmia, anophthalmia and coloboma are collectively considered in a similar spectrum of MAC. The biallelic mutations in *ALDH1A3* are considered the most frequent cause of MAC in autosomal recessive consanguineous families (Fares-Taie et al., 2013). In a small study of Pakistani families affected with A/M, (20%) solved families have *ALDH1A3* variants while 60% have *FOXE3* variants (Ullah et al., 2016). In a recent study of 19 consanguineous families affected with MAC, variants were identified in *TENM3, KIF26B, MICU1* are *CDON*. Some variants were identified in candidate genes such as *LRP6*, *WNT2B*, and *IQGAP1* (Islam et al., 2020). Mutations in *VSX2* and *PXDN* are also reported with microphthalmia and associated phenotypes in consanguineous Pakistani families (Iseri et al., 2010; Khan et al., 2011; Reis et al., 2011).

1.5. Diagnosis of Eye Disorders

Several clinical diagnostic tests are available for screening of different eye disorders, whereas genetic testing is also available for inherited eye disorders.

1.5.1. Clinical Diagnosis

Visual acuity test: This test is performed to check the reading performance, visual acuity, effects of illumination and contrast sensitivity through "Snellen charts". According to this test, 20/20 visual acuity refers to no vision loss, whereas 20/40 and 20/60 means 10% and 20% vision loss respectively. 20/200 visual acuity is generally accepted as complete vision loss (Sloan, 1951).

Slit lamp examination: The slit lamp is a uniquely designed microscope which gives a three-dimensional view of the eye structures and therefore it provides an accurate view of the abnormalities and their location. This test can be performed to visualize the anterior segment of the eye to examine mainly corneal injuries, conjunctivitis and cataracts (Ledford and Sanders, 2006). It is used before and after operative assessments of eye and for fitting lens (Martin, 2018).

Tonometry: It is performed to accurately measure the IOP in the eye. This test is performed to diagnose glaucoma a condition characterized by the increased IOP (normal range: 7-21 mm Hg) (Kniestedt et al., 2008).

Ophthalmoscopy/Fundoscopy: Fundoscopy is used to examine the inside of the eye called fundus and provides the clear images of retina, macula, fovea, blood vessels and optic nerve. This test is important for the diagnosis of diabetic retinopathies, macular degenerations, retinal degeneration, pigment depositions and retinal detachment (Chatziralli et al., 2012).

Fluorescein angiography: In this test, dye is injected through a vein and as it travels through the blood vessels of retina, images are captured for visualization of innermost layers of eye. This test is also performed for the diagnosis of diabetic and other retinopathies and macular degeneration (Yannuzzi et al., 1986).

Optical coherence tomography (OCT): OCT uses light waves to create the non-invasive cross-sectional image of the different layers in eye. This test provides the diagnosis for glaucoma, macular and other retinal dystrophies (Huang et al., 1991).

Electroretinogram (ERG): ERG uses the light stimuli to record the electrical activity of retina during scotopic and photopic vision. This test is performed for the diagnosis of IRDs (Perlman, 1995).

1.5.2. Genetic Diagnosis

Genetic diagnosis involves the identification of disease-causing variant in patients presented with different types of ocular disorders. The genetic testing strategy that can be employed for a patient's genetic test can vary but is mainly dependent on the available clinical information. A brief account of these strategies is given below;

1.5.2.1. Targeted Sanger Sequencing

Targeted Sanger sequencing (TSS) involves the capturing and amplification of single exon or part of large exons for up to 1kb through conventional PCR techniques. The captured region is then sequenced through Sanger sequencing. However, TSS can be directly employed in a limited number of patients owing to heterogenous nature of ocular disorders and very few types have single or few candidate genes which are suitable for TSS.

In majority of research settings TSS has been frequently utilized in combination with genome wide genotyping and homozygosity mapping to increase diagnostic yield of genetic test. These studies initially perform homozygosity mapping to shortlist candidate genes prior to TSS. This approach provided more accurate gene targeting as compared to random selection of genes and exons. These approaches have been proved successful in several studies for the identification of disease causing variants associated with different IRDs (Ali et al., 2009; Anjum et al., 2010; Bashir et al., 2014; Saqib et al., 2015; Ghofrani et al., 2017; Wawrocka et al., 2018; Rashid et al., 2019; Rauf et al., 2020) were only helpful in the identification of already known phenotypic variants in a particular population. This technique is accurate but provides less data and is not much beneficial for the identification of novel variants or novel genes.

1.5.2.2. Next Generation Sequencing (NGS)

Next generation sequencing (NGS) techniques have revolutionized to tackle the human genome complexities over the past decade and has increased the sequencing capacities from 100-1000 times (Kircher and Kelso, 2010). In most of NGS platforms, sequencing is performed by either of two methods; sequencing by ligation or sequencing by synthesis. In sequencing by ligation approach, a fluorophore bound probe fragment is hybridized to a DNA fragment and the bases within the sequenced fragment are identified by complementarity to specific positions in the probe. Whereas, in sequencing by synthesis, fluorophore tagged bases are used in a polymerase chain reaction and the addition of base or ionic changes in the reaction are measured to detect the sequence of the fragment. Since several fragments are sequenced together in both approaches through clonal amplification therefore pronounced and reliable signal is detected compared to background noise (Goodwin et al., 2016). The genetic community have used NGS in different ways to ensure rapid turnaround time and diagnostic yield and these are summarized in the subsequent sections.

1.5.2.2.1. Panel-Sequencing

Phenotype-directed panels are available for the diagnosis of several genetic disorders. The ultimate goal of these panels is to avoid the cost of exome sequencing and time in consuming analysis of unnecessary genes and variants of uncertain significance (VUS). While designing a panel, maximization of clinical sensitivity is also kept in consideration by possibly including all genes associated with that particular Mendelian

disorder. It is also important to include genes with the uncertain significance which have limited but emerging evidences of their relevance with the particular phenotype. The technical completeness of the panel design is also very important e.g., the coverage depth should be in appropriate range for good quality diagnosis (Bean et al., 2020). The panel testing is helpful in capturing intronic or regulatory regions as well as complex regions which may not be covered in exome sequencing. Among the disadvantages of the panel sequencing include un-identification of novel genes and variants associated with the particular disorder. Panel may not include the recently identified genes associated with a phenotype and generally panels vary depending on lab (Wojcik et al., 2023).

The recent technique used for target enrichment in most panel sequencing is single molecule Molecular Inversion Probes (smMIPs) which is fast high throughput technique. The smMIPs are oligonucleotide probes which have primers at its 3' and 5' ends. Therefore, it hybridizes with both ends to the DNA and target region is incorporated through the fill in reaction. The circular probe is then PCR amplified and sequenced after purification. The target enrichment technique is advantageous, as we can capture and tile regions as closely as necessary (Boyle et al., 2014). Several studies have highlighted the success of panel-based sequencing for the genetic diagnosis of inherited ocular defects. In a Chinese cohort of 319 patients, 41.2% diagnostic yield was achieved through panel based gene sequencing, which covers 441 genes out of which 291 genes were related to IRDs (Wang et al., 2018). In another study 56% diagnostic yield was achieved in Brazilian patients affected with retinal dystrophies by the use of panel based sequencing covering 132 genes related to retinal dystrophies (Costa et al., 2017).

1.5.2.2.2. Exome Sequencing (ES)

Exome sequencing (ES) is the sequencing of protein coding exons in a gene and this covers 1-2% of the genome. According to estimation, 85% disease causing variants are present in the coding region of the genome (Cooper et al., 1995). Therefore, sequencing of complete coding region of the genome can potentially uncover the mutations causing many rare monogenic genetic disorders (Botstein and Risch, 2003; Majewski et al., 2011). The identification of disease-causing variant has been increased from 25-40% using ES in the clinical diagnostic setup depending on the phenotype. Whereas

diagnostic rates are even higher in the populations reported with consanguinity (Sawyer et al., 2016). The ES also requires capturing of the target sequence. There are several different capturing platforms available which are improved and updated constantly. The three main providers of capturing platform include NimbleGen, Agilent and Illumina (Warr et al., 2015). The variation in diagnostic from different studies may arise due to use of different capturing method.

The first diagnosis made by the use of ES was in patient suffering from congenital chloride diarrhoea which was suspected of Bartter syndrome (Choi et al., 2009). After this the genetic cause of many heterogeneous disorders including intellectual disability, hearing loss, autism and RP have utilized ES. ES has proven successful in the identification of disease-causing variants in several eye disorders. Recently, a cohort of 90 unrelated individuals affected with different eye disorders were provided genetic diagnosis through ES. In total 71 variants were identified in 38 different genes, out of which 21 were novel disease causing variants (Ordonez-Labastida et al., 2022). In another study of 266 Dutch patients, ES provided diagnosis to 51% patients. The highest diagnostic yield was observed in IRD patients (63%) while second highest in RP (with 50%) (Haer-Wigman et al., 2017). This indicates that ES provides diagnosis in rare disorders where genetic causes are already well explained.

ES provides an intermediate coverage of the sequencing region as compared to panel and genome sequencing. It is also useful in the identification of novel genes which cannot be identified through panel sequencing. Some capturing methods fail to capture GC rich regions from the genome and may result GC biases (Meienberg et al., 2016). Some defects are caused by repeat expansion while large indels and copy number variations (CNVs) play a significant role in causing rare disorders. ES is unable to identify CNVs and large deletions accurately and also provides poor coverage in sequencing of repeat regions (Fromer et al., 2012).

1.5.2.2.3. Genome Sequencing

The genome sequencing (GS) screens the complete genome and provides information of all coding and non-coding variants in the genome, potentially expanding the information of the genes associated with the particular phenotype. The diagnostic yield of as high as 73% on average can be achieved using GS (Miller et al., 2015; Soden et al., 2014; Willig et al., 2015). In GS no capturing and enrichment is involved therefore

it provides an unbiased sequenced data which can be more reliably used for the identification of large structural variants (SVs) and CNVs due to uniform coverage. Many studies recommended GS over ES after initial panel screening for identification of disease causing variants (Meienberg et al., 2016). The GS is used for genetic diagnosis of rare diseases since 2010 but now its usage has been increased in the clinical setup.

This technique is now widely used by researchers in the field of eye genetics for providing molecular diagnosis. In two separate studies, 562 and 605 patients with ocular defects were screened through WGS. Both the studies demonstrated that GS is more advantageous in detection of SVs, CNVs and mutations in regulatory and GC-rich regions (Ellingford et al., 2016; Carss et al., 2017). Although with huge benefits, GS is very expensive, but costs are declining with time. Currently, the major disadvantages of GS includes less coverage depth and more turnaround time. The problem related to GS is the information of many VUSs and unreal SVs and CNVs which makes the analysis tiring and time taken which is not suitable for early detection of genetic diagnosis. The figure 1.5 provides a comparison of different sequencing techniques utilized for genetic testing.

1.5.2.3. Third Generation Sequencing

The third-generation sequencing technology is aimed to sequence long DNA fragments and is also known as long read sequencing. The leading company providing such sequencers is Pacific Biosciences (PacBio) and their latest sequencer is Single Molecule Real Time (SMRT) sequencer which is capable of sequencing fragments as large as 30 to 50 kb. It not only provides longer reads of genome for accurate and reliable assembly but also facilitates the identification of methylation sites and other epigenetic signatures (Slatko et al., 2018). This technique is efficient as compared to other sequencing techniques for the identification of large indels and CNVs which are inaccessible through short read ES or GS. This is a promising technique in resolving missing heritability and ultimately identification of novel disease genes and associated mechanisms. But the disadvantages associated with third generation sequencing are high capital costs, low-medium accuracy and long turnaround time.

A recent study has utilized the long read Nanopore sequencing to optimize method for the identification of mutations in *RPGR* gene which is known to cause X linked RP

(Yahya et al., 2023). *RPGR* is a commonly mutated gene in X linked RP and a specific region of this gene (referred as ORF15) is hard to sequence but is a known hot spot for RP causing mutations. They sequenced PCR amplified products of 2Kb size flanking ORF15 region and confirmed the results on SMRT platform. This type of strategy can be useful for either the sequencing of hard to sequence genes/exons of IRD genes (as specified above) or the sequencing of deep intronic and regulatory regions.

1.6. Therapeutics of Genetic Eye Disorders

Advancements in the identification of disease-causing variants responsible for eye disorders have accelerated the formulation of probable treatments or gene therapies. The identification of crucial genes provides an insight into the important genetic players which can be targeted therapeutically. The retina being an integral unit for visual transduction is the preferable target for gene therapy (Trapani and Auricchio, 2019). Since the retinal cells do not propagate therefore single dose can provide a long term expression of the transgene (Trapani and Auricchio, 2018). Eye is an isolated and small compartment, which makes it easily approachable through subretinal and intravitreal injections (Schwartz et al., 2015). The gene delivery is either aided by nanoparticles or virus-mediated approaches. Adenovirus, lentivirus, adeno-associated virus (AAV) or recombinant adeno-associated virus (rAAV) are used for this purpose. rAAV is the most preferable delivery method as the genome of rAAV is double-stranded and maintained as an extrachromosomal episome, which makes it less favourable for genomic integration and hence, preventing off target affects in the genome (Deyle and Russell, 2009).

Subretinal injections of Luxturna (delivering the normal copies of *RPE65*) is the first FDA approved gene therapy which treats *RPE65*-associated LCA (Chiu et al., 2021). Two other therapies i.e., AAV5-RPRG and AAV2-REP1 which are gene-based drugs and are under clinical trial (Phase III) for treatment of X-linked RP and choroideremia respectively (ClinicalTrials.gov, Identifier: NCT04671433 & NCT03496012). In few therapies, the antisense oligonucleotides have also been used to rectify the aberrant splicing of mutant pre-mRNA thereby nullifying the effect of mutation at transcript level. One such therapy (QR-110) which involves utilization of antisense oligonucleotides for rectification of *CEP290* aberrant splicing is also in clinical phase III trial (Cideciyan et al., 2019).

The development of such therapies is an important step forward towards the treatment of genetic disorders. Since world is moving towards the personalized medicine, therefore the foremost step required for the formulation of such therapies is to screen and identify the genetic players responsible for inherited eye disorders. Same is true for Pakistani population as knowledge of the underlying genetic players is essential for gene specific therapeutic strategies. There is still need to broaden spectrum of disease-causing variants in our population to design appropriate diagnostic panels for efficient and timely diagnosis to ensure appropriate management. This study has been initiated to explore mutations responsible for different inherited eye disorders in families recruited from different regions of Pakistan. This study also tests the utility of different sequencing approaches for future use in genetic testing.
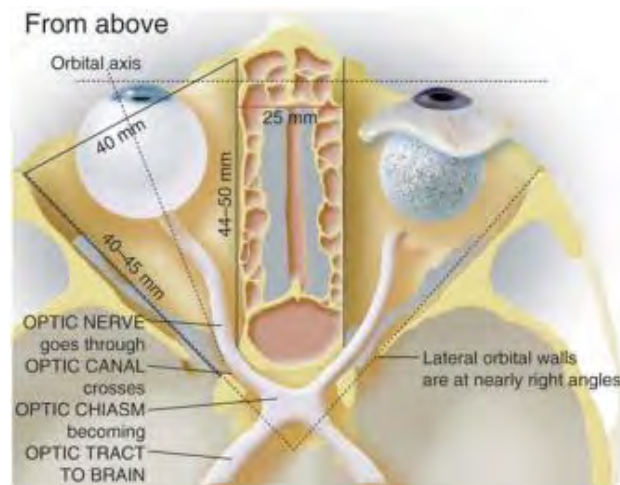
Figure 1.1: Visual representation of an eye orbit and originating optic nerves leading to brain (Adapted from Hughes, 2004).
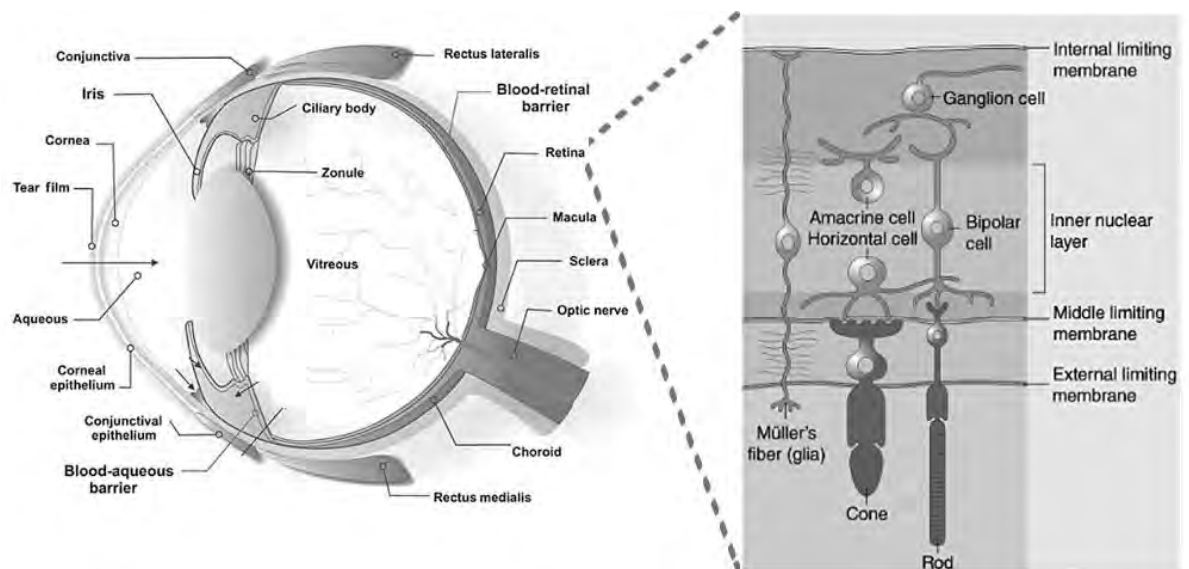
Figure 1.2: Schematic illustration presenting the eye structure and cells in the retinal layers (Adapted and modified from Willoughby et al., 2010).
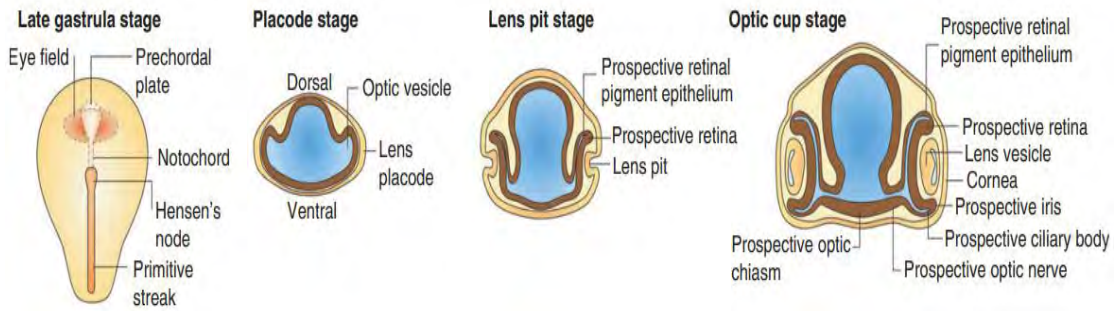
Figure 1.3: Schematic representation of development of eye from gastrula stage to optic cup formation (Adapted from Graw, 2010).
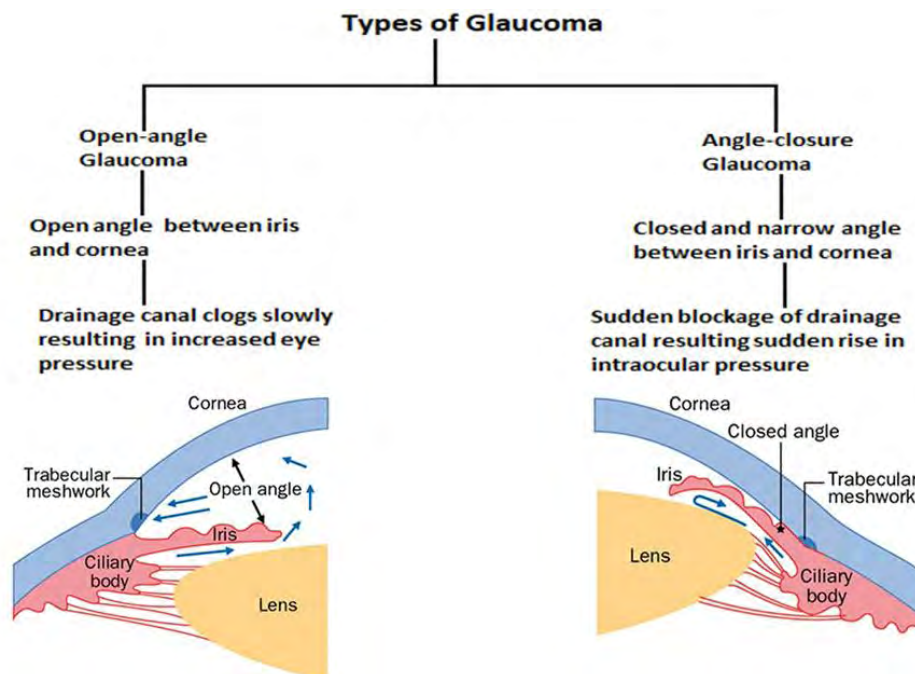
Figure 1.4: Flow chart showing two types of glaucoma and flow/obstruction of aqueous humor through trabecular meshwork (Adapted and modified from Wiggs and Pasquale, 2017).
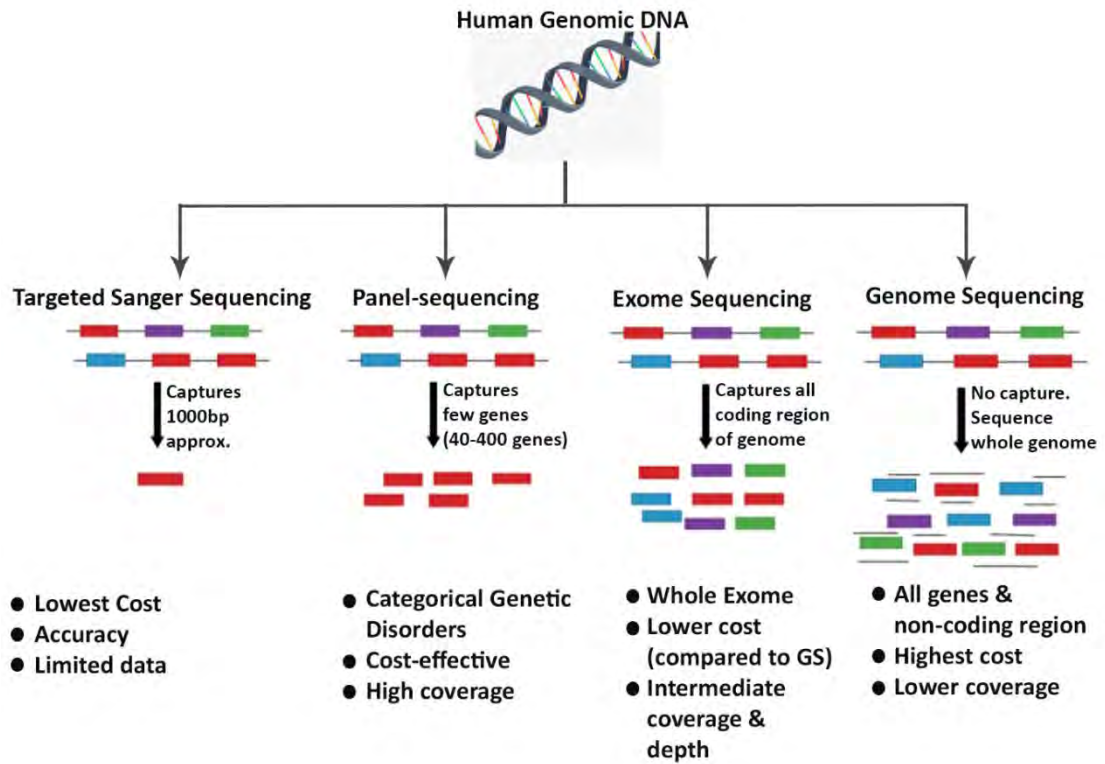
Figure 1.5: Schematic representation and comparison of targeted Sanger sequencing, panel-sequencing, exome sequencing and genome sequencing.

AIM AND OBJECTIVES

The aim of this study is to explore genes involved in different types of inherited ocular defects in Pakistani families.

The specific objectives of the study are:

- To enroll families affected with different inherited ocular defects.

- To establish molecular diagnosis in the collected families.

- To explore genotype-phenotype correlation in the families

- To compare different approaches utilized in the study.

2.0.MATERIAL AND METHODS

This study was designed according to the guidelines of Tenets of Helsinki and was approved by Bio-ethical committee (BEC) of Quaid-I-Azam University (QAU), Islamabad, Pakistan and ethical review board of the Radboud University Medical Center, Nijmegen, The Netherlands. The major part of the study was conducted in Lab of Genomics, Department of Biochemistry, QAU, Islamabad, while some part of research was also performed in the Department of Human Genetics, Radboud University Medical Center, Nijmegen, The Netherlands during a 6-month fellowship funded by Higher Education Commission (HEC), Pakistan. The participants voluntarily took part in this study. The informed consent was taken from either the subjects or the guardians of the subjects enrolled in this study.

2.1. Family Recruitment

In this study 28 multiplex consanguineous families affected with different types of eye disorders were collected from different regions of Pakistan. The participating members of each recruited family were interviewed at their residencies to obtain related information regarding phenotype, age of onset and progression of the disease. After collecting complete information, pedigrees were drawn for the assessment of phenotypic inheritance pattern running among each family.

2.2. Clinical Assessment

Clinical assessment was made after thorough investigation of the participating members by local ophthalmologist. All available information related to age of onset, any other related medical condition or extra-ocular features including hearing impairment, intellectual disability, skeletal or muscular atrophy or facial dysmorphism was gathered verbally through a questionnaire. One affected member from each family was subjected to clinical diagnosis through fundoscopy or optical coherence tomography (OCT) where available in the nearby health facilities.

All the available clinical information was compiled, and 28 recruited families were divided into four subgroups based on the clinical presentation. Group A contained 6 families (A1-A6) with glaucoma, while group B consisted of 8 families (B1-B8) presenting anophthalmia/microphthalmia (A/M) phenotype. Eleven non-syndromic

inherited retinal dystrophy (IRD) families were placed in group C (C1-C11) whereas group D had three families (D1-D3) with syndromic IRDs.

2.3. Sample Collection

From the available members, 5-8 ml peripheral blood was withdrawn in sterile EDTA vacutainers (BD, Franklin Lakes, New Jersey, USA). Tubes containing blood samples were labelled properly and stores at 4°C in a refrigerator.

2.4. Genomic DNA Extraction

Genomic DNA was extracted from all collected samples using standard phenol-chloroform method as explained below:

1. In a sterile 1.5 mL microfuge tube (Axygen, USA), 750 microliters (μL) blood sample was taken to which the equal volume of solution A (including 0.32M Sucrose, 10mM Tris-HCL pH 7.5, 5mM MgCl2 and 1% v/v Triton-X 100) was added and mixed thoroughly.

2. The mixture was incubated for 10 – 15 minutes at room temperature and then centrifuged (EBA21; Hettich, Germany) for 2 minutes at a speed of 12000 rpm.

3. The pellet obtained was washed again with 400 μL of solution A.

4. The nuclear pellet was now re-suspended in 500 μL of solution B (including 10mM Tris-HCL pH 7.5, 400mM NaCl and 2mM EDTA pH 8.0), 15 μL of 20% sodium dodecyl sulphate (SDS) and 10 μL of proteinase K (20 mg/mL). It was then incubated at 37° C in an incubator (B28; Binder, Germany) for 24 hours.

5. The freshly prepared 500 μL mixture (1:1) of solution C (24 mL Chloroform, 1 mL Isoamyl alcohol) and phenol was added to the tubes, thoroughly mixed for 10 seconds by shaking and centrifuged for 10 minutes at 12000 rpm.

6. This separated the genomic DNA in the upper clear aqueous phase which was then carefully aspirated using micropipette and transferred to a fresh 1.5 mL microfuge tube.

7. The phase separated genomic DNA was then precipitated with isopropanol (500 μL) and 3M sodium acetate (60 μL), mixed gently and centrifuged for 10 minutes at 12000 rpm.

8. The supernatant was discarded and genomic DNA pellet was washed by adding 300 μL of 70% ethanol and centrifugation at 8000 rpm for 5 min.

9. The supernatant was discarded very carefully, and the genomic DNA pellet was air dried. Depending upon the size of the genomic DNA pellet, 50 – 150 µL Tris-EDTA (TE) buffer (pH 7.4) (Cat. No. AM9849; Invitrogen) was added to dissolve the DNA. The extracted DNA was then stored at -20° C.

Quality and quantity of the extracted DNA was checked through nanodrop and 1% agarose gel electrophoresis.

2.4.1. Quantification of the DNA

Extracted genomic DNA was quantified using Colibri Microvolume Spectrophotometer (Titertak Berthhold, Germany). The concentrations were recorded in ng/µL and quality was checked by observing the 260/280 and 260/230 ratios.

2.4.2. Agarose Gel Electrophoresis

Extracted genomic DNA was confirmed by agarose gel (1%) electrophoresis. For preparing 1.0% agarose gel, 0.4g agarose powder was taken and mixed in 40.0 ml 1X TBE buffer. The flask was then warmed in microwave oven with occasional shaking for about 1 -2 minutes and then checked whether agarose granules completely disappeared. In case of presence of some undissolved granules, the flask is then heated again for 30-60 seconds. The mixture was then cooled down below 60°C. Then 4µl ethidium bromide was added and homogenized mixture of solubilized gel was then poured in the casting tray to the depth of 5-8mm. Then carefully inserted the comb into the molten gel which was removed after the gel solidification. Before loading the samples on gel, DNA loading dye was added to each sample separately. Samples were loaded carefully in wells (a single sample in a single well). The gel was run at 95 volts in 1X TBE buffer for about forty-five minutes. The gel was removed, and the bands of DNA were visualized under the UV light in the gel documentation system (Syngene, UK).

2.5. Molecular Genetic Testing

Several approaches were used for the identification of disease-causing variants in the collected 28 families. Three out of 6 glaucoma families (A1-A3) were screened through targeted Sanger sequencing (TSS), while remaining families (A4-A6) were tested through exome sequencing (ES). Similarly, for A/M group seven families (B1-B7) were initially screened through TSS, but family B8 and genetically unexplained A/M

families (After TSS) were subjected to genome sequencing (GS). All non-syndromic (C1-C11) and syndromic (D1-D3), IRD families were initially screened through panel-sequencing (PS) and the families which remained genetically unexplained after PS were subjected to GS. The schematic representation of this approach is shown in figure 2.1.

2.5.1. Targeted Sanger Sequencing (TSS)

Targeted Sanger Sequencing (TSS) of complete coding regions of *CYP1B1* (NM_000104.4) and *MYOC* (NM_000261.2), and specific exons with recurrent mutations in *TEK* (NM_000459.5) and *LTBP2* (NM_000428.3) was performed for glaucoma families (A1-A3). A/M families (B1-B7) were screened for complete coding region of *FOXE3* (NM_012186.3) through TSS.

2.5.1.1. Primer Designing

For amplification of the genes explained in the section 2.5.1, reference sequence of each selected sequence was downloaded from the Ensembl genome browser (http://asia.ensembl.org/index.html) and primers were designed using Primer3 version 0.4.0 (http://bioinfo.ut.ee/primer3-0.4.0/primer3). BLAST-like alignment tool (BLAT) (https://genome.ucsc.edu/cgi-bin/hgBlat) was used to check the primer specificity for each primer. After BLAT those primers were selected which gave single hit on human genome. The polymerase chain reaction (PCR) product's sizes and melting temperatures of primers were confirmed by In-silico PCR (https://genome.ucsc.edu/cgi-bin/hgPcr). List of all the primers used for TSS is given in table 2.1.

2.5.1.2. Polymerase Chain Reaction (PCR)

The DNA of single proband from each selected family was used for the amplification of the concerned regions using primers mentioned in table 2.1. For the amplification of *CYP1B1* and *FOXE3* regions, HotStarTaq master mix (Qiagen, Germany) was used with the protocol described below;

Reagents   Quantity

- Master Mix by Qiagen   3μl

- Forward Primer (10pmol/μl)   1μl

- Reverse Primer (10pmol/µl)   1µl

- DNA template (30ng/µl)   2µl

- Nuclease free Water   6µl

- Total Reaction Volume   13µl

Additionally, for *FOXE3* region, DMSO (8%) and betaine (0.2M) were also added to improve DNA denaturation. The reaction mixture was prepared in 0.2mL tubes, spun briefly in the centrifuge and placed in T1 thermocycler (Biometra, Germany). The PCR was completed with an initial denaturation of DNA at 95°C for 15 minutes and then followed by 39 cycles which include steps such as the denaturation at 96°C, annealing at 60°C and elongation at 72°C for 60 seconds, 50 seconds and 2 minutes 30 seconds respectively. Finally, at 72°C, the extension was given for 10 minutes.

For all the remaining primers, following protocol was used:

Reagents	Quantity
• 10X PCR Buffer (Thermo Fisher Scientific, USA)	2.5µl
• $MgCl_2$ (25mM; Thermo Fisher Scientific, USA)	1.5µl
• dNTPs (10mM; Thermo Fisher Scientific, USA)	
	0.5µl
• Forward Primer (10pmol/µl)	1µl
• Reverse Primer (10pmol/µl)	1µl
• Taq DNA polymerase (5U/µl; Thermo Fisher Scientific, USA)	0.2µl
• DNA template (30ng/µl)	2µl
• Nuclease free Water	16.3µl
• Total Reaction Volume	25µl

The PCR was completed with an initial denaturation of DNA at 95°C for 10 minutes and then followed by 39 cycles which include steps such as the denaturation at 96°C, annealing at 60°C or 62°C and elongation at 72°C for 60 seconds, 50 seconds and 1 minutes 30 seconds respectively. Finally, at 72°C, the extension was given for 10

minutes. The amplified products were then visualized on 2% agarose gel stained with ethidium bromide and observed under UV in the gel documentation system.

2.5.1.3. Purification of PCR product

The amplified PCR products were then purified for sequencing either through ExoSAP-IT (Cat. No. A55242; Thermo Fisher Scientific, USA) or GeneJET Gel Extraction Kit (Cat. No. K0691; Thermo Fisher Scientific, USA).

ExoSAP-IT purification was used for the primers which gave specific PCR products. For this standard protocol was used, according to which 2µl of ExoSAP reagent was added to 8µl of PCR product. The mixture was then incubated at 37°C for 15 minutes and then 80°C for 15 minutes.

The PCR with non-specific products were purified using GeneJET Gel Extraction Kit. For which, amplified product was run on 2% agarose gel. The sterilized blade was used to cut the gel slice which contains the DNA fragment of our required PCR product and then slice was placed in an autoclaved Eppendorf (pre-weighed) tube. The slice containing DNA fragment Eppendorf was weighed again to find the weight of gel slice. Binding buffer (Lot. No. 00850742) in 1:1 (volume of buffer in µl: weight of slice in mg) was poured in the tube. The tube which contains the mixture of gel and buffer was then incubated at 60°C for 10-15 minutes or until the gel was completely dissolved. The dissolved gel mixture was then vortexed shortly before loading on the column. Up to 800µl of the solution containing the solubilized gel was loaded to the column provided in the kit and centrifuged for 1 minute. The flow-through was discarded. The remaining mixture was loaded again to the same column and centrifuged. This process was repeated until entire mixture was processed. 100 µl of the same binding buffer was added to the purification column and centrifuged for 1 minute, after which the flow-through was discarded. 700µl of Wash Buffer (Lot. No. 00904265) (100% ethanol mixed) was added to the column and centrifuged for 1 minute. Again, the flow-through was discarded. The empty column was centrifuged for additional 1 minute to dry the residual wash buffer. Column was then transferred into the clean and sterile 1.5ml tube and 25µl of elution buffer was added in the center of the column. The column was incubated for 1 minute and then centrifuged at 12,000 RPM for 1 minute. The empty column was then discarded, and purified DNA was stored at -20°C.

2.5.1.4. Sequencing

Standard protocol for ABI Big Dye Terminator Cycle Sequencing Kit was used to for the sequencing of each fragment, 4.0μl Terminator Ready Reaction Mix, up to 4μl (30-90ng) of template (dsDNA template at a concentration of 2 ng/ μl per 100 bp length required for each reaction), 1.0μl primer, ddH$_2$O to make final volume equal to 10 μl were added in a separate 0.2ml microamp tubes and then mixed and spun briefly. These prepared tubes were then placed in thermal cycler for 25 cycles (of 96°C for 10 seconds, 50°C for 5-10 seconds, 60°C for 4 minutes), then ramp to 4°C.

2.5.1.4.1. Purification of sequencing products by isopropanol precipitation

After thermal cycler the tubes were spun, and the content were transferred in separate Eppendorfs by pipetting the entire sequencing reaction. 75% isopropanol (40 μl) and 100% isopropanol (30μl) were added in the tubes and mixed by vortexing briefly. For the precipitation of products, the tubes were left at room temperature (for greater than 15 minutes and less than 24 hours) and were centrifuged for 20 minutes. Supernatant was discarded carefully so that the DNA pellet is not disturbed. Again, pellet was washed with 75% isopropanol (125 to 250μl) and centrifuged for 5 minutes. The supernatant was again discarded. For 10-15 minutes the samples were dried in vacuum centrifuge and then stored at -20°C until ready for electrophoresis. Pellet of sample was then dissolved in 3μl loading buffer [Hi-Di Formamide, pH 8.0 with blue dextran (50 mg/ml)]. The tubes were then vortexed and centrifuged and heated at 95°C for 2 minutes before putting into the sequencer. The tubes were then chilled by placing on ice and finally purified product was sequenced on an ABI 310 sequencer.

2.5.1.5. Sequence Analysis

The sequence data were analysed using SnapGene v5.2.2 (San Diego, CA, USA). The sequence obtained after sequencing was aligned through ClustalW Multiple Alignment with the reference sequence downloaded from Ensembl/UCSC genome browser. The variants found were checked for minor allele frequency of ≤0.01 in the population database gnomAD (v3.1.2, total population frequency) and pathogenicity was assessed through various bioinformatics tools such as Mutation Taster (http://www.mutationtaster.org/), CADD-PHRED (≥15), REVEL (≥0.3), and SpliceAI (delta score ≥0.2, default settings).

2.5.2. Panel-sequencing (PS)

In this study, single-molecule molecular inversion probe (smMIP) method was used for capturing and enrichment of the target regions with Molecular Loop High-Input DNA Target Capture Kit (Molecular Loop Biosciences, USA). Two types of smMIPs based panels were used in this study.

For the families (C1-C10, D1-D2) RP-LCA smMIPs based panel sequencing was used as explained previously (Panneman et al., 2023). For families affected with ACHM we used MD smMIPs based panel sequencing as per procedure described in a prior study (Hitti-Malin et al., 2022). In general, following steps were performed for library preparation.

2.5.2.1. Probe Hybridization

1. In 96 well plate (Sapphire microplate, 96 well PCR plates, 0.2mL) which is a capture plate, 6μl of the diluted DNA sample of each proband was added, plate was sealed with Sapphire PCR plate caps and shortly centrifuged.

2. High molecular weight DNA samples were given pre-treatment at 92°C for 5 minutes in the thermocycler.

3. The probe hybridization mix (HM) was prepared by combining 115μl probe buffer and 115μl prepared probe mix in a clean 1.5ml microfuge tube.

4. After the completion of DNA pre-treatment, plate was removed from thermocycler and 2μl of the HM was added to each sample. Then shortly centrifuge the plate.

5. The capture plate was then placed in the thermocycler with the program: 95°C for 1 minute and 57°C for at least 18 hours.

2.5.2.2. Fill Reaction

1. The capture plate was removed from the thermocycler after 18 hours, centrifuged shortly.

2. The seal caps were removed and 2μl of the fill-in mix high-input (HF) available in the kit, was added in each well of the capture tube.

3. Again sealed the capture plate with new caps and was shortly vortexed and centrifuged.

4. The capture plate was again placed in thermocycler at 57°C for 1 hour.

2.5.2.3. Combined Clean-up and PCR Reaction

1. In a 1.5ml centrifuge tube, the cleanup-PCR mix was prepared by combining 204μl cleanup mix and 1224μl PCR mix available in the kit (for 96 reactions). The tube was shortly vortexed and centrifuged.

2. The capture plate was taken out of the thermocycler after completion of fill-in reaction, shortly centrifuged and seal caps were removed and discarded.

3. Another 96 well plate containing the index primers were taken out from -20°C and thawed at room temperature.

4. In each sample 2.4μl of respective index primer was added.

5. Simultaneously, 14μl of the already prepared cleanup-PCR mix was added to each sample.

6. The plate was sealed with new caps and shortly vortexed and centrifuged.

7. The plate was then placed in thermocycler to run cleanup-PCR program: 45°C for 15 minutes, then 95°C for 3 minutes, 17 cycles (98°C for 15 seconds, 60°C for 15 seconds, 72°C for 30 seconds) and finally 4°C.

After cleanup-PCR reaction, 5μl of each sample was run on 2% agarose gel. The expected product size is around 400bp (~413 bp to be more precise).

2.5.2.4. Sample Pooling

For pooling the samples, the plate was handled with extra care. 5μl of each sample was pooled first in an 8-well strip and then each well from this strip was emptied into a 1.5ml centrifuge tube using a micropipette. The tube was then shortly vortexed and centrifuged.

2.5.2.5. Library Purification

1. For the clean-up step, 100μl of the library pool was taken in 1.5ml microfuge tube.

2. The AmPureXP beads were vortexed thoroughly to re-suspend any magnetic particles that may settle down.

3. Then 1X AmPure XP beads (100μl) was added to the library pool and mixed thoroughly by pipetting up and down the mixture.

4. The tube was incubated at room temperature for 5 minutes and then placed on the magnetic rack for 3 minutes.

5. The supernatant was removed by keeping the tube in the magnetic rack.

6. The beads were washed with freshly prepared 70% ethanol, incubated at room temperature for 30 seconds before removing the ethanol.

7. The second wash with 70% ethanol was also performed as mentioned in step 6.

8. All the ethanol was carefully removed through pipette without disturbing the bead pellet.

9. The beads were air-dried on the rack for 5 minutes and then 25µl TE buffer was added for elution.

10. To ensure the complete elution, buffer was thoroughly mixed with beads by pipetting up and down to make sure no beads remained clumped.

11. The tube was incubated at room temperature for 1 minute and then placed back on the rack for 1 minute.

12. Lastly, 24µl of supernatant was transferred to a clean 1.5µl microfuge tube, in two steps of 12µl using a small pipette tip without touching the beads.

2.5.2.6. Sample Pool Quantitation and Quality Control

The Qubit (ThermoFisher Scientific, USA) was used to determine the concentration of purified pooled library and TapeStation (Agilent, USA) was used to determine the library size (bp).

For Qubit, 199µl of Qubit buffer and 1µl of Qubit reagent from Qubit dsDNA HS assay kit (ThermoFisher Scientific, USA) were added in the clean tube. Then 199µl of this mix was taken in the Qubit tube to which 1µl of the sample (purified pooled library) was added. The quantities were measured by using two Qubit standards provided with the kit. For standard, 190µl of the Qubit buffer and Qubit reagent mix was used while 10µl of the standard was added.

For TapeStation, the HS D1000 DNA kit was used. 2µl of TapeStation kit buffer and 2µl of sample (purified pooled library) were combined in an 8-well PCR strip tube. A control of 2µl TapeStation buffer and 2µl Milli-Q water was also prepared to run alongside. The 8-well PCR strip was sealed with cap, vortexed for 1 minute and centrifuged shortly. The TapeStation loading dock was checked for clean pipette tips and the TapeStation cassette. The ladder was deselected from the sample selection on

the TapeStation Controller while loading the samples. The machine was started, and samples were run against electronic ladder. The expected size was 417bp.

The megapool was prepared by combining equimolar quantities of each library pool (75ng of each) to make a final concentration of 1.5nM library in 100μl volume. This prepared megapool was sent to Radboudumc Diagnostic Department (Radboudumc, The Netherlands) where each library was sequenced by paired-end sequencing on the NovaSeq 6,000 platform (Illumina, California, United States) using SP reagent kits v1.5 (300 cycles).

2.5.2.7. Variant Calling and Annotation

All the reads which were generated by the NovaSeq 6,000 run were converted into raw sequencing data files (FASTQ) using bcl2fastq (v2.20). These files were subsequently processed using a bioinformatics pipeline developed in-house (Radboudumc), as described previously (Khan et al. 2019). According to which the random identifiers were removed from the sequencing reads and added to the read identifier for later use. After exclusion of duplicate reads, the remaining reads were added to patient specific BAM files based on the index barcoding system. In order to determine the overall average smMIPs coverage, forward and reverse read were combined and subsequently divided by two.

2.5.2.8. Average Coverage per Nucleotide

In order to determine the coverage per nucleotide in sequencing run, the base calls of reads which aligned to a reference sequence were calculated in BAM files corresponding to individual probands using the 'pileups' function of SAMtools (Li et al. 2009a). The following parameters were used to obtain data: minimum mapping quality = 0, minimum base quality = 12, anomalous read pairs were discarded, overlapping base pairs from a single paired read as a depth of 1 were counted. For each nucleotide position, an average coverage per nucleotide was generated across all the samples which were sequenced in a single run, followed by an average coverage for all genes/loci targeted in the panel. Coverage plots for all reads across each gene/locus were generated. The average coverage per nucleotide was used to assess whether regions were poorly covered (≤10 reads), moderately covered (11-49 reads), or well-covered (≥50 reads).

2.5.2.9. Variant Analysis and Classification

All SNVs and indels were prioritized on minor allele frequency in gnomAD (Karczewski et al. 2020) V2.1.1 (MAF ≤0.5 for autosomal recessive IRD genes and MAF ≤0.1 for autosomal dominant IRD genes) and in house cohort of Radboudumc (consisting of ~24,488 WES from varying clinical phenotypes). Remaining variants were prioritized by their predicted effect on protein i.e., stop gain, stop loss, frameshift, nonsense and in frame indels. Missense variants were prioritized to meet the criteria using *in silico* tools, predicting pathogenicity of the coding and non-coding variants (CADD-PHRED (Rentzsch et al. 2019) score ≥15; Grantham score (Grantham 1974) ≥80; PhyloP (Pollard et al. 2010) ≥2.7; SpliceAI (Jaganathan et al. 2019) ≥0.2) using an automated Franklin Genoox Platform (https://franklin.genoox.com/clinical-db/home). CNV analysis was performed manually based on the average coverage per smMIPs in the particular run as previously reported (Khan et al. 2020). Regions were considered deleted or duplicated if six or more consecutive smMIPs showed normalized coverage across all samples ≤0.65 or ≥1.20 respectively and if suspected, deletions and duplications were confirmed in visualized BAM files using Integrative Genomics Viewer (IGV) software V2.4. Segregation analysis was performed for all class 3-5 variants according to ACMG guidelines (Richards et al., 2015).

2.5.2.10. PCR-based Genome Walking

To identify the breakpoints of a large deletion spanning exon 50-58 of *USH2A* (NM_206933.4) observed in the smMIPs data (CNV analysis), PCR-based genome walking was performed. Seven forward primers 2kb apart were designed in the region flanking upstream to the first intact smMIPs and 6 reverse primers 2kb apart were designed in the region downstream to the last intact smMIPs between the deleted region. PCR was performed with different combinations of primers using Q5 high-fidelity polymerase (New England BioLabs, USA) with standard protocols. A product of approximately 3kb was subjected to amplicon based long read sequencing using Single Molecule Real-Time Sequencing (Pacific Biosciences) as previously described (Te Paske et al., 2022).

2.5.3. Exome Sequencing (ES)

Exome sequencing was performed on the probands of three families (A4-A6) with glaucoma. The exonic libraries either were prepared using the SureSelect Human All Exon V6 kit (Agilent Technologoes, Santa Clara, CA, USA), the TruSeq DNA exome kit (Illumina Inc, San Diego, CA, USA) or the Baylor College of Medicine Human Genome Sequencing Center VCRome 2.1 design (42Mb Nimblegen). 100bp paired-end sequencing was performed on a HiSeq2500/ 4000/ 2000 instrument (Illumina Inc, San Diego, CA, USA). The generated fastq files were aligned to the human reference sequence (hg19) using Burrows–Wheeler Aligner (BWAv0.5.9) (Heng Li, 2009) with default settings of allowing two mismatches. The variants were called using Genome Analysis Toolkit (McKenna et al., 2010).

2.5.3.1. Variant Annotation and Analysis

The variant call file (VCF) was annotated using wANNOVAR (Chang and Wang 2012) by keeping default settings. The variants were prioritized on the basis of exonic function in their respective genes and selected the variants with effect of stop gain, stop loss, frameshift, in-frame indels and canonical splice site variants. Further rare SNVs were selected on the basis of minor allele frequency (MAF<0.01) in public databases such as1000 genomes (Genomes Project et al., 2015) and Exome Aggregation Consortium (ExAC) (Karczewski et al., 2017). The pathogenic variants predicted "damaging" through tools such as MutationTaster (Schwarz et al., 2014), SIFT (Sorting Intolerant From Tolerant) (Ng and Henikoff, 2003), PolyPhen-2 (Adzhubei et al., 2010), PROVEAN (Choi and Chan, 2015) and CADD-PHRED score ≥15 (Rentzsch et al., 2019) were prioritized. Lastly the variants in the known and candidate genes of glaucoma were selected. For the selected variants, segregation analysis was performed among all the available members of respective families. For the identified pathogenic missense variants in glaucoma families, the 3-D structure of mutated proteins was predicted with Phyre2 online tool (http://www.sbg.bio.ic.ac.uk/phyre2/index.cgi) and structures were analysed in Jmol (version 2.1).

2.5.4. Genome Sequencing (GS)

WGS was performed at BGI (Hongkong, China) on a BGISeq500 using a 2×100bp paired-end reads, with a minimal median coverage per genome of 30-fold. WGS read

mapping to GRCh38/hg38 and annotation of all SNVs, CNVs, and SVs using an in-house pipeline (Radboudumc) were performed as previously described (de Bruijn et al., 2022; Fadaie et al., 2022). Single nucleotide variants (SNVs) were called using GATK Haplotype Caller (Van der Auwera et al., 2013) whereas copy number variants (CNVs) and structural variants (SVs) were called through Canvas Copy Number Variant Caller (Roller et al., 2016) and Manta Structural Variant Caller (Chen et al., 2016), respectively.

2.5.4.1. Variant Prioritization

All variants including SNVs, SVs and CNVs were analyzed. SNVs were considered with a MAF ≤0.01 in public database gnomAD (Karczewski et al., 2020) (v3.1.2) and the in-house genome database of the Radboudumc (containing ~ 1400 alleles). Variants with effect of stop gain, stop loss, frameshift, in-frame indels and canonical splice site were selected. Missense variants were selected with CADD-PHRED (Rentzsch et al., 2019) score ≥15 or REVEL (Ioannidis et al., 2016) score ≥0.3. Putative causative non-coding variants were selected with SpliceAI (Jaganathan et al., 2019) score ≥0.2 (default setting; upstream and downstream 50 bp). SVs and CNVs were prioritized with the MAF ≤0.01 in population database 1000G (Genomes Project et al., 2015).

Eventually, all prioritized homozygous and compound heterozygous SNVs, SVs and CNVs were assessed with an initial focus on currently known IRD-associated genes according to Retnet (https://web.sph.uth.edu/RetNet/) database and the VISION DISORDERS GENE PANEL DG 3.5.0 (BLIND_DG350.aspx (radboudumc.nl)) for IRD families. While for A/M families, all prioritized homozygous and compound heterozygous SNVs, SVs and CNVs were prioritized on the basis of candidate genes and genes already known to be associated with syndromic and non-syndromic A/M enlisted in OMIM (Manually curated list of 147 genes). All the prioritized variants were subjected to segregation analysis where possible (primers used are listed in table 2.1).

2.6. *In vitro* Minigene Splice Assay

The potential splice-altering effect of a deep-intronic PXDN (NM_012293.3) variant located in intron 17 was assessed using a minigene splice assay.

2.6.1. Amplification of Gene Fragment

A 693bp region of intron 17 was amplified using Q5 high-fidelity polymerase (New England BioLabs, Ipswich, MA, USA) from genomic DNA obtained from individuals V:4 (affected-mutant) and III:1 (normal-wildtype) of family B3. The primers for amplification were designed with attB1 and attB2 tags at the 5' ends to allow Gateway cloning (primers given in the table 2.1).

Reagents	Quantity
• Q5 Buffer	10µl
• 10mM dNTPs	1µl
• 5µM Forward Primer	2.5µl
• 5µM Reverse Primer	2.5µl
• DNA template (50ng/µl)	3µl
• Q5 polymerase	0.5µl
• Nuclease free Water	30.5µl
• Total Reaction Volume	50µl

The PCR was completed with an initial denaturation of DNA at 98°C for 30 seconds and then followed by 35 cycles which included steps such as the denaturation at 98°C, annealing at 63°C and elongation at 72°C for 10 seconds, 20 seconds and 1 minutes respectively. Finally, at 72°C, the extension was given for 5 minutes.

After completion of the PCR the product was run on 0.8% agarose gel to verify the presence and size of fragments. The desired size of the band was cut from the gel and gel purified initially using the protocol as explained earlier in section 2.5.1.3. and latter purified with AmpureXP beads by using protocol explained in section 2.5.2.5.

2.6.2. BP Gateway Cloning

For the BP reaction, following reagents were mixed in a 1.5mL microfuge tube kept on ice.

Reagents	Quantity
• BP Buffer	2µl
• pDONR 201 vector (150ng) (Invitrogen)	1µl
• BP enzyme	2µl
• PCR product (100ng/µl)	3µl
• Milli Q water	2µl
• Total Reaction Volume	10µl

The tube containing above mixture was incubated on a heat block for 2-18 hours at 25°C. After incubation, 1µl of the protein kinase was added to the mixture and incubated at 37°C for 10 minutes to stop the reaction.

2.6.3. Transformation of BP Clone

2.6.3.1. Preparation of LB Agar

LB agar was prepared by mixing 20.0g of ready to use LB and 15.0-16.0g of agar in 1000ml or 1 liter of distilled water. The agar was dissolved thoroughly by shaking and heating in microwave oven for 2 minutes. After mixing, in a conical flask 100ml medium was taken, covered with cotton plug and then wrapped properly with aluminium foil. The medium was then autoclaved at 15 atmospheric pressure and 121°C for 15 minutes. For antibiotic screening, 1 ml of kanamycin (5mg/ml) was added in the flask containing 100ml LB agar before pouring the plates and mixed well by shaking. Kanamycin was added when media cooled down to 50-60˚C.

The agar media after autoclaving was allowed to cool down to 45ºC roughly and then poured in the disposable electron beam sterilized Petri-plates (Hundai Micro Co., Korea) in the laminar air flow hood while following all antiseptic conditions. After solidification, the plates were placed inverted for overnight in the incubator at 37˚C to screen out any contamination.

2.6.3.2. Transformation

The following steps were performed for transformation:

1. Took commercially available DH5α cells (50µl) in 1.5ml microfuge tube and thawed them on ice.

2. Then added 2µl of the BP reaction mixture into 50µl of the cells, tapped gently and placed back on ice for 30 minutes.

3. The tube was then placed in a water bath at 42°C for 45 seconds to provide heat shock to the cells. After heat shock, tubes were immediately placed back on ice for 2 minutes.

4. Added 250µl of SOC medium to the mixture (through the wall of the tube and not directly on the cells). Incubated the mixture at 37°C in a shaker for 2 hours.

5. Poured 150µl of the above mixture on kanamycin containing plates (two different plates for complete 300µl volume) and spread the mixture using glass beads.

6. Plates were then incubated at 37°C for 20-24 hours.

2.6.3.2.1. Preparation of LB

LB broth was prepared by mixing, 20.0g of ready to use LB in 400ml of distilled water and raised the final volume to 1000ml. Mixture was shaken vigorously to allow proper mixing and was poured in conical flasks in measured quantity ranging from 25 to 50ml. The flasks were covered with cotton plug, and were wrapped with aluminium foil. Autoclaving was then done at 15 lb/ inch^2 pressure and 121°C temperature for 15 minutes.

2.6.3.2.2. Inoculation of LB media

After overnight incubation, 4 colonies were selected from plates (both from mutant and wildtype BP clones) and inoculated in 3ml of LB media supplemented with 3µl of kanamycin in 10ml tubes. Colonies were picked with pipette tips and put the tips directly in 10ml tubes. The tubes were then incubated at 37°C for overnight.

2.6.3.3. Nucleospin Plasmid Easypure

After completion of incubation, growth was seen in the media and the culture were subjected to plasmid isolation using Nucleospin Plasmid Easypure kit (Macherey-Nagel, Germany). The following steps were performed for plasmid isolation:

1. Poured 2ml of each sample in 2ml Eppendorf tube and centrifuged for 3 minutes at 120 RPM to pellet down the cells.
2. Then 150µl of the buffer A1 was added in the pellet and vortexed to re-suspend the cells completely.
3. Added 250µl of buffer A2 and inverted the tube 4-5 times, incubated at room temperature for 2 minutes to lyse the cells.
4. After this 350µl of buffer A3 was added and inverted the tubes until the lysate turned colourless. Then centrifuged at full speed for 3 minutes to pellet down the precipitates.
5. Placed nucleospin plasmid easypure column into a 2ml collection tube and loaded 700µl clear supernatant onto the spin column without disturbing the pellet.
6. Centrifuged the column for 1 minute at 6000g and discarded the flow-through.
7. Added 450µl of buffer AQ to the spin column and centrifuged for 1 minute at full speed. Discard the flow-through and centrifuged the empty column once again to completely dry the spin column.
8. Discarded the collection tube and placed the spin column into a clean labelled 1.5ml microfuge tube.
9. Added 50µl of the Milli Q onto the filter membrane of the column and incubated at room temperature for 5 minutes.
10. Centrifuged for 1 minute at full speed.

2.6.3.4. BP Plasmid Validation

About 150-200ng of the isolated plasmid was run on the 0.8% agarose gel against empty pDONR 201 vector to confirm the size, along with ladder.

The samples with quality and expected size were selected for second round of validation by restriction digestion. The digestion mix was prepared in 1.5ml microfuge tube as follows:

Reagents	Quantity
• 1X NEB buffer r3.1	2µl

- BP plasmid isolated (~100ng/µl)   2µl

- BsmBI enzyme   0.5µl

- Milli Q water   5.5µl

- Total Reaction Volume
                                                                                                             10µl

Incubated the above mixture at 37°C for 1 hour. The mix was then run on 1% agarose gel to see the expected band pattern. The BP clone was then linearized and product was subjected to amplicon based long read sequencing using Single Molecule Real-Time Sequencing (Pacific Biosciences) on a Sequel II system as previously described (Te Paske et al. 2022). After confirmation, both wildtype and mutant BP clones were subjected to LR cloning.

2.6.4. LR Gateway Cloning

The LR gateway cloning is almost same as BP cloning, with the difference that instead of PCR product BP clone is used as an insert. The following LR reaction mixture was prepared in 1.5ml microfuge tube.

Reagents	Quantity
• LR Buffer	2µl
• pCl-neo *RHO* vector (150ng)	1µl
• LR enzyme	2µl
• BP clone (100ng/µl)	3µl
• Milli Q water	2µl
• Total Reaction Volume	10µl

Incubated the tube containing above mixture for overnight at 25°C. After completion of incubation, 1µl of protein kinase was added to the mixture and incubated for 10 minutes at 37°C for enzyme inactivation.

After completion of LR gateway cloning, the reaction mix was used for transformation and plasmid isolation as explained previously in sections 2.6.3.2. and 2.6.3.3. respectively.

2.6.4.1. LR Plasmid Validation

About 150-200ng of the isolated plasmid was run on 0.8% agarose gel against empty pCl-neo *RHO* vector to confirm the size, along with the ladder. The samples with quality and expected size were selected for second validation by restriction digestion. The digestion mix was prepared in 1.5ml microfuge tube as follows:

Reagents	Quantity
• 1X NEB buffer rCutSmart	1µl
• LR plasmid isolated (~100ng/µl)	2µl
• NdeI enzyme	0.5µl
• Milli Q water	6.5µl
• Total Reaction Volume	10µl

Incubated the above mixture at 37°C for 1 hour. The mix was then run on 1% agarose gel to see the expected band pattern.

2.6.5. Transfection of HEK293T Cells

The LR clones (both mutant and wildtype) which showed best validation results through digestion and concentration were selected for transfection in HEK293T cells.

2.6.5.1. Splitting of HEK293T Cells

All the reagents were used at room temperature. The confluency of the HEK293T cells was observed under microscope. On reaching 70% confluent, medium was removed from the cells using vacuum while holding the flask in a tilted position, in order to avoid disturbance of cell layer. The cells were gently washed with 10ml 1X PBS (phosphate buffer saline) solution. The PBS solution was not directly poured onto cell. After PBS was removed from the flask through pipette, 2ml of trypsin (0.25%) was added over the cells and flask was moved back and forth gently for few times. Then flask was placed in an incubator for few minutes to detach the cells before adding 9ml of DMEM

medium (supplemented with 10% FBS, 1% sodium pyruvate and 1% penicillin streptomycin). Then all the cells stuck to the flask were washed out by pipetting up and down and moving pipette over the whole flask. When all the cells were completely detached from the flask, the whole volume was transferred to a 50ml falcon tube. Again, pipetted up and down the cells at least 50 times to remove all the clumps, this was our fresh stock of cells.

2.6.5.2. Seeding of HEK293T cells

The seeding of the cell was performed in 6 well plate for transfection. The cells and DMEM medium were added in the ratio of 1:6 in each well of the plate. For this, 3ml of the cell stock was added in 15ml of DMEM medium to make a final volume of 18ml in a 50ml falcon tube. In each well 2ml of the mixture of cells and DMEM medium was added in a way to avoid bubble formation. After seeding cells were left to grow for 24 hours at 37°C in an incubator.

2.6.5.3. Transfection

In three 1.5ml microfuge tubes, transfection reagent was mixed with prepared clones. In first tube, 90µl of PEI transfection reagent was mixed with 500ng of wildtype clone, in second tube, 90µl of PEI was mixed with 500ng of mutant clone while in the third tube only 90µl of the PEI reagent was added. These three tubes were incubated for 10 minutes at room temperature. The 6 well seeded plate was taken out of the incubator and confluency of the cells was observed under microscope. The transfection was performed when cells reached 70% confluent. The medium of the cells was replaced by fresh DMEM medium and transfection mixture was added slowly and dropwise in 3 different wells. Placed the plate in the incubator at 37°C for 24 hours.

2.6.5.4. Harvesting of Cells

After 24 hours of incubation, plate was taken out from the incubator, cells were observed under the microscope. The medium was removed from all wells. The cells were washed carefully by adding 1ml PBS through walls of the well, moved it carefully all over the well and pipetted it out from the well. After this, 1ml of PBS was added again over the cells to detach them from the well. Washed the cells and moved the PBS all over the cells until they are detached from the well. After detaching the cells, they

were put into the 1.5ml tube and placed on ice. This process was done for four wells (wildtype, mutant, PEI treated and empty HEK293T cells).

2.6.6. RNA Extraction from Cells

The harvested cells were then centrifuged for 5 minutes at maximum speed and supernatant was removed. The RNA was extracted from the pelleted cells using NucleoSpin RNA extraction kit (Macherey-Nagal, Germany) with following protocol:

1. To the pelleted cells, 350µl of the buffer RA1 and 3.5µl of ß-mercaptoethanol was added and vortexed vigorously for cell lysis.

2. The lysate was then filtered through NucleoSpin filter (violet ring). For this, filter column was placed in the 2ml collection tube and lysate was poured on the filter.

3. The column was then centrifuged at 11,000g for 1 minute.

4. The filter column was discarded and 350µl 70% ethanol was added to the filtrate. The mixture was then homogenized by pipetting up and down several times.

5. For binding the RNA to column, the NucleoSpin RNA column (light blue ring) was placed in the new 2ml collection tube. The lysate was then loaded onto this column. The column was then centrifuged for 30 seconds at 11,000g. Discard the flow-through and placed the column into new 2ml collection tube.

6. After this, 350µl of MDB (membrane desalting buffer) was added onto the column and centrifuged for 1 minute at 11,000g.

7. DNase reaction mixture was prepared in a sterile 1.5ml microfuge tube by adding 10µl of reconstituted rDNase and 90µl of reaction buffer for rDNase. The mixture was homogenized by flicking the tube. Added 95µl of this mixture directly onto the center of the membrane of column. Incubated the column at room temperature for 15 minutes.

8. Then for washing and inactivation of rDNase, 200µl of the buffer RAW2 was added to the column and centrifuged the column for 30 seconds at 11,000g.

9. After this the collection tube was replaced by new collection tube and 600µl of the buffer RA3 was added onto the spin column and centrifuged for 30 seconds at 11,000g.

10. Again washed the column with 250µl of the buffer RA3 and centrifuged at 11,000g for 2 minutes to completely drying the column.

11. The collection tube was replaced by new clean nuclease free 2ml tube. Eluted the RNA in 60µl RNase free water (available in the kit) and centrifuged at 11,000g for 1 minute.

2.6.7. cDNA Synthesis

The extracted RNA was quantified with nanodrop and calculated the volume of each sample needed to make 1µg cDNA.

Required volume of RNA = 1000/ [C].

C= Conc. of extracted RNA (ng/µl).

The cDNA synthesis was performed using iScript cDNA synthesis kit (Bio-Rad, USA) with the following protocol:

Reagents	Quantity
• Reverse transcriptase Buffer	1µl
• Reverse transcriptase enzyme	4µl
• RNA	1000/[C]
• Nuclease free water	Up to 20µl
• Total Reaction Volume	20µl

The above mixture was prepared in 0.2ml sterilized tube and placed in the thermocycler for reverse transcription at 25°C for 5 minutes, 46°C for 20 minutes, 95°C for 1 minute and at 4°C to hold.

2.6.8. Amplification of Splice Isoforms

The prepared cDNA libraries were then amplified using AmpliTaq gold master mix (Thermo Fisher Scientific, USA), with protocol as described in section 2.5.1.2. The primers used are listed in table 2.1. The amplified products were then run on 2% agarose

gel and the bands were gel purified as described earlier in section 2.5.1.3. The purified products were then Sanger sequenced to observe the splicing pattern.

Table 2.1: List of all primers designed and used for this study

Primers used for Targeted Sanger Sequencing	
Primer ID	**Primer Sequence (5'-3')**
*MYOC*_Ex1 F	CCAAACAGACTTCTGGAAGGTTA
*MYOC*_Ex1 R	GTGATCGCTGTGCTTTCCTTA
*MYOC*_Ex2 F	ACACCATATCTTTGGGAGCCTA
*MYOC*_Ex2 R	CTCTGCTCCCAGGGAAGTTAAT
*MYOC*_Ex3 F	AACAGCCCTACTACCCAAAACA
*MYOC*_Ex3 R	ACCATGTTCATCCTTCTGGATT
*TEK*_Ex2 F	GGCACATGGTCAGAATAGCA
*TEK*_Ex2 R	GACAGGCAAGATCGTCAAGC
*TEK*_Ex3 F	AGCCACCACTGTTTTTCACC
*TEK*_Ex3 R	TGAAAGCTTGCATCATAGCAG
*TEK*_Ex4 F	TCATGTGTTTGGTGGTAGATCC
*TEK*_Ex4 R	TGGGTTTCTCTGTCATTCCTCT
*TEK*_Ex5 F	CTCCTTGTCTTTGTTTCTGTCG
*TEK*_Ex5 R	CACACACAGGTACCATCTGACC
*TEK*_Ex6 F	CAGCTGAGATTTGACTGTTTCC
*TEK*_Ex6 R	GGGTAGCTAAGCAGTCCAGGTA
*TEK*_Ex7 F	CCCCTACCTTACACAAATCAGC
*TEK*_Ex7 R	CTATTCCCAACTTCTGGATGGA
*TEK*_Ex9 F	ACAACAGCAGGATCTGACAGG
*TEK*_Ex9 R	GCCACCCACAAGATTATGAGC
*TEK*_Ex12 F	GGAAGTCACACTCATCAACCAA
*TEK*_Ex12 R	GGGGCACTAATTAGCCTTCTCT
*TEK*_Ex14 F	GGCTGCTGTTAAGTTCCCATTA
*TEK*_Ex14 R	GAAAGCCAAAGAGAAGATGAGG
*TEK*_Ex17-18 F	GGTGGTGTTGCTAGATGTGTTT
*TEK*_Ex17-18 R	CACATGACAGTGCCTTCTTCAT
*TEK*_Ex21 F	CCTCTCTTGCCATACCATGTCT
*TEK*_Ex21 R	TTGGGATCTCTGTGTGTAGGTG
*TEK*_Ex22 F	CCTAGGGGCTGTACTTTGGTTA
*TEK*_Ex22 R	GGAGGGACATCCTTTGTTTCTA
*LTBP2*_Ex1 F	GAGCCCAGCTGGAGTAGGAG
*LTBP2*_Ex1 R	GGCTGTTTCCCGAAGTACTAAA
*LTBP2*_Ex6 F	AGGCAGGGGCTGGTTATTAT
*LTBP2*_Ex6 R	GGCTGAGAAGTTGAGGGAATG
*LTBP2*_Ex7 F	GGCTCCTTCAGTGACAGAGTTT
*LTBP2*_Ex7 R	AGGCCCAGACTCTCCATACAT
*LTBP2*_Ex36 F	GCCTCTGGCTGTCACACTTAG
*LTBP2*_Ex36 R	GCTGAAGCATTAAAGCGATTG

*CYP1B1*_Ex2 F	TCTTCTCCAAGGGAGAGTG
*CYP1B1*_Ex2 R	GATCTTGGTTTTGAGGGGTGG
*CYP1B1*_Ex3 F	AGTCATGCAAGGCCTATTACAG
*CYP1B1*_Ex3 R	TGAGAAGCAGCACAAAAGAGG
*FOXE3*_Ex1 F	GGGTACCGTGAACAGAGTAAG
*FOXE3*_Ex1 R	TGTAGCAGGAGTTTGAGTCCAG
Primers for Segregation Analysis	
Primer ID	**Primer Sequence (5'-3')**
*PXDN*_Int 17 F	GTCCACACCTTTTCCCAGAG
*PXDN*_Int 17 R	GCTAGGTCCCTGGTAAAGAAG
*VSX2*_Ex2 F	ACGAAATCTGTTCAAAACCTCCG
*VSX2*_Ex2 R	CTCATCCTGCTCAACCGGTG
*PXDN*_Ex17 F	GGAGTTCATGAGCAGCGAAG
*PXDN*_Ex17 R	GAATGGCTTCAACACCCCTC
*SIX6*_Ex1_F	CAATCCGCCTCATCAACAAGC
*SIX6*_Ex1_R	GTGAAGCCTTGGTTTGGTGAC
*ATOH7*_Ex1 F	TGAAGAGATATCAGCCTGGTCA
*ATOH7*_Ex1 R	AAATGATTGCGTCCATAGGTCT
*NMNAT1*_Ex2 F	TTGGTATGTGCCTGTGTTCC
*NMNAT1*_Ex2 R	GATGGTGTCTTGCTCTGTCTC
*TULP1*_Ex14 F	AGCCATCTCAGCCATCTC
*TULP1*_Ex14 R	CTTGAATGAAGGTCAGCATC
*PRPF8*_Ex43 F	CAACACAAGCACAGACAGAGG
*PRPF8*_Ex43 R	GATGTGGGGATAGCAGTAGGG
*CDHR1*_Ex9 F	AGAGGAGAGTAGGGCCATGC
*CDHR1*_Ex9 R	AGCACACAACCCAGAGACTTG
*HGSNAT*_Ex18 F	TCTCGAACTCCTGGCCTTAAG
*HGSNAT*_Ex18 R	CACCCATGGCAATTCCCTTTTG
*PROM1*_Ex15 F	TCTAGTTATAAGTTGGAAATCAACCAG
*PROM1*_Ex15 R	AAATGCAAAATTCTCATTCCAG
*TULP1*_Ex9-10-11 F	CCAGAGCCTCCTAACTTGG
*TULP1*_Ex9-10-11 R	CACAGCAGGACAGAGATGAC
*MERTK*_Ex2 F	CAGTGCTCTCTCTTCTTGGC
*MERTK*_Ex2 R	GAGGTGGAGGTTGCAATGAG
*CNGB1*_Ex26 F	TGCACAACATGCATCTATCAG
*CNGB1*_Ex26 R	ACATTCTGGCAACAGTGG
*CNGA3*_Ex7a F	GTGGGTGTTCTGATTTTTGC
*CNGA3*_Ex7a R	CCCAATATCTCCCTTCTTGC
*CNGA3*_Ex7b F	GCATACTGTGTAGCCGTGAGG
*CNGA3*_Ex7b R	CCGTGAGGCATTCATATTCG
*CNGA3*_Ex7c F	GTGGGTGTTCTGATTTTTGC

*CNGA3*_Ex7c R	CCCAATATCTCCCTTCTTGC
*CDH23*_Ex36 F	GATATCCTAGCCCCGGAAC
*CDH23*_Ex36 R	CACCTCAACTACCTCCTCCTG
*CDH23*_Ex53 F	TCCACATCTTCTGGCACTCTG
*CDH23*_Ex53 R	GGCAAAGATTTCTCCCAGAGG
*DMD*_Ex51 F	TGTGTTTGCTGAGAGAGAAAC
*DMD*_Ex51 R	TTGTCCAGGCATGAGAATGAG
*ABCA4*_Ex11 F	GGAGATGTGAAGAGGAAACCG
*ABCA4*_Ex11 R	CATGGACTTGGGGAAATGGG
*LZTFL1*_Int4 F	CTCTTTGCATTCTTGAGACCC
*LZTFL1*_Int4 R	GGGATTGTAGAAGATGGCACC
*LZTFL1*_Ex10 F	GTCCAACGTTTATCTTAGCCAC
*LZTFL1*_Ex10 R	TGGCATGCACACAAAACATAC
*COL18A1*_Ex16 F	GTTGTGTTTCTGTGTGGCTG
*COL18A1*_Ex16 R	CTCATTCGCTCTTGGTCAGG
*NDP*_Ex1 F	TCACGGGGTCAACTATAAGAAC
*NDP*_Ex1 R	CGCACGCCTGATTGATATATG
Primers for Splice Assay	
Primer ID	**Primer Sequence (5'-3')**
*PXDN*_(Int17) F	ggggacaagtttgtacaaaaaagcaggcttcTCCCAGATGATTCTCTCTTTTGC
*PXDN*_(Int17) R	ggggaccactttgtacaagaaagctgggtgAGCTCTAAGATGTCCCCTGG
*ACTB*_Ex4-5 F	ACTGGGACGACATGGAGAAG
*ACTB*_Ex4-5 R	TCTCAGCTGTGGTGGTGAAG
*RHO*_Ex3-5 F	CGGAGGTCAACAACGAGTCT
*RHO*_Ex3-5 R	AGGTGTAGGGGATGGGAGAC
Primers for Deletion Mapping	
Primer ID	**Primer Sequence (5'-3')**
*USH2A*_Int49_P1 F	TTCAAACACCTCCCTCTCAAC
*USH2A*_Int49_P2 F	AGTTTTGCTCTTGTTGCCCAG
*USH2A*_Int49_P3 F	AATGGTCCCAAATCCTGTTGC
*USH2A*_Int49_P4 F	AACATGACCAAGACACTCAGC
*USH2A*_Int49_P5 F	CAGGGAGTGGCAGTAGGATG
*USH2A*_Int49_P6 F	CGGTTTCCAGCTTCATCCATG
*USH2A*_Int49_P7 F	ATCTCTGTTCTATCCCATTGGTC
*USH2A*_Int58_P1 R	CATCAACCTTGCTCATCACCC
*USH2A*_Int58_P2 R	TGAGGTAAGGCAGAGAAGGAG
*USH2A*_Int58_P3 R	AGCTGGTAAAAGGTGAGAGGG
*USH2A*_Int58_P4 R	GCGTTCCCTCCAATTCATCTG
*USH2A*_Int58_P5 R	CCCTGAACTGGAAAAGGTGTG
*USH2A*_Int58_P6 R	TCACAAGGTCAGGAGATGGAG
Primers for *USH2A* Deletion Segregation	

Primer ID	Primer Sequence (5'-3')
*USH2A*_S1 F	AGCACTCAGTTAACGTGACAC
*USH2A*_S1 R	ACGGTGTTTGGTTCTTTGTCC
*USH2A*_S2 F	AGCACTCAGTTAACGTGACAC
*USH2A*_S2 R	GCAAGGCATATTCAGAGAAGGG

Ex= Exon, Int= Intron, F= forward, R= Reverse.
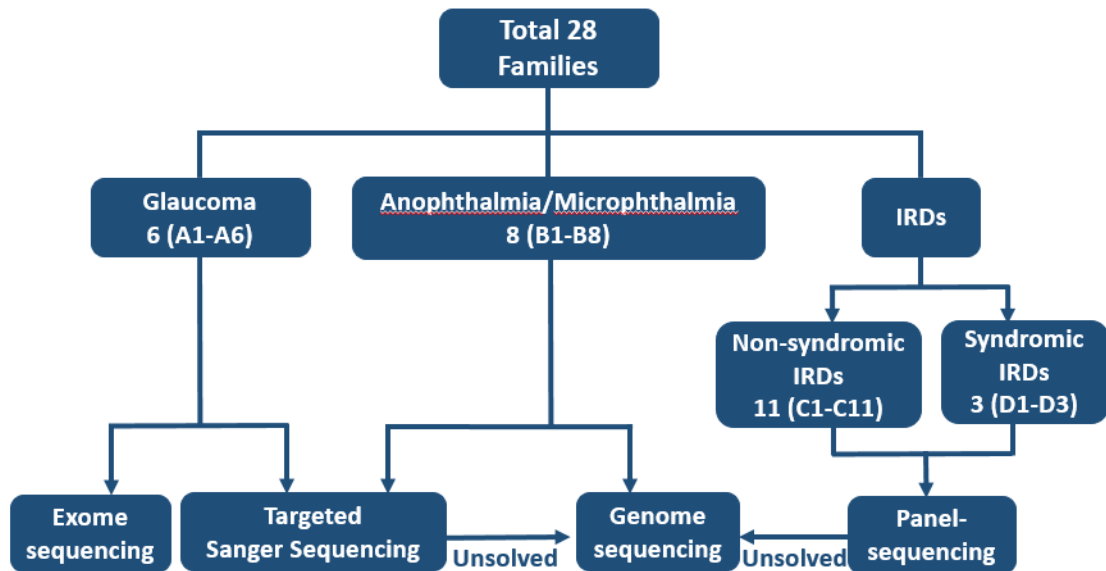
Figure 2.1: Flow chart showing sequencing approaches used for all the families recruited in this study.

RESULTS AND DISCUSSION

For this study 28 Pakistani families were recruited from different regions of Pakistan. The analysis of clinical information gathered from these 28 families led to their further subgrouping in to four types. First group included six families (Family A1 to A6) with primary congenital glaucoma whereas eight families (Family B1 to B8) in the second group presented anophthalmia/microphthalmia phenotype. Eleven families (Family C1 to C11) presented phenotype in the IRD spectrum whereas patients from three families (Family D1 to D3) presented syndromic IRDs. Therefore, results section has been divided into four sections (Chapter 3 to 6) to present data of each phenotypic group.

Available members of 28 families underwent genetic analysis as summarized in methods chapter and graphically depicted in figure 2.1. Details of the identified disease-causing variants are provided in respective sections along with their segregation patterns in other members of the family. The figures, diagrams and tables are given in each segment and a comprehensive conclusion of the findings of this study is provided with the focus on the success rate of different molecular diagnosis approaches.

3.0.PRIMARY CONGENITAL GLAUCOMA

Primary congenital glaucoma (PCG) is a birth defect which is characterized by several features including enlarged globe (buphthalmos), increased IOP, breaks in Descemet membrane (Haab striae) and optic nerve cupping. This leads to early irreversible blindness (Azmanov et al., 2011). In PCG mostly Schlemm canals are not blocked because blood flow is sufficient even after compression of jugular vein. The features of glaucoma are overlapping with megalocornea therefore the identification of glaucoma is clinically challenging. There are certain distinguishing features of megalocornea like absence of Descemet membrane breaks and corneal edema. PCG mostly exhibits autosomal recessive pattern of inheritance with a high frequency of parental consanguinity. According to an estimate most cases of PCG are sporadic but 10-40% cases are familial (Abdolrahimzadeh et al., 2015). Most frequently mutated genes in PCG include *CYP1B1, LTBP2, MYOC* and *TEK* (Aboobakar and Wiggs, 2022). Although the number of genes known to be associated with PCG is limited but the overlapping features of PCG with other forms of glaucoma makes it difficult to select genes for TSS. In this chapter we present genetic analysis of six families with PCG.

3.1. Description and Clinical Features of PCG Families

 Based on the physical appearance (buphthalmos and corneal clouding) and phenotype (vision loss, poor vision and tunnel vision) 6 families (A1-A6) were recruited from different regions of Pakistan. Four families (Family A1, A2, A4 and A6) were collected from Islamabad while two families (Family A3 and A5) belonged to Larkana and Pakpattan cities respectively. Pedigree analysis showed consanguinity among all parents of affected individuals and autosomal recessive mode of transmission of phenotype (Figure 3.1). The glaucoma was initially detected in affected individuals of six families between ages of 2 to 6 years. All recruited affected individuals have bilateral PCG, but bilateral corneal opacity was observed in affected members of three families (Family A2, A4 and A5). Similarly, cataract (Family A1 and A4) and epiphora (Family A1 and A5) were observed in two families each. Phenotypic features observed in affected members of all 6 families are presented in table 3.1.

3.2. Genetic Analysis of Families with PCG

As described in methods families with PCG were subjected to either TSS or ES to identify underlying variants. One affected member from each of three families (Family A1, A2 and A3) was screened through TSS to detect pathogenic mutations in *CYP1B1, MYOC* coding regions and selected exons of *TEK* and *LTBP2* genes. Sequence analysis identified a missense variant (NM_000104.4:c.1169G>A; p.(Arg390His)) in *CYP1B1* in two (Family A1 and A3) families (Figure 3.2, 3.3). In the third family (Family A2) a missense mutation (NM_000104.4:c.353C>T; p.(Pro118Leu)) was also identified in *CYP1B1* (Figure 3.4).

For the remaining three families (Family A4, A5 and A6) single proband (IV:3, IV:3, IV:2) from each family was selected for exome sequencing as described earlier in section 2.5.3. The VCF annotation indicated 28789, 29312 & 29598 variants in individuals A4-IV:3, A5-IV:3 and A6-IV:2 respectively. After filtration for the rare disease causing variants the number reduced to 30 in case of family A4 individual IV:3 while 22 variants in family A5 individual IV:3. Phenotype based prioritization of the candidate genes through Phenolyzer (http://phenolyzer.wglab.org/#getstart) shortlisted only *CYP1B1* variant in case of both families. Analysis of family A6 individual IV:2 identified 2 rare pathogenic variants; one in *CYP1B1* and the other on X chromosome, since our pedigree is autosomal recessive therefore the involvement of variant present on X chromosome was ruled out. After ES, we identified two known mutations (c.1169G>A; p.(Arg390His)) and (NM_000104.4:c.1325del; p.(Pro442Glnfs*15)) in the probands of families A4 and A5 respectively (Figure 3.5, 3.6). Whereas a novel mutation (NM_000104.4:c.1A>G; p.(Met1?)) was found in family A6 which is predicted to result in loss of initiation codon (Figure 3.7).

All these variants (identified in 6 PCG families) were predicted to be pathogenic through various bioinformatics tools and likely pathogenic according to guideline of American College of Medical Genetics and Genomics and Association for Molecular Pathology (ACMG/AMP) (Richards et al. 2015) (Table 3.2) except for novel variant (c.353C>T; p.(Pro118Leu)) which was found in family A2. Additionally, a haplotype was identified in all PCG families on the basis of six common single nucleotide polymorphisms (SNPs) (rs2617266, rs10012, rs1056827, rs1056836, rs1056837 and

rs1800440) present in *CYP1B1* (Table 3.3). All the *CYP1B1* variants segregated in their respective families.

3.3. Protein 3D Modelling of CYP1B1 Predict Changes in Mutant Protein

The analysis of 3D structure of protein having missense variants identified in six families included in this study predicted abnormalities in the respective mutant protein. The analysis of missense variant (NM_000104.4:c.1169G>A; p.(Arg390His)) identified in 3 families (A1, A3 and A4) showed substitution of arginine at position 390 with histidine. This Arg at position 390 is highly conserved among several species (Figure 3.8B). This substitution alters the distances between nearby amino-acid side chains as compared to normal protein. Normal Arg390 is thought to form a salt bridge and H-bonding with Glu387 in the conserved K-helix (Stoilov et al. 1998; Su et al. 2012). Salamanca Viloria et al., (2017) identified the optimal cut off distances to be 5Å or 0.5nm between two amino acid residues to influence each other's bonding in the field. When arginine is replaced with histidine in protein 3D structure, imidazole ring in the latter showed more bend towards Asn428 residue than Glu387 in the K-helix. The distance between His390 and Glu387 will probably increase to 0.539nm as compared to normal 0.293nm between Arg390 and Glu387 (Figure 3.8A). This increased distance may result in escape of Glu387 from the influence of His390 compared to normal R390 and thus expected to alter the normal interactions in the CYP1B1 protein and eventually may disrupt the normal function.

Similar proline at 118 position in CYP1B1 protein is highly conserved among several species (Figure 3.9B) and the predicted 3D structure analysis of p.(Pro118Leu) variant identified in family A2 showed increase of length of helices in the surrounding region of Leu118 compared to Pro118. This change may reduce the flexibility and increase the rigidity in the mutant protein structure compared to normal protein. Our predicted protein 3D modelling of the Leu118 indicated that it alters the normal 3D conformation of the protein. The normal length of D, G and K helices in the predicted protein structure is increased with the replacement of proline residue with leucine at 118 position. These conserved helices are carrying several amino acid residues which are important in the formation of active site of the enzyme. Hence the increased length of the helices may result in the loss of flexibility in this region and in turn may affect the active site in this region. Moreover, arginine 117 adjacent to proline 118 is thought to be the part of heme

interaction with enzyme (Wang et al., 2011). The normal amino acid distance between Pro118 and Arg117 is increased in mutant Leu118 and Arg117 (Figure 3.9A). This increased distance may result in escape of bonding effect between amino acids at position 118 and 117 and may affect the interaction of Arg117 with the heme co-factor.

3.4.   Discussion

CYP1B1 gene encodes cytochrome P450 1B1 protein which is involved in steroid metabolism, retinol metabolism and lipid metabolism (Lee et al. 2003; Choudhary et al. 2004). Cytochrome P450 1B1 is expressed in IOP maintaining structures such as trabecular meshwork and ciliary bodies as well as in the iris and retina (Yamazaki et al., 1993). The knockout of *CYP1B1* in mice induced defective trabecular meshwork and increase in the oxidative stress, suggesting the role of *CYP1B1* in glaucoma (Zhao et al., 2015). Previously it was thought that *CYP1B1* mutations and failure of surgical treatments in patients have no significant correlation (Abu-Amero et al., 2011), but a later study (Khafagy et al., 2019), observed that the populations with increased consanguinity and higher rates of *CYP1B1* mutations are more prone to failure of the trabeculectomy and other initial procedures. This indicates that *CYP1B1* has more roles to play in development of glaucoma than its predicted role in development of malformed Schelmm's canal. However, the mechanism through which *CYP1B1* is causing the disease is not understood completely. This study of six PCG families have identified known and novel variants in *CYP1B1*.

In three families (Family A1, A3 and A4) we identified a missense variant (c.1169G>A; p.(Arg390His)) in *CYP1B1* (Figure 3.8B). The arginine present at 390 position is also evolutionary conserved among several species (Figure 3.8B). This variant was first identified in 1998 (Stoilov et al., 1998) in a Pakistani family but is now considered as most common *CYP1B1* mutation in several populations including Indian, Chinese, Iranian and Pakistani. In two different studies conducted in Pakistan, 5 and 13 families identified with this variant respectively has the same haplotype C-C-G-C-C-G; (constructed on the basis of SNPs) around *CYP1B1* gene (i.e. rs2617266, rs10012, rs1056827, rs1056836, rs1056837 and rs1800440) (Sheikh et al., 2014; Rauf et al., 2016). Whereas analysis of genotypes of above mentioned six SNPs in our three families identified different haplotypes in two families. Family A4 showed previously reported haplotype C-C-G-C-C-G while family A1 and A3 have C-C-G-G-C-C and C-

C-G-C-T-G haplotypes respectively (Table 3.3). These differences in the haplotypes are emphasizing on the founder effect of this mutation but further confirmation is required to clarify this notion as it can be a mutational hot spot because two additional allelic variants have also been identified at the same position i.e, p.(Arg390Ser) in Saudi, Spanish, European and Italian populations and p.(Arg390Cys) in Indian, Egyptian and German populations (Bejjani et al., 2000; Reddy et al., 2003; Sivadorai et al., 2008; Campos-Mollo et al., 2009; Weisschuh et al., 2009; Giuffre, 2011; Lopez-Garrido et al., 2013). Although Arg390His variant is commonly known to cause PCG in Pakistani population with early onset indicating the presence of severe phenotype in patients with this variant. There are certain studies which presented the same variant with association to juvenile open angle glaucoma (JOAG) (Yang et al. 2009; Su et al. 2012). This indicates the involvement of Arg390His variant with varying degree of phenotypic expression, however in our three families (A1, A3 and A4) p.(Arg390His) variation is responsible for early onset of severe phenotype with the presentation of buphthalmos. Additionally, cataract and epiphora (watery eyes) was also observed in all the affected members of family A1.

A single nucleotide frameshift deletion observed in family A5 (c.1325del; p.(Pro442Glnfs*15)) replaced proline at 442 position with glutamine and introduces a pre-mature termination codon (PTC). This PTC might not result in non-sense mediated decay (NMD) as it is present in the last exon and there is no exon-exon junction (EEJ) downstream for the binding of exon junction complex (EJC). In our prediction this variant, which we are reporting for the second time in Pakistani population (Rauf et al., 2016), will result in the formation of truncated protein causing loss of function. Cysteine residue at 470 position at the C-terminus is conserved and essential for the binding of heme (co-factor of *CYP1B1*) (Wang et al., 2011) and it will be lost in the truncated protein, rendering it non-functional. Same variant p.(Pro442Glnfs*15) is previously found associated with phenotype showing anterior segment dysgenesis and congenital glaucoma (Reis et al., 2016). Previously reported Pakistani family with the same variant was affected with PCG showing additional features of buphthalmos, corneal haze and photophobia (Rauf et al., 2016). All members affected with PCG in family A5 also showed buphthalmos and corneal opacity without photophobia. The members of family A5 also presented epiphora (watery eyes).

A novel missense variant (c.353C>T; p.(Pro118Leu)), identified in the family A2 will probably replace proline at 118 position with leucine. Previously 2 variants at the same amino acid position (which is residing in the substrate recognition site of the enzyme (Chen et al., 2008)), have been identified with the similar phenotypes. A heterozygous variant P118T (in compound heterozygous state) was found associated with Peter's Anomaly (Vincent et al., 2006) whereas homozygous P118S in Chinese population was found associated with PCG (Chen et al., 2008). According to ACMG/AMP guidelines this variant is a VUS. Several pathogenicity prediction tools predicted deleterious effect of this variant on the protein. This amino acid is present in the evolutionary conserved region among several species (Figure 3.9B). This is a very rare variant, with 0.000004887 allele frequency in previous version of gnomAD (v2.1.1) (one heterozygote in Latino/Admixed American population; allele frequency 0.00003050) while with 0 allele frequency (all population) in the latest gnomAD version (v3.1.1). The absence of this variant in population database, prediction of bioinformatics tools (deleterious), segregation results and our predicted amino acid change effect on the 3D protein structure emphasizes on the pathogenic nature of p.(Pro118Leu) variant. Therefore, in our view, this is a potential pathogenic variant possibly involved in the dysfunctional CYP1B1 protein ultimately responsible for PCG in family A2.

Another missense variant identified in the family A6 (c.1A>G; p.M1?) probably result in the loss of initiation codon in open reading frame (ORF) of the gene. Since subsequent ATG appears 393 nucleotides downstream, therefore this variant may result in the loss of 131 amino acids at the N-terminus of the protein. CYP1B1 is a microsomal membrane-bound enzyme having a leader sequence at its N-terminus which directs its localization in the endoplasmic reticulum (Wang et al., 2011) where N-terminus along with hinge region provides flexibility to its structure for properly residing in the membrane and extending the cytoplasmic domain in the cytoplasm (Yamazaki et al., 1993). Therefore, we anticipate that the delocalization of the CYP1B1 in the family A6 is the cause PCG phenotype. This variant is novel but a different variant i.e., c.2T>C (with similar probable effect on the protein p.M1?) was identified for the first time in a patient affected with Peter's anomaly with increased IOP and bilateral corneal opacity (Vincent et al., 2001). Later c.2T>C was reported in many populations; Indian, Canadian, Israeli, Italian causing congenital glaucoma and Peter's anomaly (Vincent et

al. 2006; Geyer et al. 2011; Giuffre 2011). Our variant (c.1A>G; p.(Met1?)) is present in the homozygous state in affected individuals and is responsible for PCG while in one affected female, unilateral cataract was also observed.

Since 1990s several variants in *CYP1B1* have been reported to cause glaucoma and to date the number raised to more than 250 (Source: HGMD). But in our prediction, several identified variants might represent the incidental findings and therefore all of these may not play major role in the phenotype development. For example, two *CYP1B1* mutations; p.(Arg390His) and p.(Arg368His) are not only common in Pakistani population but also in several other populations like Middle-Eastern and Caucasian (Li et al., 2011). The p.(Arg390His) is a previously reported mutation but p.(Arg368His) is present in one of our previously screened families and did not segregate in the family (*unpublished data*). Recently in another study p.(Arg368His) variant was negated as pathogenic on two bases; (i) they found it in less number of samples in glaucoma cohort than expected (ii) they found this variant in a comparable number of individuals from another cohort of intellectually disabled children (Alsaif et al. 2019). Previous finding by Alsaif et al., (2019), presence of this variant in gnomAD database in homozygous state (n=13), with an allele frequency of 0.03035 in South Asian population and our finding strongly endorse the recommendation of changing the "pathogenic" state of the said variant in the public databases. Previously p.(Glu229Lys) was found associated to POAG in heterozygous state with low penetrance but latter in 2010 significant number of times it was found in the control group as compared to patients (Pasutto et al., 2010). Similarly, in some Indian families *TEK* heterozygous variants along with *CYP1B1* variants were found associated with PCG. Functional analysis of these variants revealed that certain combination of variants in both genes resulted in perturbed or reduced interaction between both proteins. The variant p.(Glu229Lys) in *CYP1B1* when occurred in combination with TEK variant p.(Gln214Pro), only then showed reduced interaction, otherwise p.(Gln214Pro) in combination with p.(Gly743Ala) *TEK* variant showed normal interaction as of wild type (Kabra et al. 2017). We found p.(Glu229Lys) in two of our previously screened families in heterozygous state (*unpublished data*) but this variant has 0.01 frequency in gnomAD therefore we assume it as a risk factor rather than pathogenic variant. Although, *CYP1B1* has been associated with glaucoma since long, even then the

pathway or mechanism through which this gene may cause the disease in not known yet. In our view, variants of uncertain significance (VUS) in this gene are one of the hurdles in identification of new genes which might have important role in developing the disease and unwinding the *CYP1B1* mystery. Advancements in techniques has provided the information of variations among normal individuals through different public databases, which is indicating that certain variants in *CYP1B1* might not be the actual cause of disease. There is a need to revisit the literature in order to sketch the clear picture of *CYP1B1* variants.
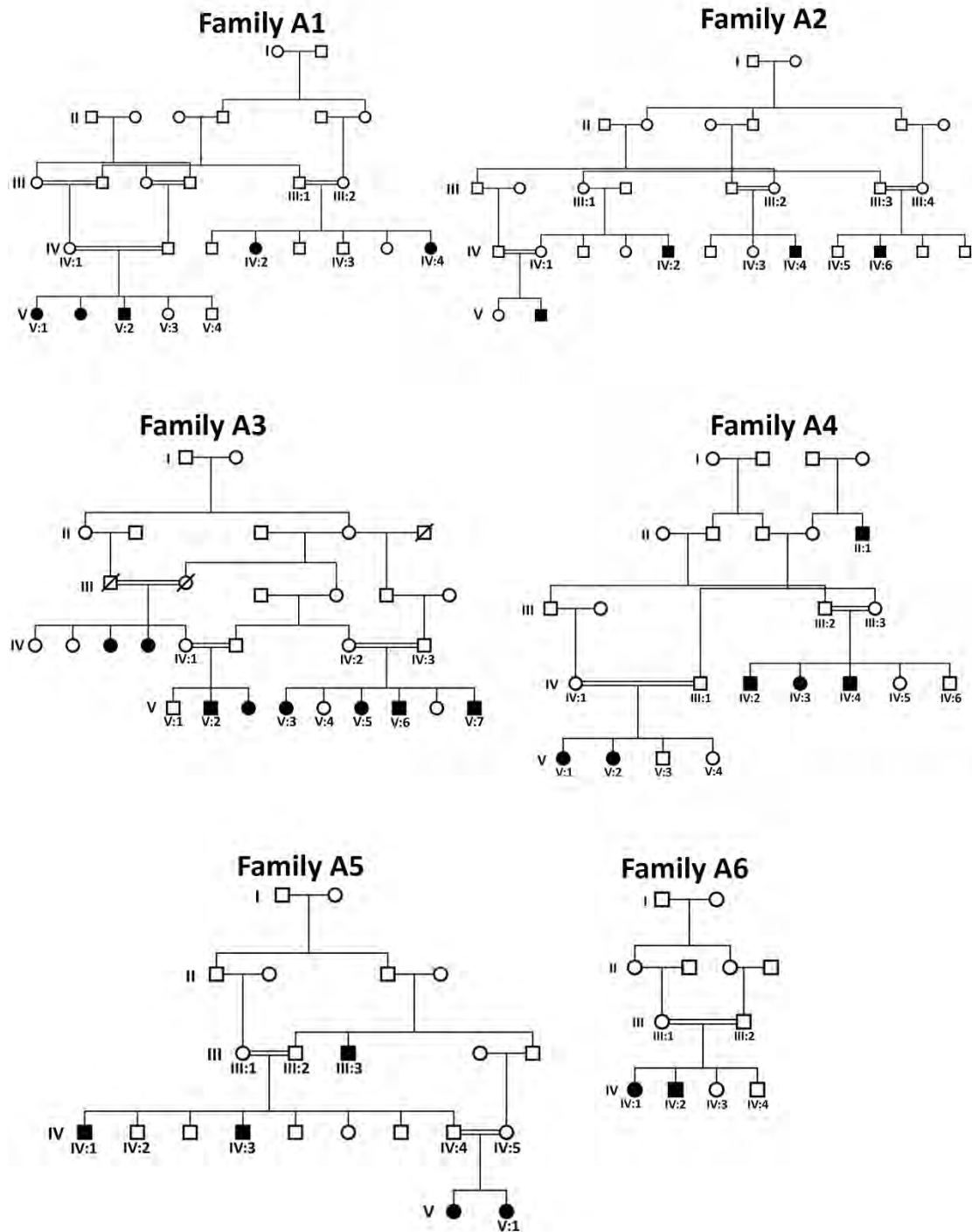
Figure 3.1: Pedigrees of six families with glaucoma. Numbers are given in each pedigree only to the participating members. The autosomal mode of inheritance and consanguinity is clearly seen among six families.
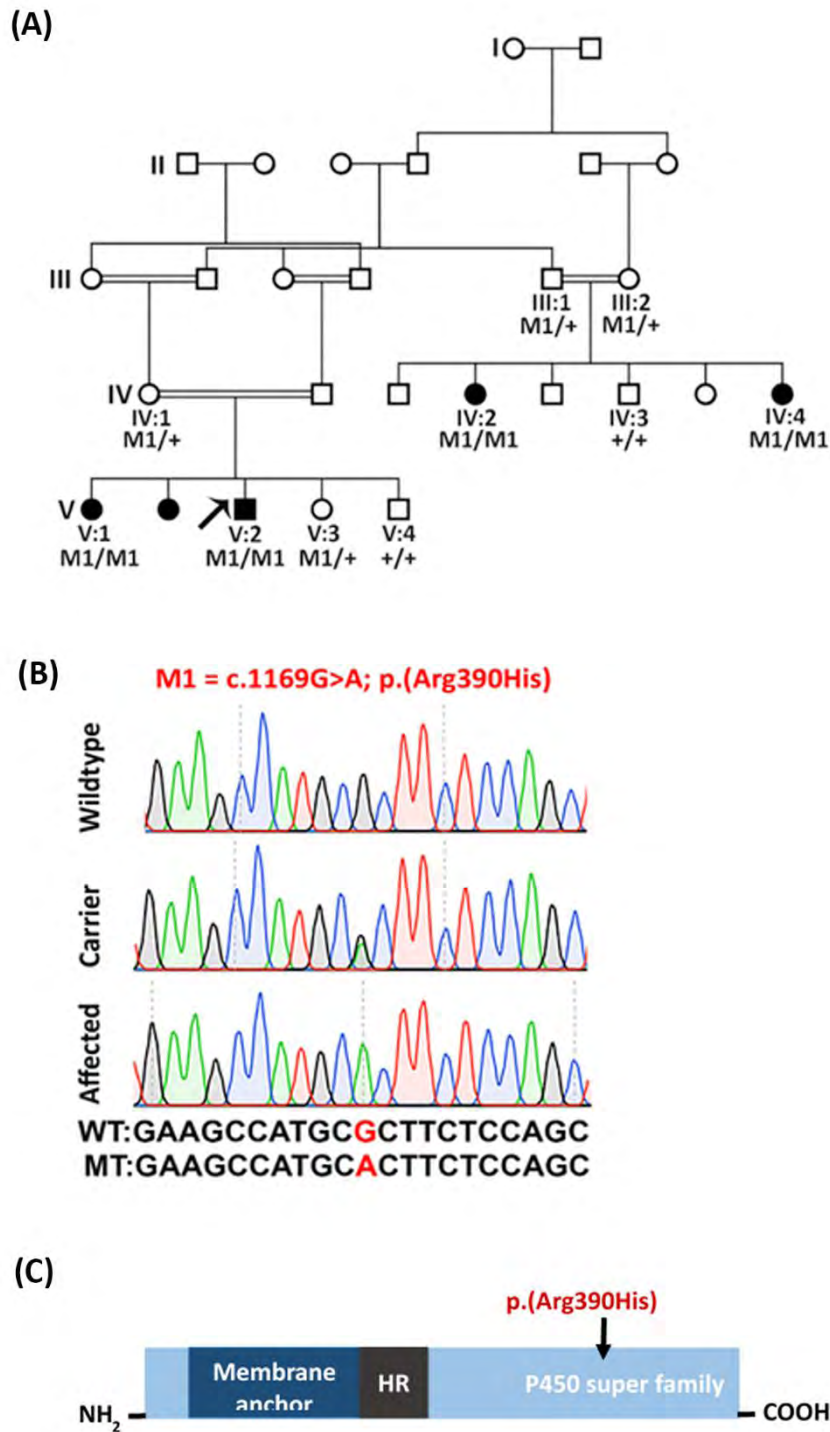
Figure 3.2: (A). Pedigree of Family A1 where arrow is indicating the proband and below each participating member is shown the segregation results. (B). Chromatogram of the variant M1 (c.1169G>A; p.(Arg390His)) identified in *CYP1B1* in wildtype, carrier and affected individuals. (C). Schematic representation of amino-acid change in protein domain of cytochrome P450 1B1.
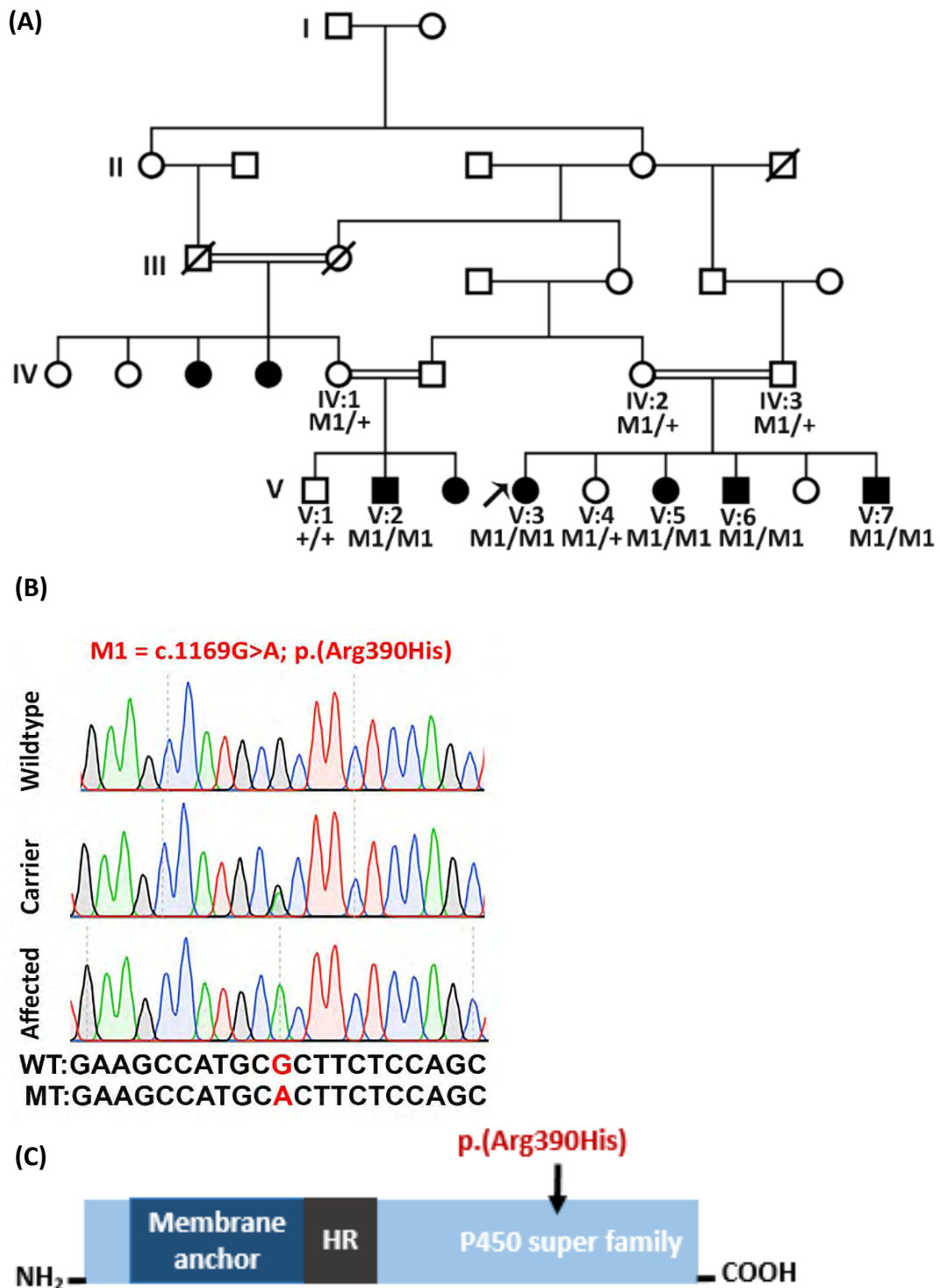
Figure 3.3: (A). Pedigree of Family A3 where arrow is indicating the proband and below each participating member is shown the segregation results. (B). Chromatogram of the variant M1 (c.1169G>A; p.(Arg390His)) identified in *CYP1B1* in wildtype, carrier and affected individuals. (C). Schematic representation of amino-acid change in protein domain of cytochrome P450 1B1.
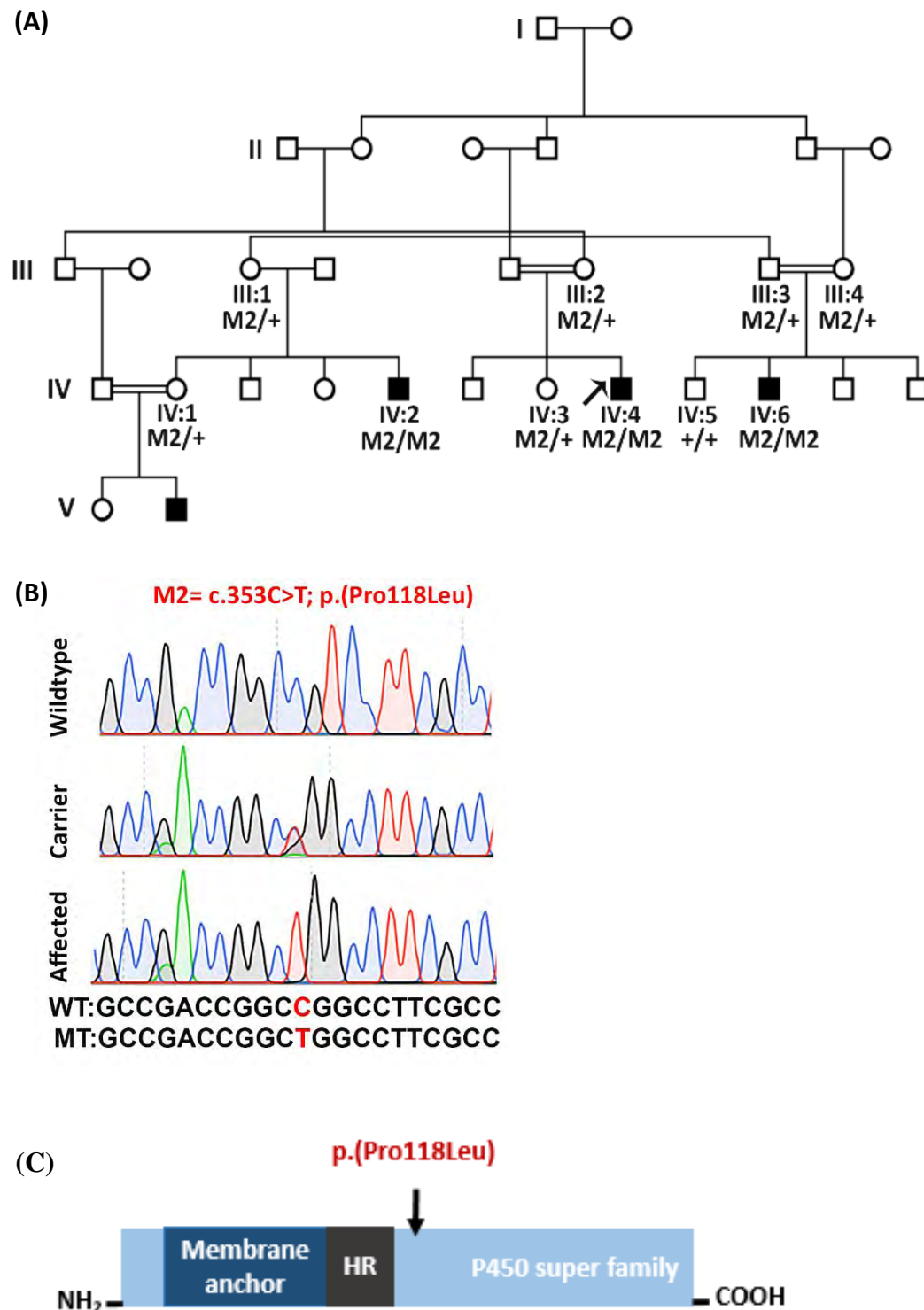
Figure 3.4: (A). Pedigree of Family A2 where arrow is indicating the proband and below each participating member is shown the segregation results. (B). Chromatogram of the variant M2 (c.353C>T; p.(Pro118Leu)) identified in *CYP1B1* in wildtype, carrier and affected individuals. (C). Schematic representation of amino-acid change in protein domain of cytochrome P450 1B1.
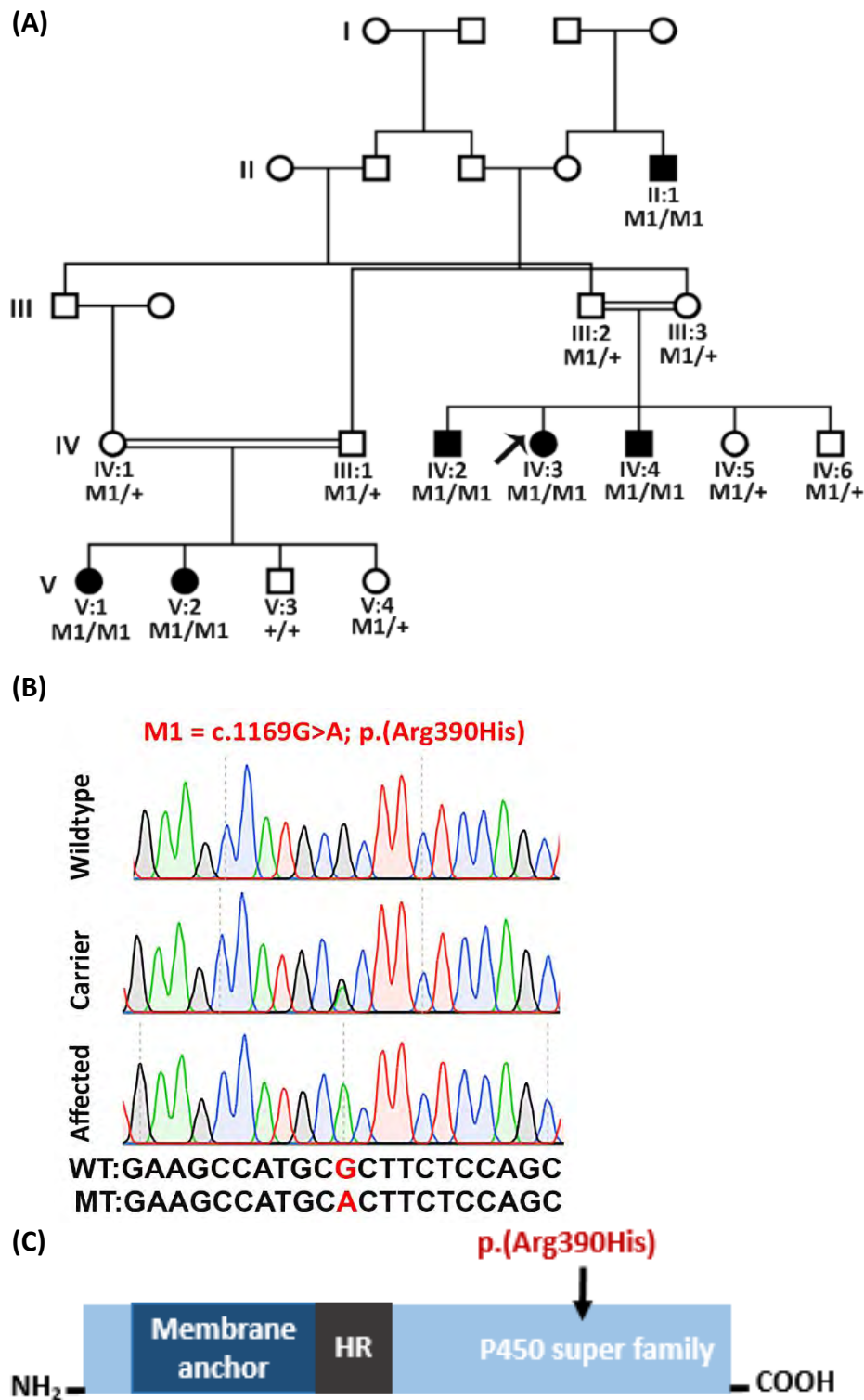
Figure 3.5: (A). Pedigree of Family A4 where arrow is indicating the proband and below each participating member is shown the segregation results. (B). Chromatogram of the variant M1 (c.1169G>A; p.(Arg390His)) identified in *CYP1B1* in wildtype, carrier and affected individuals. (C). Schematic representation of amino-acid change in protein domain of cytochrome P450 1B1.

(A)

(B)

M3= c.1325del; p.(Pro442Glnfs*15)

WT: T C G A G C T **G** G A T C A A A
MT: T C G A G C T **-** G A T C A A A

(C)
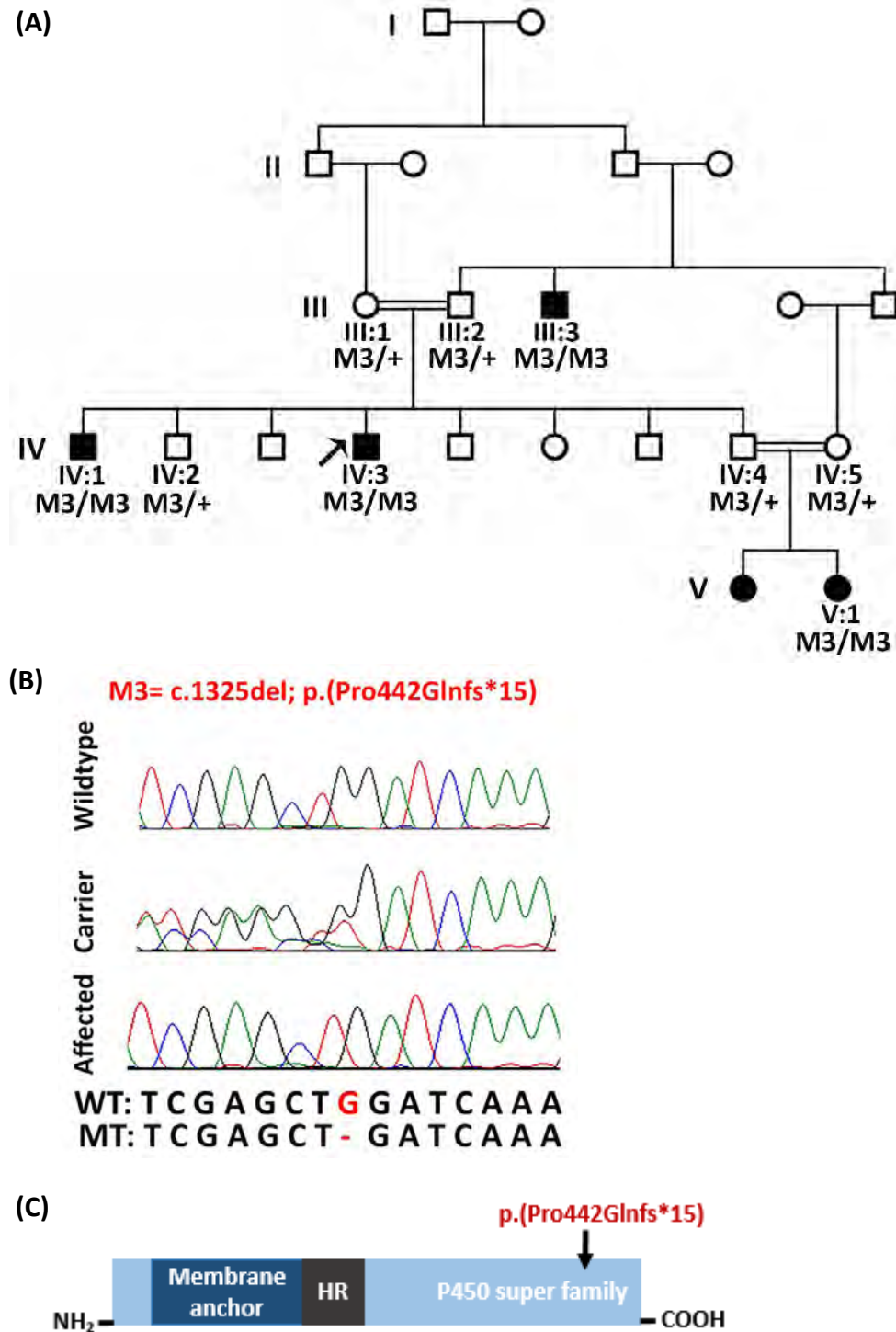
p.(Pro442Glnfs*15)

Figure 3.6: (A). Pedigree of Family A5 where arrow is indicating the proband and below each participating member is shown the segregation results. (B). Chromatogram of the variant M3 (c.1325del; p.(Pro442Glnfs*15)) identified in *CYP1B1* in wildtype, carrier and affected individuals. (C). Schematic representation of amino-acid change in protein domain of cytochrome P450 1B.

(A)

(B)

M4 = c.1A>G; p.(Met1?)

WT: T G T C C C C A G C **A** T G G G C A C C A G
MT: T G T C C C C A G C **G** T G G G C A C C A G

(C) p.(Met1?)

NH₂ — Membrane anchor | HR | P450 super family — COOH
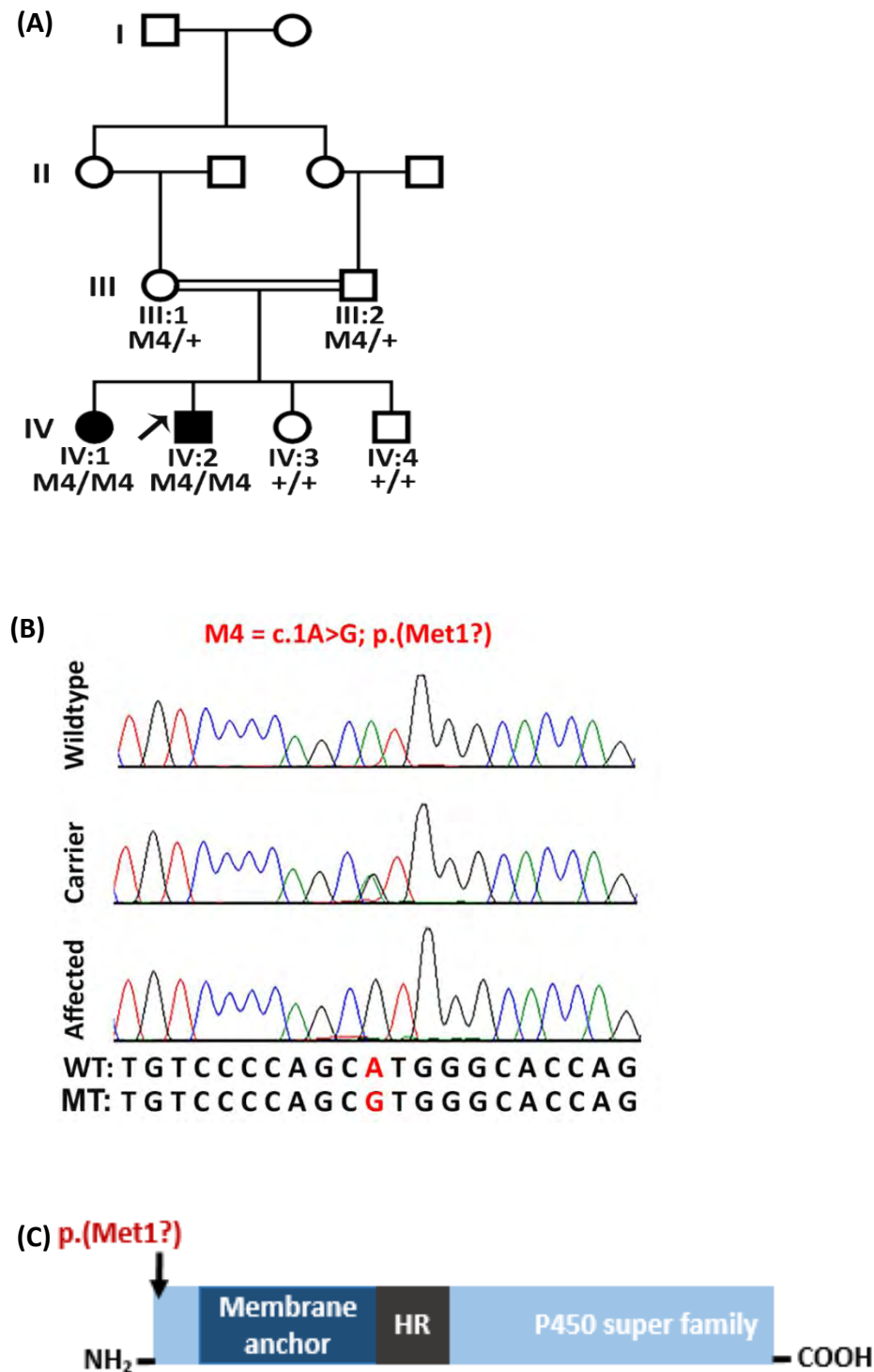
Figure 3.7: (A). Pedigree of Family A6 where arrow is indicating the proband and below each participating member is shown the segregation results. (B). Chromatogram of the variant M4 (c.1A>G; p.(Met1?)) identified in *CYP1B1* in wildtype, carrier and affected individuals. (C). Schematic representation of amino-acid change in protein domain of cytochrome P450 1B1.
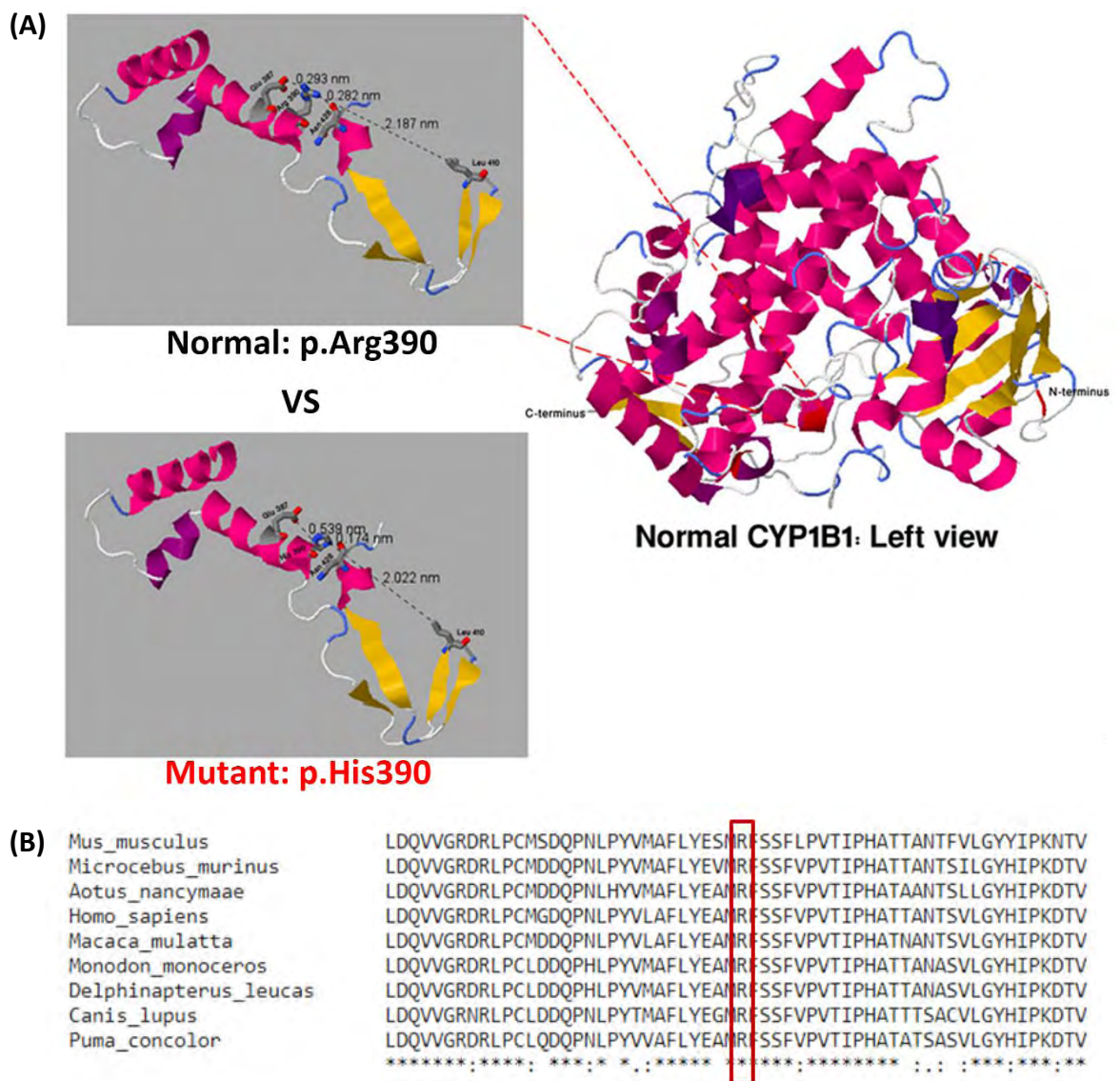
Figure 3.8: (A). Protein 3D structure showing changes in mutant containing variant p.(Arg390His). In bottom left panel the distance between His390 and Glu387 is increased to 0.539nm as compared to normal 0.293nm shown in top right panel. (B). The *CYP1B1* variant p.(Arg390His), disrupts the amino acid which is evolutionary conserved among several species (source: pBLAST).

(A)

Normal CYP1B1: Left view

Normal: p.Pro118

VS

Mutant: p.Leu118

(B)

Mus_musculus	GNAAAVGQASHLYFARLARRYGDVFQIRLGSCPVVVLNGESAIHQALVQQGSIFADF PPF
Microcebus_murinus	GNALAVGRAAHLSFARLARRYGDVFQIRLGSCPIVVLNGERAIHQALVQQSAVFAGF PPF
Aotus_nancymaae	GNAAAVGQAAHLSFARLARRYGDVFQIRLGSYPIVVLNGERAIHQALLQQGAAFADF PSF
Homo_sapiens	GNAAAVGQAAHLSFARLARRYGDVFQIRLGSCPIVVLNGERAIHQALVQQGSAFADF PAF
Macaca_mulatta	GNAAAVGQASHLSFARLARRYGDVFQIRLGSCPIVVLNGERAIHQALVQQGSAFADF PSF
Monodon_monoceros	GNAASMGPAPHVSFARLARRYGDVFQIRLGSCPVVVLNGERAIRQALVQQGAAFADF PPF
Delphinapterus_leucas	GNAASMGPAPHVSFARLARRYGDVFQIRLGSCPVVVLNGERAIRQALVQQGAAFADF PPF
Canis_lupus	GNAAAMGPAPHLSFARLARRYGDVFQIRLGSCPVVVLNGERAIRQALVQQGAAFADF PRF
Puma_concolor	GNAAAMGPAPHLSFARLARRYGDVFQIRLGNCPVVVLNGERAIRQALVQQGAAFADF PRF
	*** ::* * *; ***************. *;****** **;***;**.: **.:* *

Figure 3.9: (A). Protein 3D structure showing changes in mutant CYP1B1 protein containing variant p.(Pro118Leu). In bottom right panel the distance between Leu118 and Arg117 is increased to 0.66nm compared to 0.42nm in normal shown in top right panel. (B). The *CYP1B1* variant p.(Pro118Leu), disrupts the amino acid which is evolutionary conserved among several species (source: pBLAST).

Table 3.1: Clinical features of six glaucomatous families recruited in this study.

Phenotypic features	Family ID																							
	A1				**A2**			**A3**					**A4**						**A5**				**A6**	
Individual ID	IV:2	IV:4	V:1	V:2	IV:2	IV:4	IV:6	V:2	V:3	V:5	V:6	V:7	II:1	IV:2	IV:3	IV:4	V:1	V:2	III:3	IV:1	IV:3	V:1	IV:1	IV:2
Gender	F	F	F	M	M	M	M	M	F	F	M	M	M	M	F	M	F	F	M	M	M	F	F	M
Age onset (yrs)	3	3	3	3	6	6	6	3	3	3	3	3	3	3	3	3	3	3	2	2	2	2	3	3
Affected eye	BL	BL	BL	BL	BL	BL	BL	BL	BL	BL	BL	BL	BL	BL	BL	BL	BL	BL	BL	BL	BL	BL	BL	BL
Buphthalmos	+	+	+	+	-	-	-	+	+	+	+	+	+	+	+	+	+	+	+	+	+	+	+	+
Corneal Opacity	-	-	-	-	BL	BL	BL	-	-	-	-	-	BL	BL	BL	BL	BL	BL	BL	BL	BL	BL	-	-
Cataract	+	+	+	+	-	-	-	-	-	-	-	-	+	+	+	+	+	+	-	-	-	-	RE	-
Epiphora	+	+	+	+	-	-	-	-	-	-	-	-	-	-	-	-	-	-	+	+	+	+	-	-

BL= Bilateral, F= Female, M= Male, RE= Right eye, yrs= Years, "+" means present, "-" means absent.

Table 3.2: Mutations identified in this study with their pathogenicity predictions.

Family ID	cDNA	Protein	gnomAD (v2.1.1)	Mutation Taster	PolyPhen	SIFT	Provean	CADD (PHRED)	MutPred2	ACMG/AMP	Status
A1, A3, A4	c.1169G>A	p.(Arg390His)	0.0001032	Disease causing	Probably Damaging	Damaging	Deleterious	32	0.759	Likely pathogenic	(Stoilov et al. 1998)
A2	c.353C>T	p.(Pro118Leu)	0.000004887	Disease causing	Probably Damaging	Damaging	Deleterious	23.6	0.89	VUS	This study
A5	c.1325del	p.(Pro442Glnfs*15)	-	Disease causing	-	-	-	-	-	Likely pathogenic	(Rauf et al. 2016)
A6	c.1A>G	p.(Met1?)	0.000008156	Disease causing	-	-	-	19.53	0.739	Likely pathogenic	This study

Reference transcript NM_000104.4; VUS, variant of uncertain significance, '-' indicates not applicable.

Table 3.3: List of Common SNPs in *CYP1B1* gene which were used for haplotype analysis.

Individual ID	Intronic g.34501C>T rs2617266	R48G c.142C>G rs10012	A119S c.355G>T rs1056827	V432L c.1294G>C rs1056836	D449D c.1347T>C rs1056837	N453S c.1358A>G rs1800440
A1-V:2	-	-	-	-	Homo	Homo
A2-IV:4	-	-	-	-	-	-
A3-V:3	-	-	-	Homo	-	Homo
A4-IV:3	-	-	-	Homo	Homo	Homo
A5-IV:3	-	-	-	-	-	-
A6-IV:2	-	-	-	-	-	-

Coding positions are given with the reference transcript NM_000104.4
Homo= Homozygous alternative allele, '-' Means absence of alternative allele.

4.0. ANOPHTHALMIA AND MICROPHTHALMIA

Anophthalmia and microphthalmia (A/M) is a group of inherited structural eye defects which are either present in the isolated form (Nonsyndromic types) or present along with other anomalies (Syndromic types). The combined prevalence of A/M is up to 30 per 100,000 population, with microphthalmia reported in up to 11% of blind children (Verma and Fitzpatrick, 2007). The exact pathogenesis of both anophthalmia and microphthalmia is unknown. But it is believed that failure of anterior neural tube development give rise to secondary anophthalmia while failure in enlargement of optic pit or optic vesicle is responsible for secondary anophthalmia (Mann, 1953). Similarly, when the posterior segment of the eye is not well-developed as compared to the anterior segment then it results in microphthalmia. To date approximately 150 genes are known to be associated with syndromic and non-syndromic forms of A/M (OMIM, assessed 1st December 2022). Due to increased heterogeneity only 20-30% of the patients receives genetic diagnosis, although detection rates are higher in case of severe bilateral cases (Plaisancie et al., 2019). Here we have selected seven families affected with severe bilateral A/M depicting consanguinity and autosomal recessive mode of inheritance.

4.1. Description and Clinical Features of Families

A total of 8 families (B1-B8) with 23 affected individuals showed A/M with or without anterior segment dysgenesis or corneal opacity and were included in this study. All eight families were consanguineous and showed an autosomal recessive inheritance of A/M phenotype (Figure 4.1). All affected individuals were diagnosed with bilateral, congenital microphthalmia (n = 13) or anophthalmia (n = 10). The affected members of three families (B1, B4 and B5) showed complete absence of eye tissue and ocular structures with no light perception. Therefore, they were included in the category of bilateral clinical anophthalmia. The members of all these families had flat nasal bridge but no other facial dysmorphism, skeletal deformities or polydactyly was observed.

Both the affected individuals of family B2 and B7 showed bilateral microphthalmia with corneal opacity and anterior segment dysgenesis, whereas individuals of family B6 showed microphthalmia with corneal opacity and flat nasal bridge. All the affected individuals of family B3 showed phenotypic variations. Individual B3 (V:4) showed

bilateral microphthalmia with corneal opacity and anterior segment dysgenesis, B3 (V:2) had severe/extreme bilateral microphthalmia with corneal opacity. The individual B3 (V:3) exhibited bilateral microphthalmia but unilateral corneal opacity. All the three affected individuals of family B3 had somewhat flat nasal bridge. Three affected members of family B8 (IV:1, IV:3, IV:5) presented microcornea with congenital blindness (had perception of light) while individual B8-IV:3 additionally showed sclerocornea/corneal opacity. Varying degree of cataract development was also observed in the affected individuals of family B8. Detailed clinical features for all individuals are provided in table 4.1.

4.2. Targeted Sanger Sequencing Revealed Pathogenic Variants in Four A/M Families

Since phenotype of 60% of the A/M families from a similar Pakistani cohort was previously explained by pathogenic *FOXE3* variants (Ullah et al., 2016). Therefore, all probands from eight families were subjected to *FOXE3* screening through Sanger sequencing. For the probands of families B1, B2, B6, and B7, likely pathogenic biallelic variants were identified, which segregated in the respective families. For three of these families (B1, B2 and B7), an identical homozygous nonsense pathogenic variant (NM_012186.3:c.720C>A; p.(Cys240*)) was identified in *FOXE3* (Figure 4.2-4.4). The variant has allele frequency of 0.00001334 (only heterozygote state) in gnomAD and most likely result in the formation of a truncated protein. The variant is previously reported as pathogenic in ClinVar (Landrum et al., 2018) and classified as pathogenic according to the ACMG/AMP classification system with high CADD-PHRED score of 36. In the fourth (Family B6) a known (Ullah et al. 2016; Rashid et al. 2020) *FOXE3* homozygous pathogenic missense variant (NM_012186.3:c.289A>G; p.(Ile97Val)) was identified (Figure 4.5). This amino acid change affects an evolutionary conserved region of the protein (Figure 4.5D) and is predicted as pathogenic by *in silico* tools (Table 4.2). None of potentially pathogenic variants were identified in *FOXE3* in investigated probands of other four families.

4.3. Genome Sequencing Revealed Pathogenic Variants in *PXDN* and *VXS2*

Four families (B3, B4, B5 and B8) remained unsolved after targeted sequencing of *FOXE3*. Therefore, the probands B3 (V:4), B4 (IV:4), B5 (IV:2) and B8 (IV:5) were subjected to genome sequencing. Variant prioritization on the basis of minor allele

frequency, prediction of pathogenic tools and finally on the basis of genes already known to cause A/M (curated manually from OMIM entries accessed on December, 2022; Attached as Appendix I) revealed possibly pathogenic variants in *PXDN, VSX2,* and *SIX6* which also segregated in the respective families (Figures 4.6, 4.7, 4.8 and 4.9).

In family B4, a 13bp deletion in *VSX2* (NM_182894.3:c.413_425del; p.(Ser138*)) was identified (Figure 4.7). Pathogenic variants in *VSX2* are associated with isolated microphthalmia and microphthalmia with coloboma (Ammar et al., 2017). This frameshift variant has not been previously reported and results in the formation of a premature termination codon in exon 2 and may induce nonsense mediated decay (NMD) or the formation of a truncated protein. In family B5, a known pathogenic (Khan et al., 2011) single nucleotide deletion (NM_012293.3:c.2568del;p.(Cys857Alafs*5)) was identified in *PXDN* (Figure 4.8). Both the identified *VSX2* and *PXDN* frameshift variants were classified as pathogenic according to the ACMG/AMP classification system.

In family B8, a known disease-causing variant (NM_007374.3:c.547G>C; p.(Asp183His)) (Figure 4.9), which is recently reported in ClinVar as pathogenic by a single submitter, in association with congenital cataract, microcornea, sclerocornea and nystagmus was identified in *SIX6* gene. The *SIX6* gene is known to cause optic disc anomalies with retinal or macular dystrophy (OMIM: 606326). Many studies have indicated the association of *SIX6* with anophthalmia, microphthalmia and complex microphthalmia (Aijaz et al., 2004; Deepthi et al., 2021; Mayank and Amita, 2023).

In family B3, a novel homozygous deep-intronic variant in intron 17 of *PXDN* (NC_000002.12:g.1646059C>T (c.3609-1307G>A; p.(?)) was identified. The potential splice-altering effect was predicted by SpliceAI (acceptor gain, 0.97) and other prediction tools embedded in the Alamut Visual software version 1.4 (Interactive Biosoftware, Rouen, France; http://www.interactive-biosoftware.com) including MaxEntScan, SpliceSiteFinder-like, NNSPLICE, and GeneSplicer. Based on the high prediction scores of SpliceAI (0.97), Splice site finder-like (88.9), MaxEntScan (8.5), NNSPLICE (1.0), and GeneSplicer (9.9), the identified splice site variant was predicted to create a strong splice acceptor site, potentially leading to the activation of a pseudoexon (Figure 4.10). No other homozygous or compound heterozygous candidate

variants (SNVs, CNVs, or SVs) in A/M-associated genes were identified in any of the probands in family B3.

4.4. Pseudoexon Activation in *PXDN* Caused by a Deep-intronic Splice Variant

To investigate the potential splice effect of the *PXDN* deep-intronic variant (c.3609-1307G>A), identified in family B3, an *in vitro* minigene splice assay was performed. The variant was present in intron 17, and SpliceAI predicted a 137bp pseudoexon insertion in this intron resulting from this variant (Figure 4.10). The splice assay construct (Figure 4.11A) has *PXDN* insert which is flanked between *RHO* exon 3 and *RHO* exon 5. The splice isoforms were investigated using *RHO* exon 3 and *RHO* exon 5 primers and the mutant band was observed to be approximately 137bp larger than the band from wildtype construct (Figure 4.11B). Further, mutant and wildtype splice isoforms were Sanger sequenced which confirmed the pseudoexon activation in intron 17 (c.3609-1305_3609-1169) in *PXDN* (Figure 4.11C), which matches the predictions of SpliceAI, and other splicing tools as discussed earlier. This out-of-frame pseudoexon inclusion, results in the formation of a premature termination codon and will most likely cause either NMD or the formation of a truncated PXDN protein (p.Arg1203Serfs76*), that lacks the essential peroxidase domain of peroxidasin homolog protein (Figure 4.11D). No wildtype transcript could be observed when transfection was performed with the mutant construct, suggesting the variant has a severe and complete effect on splicing. Based on the splice assay results and confirmed splice-altering effect for the *PXDN* variant, the variant is classified as likely pathogenic according to ACMG/AMP guidelines (Richards et al., 2015).

4.5.   Discussion

A/M is a group of structural ocular defects with varying degrees of severity, ranging from unilateral to bilateral and from simplex (non-syndromic) to complex (syndromic) types. A/M is a complicated disorder, and the underlying mechanisms of the disease are still poorly understood. Some suggest that A/M disorders arise due to secondary regression during ocular development (Fitzpatrick and van Heyningen, 2005), while others hypothesize that these are the results of either lens induction failure (Inoue et al., 2007), disruptions in optical invagination or during early differentiation of the retina (Winkler et al., 2000; Stigloher et al., 2006). Although environmental factors can contribute to the development of A/M, genetic factors are suggested to be the most

common cause of A/M. There are >90 genes reported to be associated with A/M, and yet the phenotype of significant number of cases cannot be genetically explained (Harding and Moosajee, 2019). Resolving the missing heritability for A/M is essential, as it is required to allow optimal genetic diagnostics, pre-symptomatic screening in case of a syndromic phenotype, disease management, and genetic counselling of the families but also to investigate genotype-phenotype correlations which would allow a better understanding. In the current study, we have genetically explained the phenotype of 23 affected A/M individuals from 8 unrelated Pakistani consanguineous families and investigated their genotype-phenotype correlations. Both novel and previously reported pathogenic variants were identified affecting four different genes: *FOXE3*, *PXDN*, *SIX6* and *VSX2*.

A previously investigated cohort of the same origin (n = 8) suggested that the majority of Pakistani A/M-affected families were explained by *FOXE3* pathogenic variants (60%) (Ullah et al., 2016). Similarly, in a mixed cohort of Caucasian, Hispanic, African American and Asians (n=116), 15% of the bilateral microphthalmia patients were solved with *FOXE3* variants (Reis et al., 2010). This prompted us to first screen this single exon gene that encodes the *FOXE3* transcription factor in our cohort using Sanger sequencing. The screening of *FOXE3* gene solved 50% (4/8) of our families. Although based on a relatively small cohort, this suggests that pre-screening of *FOXE3* prior to any NGS application in Pakistani A/M patients, and possibly for other ethnicities as well, is cost-effective strategy. We have identified two known pathogenic variants in *FOXE3* in four different families. One known homozygous missense (c.289A>G; p.(Ile97Val)) variant was identified in family B6 that affects an evolutionarily conserved amino acid in the DNA-binding forkhead domain of the protein (Ullah et al., 2016). Hence, it will most likely affect the DNA binding affinity of this transcription factor. A second disease-causing *FOXE3* variant (c.720C>A; p.(Cys240*)) was identified in three of the studied families (B1, B2, and B7). This variant was initially reported by (Valleix et al., 2006) in affected members of a Madagascar inbred family. Later it was identified in Bangladeshi, Kuwaiti, and Pakistani families as well (Ali et al., 2010; Anjum et al., 2010; Reis et al., 2010). This suggests that the variant could be a founder variant inherited from a common ancestor. The known pathogenic variants previously identified in *FOXE3* are predominantly

responsible to cause aphakia, sclerocornea, microphthalmia, anterior segment dysgenesis and rarely increased intraocular pressure, bilateral congenital cataract, and vitreoretinal dysplasia (Ali et al., 2010; Gillespie et al., 2014; Ullah et al., 2016; Rashid et al., 2020).

In family B6, identified with missense *FOXE3* variant (c.289A>G; p.(Ile97Val)), we observed microphthalmia with corneal opacity. With nonsense *FOXE3* variant (c.720C>A; p.(Cys240*)), patients from families B2 and B7 showed similar phenotypes including bilateral microphthalmia, corneal opacity and anterior segment dysgenesis. In comparison to this, affected individuals of family B1 harboring the same *FOXE3* variant showed complete anophthalmia. They also have a flat nasal bridge but no other facial dysmorphism was observed. This indicates that some genetic or environmental modifiers might play a role.

Using genome sequencing, pathogenic variants in *PXDN, SIX6* and *VSX2* were identified in five families. *VSX2* encodes the VSX2 retina-specific transcription factor that is highly expressed during embryonic and fetal eye development (Liu et al., 1994). *VSX2* pathogenic variants are found in 2% of A/M cases (Verma and Fitzpatrick, 2007). We identified a novel 13bp deletion in exon 2 of this gene in affected members of family B4 that presented with complete bilateral anophthalmia. The majority of pathogenic variants reported in *VSX2* cause loss of function either by NMD or by the formation of a truncated VSX2 protein that lacks a complete DNA binding homeobox domain (amino acids 148-207) (UniProt, 2023). These variants are mostly associated with bilateral A/M and coloboma and are rarely associated with other eye deformities like cataract and cone-rod dysfunction (Khan et al. 2015; Ullah et al. 2016; Ammar et al. 2017).

In family B8, disease-causing variant was identified in *SIX6* gene (c.547G>C; p.(Asp183His)). This variant is absent in public database (gnomAD) and has already been reported in the Pakistani population with microcornea (Panagiotou et al., 2022). The affected individuals in the previously reported family with the same variant showed early childhood visual impairment, microcornea, sclerocornea and nystagmus. While all the affected members of family B8 in our study showed microcornea and were completely blind since birth (slight perception of light). They also showed varying degree of cataract and corneal opacity. The male individual IV:1, presented bilateral

cataract development at the central region of lens. The individual IV:3 showed cataract in left eye while corneal opacity/sclerocornea in the right eye and individual IV:5 showed unilateral cataract development. The Six family proteins are important for transcriptional regulation. All Six proteins have two important protein domains required for their normal functioning which are a six domain which is important for protein-protein interactions and a homeobox domain. Homeobox domain is the DNA binding domain (Kawakami et al., 2000), as this domain is also present in VSX2 and FOXE3 transcription factors. The variant we identified in family B8 is residing in the homeobox domain and will most probably affect the DNA binding ability of the protein. Panagiotou et al., has showed that aspartic acid at position 183 in the SIX6 protein is evolutionary conserved among several species and 3D protein modelling indicated that negatively charged aspartic acid is present in the recognition helix which is involved in the interaction of major groove of DNA to the homeobox domain. Therefore, its replacement with imidazole side chain containing histidine will most probably disrupt the normal binding pattern of recognition helix (Panagiotou et al., 2022). Studies in animal models, also support the involvement of *SIX6* gene in eye development. In the absence of Six6 gene, mice developed hypoplasia of retina and showed no optic nerve and chiasm formation (Li et al., 2002). Similarly, in zebrafish SIX6 gene knockdown is responsible for small eyes with underdeveloped lens and reduced optic nerve diameter (Iglesias et al., 2014).

In families B3 and B5, we have identified one novel and one known disease-causing homozygous *PXDN* variant, respectively. *PXDN* encodes a peroxidasin which is expressed in epithelial layers of cornea and lens, where it may provide structural support or serve as an antioxidant enzyme to protect lens, cornea and other developing eye structures from oxidative damage (Khan et al., 2011). In family B3, a high degree of intrafamilial phenotypic heterogeneity was observed where individual V:2 exhibits severe microphthalmia with corneal opacity, individual V:3 shows bilateral microphthalmia and unilateral corneal opacity, and individual V:4 was diagnosed with microphthalmia with anterior segment dysgenesis. In family B5, we identified the previously reported 1bp deletion (c.2568del; p.(Cys857Alafs*5)) which was previously reported by (Khan et al., 2011) in a Pakistani family with corneal opacity and cataract. In a Caucasian family, a different variant with the same protein effect (c.2569delT;

p.(Cys857Alafs*5)) showed unilateral microphthalmia (Zazo-Seco et al., 2020). Contradictory to both previous studies, all affected individuals from family B5 manifest bilateral anophthalmia, suggesting the variant is responsible for a more severe phenotype in this family. Several studies previously reported intra- and interfamilial phenotypic heterogeneity caused by *PXDN* variants even in monozygotic twins, which is in line with our findings (Zhu et al., 2021). Although our study is expanding the phenotypic spectrum of families carrying previously reported pathogenic variants in *FOXE3* and *PXDN* genes, the unavailability of OCT, ERG or MRI for the patients is a limitation of our study in providing the complete phenotypic diversity.

Genome sequencing analysis in family B3 revealed a novel deep-intronic splice variant in intron 17 (c.3609-1307G>A) of *PXDN*. *In silico* splice site prediction tools predicted the activation of a pseudoexon (c.3609-1305_3609-1169) as a consequence of this variant. The expected pseudoexon insertion was evaluated by a minigene splice assay. The splice assay confirmed the activation of a pseudoexon, and an aberrantly spliced transcript could be observed that matches the *in-silico* predictions. No wildtype transcript could be observed, suggesting that the variant causes a severe splice defect. These findings are based on the severity of the mRNA defect as observed in HEK293T cells and RNA studies using patient-derived cells should be performed to completely assess the splice effect and the severity of the variant. Still, the splice assay did confirm a splice effect of the variant (c.3609-1305_3609-1169; p.(Arg1203Serfs76*)), and therefore the variant was classified as likely pathogenic and the phenotype of the family B3 was considered genetically solved.

Previously, splice variants in *ALDH1A3, NAA10, RAX, TENM3*, and *VSX2* are already described to be associated with syndromic or non-syndromic A/M but these were present either in exons or intron-exon junctions (Abouzeid et al., 2012; Esmailpour et al., 2014; Chassaing et al., 2016; Ammar et al., 2017; Lin et al., 2018). To the best of our knowledge, this is the first study reporting the association of a deep-intronic splice variant with A/M, and the first splice-altering variant identified in *PXDN*. These findings emphasize the added value of genome sequencing as a diagnostic tool for A/M and the importance of incorporating deep-intronic regions of the known A/M-associated genes in genetic analyses.

As extensively reviewed by Harding et al., (2022) the overall diagnostic solve rate of individuals affected by bilateral and severe A/M is 70%, which is reduced to only 10% when studying unilateral cases of A/M (Harding and Moosajee, 2019). Although exome sequencing is an efficient and cost-effective method to perform genetic diagnostics, most genes associated with A/M are transcription factors and are GC-rich. Therefore, there is a chance that because of PCR bias and exon capture techniques, exome sequencing may fail to efficiently capture these GC-rich regions (Meienberg et al., 2016). More recently, two studies explored the use of genome sequencing to increase diagnostic solve rates for A/M (Jackson et al. 2020; Harding et al. 2022). Both these studies did not focus on deep-intronic regions of the genome due to limitations in their bioinformatic pipelines. In a study performed by Harding et al., an improved diagnostic rate of 33% was obtained when combining targeted panel testing with genome sequencing. The increased solve ratios were consistent for both unilateral and bilateral cases (Harding et al., 2022). In a second study performed by Jackson et al., a diagnostic solve rate of 15.7% was achieved through genome sequencing for complex microphthalmia, anophthalmia and coloboma patients (Jackson et al., 2020). We anticipate that when the assessment of deep-intronic variants will be incorporated as well, the diagnostic solve rates will improve even more. Although these previous findings and findings of the current study indicate that genome sequencing is a promising and effective diagnostic tool for A/M, considering the high sequencing costs, it is not feasible to provide genome sequencing to all patients. Hence to make it cost-effective, in this study, we also used single gene *FOXE3* testing prior to genome sequencing to establish a genetic diagnosis. This approach led us to the solve rate of 100% in a relatively small cohort (eight families) exhibiting severe forms of bilateral A/M, suggesting this is a cost-effective and feasible approach. Overall, this study highlights the usage of genome sequencing for the identification of coding and non-coding novel variants which eventually will lead towards better understanding of the complex inheritance pattern, associated comorbidities and phenotypic variation among families affected with A/M.

The developmental eye disorders are under-studied group of disorders due to the certain facts that it is impossible to revert the aberrant phenotype after birth and it is difficult to develop prenatal treatments. Extensive studies are required for proper understanding of the contributing factors as well as their spatial expression and role during

developmental process. Secondly, prenatal treatments of such disorders may pose risks to both mother and foetus. But with new advancements some prenatal or postnatal treatments for disorders like severe osteogenesis imperfecta and aniridia are in clinical phase I/II trial and if performed successful will open new avenues and encourages the treatments for severe developmental eye disorders such as A/M.
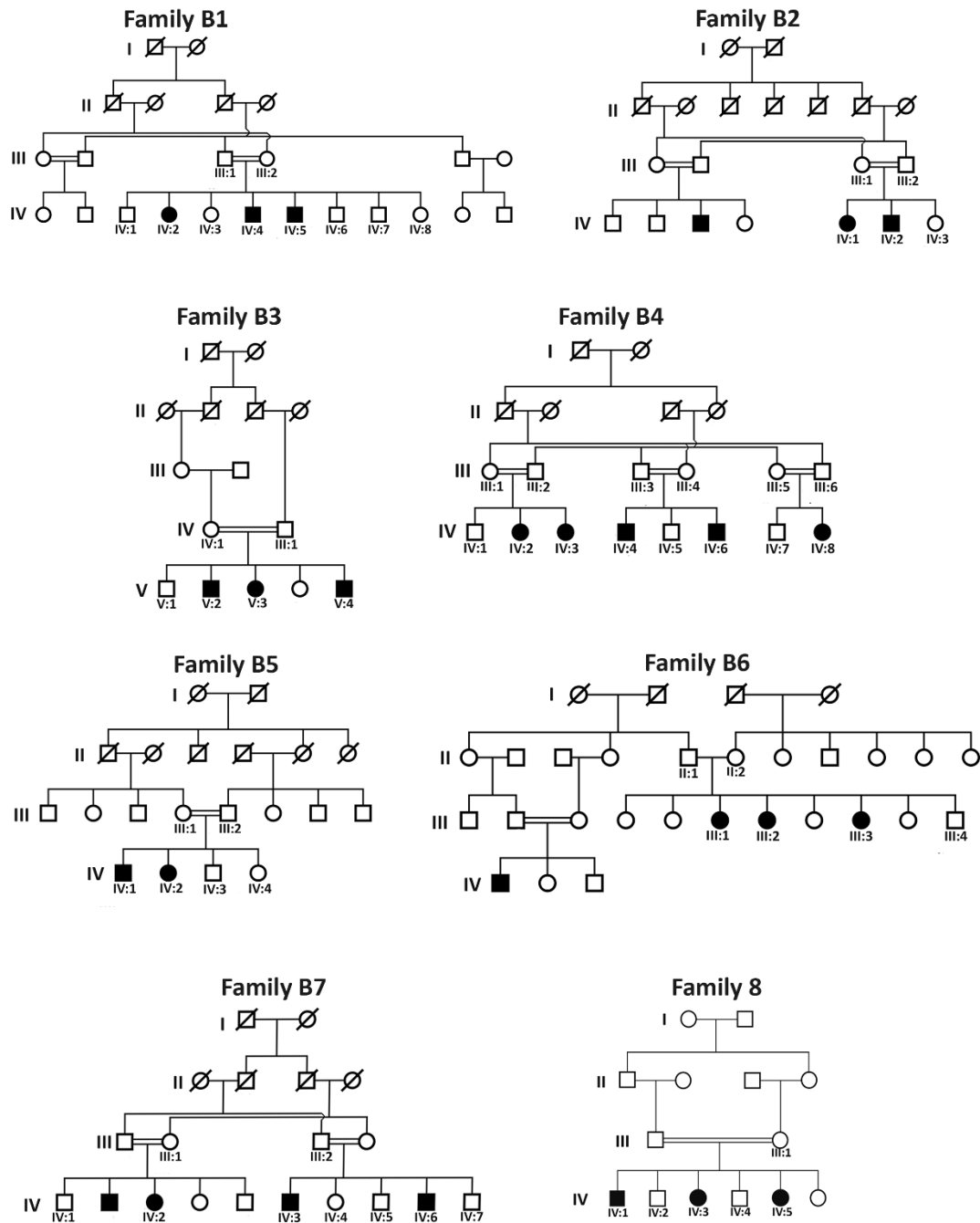
Figure 4.1: Pedigrees of eight anophthalmia/microphthalmia affected families (B1-B8). Numbers are given in each pedigree only to the participating members in this study. The autosomal mode of inheritance and consanguinity is clearly seen among all families.
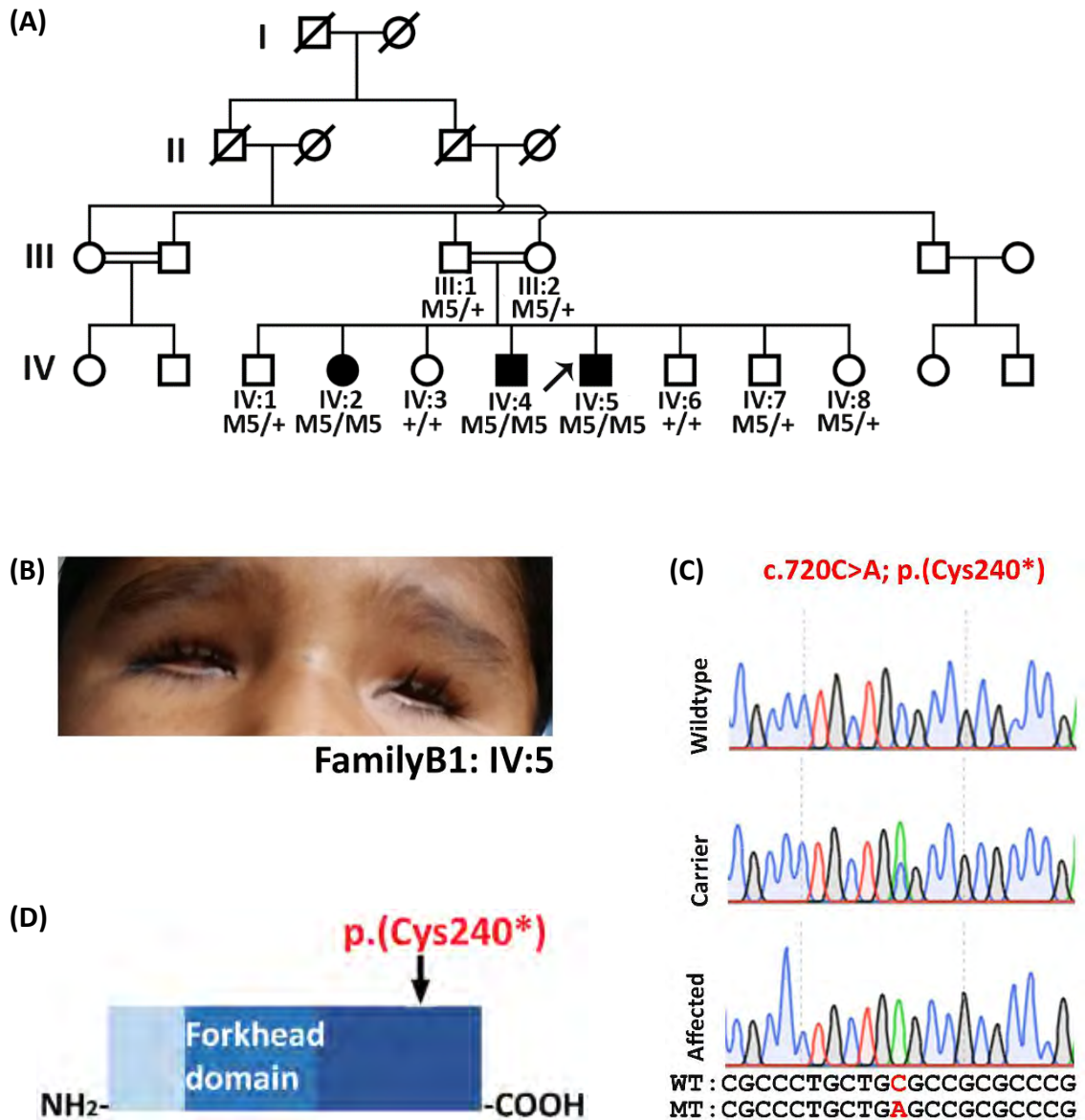
Figure 4.2: (A). Pedigree of Family B1 where arrow is indicating the proband and below each participating member is shown the segregation results. (B). Eye image of the proband IV:5 from family B1, presenting anophthalmic eyes. (C). Chromatogram of the variant M5 (c.720C>A; p.(Cys240*)) identified in *FOXE3* in wildtype, carrier and affected individuals. (D). Schematic representation of amino-acid change in protein domain of FOXE3 protein.
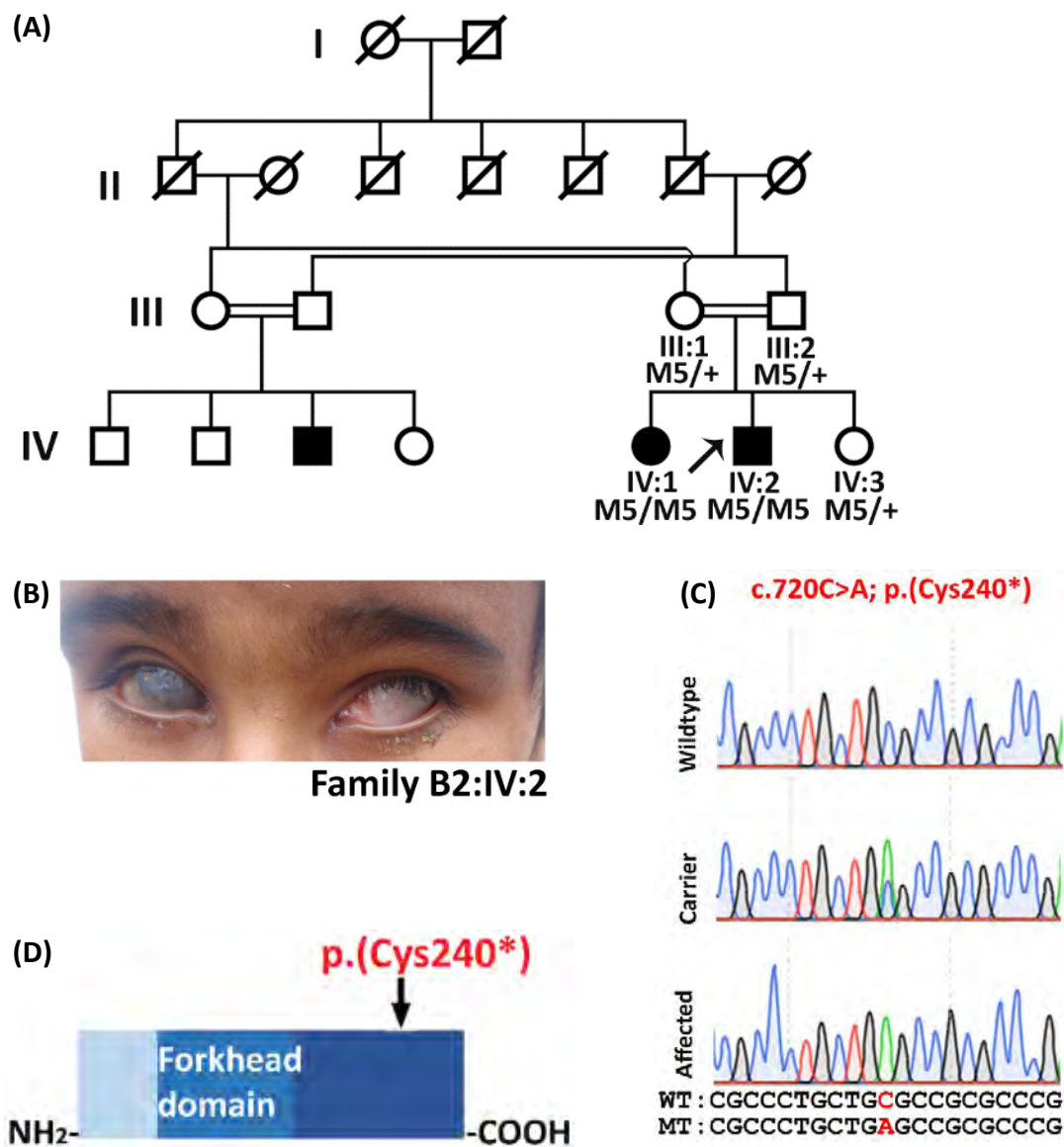
Figure 4.3: (A). Pedigree of Family B2 where arrow is indicating the proband and below each participating member is shown the segregation results. (B). Eye image of the proband IV:5 from family B1, presenting microphthalmic eyes with corneal opacity. (C). Chromatogram of the variant M5 (c.720C>A; p.(Cys240*)) identified in *FOXE3* in wildtype, carrier and affected individuals. (D). Schematic representation of amino-acid change in protein domain of FOXE3 protein.

Figure 4.4: (A). Pedigree of Family B7 where arrow is indicating the proband and below each participating member is shown the segregation results. (B). Eye image of the proband IV:2 from family B7, presenting microphthalmic eyes with corneal opacity. (C). Chromatogram of the variant M5 (c.720C>A; p.(Cys240*)) identified in *FOXE3* in wildtype, carrier and affected individuals. (D). Schematic representation of amino-acid change in protein domain of FOXE3 protein.

Figure 4.5: (A). Pedigree of Family B6 where arrow is indicating the proband and below each participating member is shown the segregation results. (B). Eye images of the proband III:3 from family B6, presenting microphthalmia. (C). Chromatogram of the variant M9 (c.289A>G; p.(Ile97Val)) identified in *FOXE3* in wildtype, carrier and affected individuals. (D). *FOXE3* missense variant p.(Ile97Val) affects an evolutionary conserved amino acid (Source: pBLAST) (E). Schematic representation of amino-acid change in protein domain of FOXE3 protein.

Figure 4.6: (A). Pedigree of Family B3 where arrow is indicating the proband and below each participating member is shown the segregation results. (B). Eye images of the all affected members V:2, V:3 and V:4 from family B2, presenting intra-familial heterogeneity. (C). Chromatogram of the variant M5 (c.720C>A; p.(Cys240*)) identified in *PXDN* in wildtype, carrier and affected individuals.
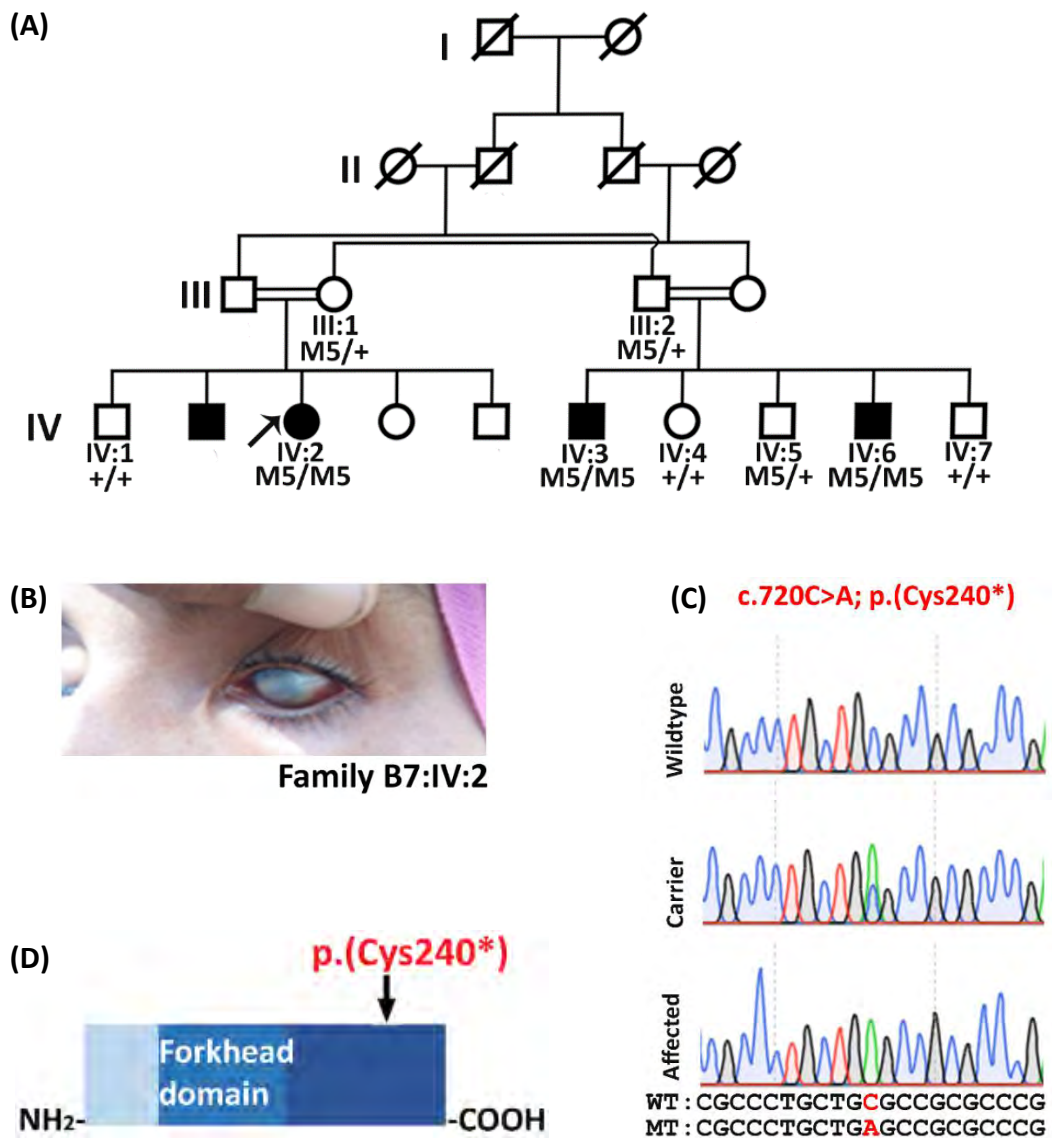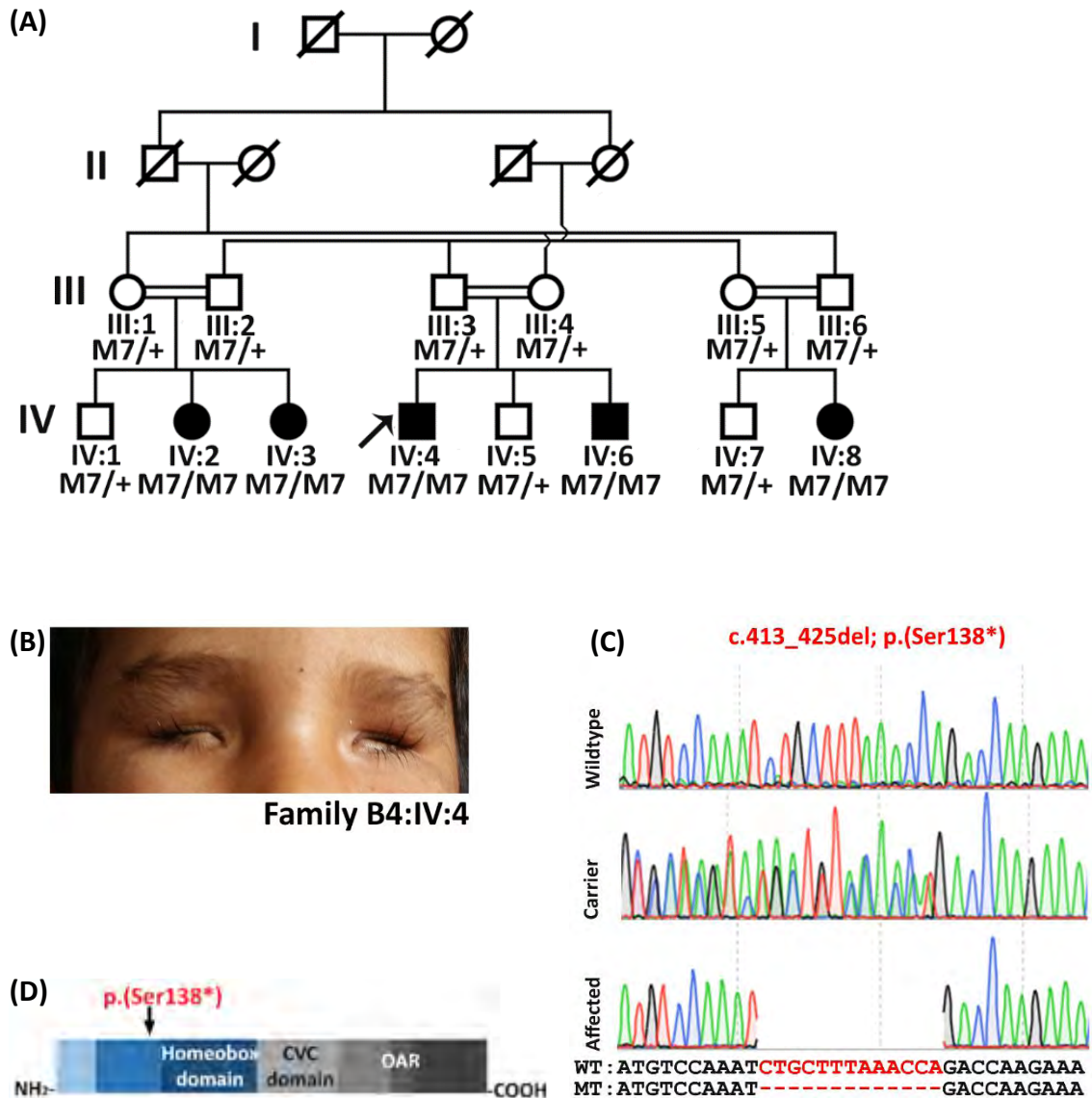
Figure 4.7: (A). Pedigree of Family B4 where arrow is indicating the proband and below each participating member is shown the segregation results. (B). Eye images of the proband IV:4 from family B4, presenting anophthalmia. (C). Chromatogram of the variant M7 (c.413_425del; p.(Ser138*)) identified in *VSX2* in wildtype, carrier and affected individuals. (D). Schematic representation of amino-acid change in protein domain of VSX2 protein.
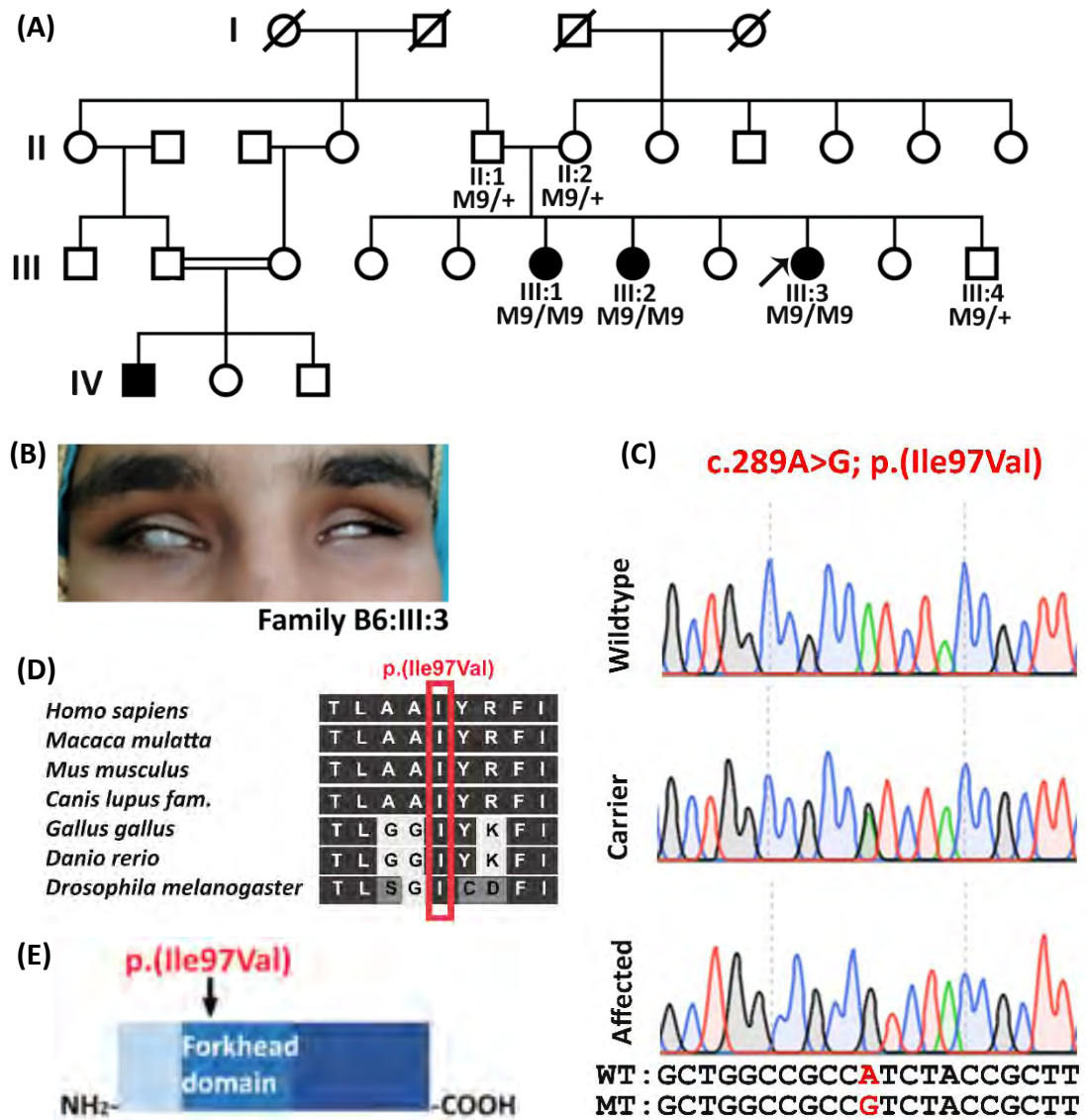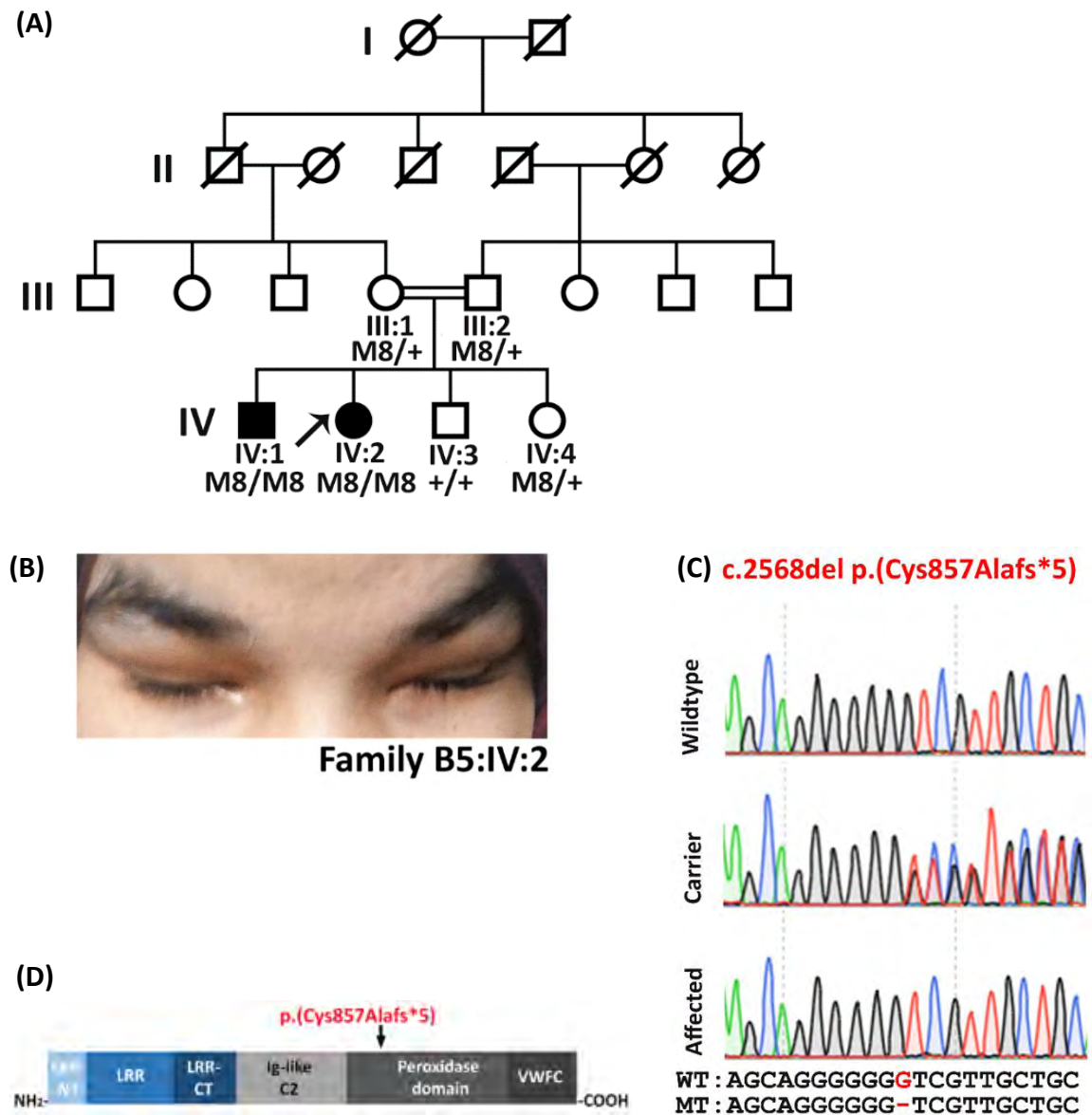
Figure 4.8: (A). Pedigree of Family B5 where arrow is indicating the proband and below each participating member is shown the segregation results. (B). Eye images of the proband IV:2 from family B5, presenting anophthalmia. (C). Chromatogram of the variant M8 (c.2568del; p.(Cys857Alafs*5)) identified in *PXDN* in wildtype, carrier and affected individuals. (D). Schematic representation of amino-acid change in protein domain of PXDN protein.
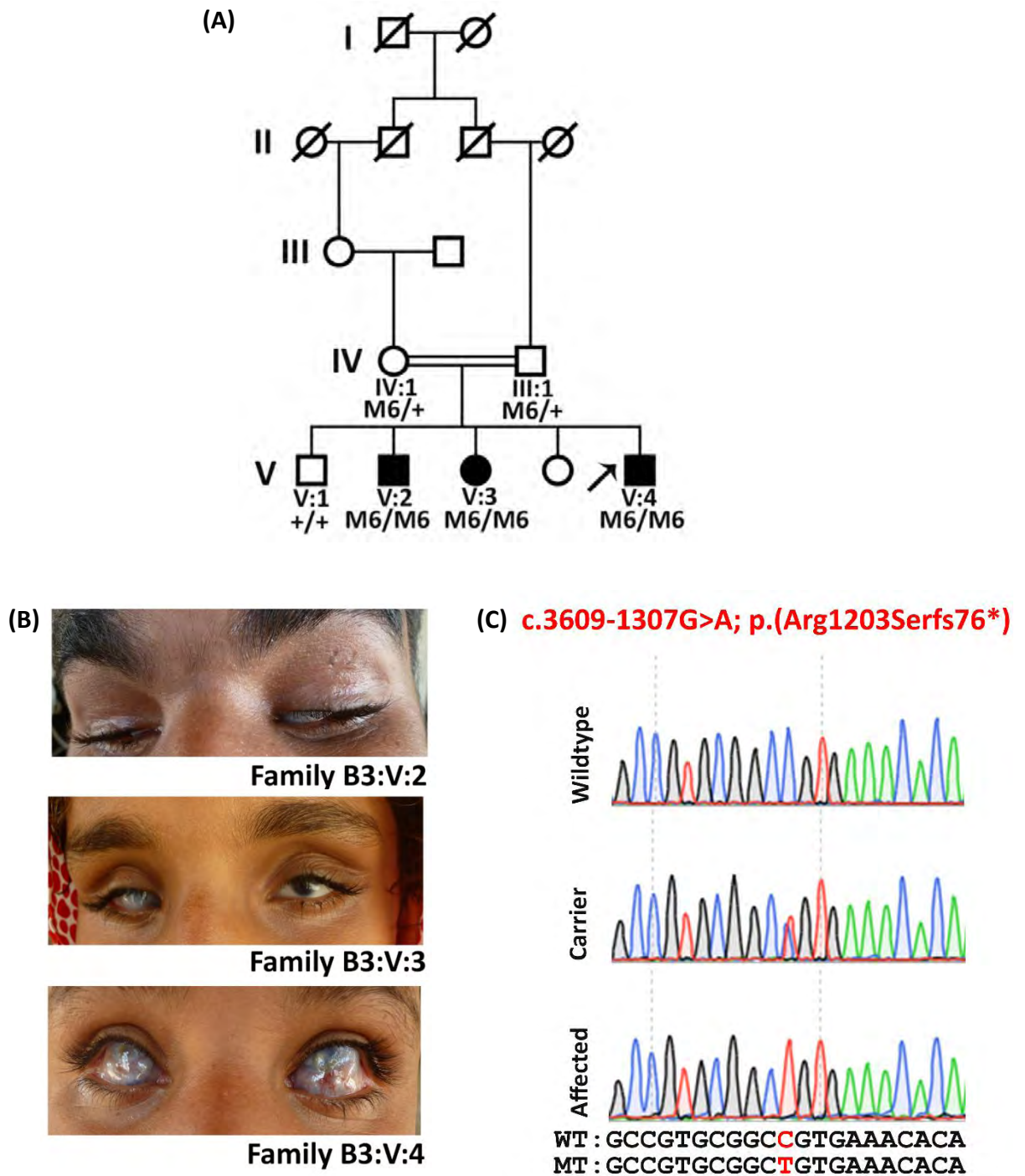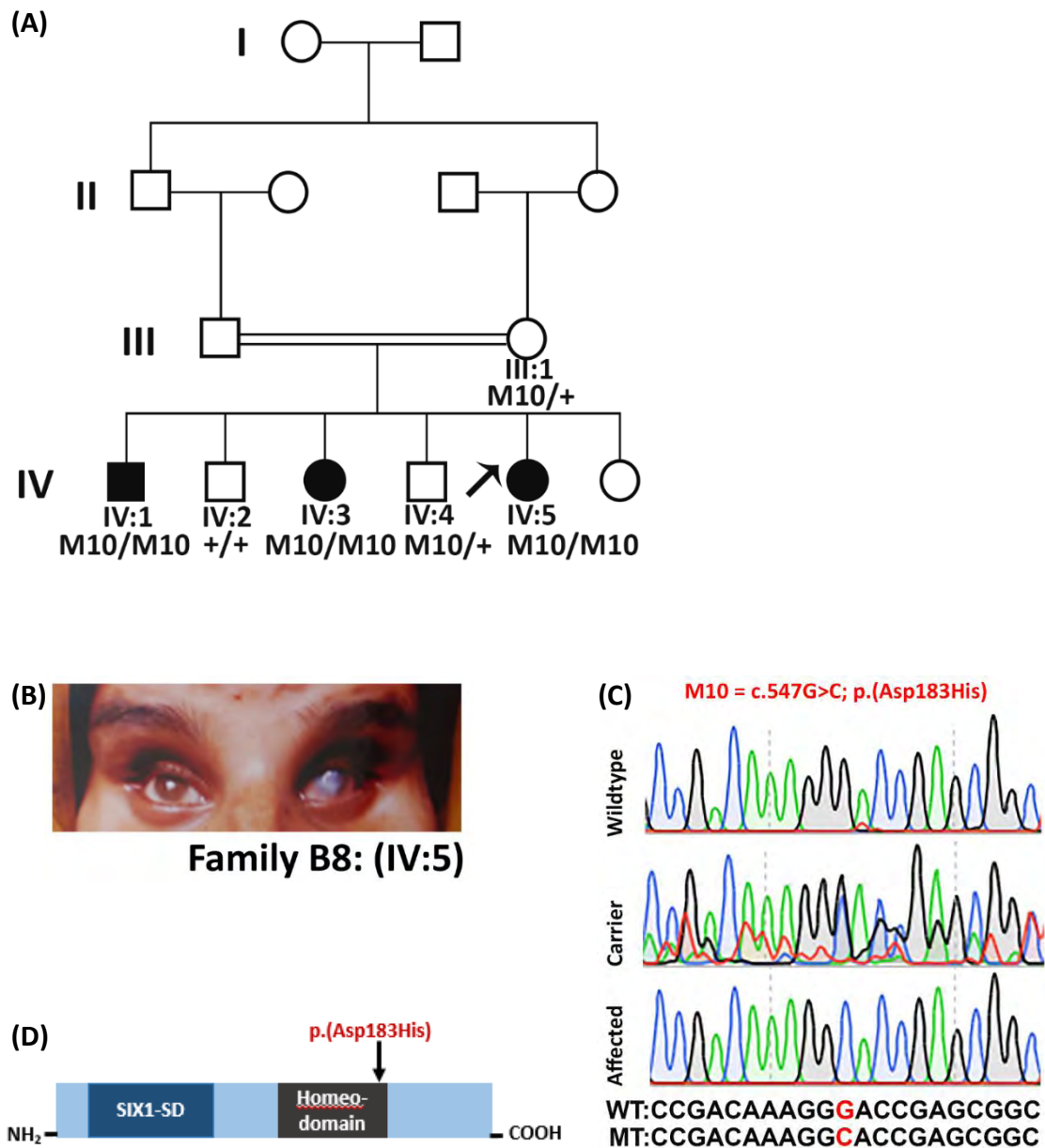
Figure 4.9: (A). Pedigree of Family B8 where arrow is indicating the proband and below each participating member is shown the segregation results. (B). Eye image of the proband IV:5 from family B8, presenting microphthalmic eyes with unilateral corneal opacity. (C). Chromatogram of the variant M10 (c.547G>C; p.(Asp183His)) identified in *SIX6* in wildtype, carrier and affected individuals. (D). Schematic representation of amino-acid change in protein domain of SIX6 protein.
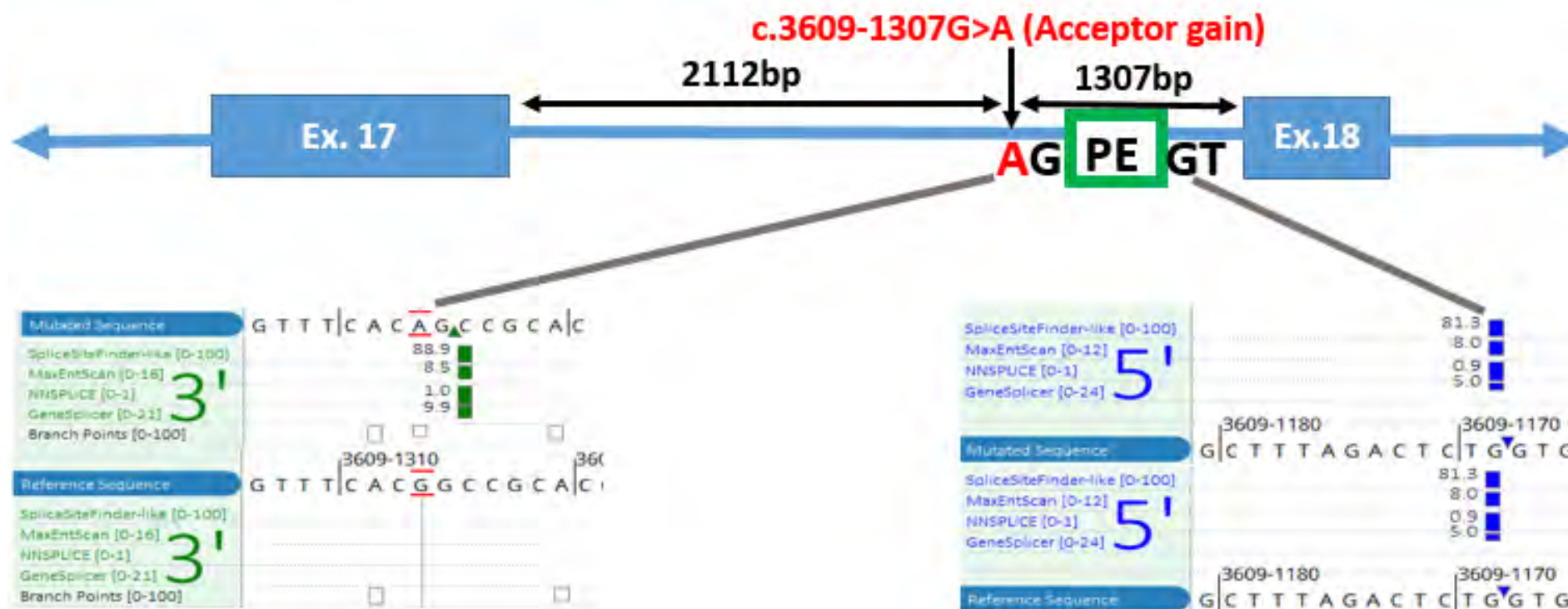
Figure 4.10: Schematic representation of deep-intronic variant (c.3609-1307G>A) identified in *PXDN* gene in family B3 along with the predicted acceptor gain scores from different splice predicting tools available (bottom left panel) and donor gain scores 137bp downstream to the identified variant (bottom right panel).
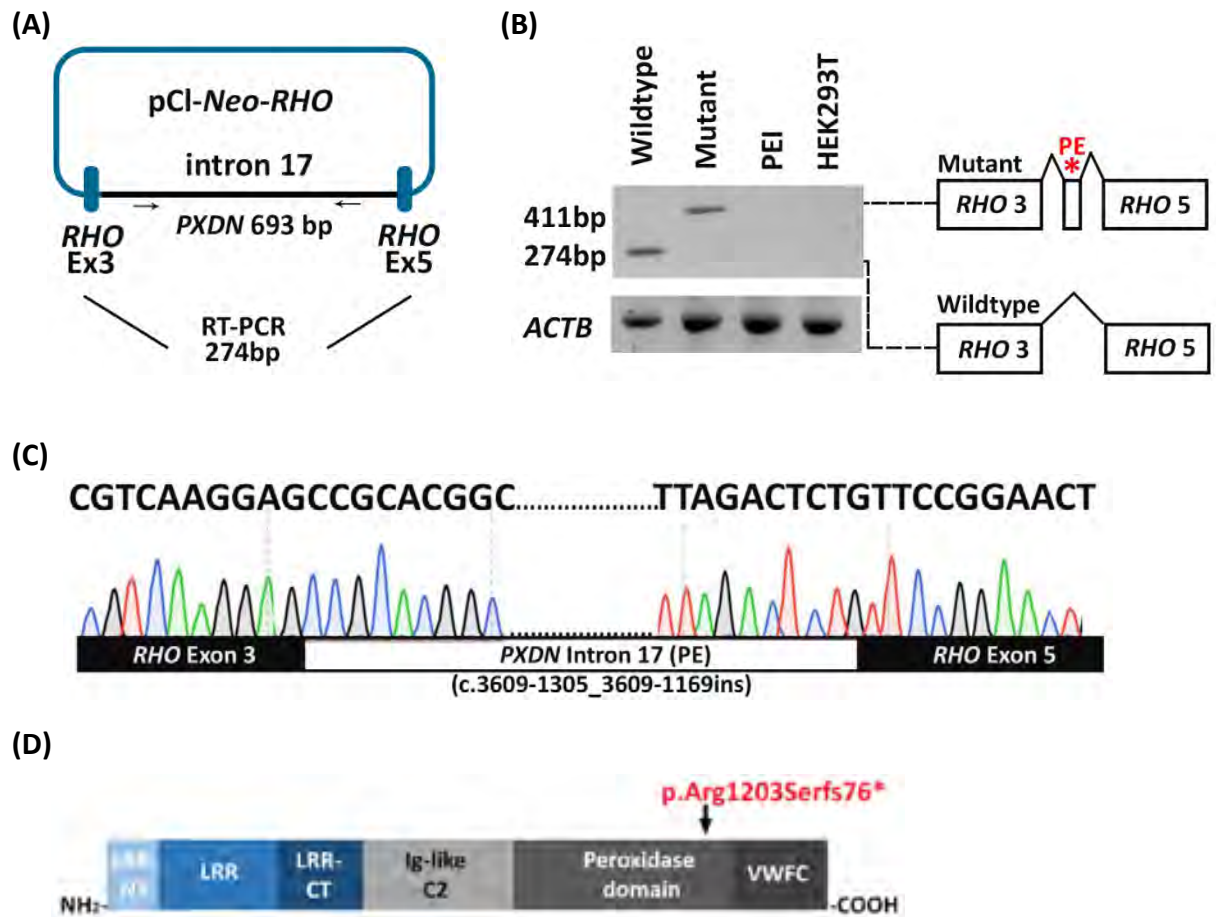
Figure 4.11: Results of the minigene splice assay with *PXDN* c.3609-1307G>A deep-intronic variant compared to wildtype. A minigene splice assay was performed in HEK293T cells to validate the effect of a deep-intronic splice variant identified in *PXDN*. The assay confirmed the activation of a 137bp out-of-frame pseudoexon (PE) (c.3609-1305_3609-1169ins; p.[Arg1203Serfs76*]) in intron 17 of *PXDN* as predicted by several *in silico* tools such as the SpliceAI, SpliceSiteFinder like, MaxEntScan, NNSPLICE, GeneSplicer. (A) Schematic illustration of the minigene construct. (B) Gel image showing wildtype (*RHO* exon 3 – *RHO* exon 5) and mutant (*RHO* exon *3* – pseudoexon (PE) – *RHO* exon 5) products amplified using *RHO* exon 3 and *RHO* exon 5 primers. (C) Sequencing chromatogram confirming the pseudoexon insertion in intron 17 of *PXDN*. (D) Probable effect of the PE in PXDN protein peroxidase domain.

Table 4.1: Clinical features of affected individuals from eight families affected with anophthalmia or microphthalmia.

Clinical feature	Family ID																						
	B1			B2		B3			B4					B5		B6			B7		B8		
	IV:2	IV:4	IV:5	IV:1	IV:2	V:2	V:3	V:4	IV:2	IV:3	IV:4	IV:6	IV:8	IV:1	IV:2	III:1	III:2	III:3	IV:2	IV:3	IV:1	IV:3	IV:5
Phenotype	A	A	A	M	M	M	M	M	A	A	A	A	A	A	A	M	M	M	M	M	M	M	M
ASD	NA	NA	NA	-	+	-	-	+	NA	NA	NA	NA	NA	NA	NA	-	-	-	+	+	-	-	-
Visual acuity	NA	NA	NA	PL	PL	NLP	PL	PL	NA	NA	NA	NA	NA	NA	NA	NLP	NLP	PL	PL	PL	PL	PL	PL
Corneal opacity	NA	NA	NA	+	+	+	RE	+	NA	NA	NA	NA	NA	NA	NA	+	+	+	+	+	-	RE	-
Cataract	-	-	-	-	-	-	-	-	-	-	-	-	-	-	-	-	-	-	-	-	BL	LE	LE
Flat nasal bridge	+	+	+	-	-	+	+	+	+	+	+	+	+	+	+	+	+	+	-	-	-	-	+

All cases were diagnosed with recessively inherited congenital bilateral anophthalmia or microphthalmia. No facial dysmorphism, intellectual disability or developmental delays were observed in any of the affected individuals. A, Anophthalmia; ASD, Anterior segment dysgenesis; BL, Bilateral; LE, Left eye; M, Microphthalmia; NA, Not applicable; NLP, No perception of light; PL, Perception of light; RE, Right eye; +, Present; -, Absent.

Table 4.2: *In silico* predictions for disease-causing variants identified in eight families affected with anophthalmia or microphthalmia.

Family ID	Gene	cDNA	Protein	gnomAD AF Total	gnomAD AF South Asian	CADD_ PHRED	REVEL	SpliceAI	ACMG/AMP	Reference
B1,B2,B7	*FOXE3*	c.720C>A	p.(Cys240*)	0.00001334 (Homo:0, Het:2)	0.0004148 (Homo:0, Het:2)	36	NA	NA	Pathogenic	Valleix et al., 2006
B3	*PXDN*	c.3609-1307G>A	p.Arg1203Serfs76*	0.000006571 (Homo:0, Het:1)	-	NA	NA	0.97 (AG)	Likely pathogenic	This study
B4	*VSX2*	c.413_425del	p.(Ser138*)	-	-	NA	NA	NA	Pathogenic	This study
B5	*PXDN*	c.2568del	p.(Cys857Alafs*5)	-	-	NA	NA	NA	Pathogenic	Khan et al., 2011
B6	*FOXE3*	c.289A>G	p.(Ile97Val)	0.000006695 (Homo:0, Het:1)	0.0002126 (Homo:0, Het:1)	24.9	0.77	NA	Pathogenic	Ullah et al., 2016
B8	*SIX6*	c.547G>C	p.(Asp183His)	-	-	31	0.83	NA	Likely pathogenic	Panagiotou et al., 2022

Candidate variants were identified in *FOXE3* (NM_012186.3), *PXDN* (NM_012293.3), *VSX2* (NM_182894.3) and *SIX6* (NM_007374.3). AG, Acceptor gain; CADD_PHRED, Combined Annotation Dependent Depletion PHRED score; cDNA, cDNA variant position based on the MANE select transcript; gnomAD AF South Asian, Allele frequency in the South Asian population according to the gnomAD (v.3.1.2) database; GnomAD AF Total, Allele frequency in the total population according to the gnomAD (v.3.1.2) database; Het, number of Heterozygotes; Homo, number of homozygotes; NA, Not applicable; SpliceAI, Splice prediction delta score; -, Absent.

5.0. NON-SYNDROMIC INHERITED RETINAL DYSTROPHIES (IRDS)

As described earlier, inherited retinal dystrophies (IRDs) are the types of eye disorders in which innermost layer of eye called retina is affected. IRDs are clinically heterogeneous and most common form of IRDs is retinitis pigmentosa (RP). The RP patients initially show nyctalopia (night blindness) and difficulty in adaptation with dark. The central part of the retina remains functional until middle age, therefore mostly complete vision loss occurs when RP patients reach middle age. However, in some cases central day vision is preserved due to residual function of some retained macular cone cells (Hamel, 2006). The hallmarks of RP include optic nerve waxy pallor, bone spicule pigment formation and retinal vessels attenuation. During early stages of disease, the fundus may comparatively appear normal but abnormal features appear later in life and exhibit variable degree of pigmentation. In some patients the pigmentation is localized towards mid-peripheral region while in others it is spread throughout the fundus (Verbakel et al., 2018). The attenuation of blood vessels in retina is believed to be an attribute due to less metabolic demands of the degenerating retinal cells. Alternatively, the degenerating photoreceptors are consuming less oxygen resulting in hyperoxic state of inner retina, this causes the vasoconstriction of retinal vessels (Yu and Cringle, 2005). OCT imaging also provides a valuable diagnosis and is also helpful in identification of other macular disorders from RP.

Early onset RP has both genetic and clinical overlap with patients affected with LCA. Therefore, age of onset can be an initial criterion for distinction between the two phenotypes. Mostly, LCA is defined as a severe vision loss at birth or within few months after birth and RP in some cases after infancy (at the age of one or two years), still there is an overlap at this age of onset (Kumaran et al., 2017). Other IRDs including cone-rod dystrophies also overlap with the clinical and genetic features of RP. Early symptoms of the disease like visual acuity, photophobia and achromatopsia (ACHM) can differentiate between RP and other cone-rod dystrophies (Hamel, 2007). Among the relatively stationary IRDs is CSNB. CSNB is predominantly characterized by dysfunctional rod photoreceptors. The patients affected with CSNB generally presents normal fundus but they have genetic overlap with RP patients (Zeitz et al., 2015). Approximately 341 genes are known to cause different forms of IRDs (Retnet: https://web.sph.uth.edu/RetNet/; assessed 22nd May, 2022). Many genes are

overlapping in different forms of RP. Therefore, clinical and genetic overlap makes diagnosis crucial for the specific forms of IRDs in different patients. In this section we have presented findings of 11 families (C1-C11) which are further grouped according to their clinical presentation.

5.1. Description and Clinical Features of IRD Families

Affected members of two families (C1, C2) were reported as completely blind since early childhood and before 1 year of age. Both the families present autosomal recessive mode of inheritance (Figure 5.1). All the affected individuals in both the families were completely blind with no perception of light. Additionally, the three affected members of family C2 (IV:4, V:1, V:3) were observed with corneal haze at the time of recruitment in this study. Details of observed clinical manifestations at the time of sampling of these two families are given in table 5.1.

However, affected members of six families initially presented night blindness and had progressive loss of day vision and were diagnosed as RP. All pedigrees showed consanguinity and autosomal recessive inheritance pattern except family C5 which shows X-linked inheritance (Figure 5.2). The family C3 had 2 affected members and their age of disease onset was between 1-2 years. Individual IV:1 lost the day vision at the age of 31 years and had no perception of light at the time of sample collection, whereas individual V:1 had visual acuity of 20/80 during day light at the age of 11 years. All the affected individuals of family C4 showed night vision loss with progressive loss of day vision. The progression of disease was slow in this family, as individuals with 35 years (oldest patient at the time of sampling) did not present complete loss of day vision. The patient VI:3 at the age of 11 years showed visual acuity of 20/40 at the day light, but later follow up investigation including OCT of patient IV:3 from family C4 detected retinal layer degeneration at the age of 21 years (Figure 5.3B). The average central retinal thickness (of inner circle) was reduced to 243.9μm (in right eye) and 253.3μm (in left eye), whereas average retinal inner circle thickness is 334.5μm in individuals without retinal abnormalities (Myers et al., 2015).

In family C5, the pedigree presents X-linked inheritance pattern, and both the affected individuals of this family showed complete vision loss in the 3rd decade of their life. Both affected individuals (VI:1 and VI:2) were male and showed complete day vision

loss with no perception of light at the age of 20 and 22 years respectively. The fundus images of individual IV:1 from family C5 showed dusty pigmentation with retinal vessel attenuation in both left and right eyes (Figure 5.4B).

The affected individuals of family C6 presented initial symptoms of RP in first decade of their life. Later at 30 years of age the female individual V:1 from the same family, completely lost day vision and was unable to see and recognize any objects around but can only sense light signal. The other 2 affected male members of this family (V:2 and V:4) with very low visual acuity, can only see objects present very close to eyes.

Similarly, affected members of family C7 presented progressive loss of day vision and all affected members above 40 years of age had complete day vision loss. However, the individuals below 30 years were able to see objects in day light. The fundus images of individual IV:4 taken at 52 years of age showed typical bone spicule pigmentation in left and right eye fundus images. Severe blood vessel attenuation was also observed in the fundus images of this individual (Figure 5.5B).

In family C8, two affected individuals were observed for clinical assessment. But only one patient (V:1) was selected for sample collecting for recruitment in this study, because the other affected female was too young and reluctant to participate. The affected individuals of this family were affected with night blindness and severe myopia at very early age (first decade of their life). Detailed clinical features for all affected individuals of these six RP families (Family C3-C8) are provided in table 5.2.

The pedigrees of families (C9-C11) showing autosomal recessive mode of inheritance are shown in figure 5.6. Two affected members of family C9 experienced night vision loss early in their life (Reported within few months after birth). While in their teen both individuals show intact day vision with reduced visual acuity. During follow-up of the patient (IV:1) after 6 years of initial sampling, no significant reduction in the day vision of the patient was observed (26 years). The fundus images of patient (IV:1) show mild dusty pigmentation more profound at the peripheral regions as compared to fovea (Figure 5.7B). While in OCT scan generalized retinal thinning was observed in both eyes along with severe degeneration of the outer retinal layer in the macular periphery, whereas the choroid appeared normal in anatomy and thickness (Figure 5.7C).

The affected members of two families C10 and C11 were reported with achromatopsia. All the affected members of both families were colour blind and presented photophobia. Though in some of the affected individuals the day vision is little compromised, and they had less visual acuity as compared to normal but in general their day and night visions were intact. No other additional features were observed in these two families. Detailed clinical features are enlisted in table 5.3.

5.2. Genetic Analysis of IRD Families

5.2.1. Family C1 with Novel *ATOH7* Variant

The family C1, since was reported with congenital blindness, therefore recruited as LCA family and initially screened through RP-LCA smMIPs panel as explained in the section 2.5.2. Through smMIPs based panel sequencing, no potential pathogenic variant was identified in this family therefore, proband VI:5 was then subjected to GS. In individual (VI:5) of family C1, three homozygous variants in *ATOH7*, *PAX6* and *SCO2* remained after variant prioritization from GS. *SCO2* and *PAX6* are associated primarily with autosomal dominant form of myopia (OMIM: 608908) and anterior segment dysgenesis (OMIM: 604229) respectively, which are not the observed phenotypes in this family. Moreover, *PAX6* (NM_001368894.2: c.865G>A; p.(Val289Ile)) variant did not segregate in the family and *SCO2* variant (NM_005138.3: c.341G>A; p.(Arg114His)) with the minor allele frequency of 0.000788571 is present in homozygous state in gnomAD database (Het: 118, Homo: 1) was not selected for further segregation analysis. *ATOH7* is known to be associated with non-syndromic retinal detachment causing congenital blindness (Ghiasvand et al., 1998). The novel frameshift variant (NM_145178.4: c.94del; p.(Ala32Profs*55)), identified in *ATOH7* segregated (Figure 5.8) and most likely explains the early onset of phenotype in family C1.

5.2.2. Family C2 with *NMNAT1* Variant

The proband V:1, from this family was screened through RP-LCA smMIPs based panel sequencing and variant prioritization identified a well-known LCA causing variant in *NMNAT1* in this family. In this family, a previously reported *NMNAT1* variant ((NM_022787.4: c.25G>A; p.(Val9Met)), was detected in a homozygous state (Falk et al. 2012). The identified variant segregated in the family and the segregating pattern in

the family along with the sequencing chromatogram is shown in figure 5.9. The details of variants identified in both families (C1 and C2) are provided in table 5.4.

5.2.3. Genetic Analysis Identified Novel and Known Variants in Six RP Families

Single proband (V:1, V:5, VI:1, V:4, V:1 and V:1) from all six (families C3, C4, C5, C6, C7, and C8) were initially screened through RP-LCA smMIPs based panel sequencing respectively. Two families were genetically explained with pathogenic variants residing in *TULP1*. In family C3, a known homozygous pathogenic variant (NM_003322.6: c.1444C>T; p.(Arg482Trp)), was identified (den Hollander et al. 2007) which segregated in the family (Figure 5.10). Another known homozygous nonsense *TULP1* variant (c.901C>T; p.(Gln301*)) was identified in proband (V:1) of family C7 in a homozygous state (Li et al., 2009b). However, this variant only segregated in one branch of the family. Screening of affected individual (IV:3) through RP-LCA smMIPs panel from the second branch identified a novel homozygous *MERTK* variant (NM_006343.3: c.436C>T; p.(Gln146*)), which segregated with the phenotype in this branch (Figure 5.5A). The segregation chromatograms are shown in figure 5.11A.

The family C6 was genetically solved with novel homozygous nonsense variant in *PROM1* (NM_006017.3: c.1649C>G; p.(Ser550*)). The segregation results for *PROM1* variant are shown in figure 5.12. However, in Family C4 a novel heterozygous, in-frame deletion (NM_006445.4: c.6920_6922del; p.(Glu2307del)), in *PRPF8* was identified in this which segregated with the phenotype in autosomal dominant pattern (Figure 5.3). *PRFP8* variants are already known to cause autosomal dominant RP. The oldest member of the family was 35 years of age but did not show progressive loss of day vision. Considering slow progression of the disease due to *PRPF8* variants as published previously (Verbakel et al., 2018), this family was considered genetically solved with identified novel heterozygous *PRPF8* variant.

In family C5, individual (VI:1) when initially screened through RP-LCA smMIPs panel, a homozygous variant was identified in *HGSNAT* (c.1843G>A; p.(Ala615Thr)), (NM_152419.3) with MAF 0.00353626 in gnomAD (2 homozygous/ 534 heterozygous alleles). *HGSNAT* is a known gene for RP (OMIM: 616544), but the variant found in family C5 is functionally proven to have negligible effect on the function of protein

alone (Fedele and Hopwood, 2010). This variant is associated with RP but in most cases it is found along with another mutation in the same gene and known as a hypomorphic mutation (Haer-Wigman et al. 2015; Carrera et al. 2021). In family C5 we have observed a severe form of RP where both the affected individuals lost their complete vision in 2nd decade of life. Even though the variant segregated in the family, considering the rapid progression of the disease we performed GS of the same proband form the family to identify any other potential pathogenic variant in the family. After variant prioritization, one novel variant (NM_001171971.3: c.785G>A; p.(Gly262Asp)), with MAF 0.000019721 (no homozygous/ 3 heterozygous alleles) identified in the known RP gene *CDHR1* (OMIM: 613660) was selected for segregation analysis. The *CDHR1* variant was absent in other affected individual (VI:2) and hence did not segregated in the family (Figure 5.4C). No other potential pathogenic variant was identified in the family, therefore we concluded that *HGSNAT* variant is responsible for the severe phenotype in family C5. The details of all the identified variants in RP families are provided in table 5.5.

Family C8 was initially screened with RP-LCA panel sequencing but we were unable to identify any potential pathogenic variant in this family. We later performed GS of the proband (V:1) and failed to identify any potential pathogenic SNV, CNV or SV after variant prioritization. We additionally looked for novel gene in this family. We selected all potential candidate variants with high pathogenic scores of CADD, PhyloP, REVEL and SpliceAI and class 3-5 variants according to ACMG/AMP guidelines. Then we looked up the expression of genes of prioritized variants in Human Eye Transcriptome Atlas (https://www.eye-transcriptome.com/) and also tried to identify pathogenic gene by looking up protein-protein interactions in string (https://string-db.org/) with any already known gene to cause RP. But we failed to identify any potential pathogenic variant in family C8 and therefore it remained unsolved in this study (Figure 5.13).

5.2.4. Genetic Analysis of CSNB and ACHM Families

Three families (C9-C11) were screened through panel sequencing. The family C9 was screened through RP-LCA smMIPs based panel while C10 and C11 were screened through MD smMIPs based panel sequencing as previously explained (Hitti-Malin et al., 2022). A known homozygous canonical splice site indel at acceptor site of exon 26

(NM_001297.5: c.2493-2_2495delinsGGC; p.(?)) in *CNGB1* was found in the family C8 (Maranhao et al., 2015). The predicted loss of acceptor site will likely result in skipping of exon 26 of *CNGB1* in affected members of family C9 (Figure 5.14B).

The two families affected with ACHM were screened through MD smMIPs panel and both the families are solved with *CNGA3* variants. In family C10, a known pathogenic variant (NM_001298.3: c.1315C>T; p.(Arg439Trp)), was identified in homozygous state (Reuter et al., 2008). While two known compound heterozygous variants (c.955T>C; p.(Cys319Arg); c.1306C>T; p.(Arg436Trp)) identified in family C11, genetically solved this family (Wissinger et al. 2001; Shaikh et al. 2015). All the identified variants in family C10 and C11, segregated in their respective families (Figure 5.15 and 5.16). *In silico* predictions and the details of identified variant in CSNB and ACHM families are given in table 5.6.

5.3.   Discussion

IRDs are clinically and genetically heterogenous group of inherited ocular disorders which are further subdivided in two different types based on clinical presentation. The most severe and earliest appearing form of IRDs is LCA and it causes childhood blindness. LCA has broad range of expression variability, but certain genes causing LCA show similar phenotypes and hence it may become easy to narrow down the number of genes for the initial screening. In total 14 genes are known to cause LCA, out of which one is responsible for autosomal dominant form of LCA while other 13 are responsible for autosomal recessive form of LCA. There are no genes which are known to cause X-linked LCA (Retnet: https://web.sph.uth.edu/RetNet/; assessed 22nd May, 2022).

However, the main hurdle in the genetic screening of LCA is that there are other ocular defects which appear phenotypically similar to LCA causing congenital blindness. The family C1 which was diagnosed with LCA in our cohort of 28 families, was identified with a 1-bp deletion in *ATOH7* gene. *ATOH7* is an intron-less transcription factor which has a DNA binding region. It binds to the gene promotor and gene enhancer elements and regulates the transcription of RGC determinant genes. It is thought to be involved in RGCs development, survival and determination though exact mechanism through which *ATOH7* regulates RGCs' development is still unknown. *ATOH7* is an auto-regulated gene as it binds to its own promotor and enhancer regions (UniProt:

https://www.uniprot.org/, assessed on 20th June, 2023). This gene in known to cause persistent hyperplastic primary vitreous (PHPV), a developmental disorder in which failed regression of primary vitreous results in the formation of fibrovascular membrane behind the eye. This fibrovascular layer is an abnormal development and exerts a pull on the retina causing retinal detachment. The retinal detachment separates retina from the underlying layers cutting off the blood supply to retina leading to non-functional retinal layer causing vision loss. In some cases, PHPV resulted in under-developed retina where retina initially fails to attach to the underlying tissues leading towards congenital retinal nonattachment (Reese, 1955; Pruett, 1975; Haddad et al., 1978; Shastry, 2009). In chicken, it was observed that ectopic expression of human *ATOH7* resulted in earlier formation of nerve cells by speeding up the differentiation of undifferentiated cells and encouraging their cell cycle exit, and also by expanding the neurogenesis area in retina. These findings also provide insight into the role of *ATOH7* in development of nerve cells in retina (Zhang et al., 2018). The novel pathogenic variant identified in *ATOH7* gene in affected members of family C1 will most probably result in the early truncation of protein causing loss of important bHLH domain in the protein (Figure 5.8C) required for DNA binding of this transcription factor. (Atac et al., 2022) provided an overview of the variants identified in *ATOH7* and their association with different phenotypes. Mostly missense variants are known to cause optic nerve hypoplasia, PHPV or foveal hypoplasia (FVP), while frameshift and truncating variants are associated with non-syndromic congenital retinal nonattachment (NCRN). The fundus or OCT scans for family C1 are not available, therefore it is difficult to exactly identify the possible phenotypes such as PHPV, FVP or NCRN caused by this specific 1-bp deletion leading towards congenital blindness. But no other phenotypic variations such as microphthalmia, glaucoma, anterior segment dysgenesis or corneal opacity were observed as previously explained by other affected Pakistani families harbouring *ATOH7* mutations (Khan et al., 2012).

In family C2, a variant (c.25G>A; p.(Val9Met)) in *NMNAT1* was identified which is already known in Pakistani and other populations (Falk et al., 2012; Hedergott et al., 2015). The *NMNAT1* variants are responsible for early onset of retinal degeneration causing LCA and complete vision loss occur in first or second decade of life (den Hollander et al., 2008; Kumaran et al., 2017). *NMNAT1* encodes an enzyme which is

ubiquitously expressed in all cells. This enzyme is responsible for providing energy by regenerating $(NAD)^+$ in the cell nucleus and is involved in cell signalling and DNA metabolism. Since NMNAT1 is ubiquitously expressed it is still difficult to explain that the absence of *NMNAT1* or dysfunctional *NMNAT1* only induces retinal degeneration. Although two other paralogues of *NMNAT1* with similar functions are *NMNAT2* and *NMNAT3* but these reside in Golgi complex and mitochondria respectively (Berger et al., 2005; Lau et al., 2009). It has been experimentally proved that *Nmnat1* knockout mice are lethal while in Drosophila photoreceptors lacking nmnat causes photoreceptor degeneration (Zhai et al., 2006; Conforti et al., 2011). The variant p.(Val9Met) was functionally tested and this variant does not affect the nuclear localization of the protein, as shown in figure 5.9C, the variant is not residing in the nuclear localization signal region of the protein. But the enzyme activity of the NMNAT1 protein is significantly reduced in mutant protein harbouring p.(Val9Met) variation as compared to the wildtype protein (Falk et al., 2012). This indicates that NMNAT1 protein is required for normal retinal function and this particular variant is causing dysfunctional NMNAT1 protein. Recently, the retinal structure and function was rescued in mice harbouring p.(Val9Met) variant in Nmnat1 when supplemented with adeno-associated virus (AAV) containing normal human *NMNAT1* copy through subretinal injections (Greenwald et al., 2020). This initial study is an indication that *NMNAT1* associated LCA can be treated but rapid detection is required as due to early onset of the disease we have narrow therapeutic window.

RP, which is also a common form of IRD is inherited in all three forms of Mendelian inheritance. In addition to these Mendelian inheritance, incomplete dominance and digenic cases of RP have also been observed (Wang et al., 2001; Hamel, 2006). Approximately 87 genes and 7 loci are known to be associated with RP (Retnet: https://web.sph.uth.edu/RetNet/; assessed 18th August, 2023) yet 60% of the RP cases remained unsolved. This indicates that still many genes responsible for causing RP are yet to be identified. It is estimated that half of the RP cases (50%) are sporadic in most populations (Kim et al., 2021b) and genetic heterogeneity and overlapping clinical features makes it critical to identify the disease causing variants. The implementation of panel-based gene sequencing has proven effective in genetic diagnosis of retinal dystrophies (Glockle et al., 2014). Here, in this study we performed smMIPs based

panel sequencing of 113 RP and LCA related genes as previously explained (Panneman et al., 2023) to identify the disease causing variant in six consanguineous RP suspected families of Pakistani origin.

Previous studies showed that *RPE65* and *TULP1* are the most frequently mutated genes known to be associated with Pakistani RP affected families (Li et al., 2017). In our small cohort of 6 RP families, two families (Family C3 and C7) were identified with *TULP1* known variants. The family C3, was identified with known homozygous *TULP1* variant (c.1444C>T; p.(Arg482Trp)) with a frequency of 0.00001314 in all populations but absent in South Asian population. This mutation was first identified in Surinamese family in compound heterozygous state with another 11-bp frameshift mutation (p.(Leu504fs*140)) in *TULP1* (den Hollander et al., 2007). Later this variant was identified in Chinese population twice in compound heterozygous state along with the variants (p.(Arg440*)) and p.(Arg400Trp) in *TULP1* (Chen et al., 2013; Wang et al., 2015). Recently, Hull et al., (2020) identified this variant again in compound heterozygous state in combination with p.(Leu461Pro) variant in *TUPL1* gene. So, to the best of our knowledge this variant is first time identified in homozygous state in Pakistani family affected with RP. However, a different mutation responsible for the amino acid change at similar position (c.1445G>A; p.(Arg482Gln)) in TULP1 protein is already known in Pakistani population causing early onset autosomal recessive RP (Ajmal et al., 2012). Through structural analysis Amjad et al, (2012) indicated that p.(Arg482Gln) most probably will destabilize the mutant protein and will cause severe consequences on the normal function of the protein. Moreover, amino acid Arg482 is present in the signature sequence among 11 highly conserved amino acids of the tubby domain of TULP family proteins (North et al., 1997). The affected female proband (V:1) from the right loop of the family C7 (Figure 5.5A) when screened through RP-LCA smMIPs panel sequencing resulted in the identification of variant (c.901C>T; p.(Gln301*)) in homozygous state in *TULP1* gene. The variant did segregate in this loop of the family while the other loop remained genetically unexplained. Another proband (IV:4) from the same extended family when screened later through RP-LCA panel was identified with homozygous nonsense variant (c.436C>T; p.(Gln146*)) in *MERTK* gene. All the affected and normal individuals from this loop of the family harbours the normal wildtype allele for the *TULP1* variant. Likewise, all the

participating members from the left loop of the family were homozygous for normal wildtype allele for *MERTK* variant (Segregation pattern shown in figure 5.5A and chromatograms are shown in figure 5.11A). Here, we have observed the phenomenon of intra-familial locus heterogeneity, where two different variants in two different genes are explaining the similar phenotype underlying a Mendelian trait. Such phenomenon of intra-familial and inter-sibship familial locus heterogeneity was previously explained in 10 Pakistani families affected with hearing impairment (Rehman et al., 2015). Large consanguineous families with rare autosomal recessive disorders are frequently genetically explained by linkage analysis and homozygosity mapping approaches (Alkuraya, 2010), but such studies are frequently hindered by different issues. It is difficult to genetically solve families with intra-familial heterogeneity using homozygosity mapping and linkage analysis. However, Rehman et al. (2015), also provided a solution to tackle such issues by analysing such families in small family loops, which again cannot be used for inter-sibship familial locus heterogeneity. Gene based panel sequencing can be a time efficient and cost-effective approach to solve such families with proper selection of individuals from different loops.

All the TULP family proteins play important role in embryonic development and proper functioning of the central nervous system. TULP1 specifically is highly expressed in retina and resides in the inner segments where it is involved in trafficking of proteins mainly rhodopsin. It basically transport proteins by connecting cilium in the inner segment of the photoreceptor cells to the outer segments (Hagstrom et al., 2001; Xi et al., 2005). As thoroughly reviewed by Verbakel et al. in (2018), the RP patients harbouring *TULP1* variants has age onset of disease before 5 years. Our findings are also in line and both families identified with *TULP1* variants present disease phenotype before 5 years of age.

In normal human eye physiology, the photoreceptor cells present at the outer segment of the retina are prone to photooxidative damage. Therefore, damaged and aged photoreceptor cells are shed and phagocytosed by RPE cells for recycling. *MERTK* is an important gene present on chromosome 2, which encodes a 999 amino acid long receptor tyrosine-kinase Mer. This is a transmembrane protein which regulates the phagocytotic activity of apoptotic cells, expressed in RPE and facilitates the phagocytosis of damaged photoreceptor cells in RPE (Feng et al., 2002; Kevany and

Palczewski, 2010). Tulp1 protein is a proven ligand to MerTK to initiate phagocytosis of photoreceptor cells in RPE (Caberoy et al., 2010). Since *TULP1* and *MERTK* both participates in the same pathway, hence the similar phenotype in all the affected members of family C7 either harbouring *TULP1* homozygous variant or *MERTK* homozygous variant is well explained. Both *TULP1* variant p.(Gln301*) and *MERTK* variant p.(Gln146*) with their premature termination codons will most probably be responsible for NMD with complete loss of protein or will produce a truncating proteins with the loss of important and functional protein domains rendering them non-functional.

In the family C4, autosomal recessive mode of inheritance was observed but all the affected individuals were males (n=6) i.e., more affected males in the pedigree is also compatible with X-linked inheritance pattern (Figure 5.3). The disease progression was slow in the affected individuals of this family. In all the affected individuals, visual acuity of day vision reduced but none of the affected individuals lost complete day vision even at the age of 35 years when initially sampled and family history recorded. Therefore, initially this family was diagnosed with CSNB. RP-LCA panel-based sequencing revealed a novel heterozygous *PRPF8* inframe deletion (c.6920_6922del) in family C4. *PRPF8* inframe deletion identified in the family was likely pathogenic according to ACMG/AMP guidelines and segregated in the family in autosomal dominant manner. The gene is already known for autosomal dominant RP (Retnet: https://web.sph.uth.edu/RetNet/). But in the pedigree parents of generation (V) are phenotypically normal. Follow-up studies for the parents of this generation was not possible because they were deceased when follow-up was performed for OCT scan. Since the genetic screening of generation (V) parents is not performed, we cannot identify whether it is a case of incomplete dominance and their parents remain asymptomatic even after carrying mutation. Moreover, there is a possibility that one of the parents was affected with mild RP which remained unnoticed throughout their life span. Previous reports, indicated that patients with *PRPF8* mutations show slow progression and in most cases their visual acuity remain normal even at 3rd and 4th decade of life and they lose complete vision at the 7th decade in their life (Verbakel et al., 2018). As discussed earlier, the affected members of this family showed slow

disease progression is also an indication that the identified *PRPF8* variant is the potential pathogenic variant in this family.

PRPF8 is one of the six pre-mRNA processing factor (*PRPF*) proteins which are known to cause autosomal dominant RP. The spliceosome complex formed during splicing is composed of 5 small nuclear ribonucleoproteins (snRNPs) which are U1, U2, U4, U5, U6 and many other protein factors. *PRPF8* encodes one of the components of U5 snRNP (Liu et al., 2006). *PRPF8* was associated with autosomal dominant RP for the first time in 2001 (McKie et al., 2001) and 64 mutations are known to be associated with autosomal dominant RP to-date. Most of the mutations identified in PRPF8 are residing towards the C-terminal of the protein. The C-terminal of the protein contains a Jab1/MPN domain, region of PRPF8 protein which interacts with SNRNP200 (another snRNP protein required for spliceosome complex formation) for unwinding of U4/U6 duplex for proper spliceosome complex activation (Yang et al., 2021). According to (Wang et al., 2022) the macular region of the RP patients harbouring *PRPF* mutations is more affected than other autosomal dominant RP patients. The OCT scan of the affected member IV:3 of this family (Figure 5.3B) also showed similar results with reduced central macular thickness of the retinal layer.

In family C5, we observed X-linked pattern of inheritance, where all affected members are male and mothers of affected individuals are linked in the pedigree. It was also noted that in family C5, generation V has more male members and generation VI has only male members which is creating a gender bias. Hence, there is a possibility of autosomal recessive pattern of inheritance over-interpreted as X-linked. For the genetic diagnosis in this family initially RP-LCA panel based sequencing was performed which resulted in the identification of disease causing variant (c.1843G>A; p.(Ala615Thr)) in *HGSNAT* gene in homozygous state. *HGSNAT* gene is located on chromosome 8 and was first time associated with nonsyndomic RP in 2015 (Haer-Wigman et al., 2015). Previously *HGSNAT* variants were known to cause mucopolysaccharidosis Type IIIC (MPS IIIC) or alternatively known as Sanfilippo syndrome Type C. MPS IIIC is characterized by hearing impairment, vision loss, sleep disorders, seizures, skeletal, developmental and neurologic defects which are the result of heparan sulfate accumulation in the tissues. HGSNAT protein is involved in the degradation of heparan sulfate by its acetylation (Valstar et al., 2008; Feldhammer et al., 2009). The variant

p.(Ala615Thr) is residing in the transmembrane towards the C-terminal of the protein and the variants in the hydrophobic transmembrane domains may result in the misfolding of the protein leading it to reside in the endoplasmic reticulum (Feldhammer et al., 2009). But the functional assays have indicated that the p.(Ala615Thr) change does not alter the size of the protein and the enzymatic activity is also retained upto 60% (Fedele and Hopwood, 2010). Haer-Wigman et al., (2015) also observed the nonsyndromic RP patients with *HGSNAT* variants slow reduced blood leukocyte enzymatic activity while MPS IIIC patients have higher enzymatic activity as compared to healthy control. Through this, it can be proposed that retina requires higher enzymatic activity from HGSNAT as compared to other tissues. The variants in *HGSNAT* are known to cause pericentral RP where pigmentation is profound towards the peripheral region of retina (Comander et al., 2017). Moreover, HGSNAT variants in general are known for slow progression of the disease and the identified variant p.(Ala615Thr) is specifically known for mild nonsyndromic RP and is also found in asymptomatic carriers even at age 73 (Zlotogora et al., 2023). Contrary to these findings, both the affected individuals (VI:1 and VI:2) from the family C5 showed early onset with rapid progression of the disease leading to complete vision loss in early 2nd decade of their life. The fundus images of the proband also indicated that the individual is not affected with pericentral RP but pigmentation is observed in peripheral as well as central region of the retina. Considering the fact that p.(Ala615Thr) variant in *HGSNAT* in not a severe variant hence might not be the only cause of severe phenotype observed in the patients of family C5, we additionally performed GS of the proband VI:1. After variant prioritization, we identified a potential pathogenic variant (c.785G>A; p.(Gly262Asp) in *CDHR1* in homozygous state. *CDHR1* variants are known to cause RP, cone dystrophy or cone-rod dystrophy (Stingl et al., 2017). But the variant was absent in another affected individual (VI:2) hence did not segregate with the phenotype. No other potential pathogenic variant was identified in this family and hence we fail to identify any other genetic modifier to explain the severity of phenotype in the family C5. *HGSNAT* variants have been known to cause mucopolisacaridosis but no variants in *HGSNAT* are yet found to be associated with nonsyndromic RP in Pakistani population. To the best of our knowledge, this is the first study explaining *HGSNAT* hypomorphic homozygous variant to be associated with severe nonsyndromic RP in a Pakistani family.

In the family C6, a novel homozygous nonsense variant (c.1649C>G; p.(Ser550*)) was identified in *PROM1* through RP-LCA panel based sequencing. PROM1 is known to cause autosomal dominant cone or cone-rod dystrophies and macular degeneration while it is also known to cause autosomal dominant RP (Retnet: https://web.sph.uth.edu/RetNet/sum-dis.htm). *PROM1* encodes a transmembrane glycoprotein which is expressed in progenitor and hematopoietic stem cells. It is also expressed in retinoblastoma and adult retinal cells and is located on the apical surfaces of the cell (Miraglia et al., 1997). This gene was first time reported with retinal degeneration in 2000, where siblings carrying homozygous frameshift deletion were affected with severe early-onset retinal degeneration while the mother harbouring heterozygous deletion presented late onset unilateral retinal degeneration (Maw et al., 2000). This is a clear example where same *PROM1* variant is responsible for autosomal dominant and autosomal recessive forms of retinal degeneration. The variant identified in the first study associated it with retinal degeneration was predicted to truncate protein after 614 amino acid residues. The nonsense variant (c.1649C>G; p.(Ser550*)) identified in our family C6 most probably will cause the NMD of the transcript or may produce a truncated protein. The protein truncation at 550 amino acid causes loss of extracellular, transmembrane and cytoplasmic domains towards the C-terminal of the protein, but this variant has not shown any diseased phenotype in mother carrying heterozygous variant. Recently, 10 Japanese families with cone-rod dystrophies and macular degeneration are associated with *PROM1* variants (Fujinami et al., 2020). Although, the identified variant p.(Ser550*) in our family is novel but the variants in this gene are already reported to cause autosomal recessive RP in Pakistani population (Zhang et al., 2007). The phenotype of the previously reported Pakistani RP family harbouring a different nonsense PROM1 mutation p.(Gln576*) (Zhang et al., 2007) had severe and rapid progression of disease where severe central vision loss was observed in 2nd decade of their life with visual acuity of 6/120 at ages between 15-44 years. In our family C6, severe phenotype was observed in female affected individual (V:1) which has severely affected day vision at the age of 30 years and can only sense light signal. While the both affected males (V:2 and V:4) show reduced visual acuity 20/40 and 20/60 respectively, but their day vision is relatively remained intact even at 26-28 years.

In the family C8, we fail to identify any potential pathogenic variant in already known RP genes during initial variant prioritization. Later we looked for other genes known to cause different forms of eye disorders but failed to identify any potential pathogenic variant in this family. All identified genes with class 3-5 variants according to ACMG/AMP guidelines were also checked for expression in Human Eye Transcriptome Atlas (https://www.eye-transcriptome.com/). Additionally, class 3-5 variants were also checked for their protein-protein interactions in string (https://string-db.org/) to establish any relation of the genes with already known gene to cause RP. But we failed to identify any potential pathogenic variant in family C8 and therefore the phenotype of this family remained genetically unsolved. Additionally, the affected individuals of family C8 manifest high myopia, therefore there is a possibility that the family was misdiagnosed as RP, while it was affected with myopia only (since patients were very young and oldest individual has 7 years of age). The genetic diagnosis of myopia is complex as limited studies are available. In our small family C8, only two affected individuals were present, and sample was available from only one individual. Therefore, the identification of myopia related variant is not possible at this age and further studies are required to solve the patients from this family. For further genetic analysis in future, long read sequencing can be performed to identify if any heterozygous deletions were missed in short read GS or alternatively multi-omics approaches can be used to identify any epigenetic causes of the disease in the family C8.

CSNB is the non-progressive form of IRDs, characterized by dysfunctional rod cells resulting in loss of signal transduction between bipolar and photoreceptor cells. The clinical features include night blindness with refractive errors, reduced visual acuity during day light and often accompanied by strabismus or nystagmus (Zeitz et al., 2015). Recently it has been observed that CSNB affected children before school age presented myopia, strabismus and nystagmus but did not complaint about night vision loss. Later genetic testing and full-field ERG revealed CSNB in those children (Miraldi Utz et al., 2018). Many features of CSNB are also overlapping with other IRDs therefore accurate diagnosis is of prime importance for the prediction of future visual outcomes.

In family C9 an already known homozygous canonical splice site indel (c.2493-2_2495delinGGC; p(?)) in *CNGB1* was identified through RP-LCA panel sequencing.

CNGB1 is a gene containing 33 exons and encode β-subunit of cyclic nucleotide-gated (CNG) channel. These are the rod specific gated channels which regulate the flow of cations during phototransduction (Biel et al. 1996). The identified variant (c.2493-2_2495delinGGC; p(?)) will most probably result in the skipping of exon 26 (Figure 5.14B) which is predicted to introduce a frameshift in the open reading frame (ORF) creating PTC. The PTC will either produce a truncating protein with the loss of transmembrane and CNBD domains at the C-terminal of the protein or will cause NMD of the pre-mRNA resulting no protein. Previously, two different studies have reported the same variant in *CNGB1* gene with RP (Maranhao et al., 2015; Li et al., 2017). A different canonical splice site variant (c.2493-2A>G; p(?)) with a similar predicted effect of exon 26 skipping has also been reported with RP in another Pakistani family (Maria et al., 2015). The affected individuals of the family C9 in this study, show reduced visual acuity but no peripheral loss of day vision was observed in both patient (oldest 26 years). Recently, *CNGB1* variants are also found associated with CSNB in two separate studies (Ba-Abbad et al., 2019; Kim et al., 2021a). In one of these studies, a 61-year old woman harboring *CNGB1* one missense and one truncating variant in trans was asymptomatic. But ERG showed delayed rod responses while cone related responses were normal (Ba-Abbad et al., 2019). Fundus images and ERG results are also used to categorize CSNB into four types; fundus albipunctatus, Oguchi, Riggs type and Schubert-Bornschein. The Riggs type and Schubert-Bornschein are the types where fundus images appear normal, and recently Riggs type CSNB was genetically explained with *CNGB1* variant in Korean population (Kim et al., 2021a). The fundus images of proband IV:1 from family C9 does not have Riggs type and Schubert-Bornschein appearance but the dusty pigmentation was present in the peripheral region of fundus, an indication to rod dysfunction. To the best of our knowledge this is the first study highlighting the role of *CNGB1* variant with CSNB in Pakistani population.

Another protein encoded by *CNGA3* forms the α-subunit of the CNG channel and is specifically expressed in cone photoreceptors where it is involved in the phototransduction cascade (Reuter et al., 2008). *CNGA3* is known to be associated with 25% achromatopsia (ACHM) cases which are characterized by partial or complete color blindness, nystagmus and photophobia during daylight (Wiszniewski et al., 2007). In this study both families C10 and C11 affected with complete ACHM were screened

through MD-panel based sequencing as explained previously in section 2.5.2. The panel sequencing analysis and variant prioritization lead to the identification of CNGA3 variants in both families. In family C10 a known (Reuter et al., 2008) homozygous missense variant (c.1315C>T; p.(Arg439Trp)) was identified which explained the phenotype of the family. In family C11 two known (Wissinger et al., 2001; Shaikh et al., 2015) heterozygous missense mutations were identified in trans [c.955T>C, p.(Cys319Arg); c.1306C>T, p.(Arg436Trp)]. All three variants identified in CNGA3 were present in exon 7 and in a Chinese cohort of 46 families, 74.4% mutations were clustered in this exon (Li et al., 2014).
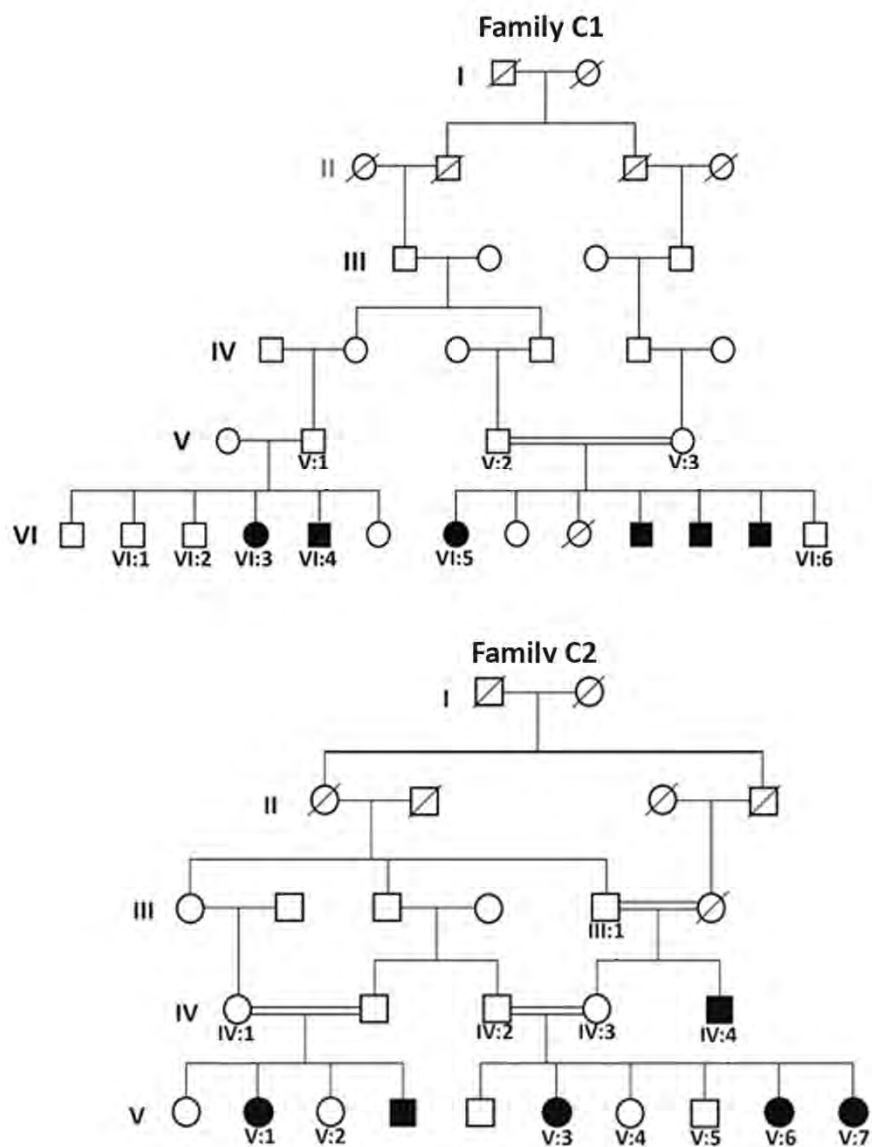
Figure 5.1: Pedigrees of both Leber congenital amaurosis (LCA) affected families (C1, C2) collected from different regions of Pakistan. Numbers are given in each pedigree only to the participating members in this study. The autosomal mode of inheritance and consanguinity is clearly seen among both families.
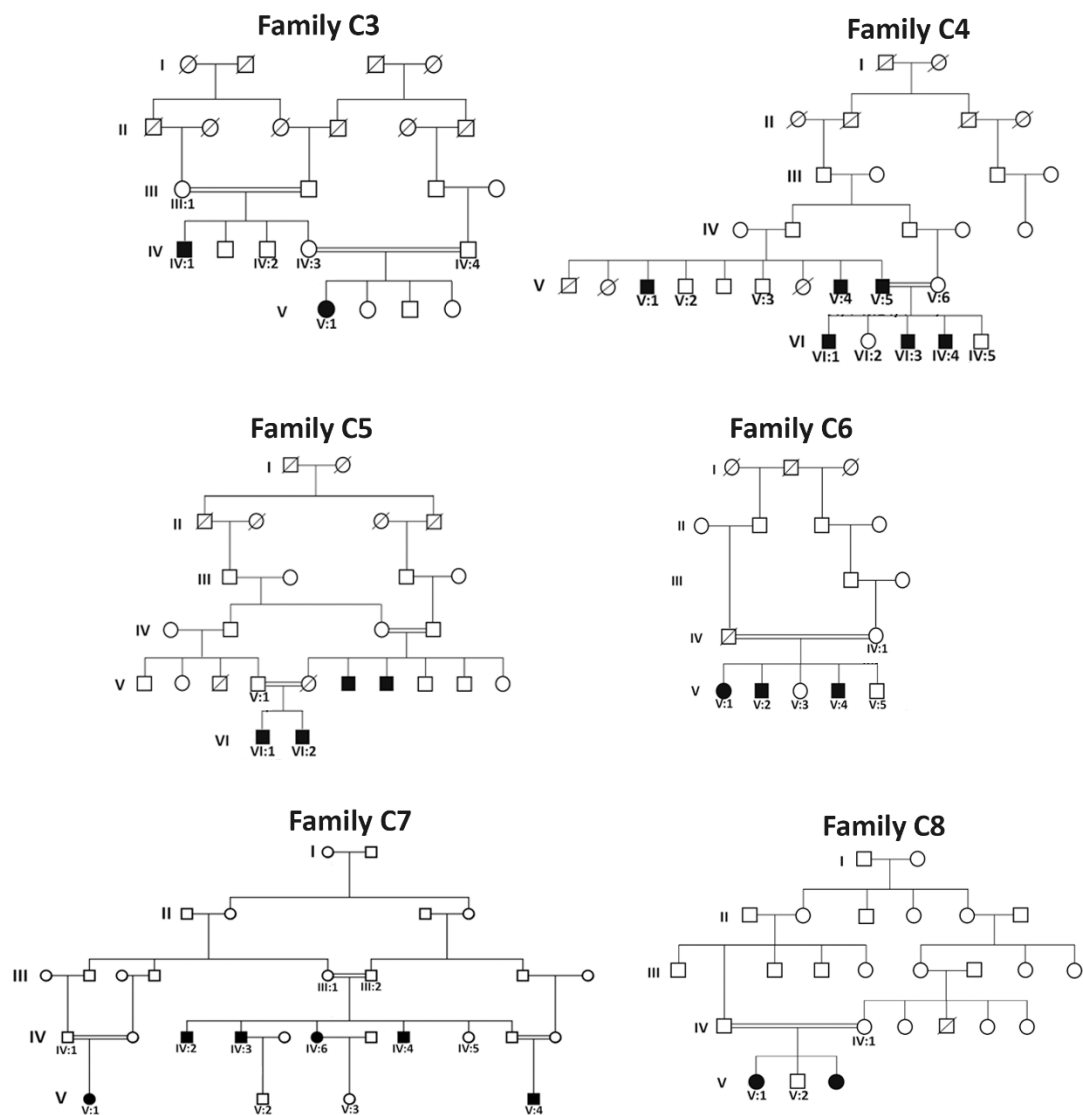
Figure 5.2: Pedigrees of six retinitis pigmentosa (RP) families (C3-C8) collected from different regions of Pakistan. Numbers are given in each pedigree only to the participating members in this study. The autosomal mode of inheritance and consanguinity is clearly seen among families C3, C6, C7 and C8, while families C4 and C5 show X-linked pattern of inheritance with only males affected.

(A)

(B)

Family C4: IV:3 (Right eye)

Family C4: IV:3 (Left eye)

(C)

M14 = c.6920_6922del; p.(Glu2307del)

WT:AGAGGGCCTGTGCACCTCGTGGTAGAACT
MT:AGAGGGCCTGTGCA---CGTGGTAGAACT

(D)

p.(Glu2307del)

NH₂ — NT — PROCN — RT — Linker — Endo — RH — Jab1 — COOH
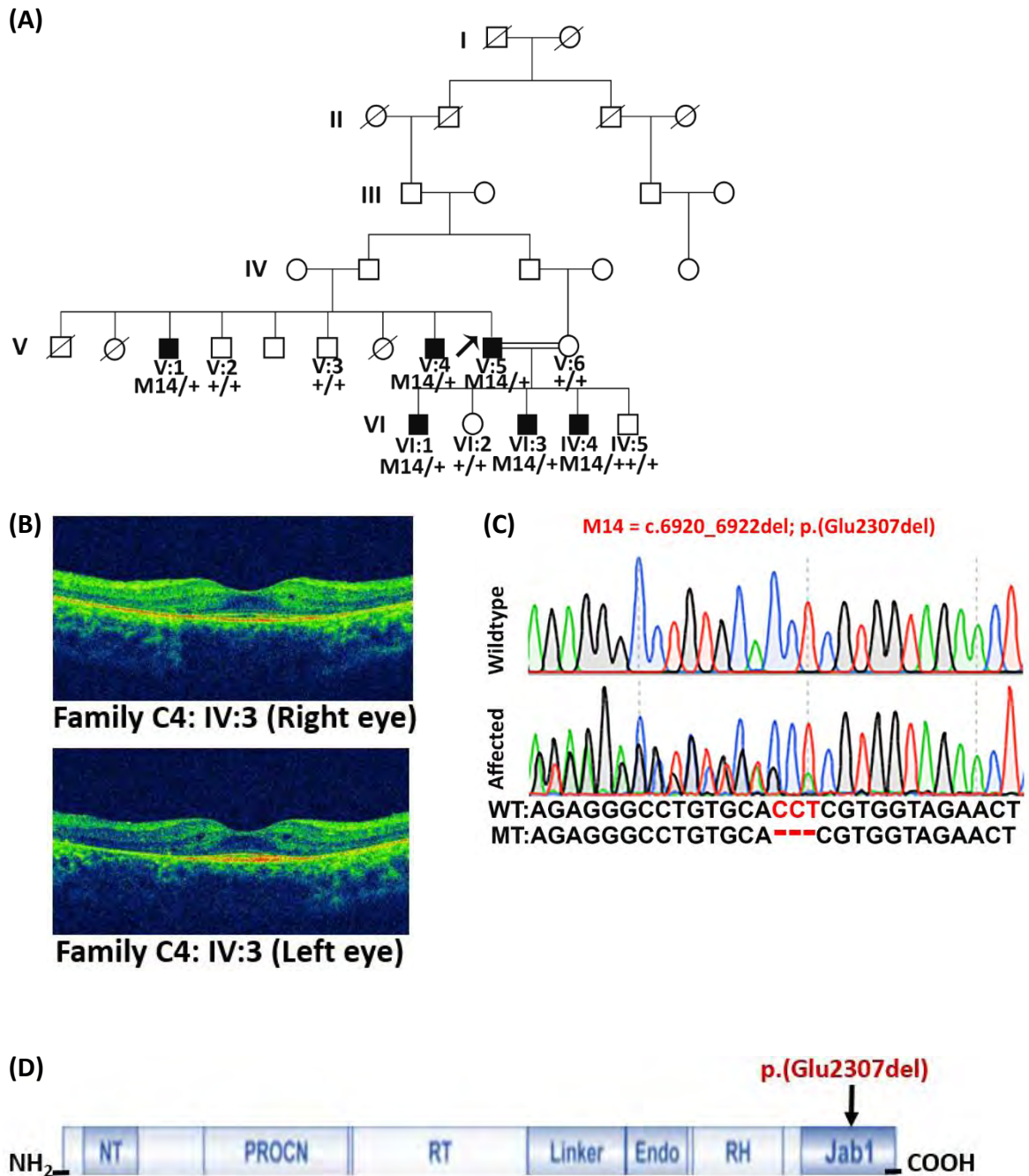
Figure 5.3: Pedigree of Family C4 where arrow is indicating the proband and below each participating member is shown the segregation results. (B). Optical coherence tomography (OCT) images of both eye of patient IV:3 from family C4 is indicating retinal layer degeneration. (C). Chromatogram of the variant M14 (c.6920_6922del; p.(Glu2307del)) identified in *PRPF8* in wildtype and affected individuals. (D). Schematic representation of amino-acid change in protein domain of PRPF8 protein.

Figure 5.4: Pedigree of Family C5 where arrow is indicating the proband and below each participating member is shown the segregation results. (B). Fundoscopy images of both eyes of patient IV:1 from family C5 is indicating pigment deposition towards periphery and central retina. (C). Chromatogram of the variant M15 (c.1843G>A; p.(Ala615Thr)) identified in *HGSNAT* in carrier and both affected individuals (left panel) and *CDHR1* variant which did not segregate with the phenotype (right panel). (D). Schematic representation of amino-acid change in protein domain of HGSNAT protein.

Figure 5.5: Pedigree of Family C7 where arrow is indicating the proband and below each participating member is shown the segregation results of variant M17=c.901C>T; p.(Gln301*) and M18=c.436C>T; p.(Gln146*) in *TULP1* and *MERTK* respectively. (B). Fundus images of both eyes of affected individual IV:4 from family C7 (affected with RP) indicating pigment deposition.

Figure 5.6: Pedigrees of family C9 affected with congenital stationary night blindness (CSNB) and two families (C10, C11) affected with achromatopsia (ACHM), collected from different regions of Pakistan. Numbers are given in each pedigree only to the participating members in this study. The autosomal mode of inheritance and consanguinity is clearly seen among all three families.
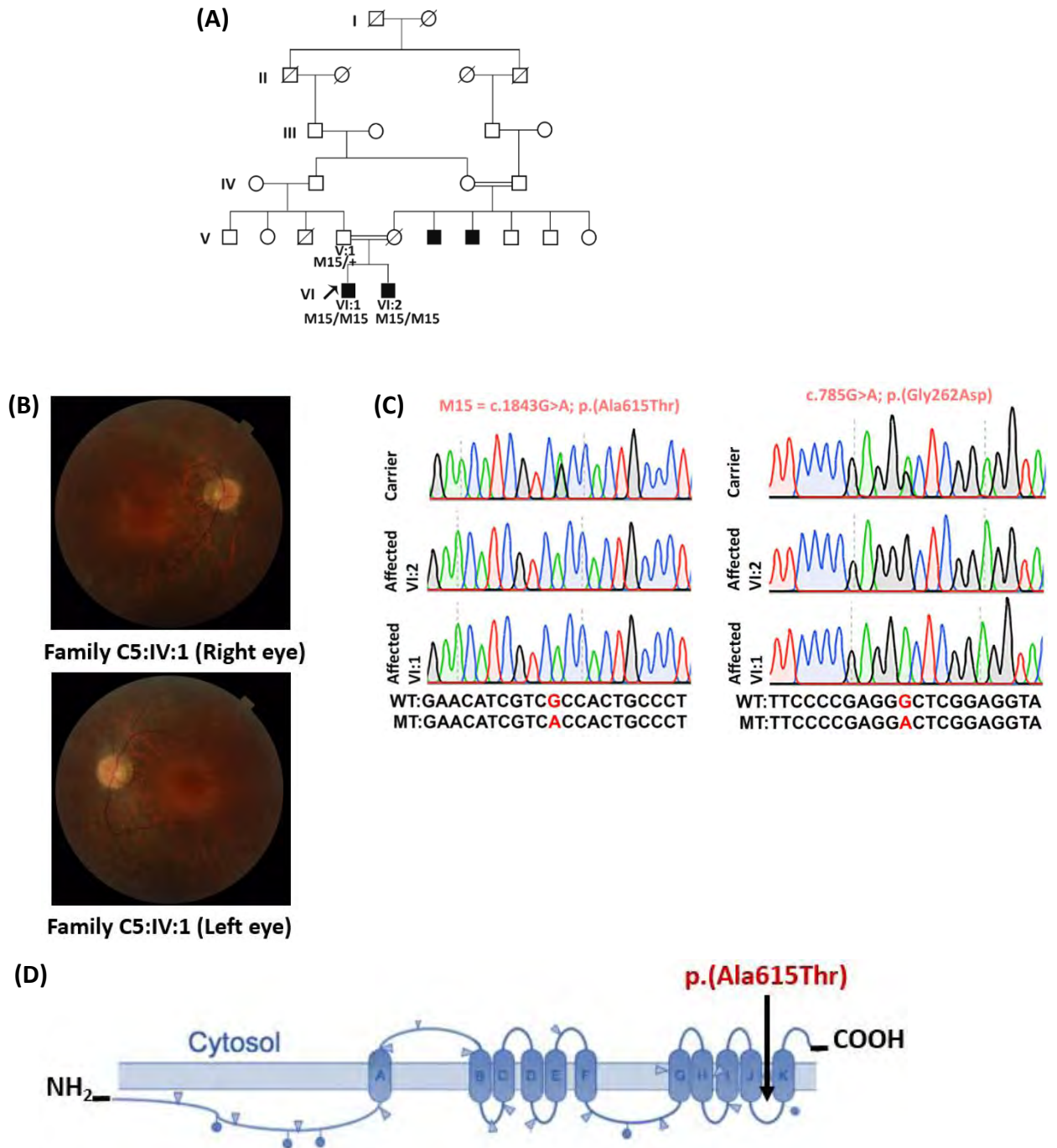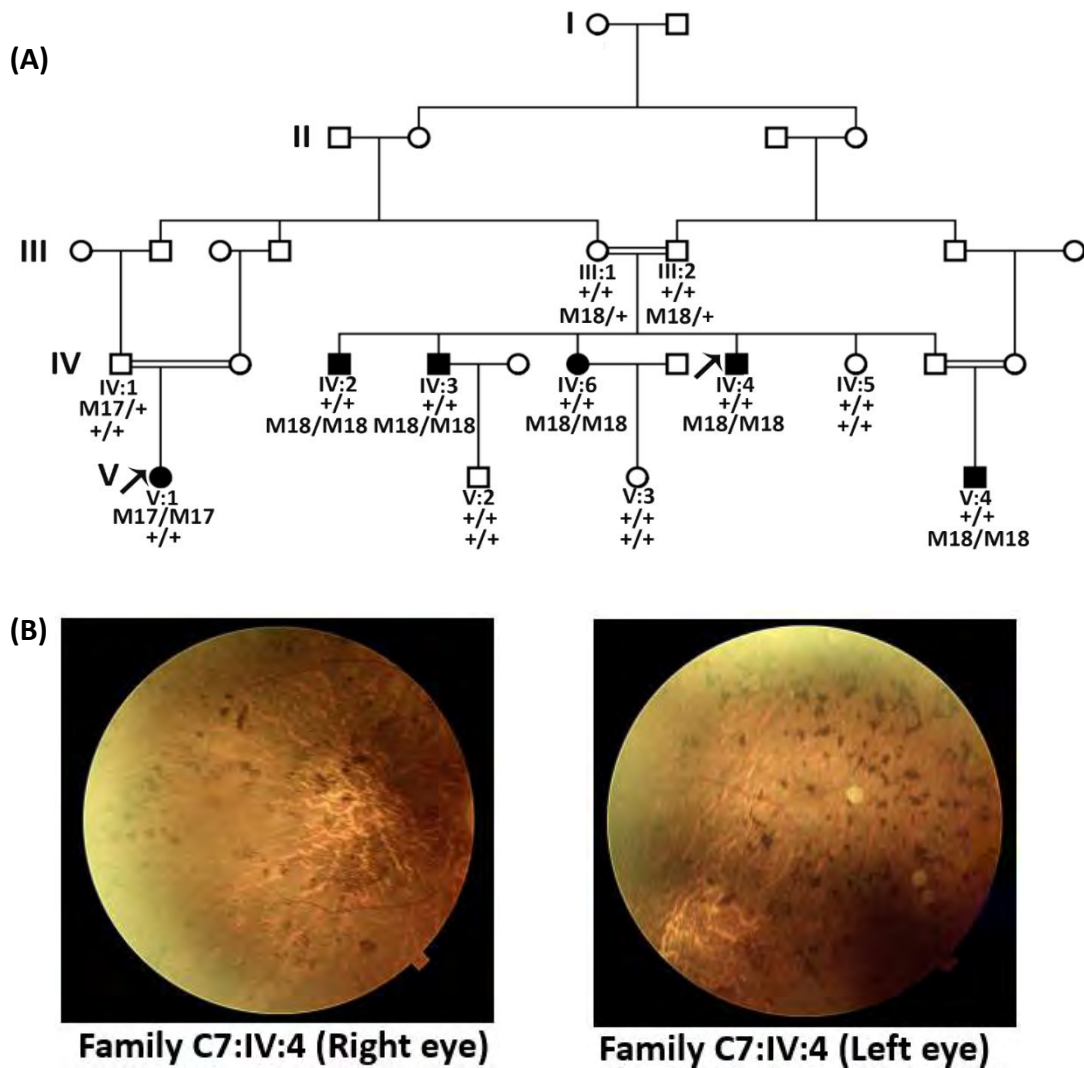
Figure 5.7: Pedigree of Family C9 where arrow is indicating the proband and below each participating member is shown the segregation results of variant M19=c.2493-2_2495delinsGGC; p.(?) in *CNGB1* causing congenital stationary night blindness (CSNB). (B). Fundus images of both eyes of affected individual IV:1 from family C9 (affected with CSNB) indicating pigment deposition more towards the peripheral region if the retina. (C). Optical coherence tomography (OCT) images of both eyes of affected individual IV:1 from family C9 indicating retinal layer degeneration.

(A)

(B)

M11 = c.94del ; p.(Ala32Profs*55)

WT: CACGTGCGCCGGGGCCGGGCGGCTGGA
MT: CACGTGCGCCGGG-CCGGGCGGCTGGA
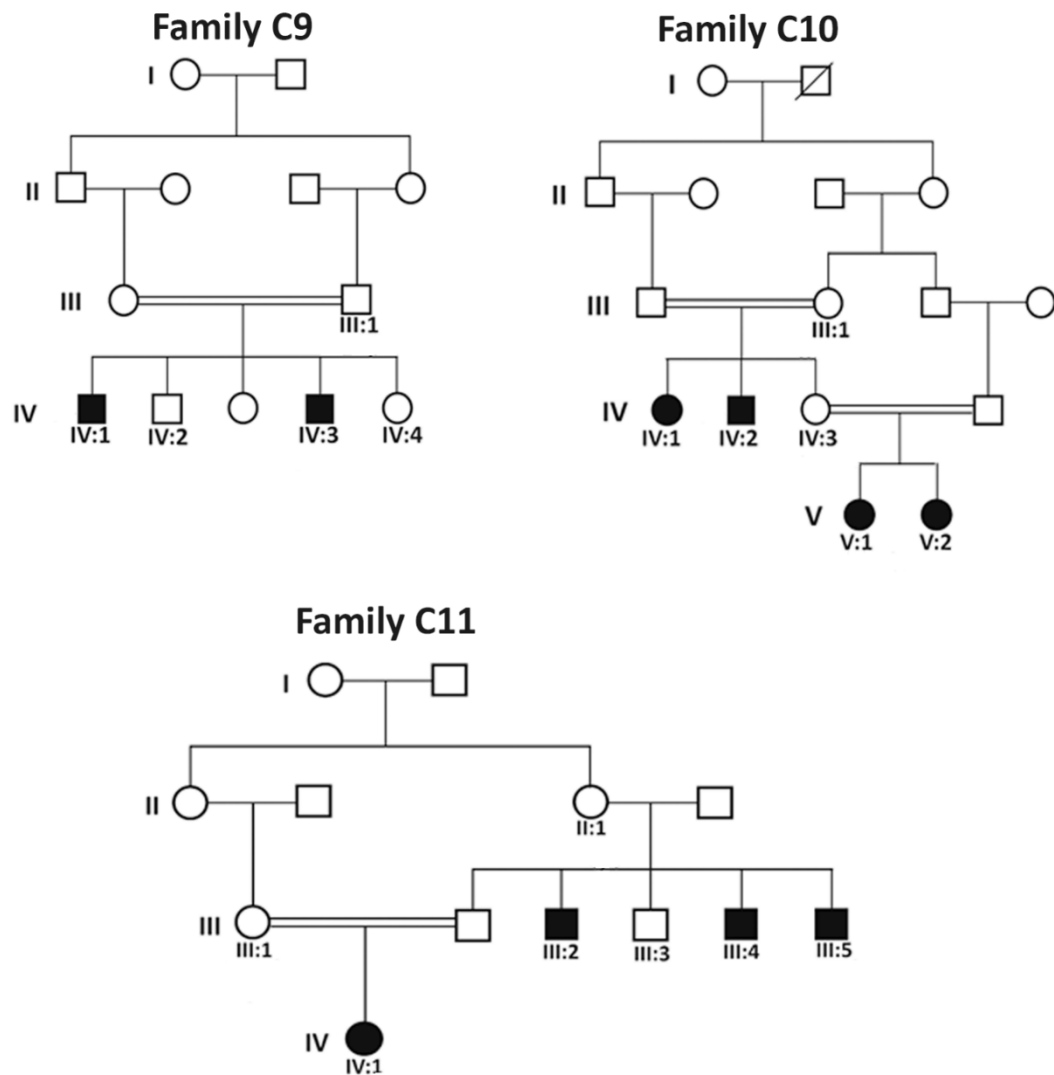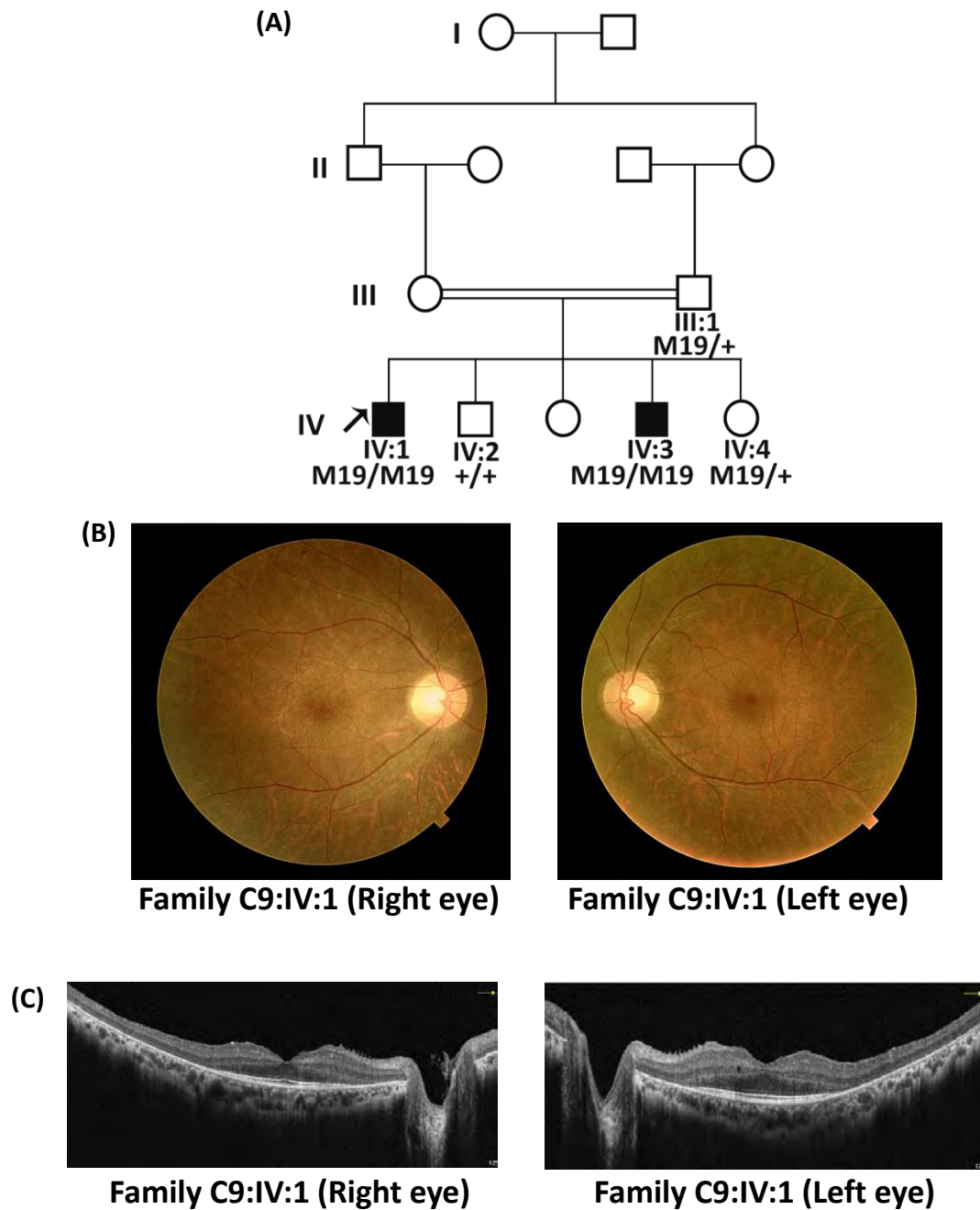
(C)

p.(Ala32Profs*55)

Figure 5.8: Pedigree of Family C1 where arrow is indicating the proband and below each participating member is shown the segregation results. (B). Chromatogram of the variant M11 (c.94del; p.(Ala32Profs*55)) identified in *ATOH7* in wildtype, carrier and affected individuals. (D). Schematic representation of amino-acid change in protein domain of ATOH7 protein.

(A)

(B) **M12 = c.25G>A; p.(Val9Met)**

WT: GAAGACTGAA**G**TGGTTCTCCT
MT: GAAGACTGAA**A**TGGTTCTCCT
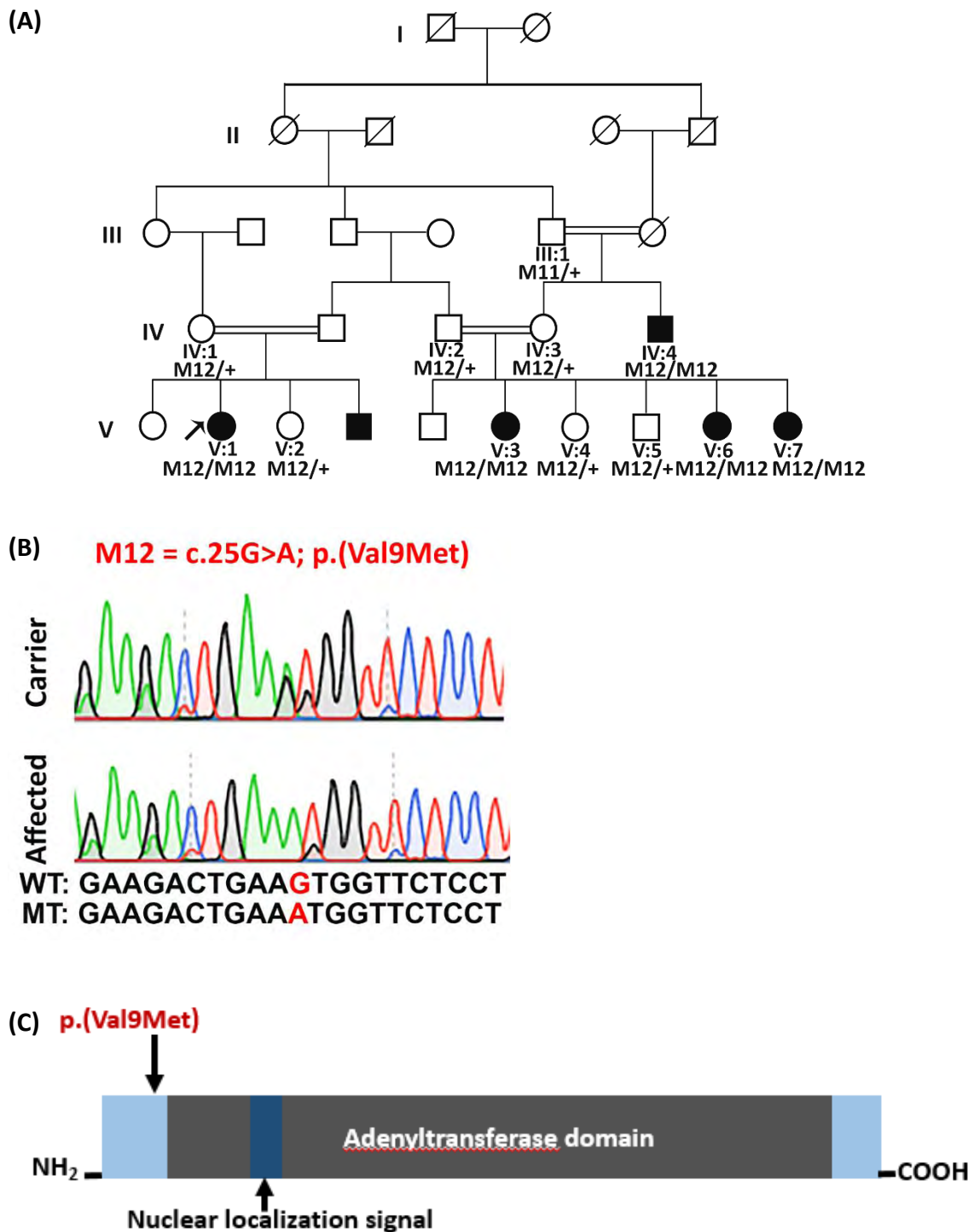
(C) p.(Val9Met)

Figure 5.9: Pedigree of Family C2 where arrow is indicating the proband and below each participating member is shown the segregation results. (B). Chromatogram of the variant M12 (c.25G>A; p.(Val9Met)) identified in *NMNAT1* in wildtype and affected individuals. (D). Schematic representation of amino-acid change in protein domain of NMNAT1 protein.
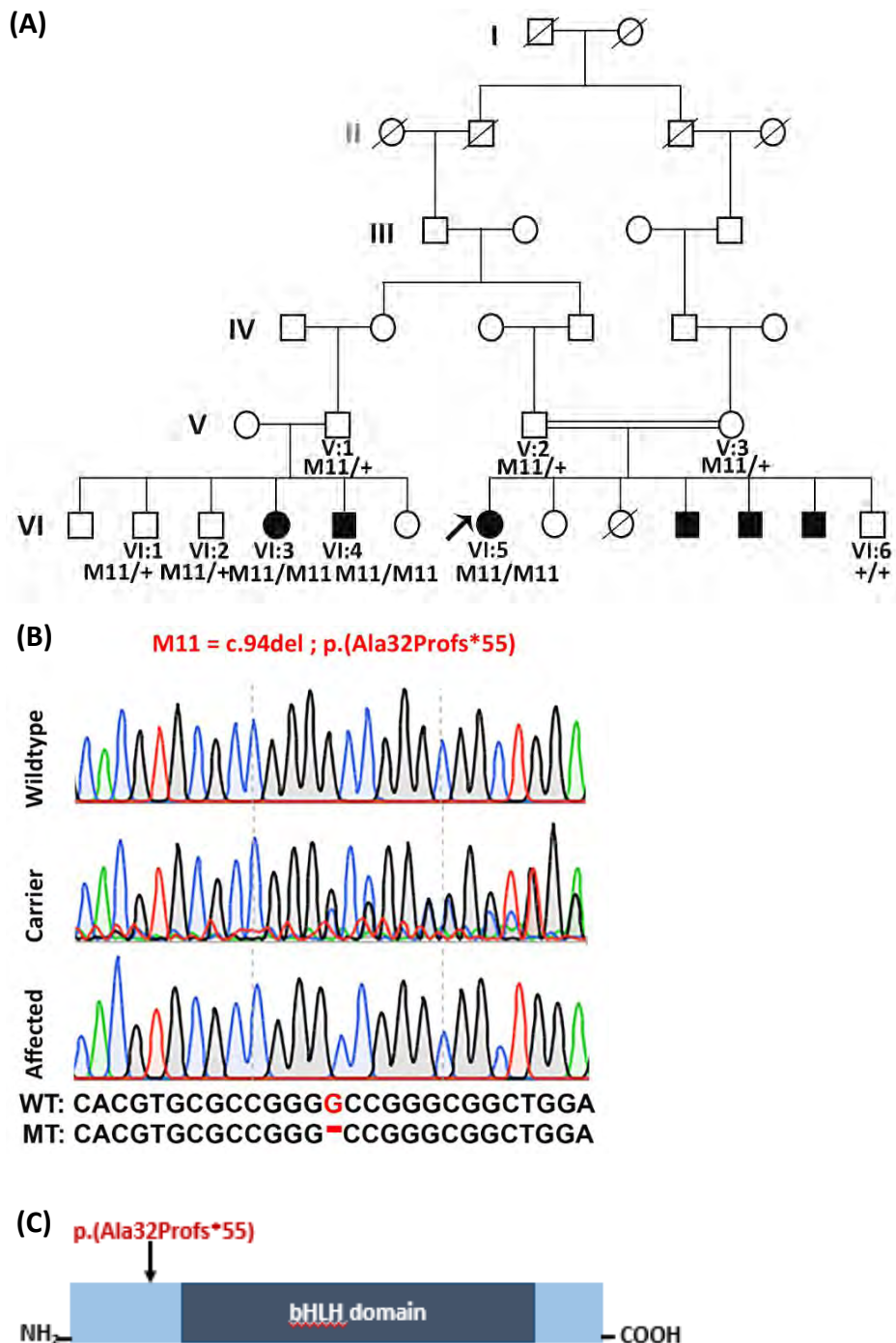
Figure 5.10: Pedigree of Family C3 where arrow is indicating the proband and below each participating member is shown the segregation results. (B). Chromatogram of the variant M13 (c.1444C>T; p.(Arg482Trp)) identified in *TULP1* in wildtype and affected individuals. (D). Schematic representation of amino-acid change in protein domain of TULP1 protein.

Figure 5.11: (A). Chromatograms of the variant M17=c.901C>T; p.(Gln301*) and M18=c.436C>T; p.(Gln146*) in *TULP1* and *MERTK* genes identified in left and right loops of the family C7 respectively in wildtype, carrier and affected individuals. (B). Schematic representation of amino-acid changes in protein domain of TULP1 (*top panel*) and MERTK (*bottom panel*) proteins.
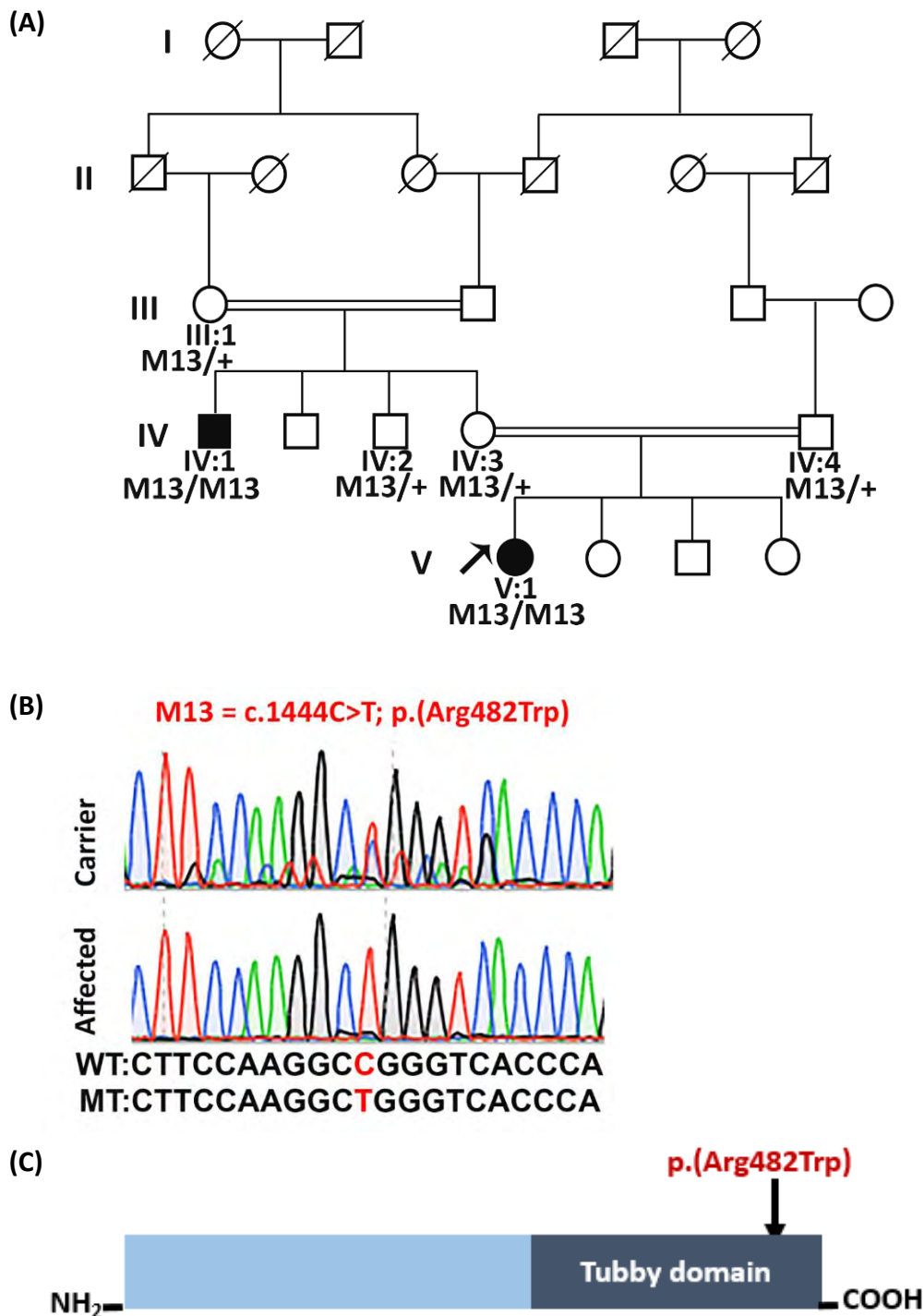
Figure 5.12: Pedigree of Family C6 where arrow is indicating the proband and below each participating member is shown the segregation results. (B). Chromatogram of the variant M16 (c.1649C>G; p.(Ser550*)) identified in *PROM1* in affected and carrier individuals. (C). Schematic representation of amino-acid change in protein domain of PROM1 protein.

(A)

(B)
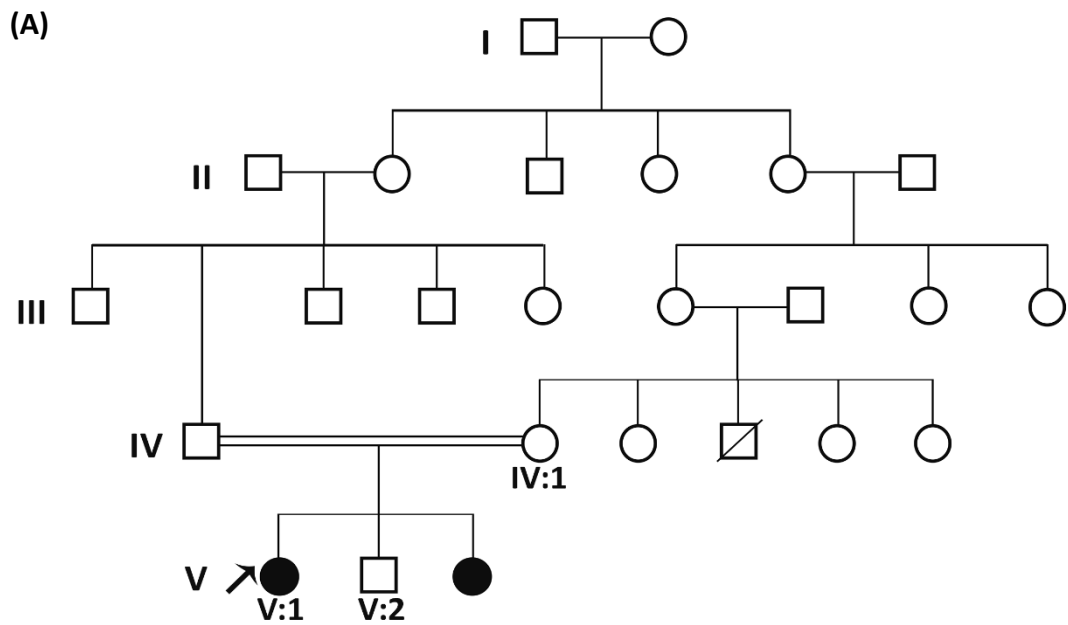
Family C8:V:1

Figure 5.13: (A). Pedigree of Family C8 where arrow is indicating the proband and individual number is given below each participating member. (B). Eye images of affected individual V:1 from the family C8 affected with RP.

(A)

M19 = c.2493-2_2495delinsGGC; p.(?)

Wildtype

Carrier

Affected

WT:TCTCCTCTCTCTCCAGTTATATTCGCTGTTACTACT
MT:TCTCCTCTCTCTCCGGC‑‑TATTCGCTGTTACTACT

(B) *CNGB1* (NM_001297.5)

c.2493-2_2495delinsGGC

1   26   33

1   25 27 28   33

Mutant Transcript

Skipping of exon 6

Figure 5.14: (A). Chromatograms of the variant M19=c.2493-2_2495delinsGGC; p.(?) in *CNGB1* gene identified in the family C9 respectively in wildtype, carrier and affected individuals. (B). Schematic representation of *CNGB1* gene and location of identified variant in the at the donor site of exon 26, which will cause the loss of donor site resulting in skipping of exon 26 in the mutant transcript.
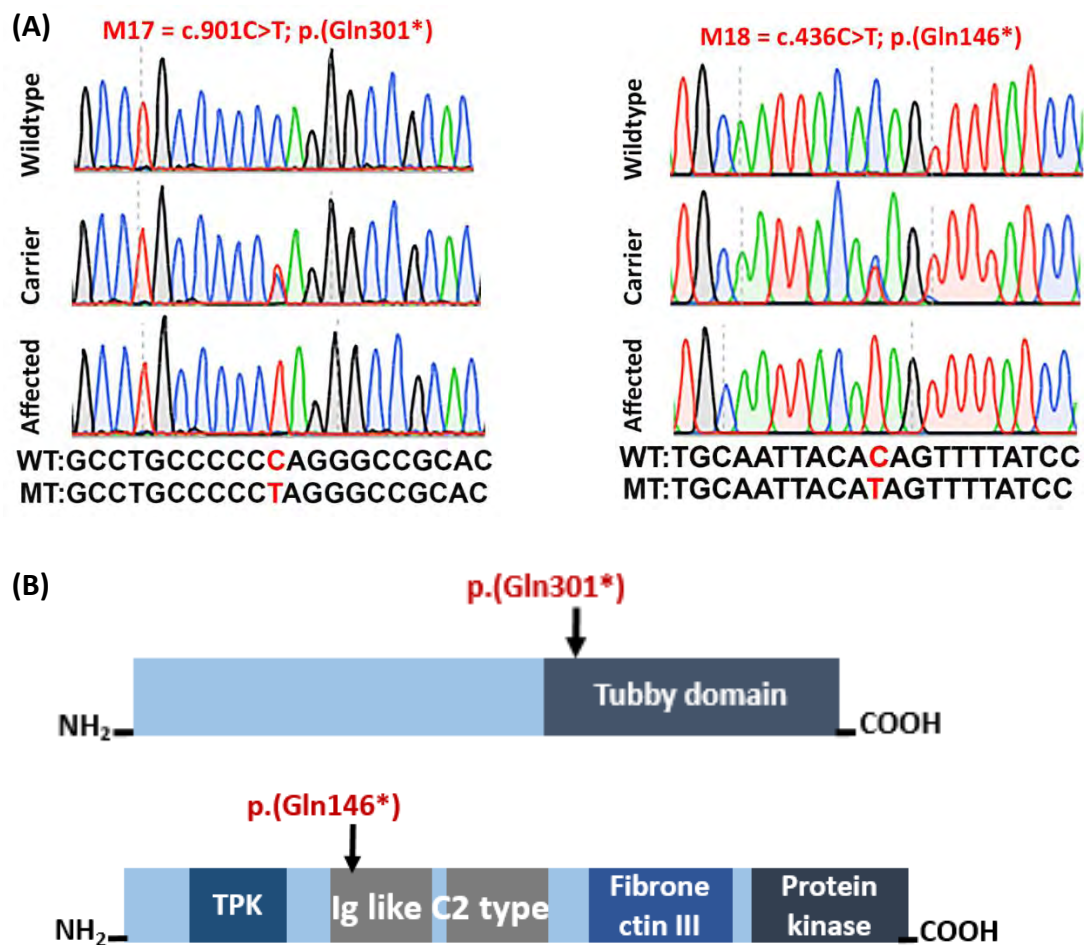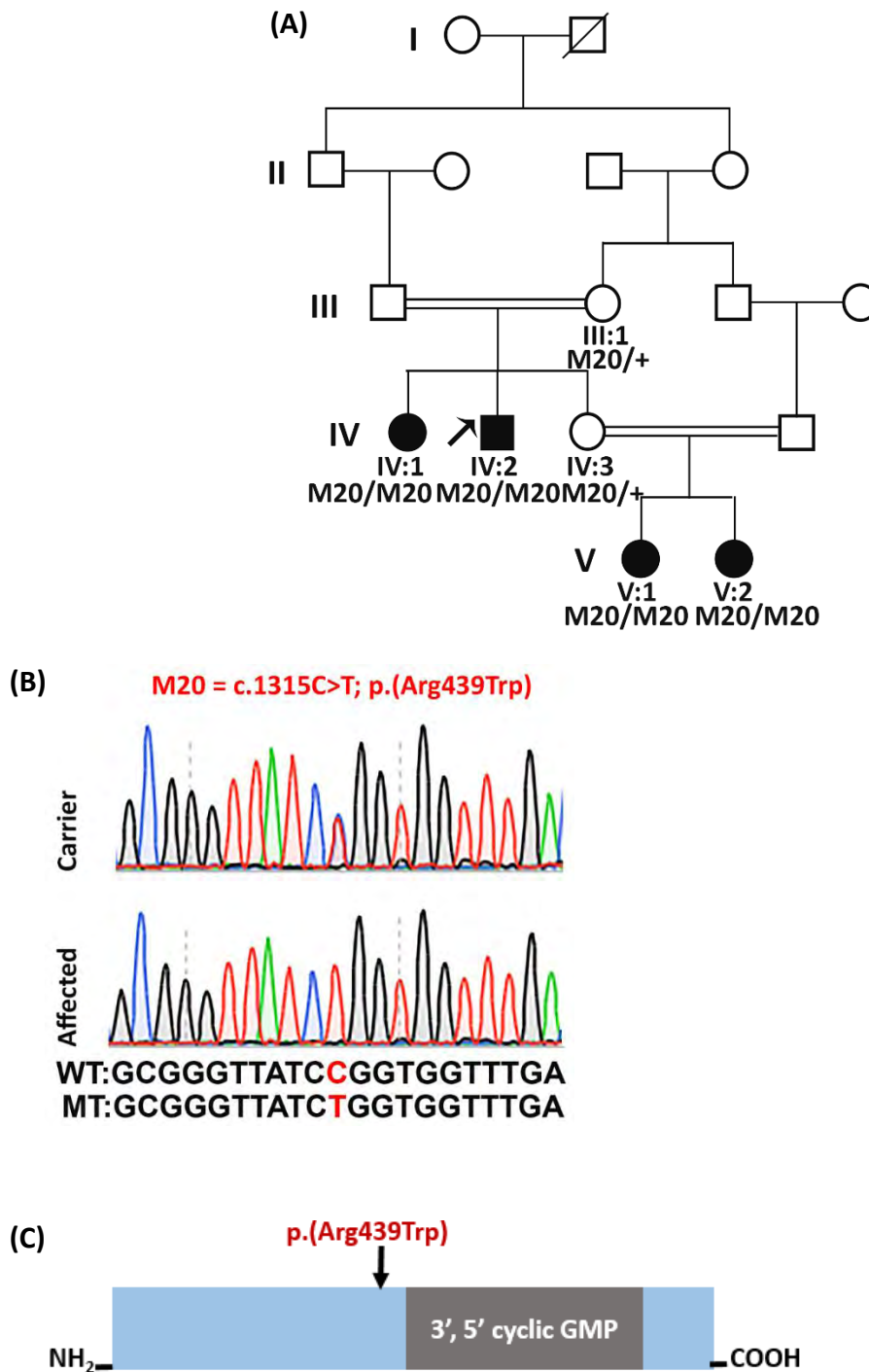
Figure 5.15: Pedigree of Family C10 where arrow is indicating the proband and below each participating member is shown the segregation results. (B). Chromatogram of the variant M20 (c.1315C>T; p.(Arg439Trp)) identified in *CNGA3* in affected and carrier individuals. (C). Schematic representation of amino-acid change in protein domain of CNGA3 protein.
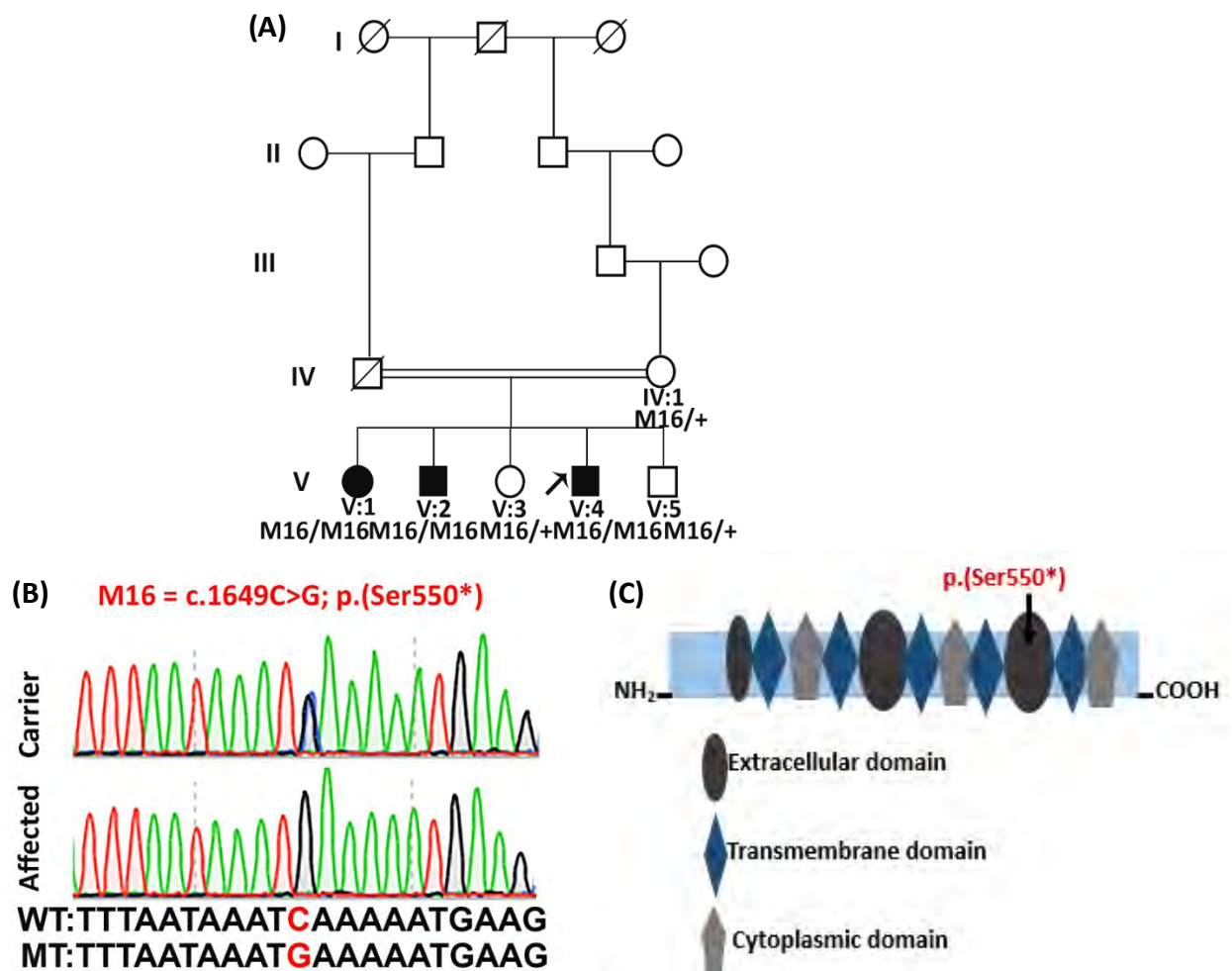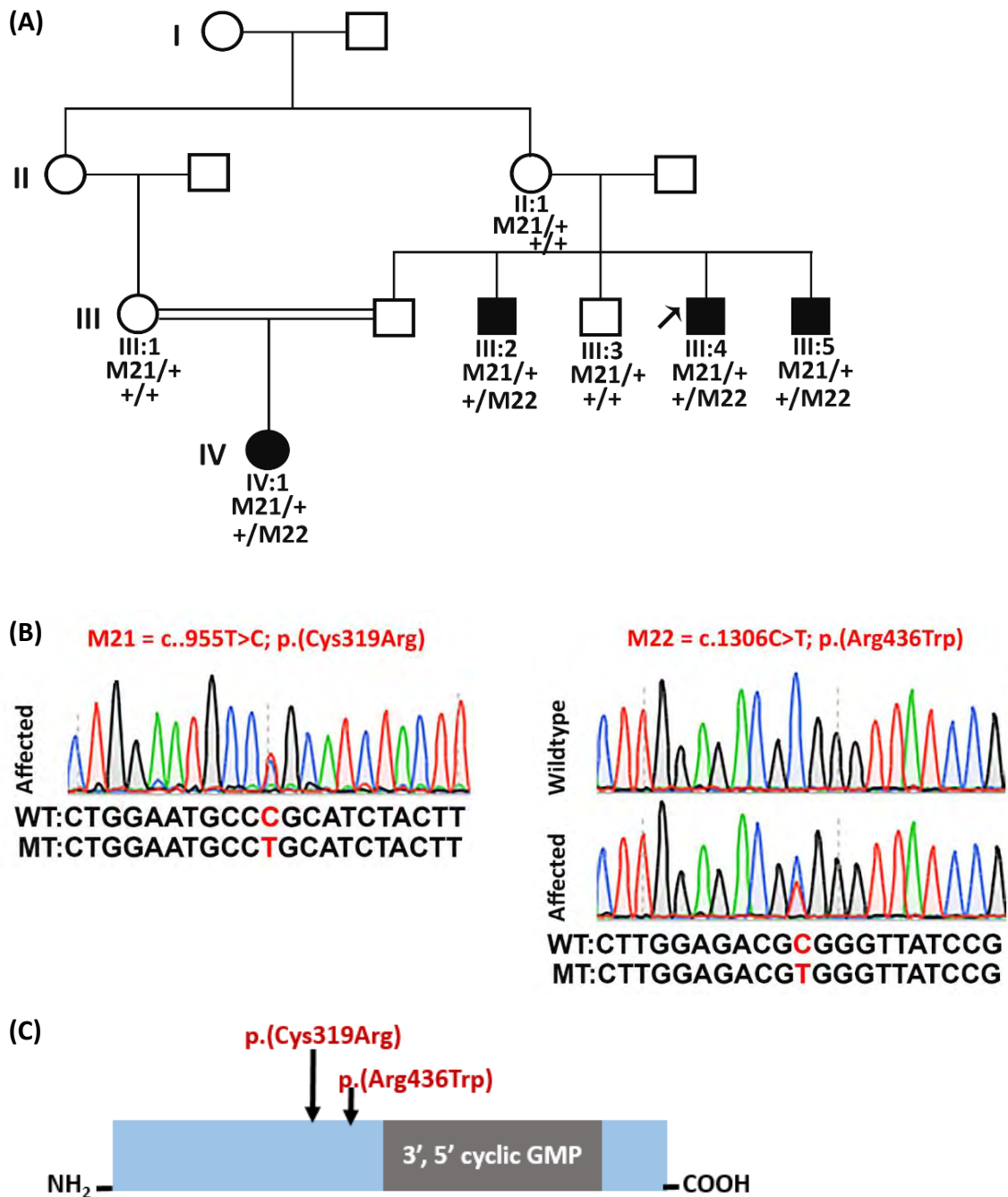
Figure 5.16: Pedigree of Family C11 where arrow is indicating the proband and below each participating member is shown the segregation results. (B). Chromatograms of the variants M21 (c.955T>C; p.(Cys319Arg)) and M22 (c.1306C>T; p.(Arg436Trp)) identified in *CNGA3* gene in compound heterozygous state. (C). Schematic representation of amino-acid changes due to both variants in protein domain of CNGA3 protein.

Table 5.1: Clinical features of affected individuals from two families (C1 and C2) affected with congenital blindness.

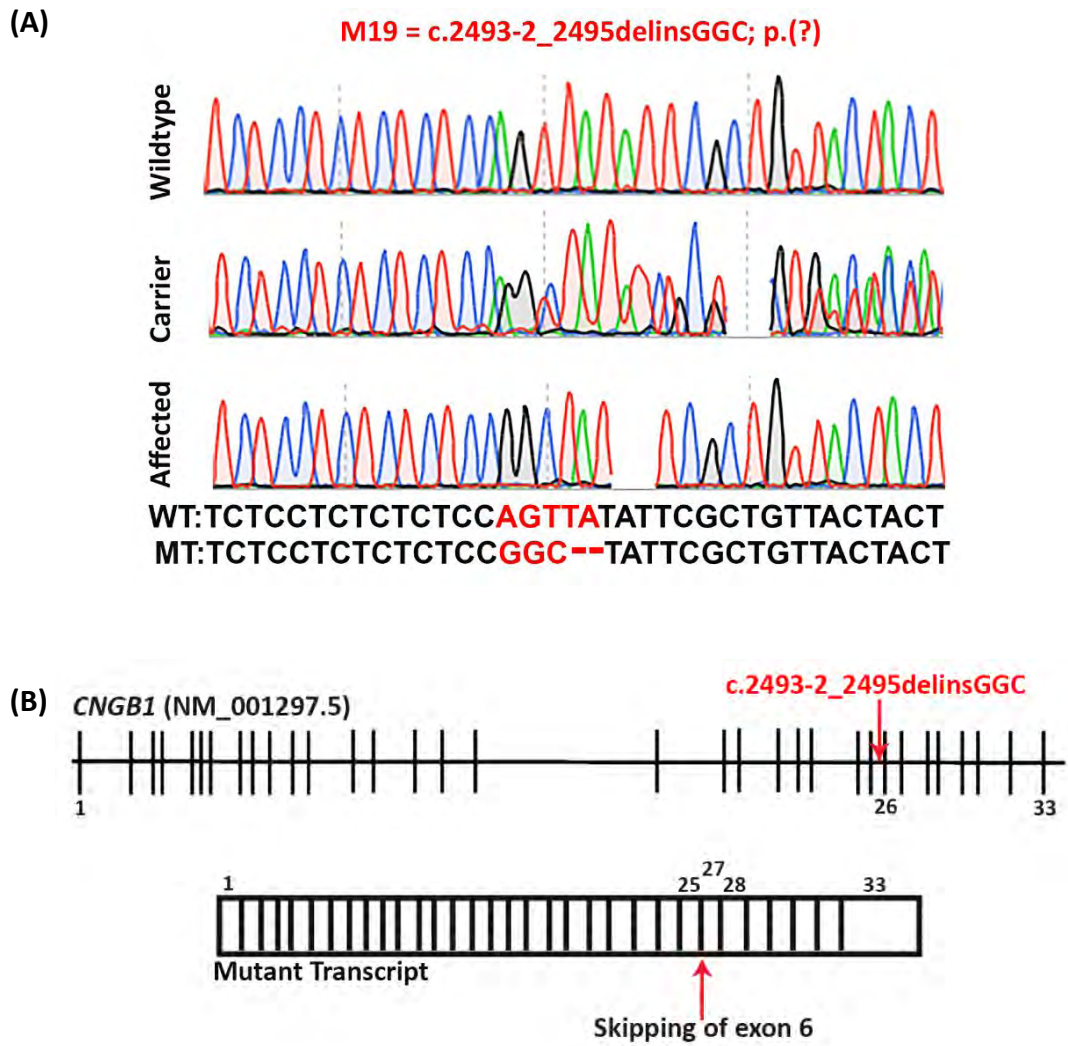| Family ID	Inheritance Pattern	Phenotype	Individual ID	Gender	Age onset (age at the time of sampling)	Observation at the time of sampling			Nystagmus	Corneal haze	Photophobia	Additional features (if any)
						Night vision	Day vision	Color vision				
C1	AR	LCA	VI:3	F	By birth (20 yrs)	No	NPL	NA	-	-	-	-
			VI:4	M	By birth (25 yrs)	No	NPL	NA	-	-	-	-
			VI:5	F	By birth (17 yrs)	No	NPL	NA	-	-	-	-
C2	AR	LCA	IV:4	M	By birth (45 yrs)	No	NPL	NA	-	BL	-	-
			V:1	F	By birth (19 yrs)	No	NPL	NA	-	BL	-	-
			V:3	F	By birth (25 yrs)	No	NPL	NA	-	BL	-	-
			V:6	F	By birth (17 yrs)	No	NPL	NA	-	-	-	-
			V:7	F	By birth (22 yrs)	No	NPL	NA	-	-	-	-

AR= Autosomal recessive, BL= Bilateral, F= Female, LCA= Leber congenital amaurosis, M= Male, NA= Not applicable, NLP= No perception of light, yrs= years, - = Absent.

Table 5.2: Clinical features of affected individuals from six families (C3-C8) affected with retinitis pigmentosa (RP).

Family ID	Inheritance Pattern	Phenotype	Patient ID	Gender	Age onset (age at the time of sampling)	Observation at the time of sampling			Nystagmus	Corneal haze	Photophobia	Additional features (if any)
						Night vision	Day vision	Color vision				
C3	AR	RP	IV:1	M	2 yrs (31 yrs)	No	NPL	NA	-	-	-	-
			V:1	F	1-2 yrs (11 yrs)	No	20/80	Normal	-	-	-	-
C4	AD	RP	VI:1	M	5 yrs (8 yrs)	No	20/30	Normal	-	-	-	-
			VI:3	M	5 yrs birth (11 yrs)	No	20/40	Normal	-	-	-	-
			VI:4	M	5 yrs (7 yrs)	No	20/30	Normal	-	-	-	-
			V:1	M	6 yrs (30 yrs)	No	20/100	Normal	-	-	-	-
			V:4	M	5-6 yrs (33 yrs)	No	20/100	Normal	-	-	-	-
			V:5	M	5 yrs (35 yrs)	No	20/80	Normal	-	-	-	-
C5	AR	RP	VI:1	M	3-4 yrs (20 yrs)	No	NPL	Normal	-	-	-	-
			VI:2	M	3-4 yrs (22 yrs)	No	NPL	Normal	-	-	-	-
C6	AR	RP	V:1	F	10 yrs (30 yrs)	No	PL	NA	+	-	-	-
			V:2	M	10 yrs (26 yrs)	No	20/40	Normal	+	+	-	-
			V:4	M	14 yrs (28 yrs)	No	20/60	Normal	+	-	-	-
C7	AR	RP	IV:2	M	2 yrs (55 yrs)	No	NPL	NA	-	-	-	-
			IV:3	M	2 yrs (46 yrs)	No	NPL	NA	-	-	-	-
			IV:4	M	2 yrs (42 yrs)	No	NPL	NA	-	-	-	-
			IV:6	F	2 yrs (51 yrs)	No	NPL	NA	-	-	-	-
			V:1	F	2 yrs (8 yrs)	No	20/100	Normal	-	-	-	-
			V:4	M	2 yrs (24 yrs)	No	20/80	Normal	-	-	-	-
C8	AR	RP	V:1	F	2-3 yrs (8 yrs)	No	20/80	Normal	+	-	-	Frequent urination

AD= Autosomal dominant, AR= Autosomal recessive, F= Female, M= Male, NA= Not applicable, NLP= No perception of light, RP= Retinitis pigmentosa, yrs= years, + = Present, - = Absent.

Table 5.3: Clinical features of affected individuals from one family (C9) affected with congenital stationary night blindness (CSNB) and two families (C10, C11) affected with achromatopsia (ACHM).

Family ID	Inheritance Pattern	Phenotype	Patient ID	Gender	Age onset (age at the time of sampling)	Observation at the time of sampling			Nystagmus	Corneal haze	Photophobia	Additional features (if any)
						Night vision	Day vision	Color vision				
C9	AR	CSNB	IV:1	M	By birth (19 yrs)	No	20/100	Normal	-	-	-	-
			IV:3	M	By birth (11 yrs)	No	20/80	Normal	-	-	-	-
C10	AR	ACHM	IV:1	F	6 months (15 yrs)	Normal	20/80	Nil	-	-	+	-
			IV:2	M	6 months (26 yrs)	Normal	20/120	Nil	-	-	+	-
			V:1	F	8-10 months (11 yrs)	Normal	20/60	Nil	-	-	+	-
			V:2	F	6 months (10 yrs)	Normal	20/60	Nil	-	-	+	-
C11	AR	ACHM	III:2	M	By birth (20 yrs)	Normal	20/100	Nil	-	-	+	-
			III:4	M	By birth (31 yrs)	Normal	20/120	Nil	-	-	+	-
			III:5	M	By birth (18 yrs)	Normal	20/80	Nil	-	-	+	-
			IV:1	F	By birth (9 yrs)	Normal	20/40	Nil	-	-	+	-

ACHM= Achromatopsia, AR= Autosomal recessive, CSNB= Congenital stationary night blindness, F= Female, M= Male, yrs= years, += Present, - = Absent.

Table 5.4: 2: *In silico* predictions for disease-causing variants identified in 2 families (C1, C2) affected with congenital blindness.

Family ID	Gene	cDNA	Protein	gnomAD G.AF	CADD-PHRED	Grantham	PhyloP	REVEL	SpliceAI	ACMG classification	Reference
C1	*ATOH7*	c.94del	p.(Ala32Profs*55)	Not found	NA	NA	NA	NA	NA	Likely pathogenic	This study
C2	*NMNAT1*	c.25G>A	p.(Val9Met)	Not found	23.6	21	4.1	0.82	NA	Pathogenic	Falk et al., 2012

gnomAD.G.AF= Allele frequency in genomes of gnomAD database, NA= Not applicable, * = stop codon.

Table 5.5: *In silico* predictions for potential disease-causing variants identified in six families (C3-C8) affected with retinitis pigmentosa (RP).

Family ID	Gene	cDNA	Protein	gnomAD.G.AF	CADD-PHRED	Grantham	PhyloP	REVEL	SpliceAI	ACMG classification	Reference
C3	*TULP1*	c.1444C>T	p.(Arg482Trp)	0.00001591	28.2	101	1.2	0.96	NA	Pathogenic	den Hollander et al., 2007
C4	*PRPF8*	c.6920_6922del	p.(Glu2307del)	Not found	31	NA	7.78	NA	NA	Likely pathogenic	This study
C5	*HGSNAT*	c.1843G>A	p.(Ala615Thr)	0.003536	22.7	58	7.64	0.45	NA	VUS	Hrebicek et al., 2006
	CDHR1	c.785G>A	p.(Gly262Asp)	0.000019721	27.3	94	5.01	0.65	NA	VUS	This study
C6	*PROM1*	c.1649C>G	p.(Ser550*)	Not found	36	NA	5.1	0.13	NA	Likely pathogenic	This study
C7	*TULP1*	c.901C>T	p.(Gln301*)	Not found	40	NA	7.6	0	NA	Pathogenic	Li et al., 2009
	MERTK	c.436C>T	p.(Gln146*)	0.00000398	36	NA	3.8	0.08	NA	Likely pathogenic	This study

gnomAD.G.AF= Allele frequency in genomes of gnomAD database, NA= Not applicable, * = stop codon.

Table 5.6: *In silico* predictions for potential disease-causing variants identified in family (C9) affected with congenital stationary night blindness (CSNB) and two families (C10, C11) affected with achromatopsia (ACHM).

Family ID	Gene	cDNA	Protein	gnomAD.G.AF	CADD-PHRED	Grantham	PhyloP	REVEL	SpliceAI	ACMG classification	Reference
C9	*CNGB1*	c.2493-2_2495delinsGGC	p.(?)	Not found	NA	NA	NA	NA	NA	Likely pathogenic	Maranhao et al., 2015
C10	*CNGA3*	c.1315C>T	p.(Arg439Trp)	0.00001993	26.8	101	4.25	0.833	NA	Pathogenic	Reuter et al., 2008
C11	*CNGA3*	c.955T>C	p.(Cys319Arg)	0.00001767	26.6	180	7.5	0.99	NA	Likely pathogenic	Shaikh et al., 2015
		c.1306C>T	p.(Arg436Trp)	0.00009574	24	101	1.4	0.85	NA	Likely pathogenic	Wissinger et al., 2001

gnomAD.G.AF= Allele frequency in genomes of gnomAD database, NA= Not applicable.

6.0. SYNDROMIC INHERITED RETINAL DYSTROPHIES

Inherited retinal dystrophies (IRDs) can be syndromic and found with extra-ocular features. Mostly the genes which are involved in syndromic IRDs are involved in ciliary functions. Hence the disorders are also known as ciliopathies. The two most common ciliopathies are Usher syndrome and Bardet-Biedl syndrome (BBS). The Usher syndrome is recognized by RP with varying degree of hearing loss. In BBS many features additional to RP might present including, obesity, hypogonadism, renal diseases and most frequently postaxial polydactyly (Mockel et al., 2011). Sometimes syndromic RP is also present with mitochondrial and other metabolic disorders. In such cases, where the other systemic features are not clearly seen may be overlooked by clinical ophthalmologist (e.g., renal disease or cardiovascular disease history of the patient) or if some features are surgically corrected early in life (e.g., polydactyly). Hence, obtaining a thorough family and clinical history is important for proper diagnosis of the disease (Verbakel et al., 2018). Syndromic IRDs also exhibit genetic heterogeneity as well as phenotypic heterogeneity. More than 100 genes are known to be associated with different types of autosomal dominant, autosomal recessive and X-linked syndromic IRDs (RetNet: https://web.sph.uth.edu/RetNet/sum-dis.htm). In this section three families (D1-D3) affected with syndromic IRDs are explained with their genetic diagnosis.

6.1. Description and Clinical Features of Syndromic IRD Families

The family D1 was affected with Usher syndrome (Figure 6.1). At the time of initial sampling and family recruitment, the hearing loss feature of the family was overlooked. Although two members V:2 and V:3 from this sample were observed with low IQ levels as compared to a normal individual. Therefore, these two patients were considered with mild intellectual disability (ID). However, after genetic analysis, follow-up study was performed to obtain fundus and OCT scans of the proband (IV:4) and mild hearing loss was observed in all the affected members of the families. Audiometry was not performed due to unavailability of audiometer in the nearby hospital. The fundus images of the patient IV:4 taken at age 40 showed dusty pigmentation towards periphery (Figure 6.2A). The OCT scans showed reduced central macular thickness i.e., 306μm and 230μm for right and left eye respectively (Figure 6.2B).

Affected members of the family D2 were presented with night blindness with severe and progressive loss of day vision early in their life (Figure 6.1). The affected members of family D3 were initially observed with congenital blindness and therefore miss diagnosed as LCA (Figure 6.1). However, in the affected members of D2 flat nasal bridge was present. Two affected individuals (IV:3 and IV:6) had nystagmus and individual IV:3 also present unilateral central corneal haze (left eye). In family D3 along with congenital blindness slight microcornea and central corneal haze was also observed. The detailed clinical features are given table 6.1.

6.2. Genetic Analysis Identified Novel Variants in all Syndromic IRD families

The proband (IV:4) of family D1 remained genetically unexplained after SNV analysis of RP-LCA smMIPs panel sequencing. However, CNV analysis identified the homozygous deletion of exon 50 to exon 58 in *USH2A* (NM_206933.4) gene (Figure 6.2C). PCR-based genome walking was performed with the combination of multiple forward and reverse primers designed in the intact region identified through smMIPs. One combination of forward primer (P5F) and reverse primer (P3R) amplified a fragment of approximately 3kb in affected and carrier individuals (Figure 6.3). The subsequent amplicon based long-read sequencing of the amplified product through PacBio, confirmed the novel deletion of approximately 51.47kb region in *USH2A* (chromatogram shown in figure 6.4). The breakpoints of the deletion lie within intron 49 and intron 58 (c.9740-5487_ c.11389+5457) causing deletion of exon 50-exon 58, likely resulting in the in-frame deletion p.(Glu3248_Gly3797del)). The segregation analysis of the identified mutation was performed by two primer pairs (S1 and S2). Where S1 is designed to cover the region of intron 49 and intron 58. The expected product from this pair was 52kb approximately from normal individual, which is likely impossible to be amplified through normal PCR. The product size expected due to deletion was reduced to 890bp. Therefore, this small fragment was amplified only from the individuals which were either homozygous or heterozygous for the identified deletion. The pair S2 was designed to amplify exon 54 of *USH2A* gene. This region was amplified either in normal individuals or individuals carrying heterozygous deletion. The gel image and primer map for segregation are shown in figure 6.5 while the segregation results are given below each participating member in the pedigree shown in figure 6.6.

In family D2, night-blindness with progressive loss of day vision was observed. GS variant prioritization resulted in the selection of two homozygous variants (NM_022124.6: c.7441C>A; p.(Pro2481Thr)) and (c.4405A>G; p.(Ile1469Val)) in gene *CDH23,* one homozygous variant (NM_004009.3: c.7520A>G; p.(Asn2507Ser)) in *DMD* and one homozygous indel (NM_030582.4: c.1785_1786delinsG, p.(Pro597Leufs*127) in *COL18A1* while compound heterozygous variants in *ABCA4* (NM_000350.3: [c.1371C>A; p.(Asn457Lys) c.1532G>A; p.(Arg511His)]) and *LZTFL1* (NM_001276378.2: [c.129-724A>G; p.(?); c.646G>A; p.(Ala216Thr)]). Out of all the selected variants, only a novel homozygous indel (NM_030582.4: c.1785_1786delinsG; p.(Pro597Leufs*127)), identified in *COL18A1*, segregated in the family (Figure 6.7). *COL18A1* is known to be associated with autosomal recessive Knobloch syndrome (OMIM: 267750). The main features of Knobloch syndrome includes occipital encephalocele, vision loss, myopia, nystagmus and retinal detachment. Previously, a large Pakistani family depicted a diverse form of Knobloch syndrome associated with *COL18A1* variant (Joyce et al., 2010). The affected members of family D2 also present similar progressive night blindness with early loss of day vision but lack nystagmus and occipital encephalocele or occipital scalp defect.

The family D3, was initially reported with congenital blindness and depicting X-linked inheritance pattern. One variant selected after GS variant prioritization in this family was (NM_001291867.2: c.566-145363T>G; p.(?)) in *NHS*, a gene known to be associated with Nance-Horan syndrome (OMIM: 302350) which is characterized by dental anomalies, cataract, dysmorphic features, microcornea and mental retardation. This variant is present in gnomAD with allele frequency (0.0002203) where 6 individuals are hemizygotes. Moreover, splice AI score for this variant was 0.22 (donor gain, -5bp), and this effect is similar for wildtype allele in Alamut predictions. Therefore, this variant was not selected as potential candidate disease causing variant in family D3. We additionally looked up for high nucleotide conservation scores (PhyloP $\geq$ 2.7) for all homozygous variants with MAF$\leq$0.01 in gnomAD. This leads us to the selection of a novel variant (NM_000266.4; c.-208G>A; p.(?)), residing in the 5'UTR of *NDP* (a gene known to cause familial exudative vitreoretinopathy (FEVR) (OMIM: 305390)) was also identified in this family (Figure 6.8). This variant was selected because it was absent in gnomAD and only identified variant relevant to the

phenotype. The 5'UTR variants in *NDP* gene are known to cause Norrie disease (Jia and Ma, 2021). The details of all the identified variants are given in table 6.2.

6.3. Discussion

There are many syndromes which affect sensory organs like vision and hearing together. Usher syndrome is one of the most common form of such disorders. It was first described by a German ophthalmologist in 1858, when he observed the co-segregation of visual impairment and hearing loss (VonGraefe, 1858). The prevalence of Usher syndrome is 3.8-4.4 in 100,000 births (Rosenberg et al., 1997). This syndrome is more prevalent in individuals with retinitis pigmentosa than hearing loss (Haim, 1992; Hope et al., 1997). There are mainly three different categories of Usher syndrome. The first type is where hearing impairment is more profound than other systemic issues. In the second type where hearing loss is less severe and the third category which is more common in Finnish patients which show progressive vision loss and hearing impairment with variable degree of vestibular dysfunction. While there are certain patients which cannot be categorized in any of these three types (Smith et al. 1994; Sankila et al. 1995; Wagenaar et al. 1999; Otterstedde et al. 2001; Tsilou et al. 2002). The most common form of blindness in deaf individuals is Usher syndrome worldwide. But the incidences of Usher syndrome in Pakistan is unknown as in most cases the symptoms remained unnoticed in young patients or in some cases symptoms become more profound later in life. Some of the genetic variants associated with non-syndromic RP are also causing Usher syndrome and some of the variants causing non-syndromic hearing loss are also causing Usher syndrome. Therefore, even after genetic diagnosis the symptoms of Usher syndrome may remain un-notified (Naz, 2022).

The family D1 with syndromic IRD, was affected with retinitis pigmentosa, while 2 male members (V:2 and V:3) were initially reported with mild intellectual disability. The genetic screening through RP-LCA panel sequencing of the proband (IV:4) was initially performed considering the reported RP case. No potential pathogenic variant was identified in SNV analysis and variant prioritization. Later CNV analysis was performed, by calculating the average smMIPs coverage per sample, calculating estimated reads per smMIPs and comparing it with actual reads received per smMIPs from each sample. It leads us to the identification of absence of reads from the smMIPs covering region of intron 49 to intron 59 in *USH2A* gene from the proband. The genome

walking within the intact regions on both sides of deletion, identified through smMIPs reads was performed to identify the exact breakpoints of deletion. Approximately 51.47kb region was identified to be deleted in this proband which covers the important coding regions of exon 50-58 within *USH2A* gene. This SV seems to be the outcome of non-homologous end joining after double stranded DNA break repair mechanism where microhomology of 2-20bp is observed at the junction point (Sfeir and Symington, 2015). This deletion also contains an overlap stretch of 22 bp at breakpoint which is completely aligned to both regions of intron 49 and intron 58. The deleted *USH2A* region encodes an important fibronectin type III repeat domain, but the exact consequences of this deletion cannot be predicted based on current knowledge. However, we anticipate that deletion of exons 50-58 most probably will cause an in-frame deletion of p.(Glu3248_Gly3797del).

The variants in *USH2A* are also known for nonsyndromic RP therefore the gene was included in panel and later follow-up studies of our affected family confirmed that all the affected patients were exhibiting mild hearing loss which remained unnoticed at the time of initial visit. Unfortunately, the audiometry test was not conducted due to unavailability of audiometer in the nearby hospital facility and the extent of hearing loss was not measured. Thus, the identified SV in *USH2A* is causing a type 2 Usher syndrome in family D1. Very few incidences of the Usher type 2 has been reported in Pakistani population. To date, three families with biallelic missense or nonsense variants in USH2A has been reported in Pakistani population (Wang et al. 2017; Richard et al. 2019; Ahmed et al. 2021). A comprehensive review of *USH2A* gene by Su et al., has indicated that 10 exons out 72 *USH2A* exons are most frequently mutated which include exon 2, 13, exon 41-43, 50, 54, 57, 61 and 63. These exons corresponds to the 50% of the *USH2A* mutant alleles. It was also observed that among the already known *USH2A* mutations, the patients with biallelic null mutations manifest Usher syndrome while those with biallelic missense variant or with the combination of one missense and one null mutation are likely to develop non-syndromic RP (Su et al., 2022). Similarly, null variant identified in *USH2A* gene in our family D1 is also responsible for Usher syndrome. This is the first report of large novel *USH2A* SV causing Usher syndrome in Pakistani population.

In family D2, progressive loss of day vision was observed and initially family was diagnosed with autosomal recessive RP. The disease progression was very rapid. All the affected individuals showed reduced visual acuity (average 20/120) at as early as 7 years of age. Additionally, flat nasal bridge was observed in all affected members of the family. Initial diagnosis of the family lead to the screening of family D2 through RP-LCA panel-based sequencing, but none of the pathogenic variant was identified as a potential cause for the observed phenotype. GS of the proband identified a novel indel (c.1785_1786delinG; p.(Pro597Leufs*127) in *COL18A1* gene. COL18A1 encodes the alpha subunit of collagen XVIII protein and this protein is present on the basement membrane of tissues (National Library of Medicine, MedlinePlus: https://medlineplus.gov/genetics/gene/col18a1/#conditions). It is expressed in retina, iris and vitreous humour and is an important player in retinal and visual function beside its role in neuronal migration and closure of neural tube during development (Sertie et al. 2000; Menzel et al. 2004). In 2014 the expression of collagen XVIII was also identified in the blood vessels of developing human cerebral cortex (Caglayan et al., 2014). Literature shows that variants in the *COL18A1* are responsible to cause Knobloch syndrome which is characterized by eye malformations including cataracts, high myopia, retinal detachment or vitreoretinal degeneration along with developmental delay and severe or mild ID (Kliemann et al., 2003; Najmabadi et al., 2011). The affected members of family D2 had severe eye abnormality but at the time of family recruitment, ID was not reported, although some behavioral problems were seen. This family belongs to a very underdeveloped region of Pakistan (Balochistan) therefore due to limited logistics, access to the family again for follow-up study is not possible. From our previous experience of Usher syndrome and reviewed literature by (Naz, 2022), we may conclude that the mild symptoms sometimes remain un-noticed in the Pakistani families during initial diagnosis. Similarly, affected individuals from the family D2 may also manifest mild ID which was not observed during initial diagnosis. Considering this, we may conclude that the family D2 was affected with Knobloch syndrome. Previously, a different *COL18A1* variant p.(Gly892Aspfs*17) was identified in a Pakistani family initially diagnosed with ID. Later reverse phenotyping confirmed the presence of eye abnormality in the affected individuals. The novel variant p.(Pro597Leufs*127) identified in *COL18A1* in D2 family will result in frameshift which will either produce no protein due to NMD of the transcript or will

produce a truncated protein with the absence of important protein domains like trimerization (TRI) domain and endostatin domain required for proper protein functioning (UniProt; assessed on 8th September, 2023: https://www.uniprot.org/uniprotkb/P39060/entry).

The family D3, was identified with congenital blindness, additionally microcornea and corneal haze was also observed in the affected members of this family. Pedigree analysis showed X-linked inheritance and initially proband (III:2) was screened through RP-LCA panel-based sequencing to identify any disease-causing variant. However, no potential pathogenic variant was identified in RP-LCA associated genes through panel sequencing, which led to further follow up with genome sequencing. The initial variant prioritization of GS data did not identify any potential pathogenic variant in this family, but later based on nucleotide conservation scores (PhyloP score $\geq$ 2.7), a homozygous variant (c.-208G>A) was identified in the *NDP* gene. *NDP* variants are known to cause Norrie disease which is characterized by profound degenerative changes to neuroretina leading towards congenital or early childhood blindness. Other symptoms include microcornea, mental retardation in 50% cases or mild hearing loss in approximately one-third of cases after 2nd decade of life (Bleeker-Wagemakers et al., 1985). *NDP* gene encodes a norrin protein which is a cysteine rich 133 amino acid long protein (Meindl et al., 1992). This protein binds with frizzled-4 receptor and activates Wnt signalling pathway which is involved in retinal vascularization (Ye et al., 2010). The variant identified in this study resides in the 5' UTR region of the *NDP* gene. The variants in the 5' UTR region of this gene are already known to cause FEVR in Chinese population (Jia and Ma, 2021). Prior *in vitro* studies has proved that the sequence c.-219 to c.-107 contains a putative repressing region and when deleted it results in unregulated expression of downstream region in retinoblastoma cells (Kenyon and Craig, 1999). Two variants in NDP are known to cause FEVR in Pakistani families (Keser et al., 2017) and one single nucleotide deletion p.(Val17fs*1) is known to cause Norrie disease (Waryah et al., 2011). This is the first study presenting 5' UTR variant in *NDP* gene to cause Norrie disease in Pakistani population.
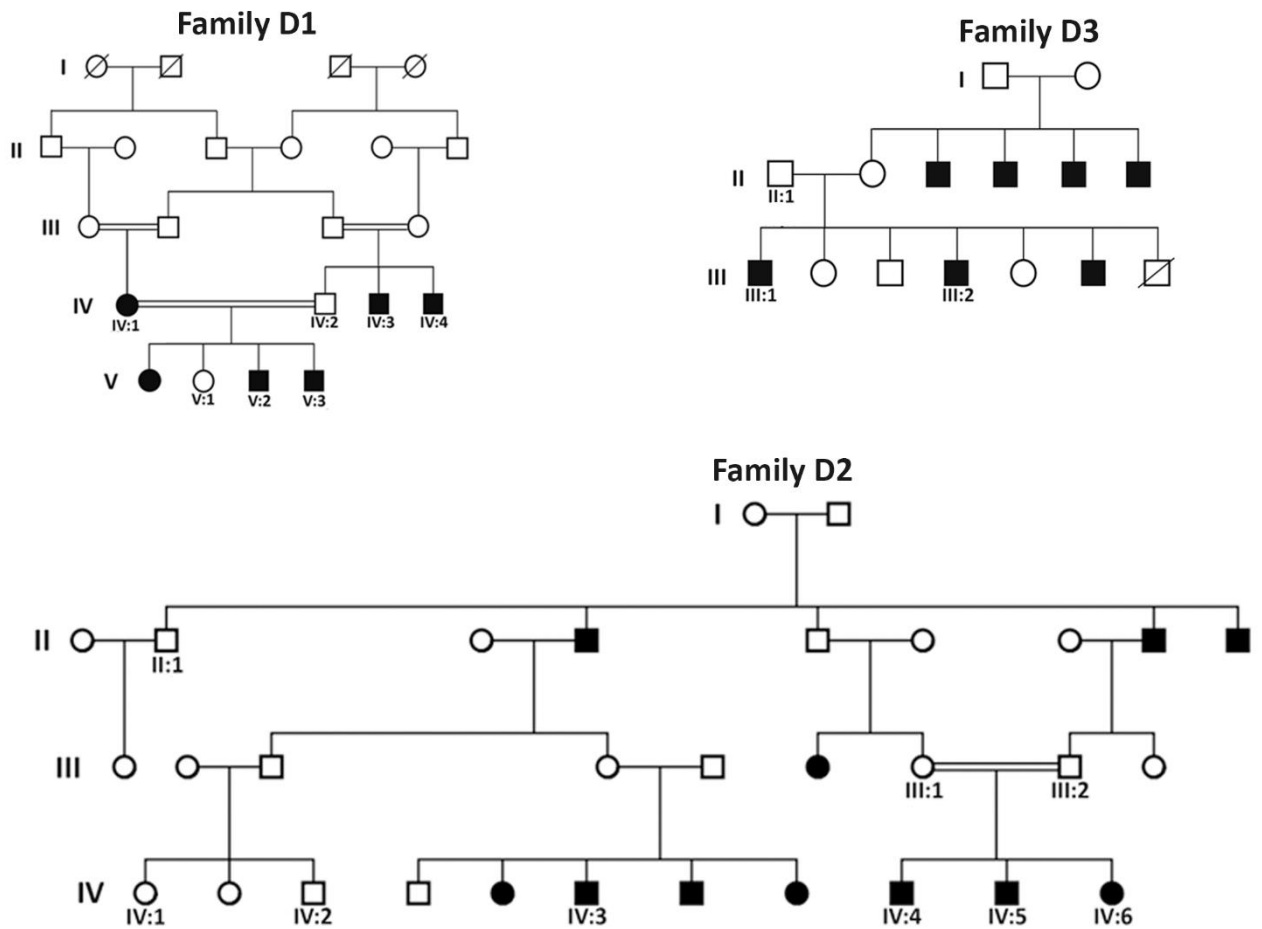
Figure 6.1: Pedigrees of three families with Usher syndrome (D1), Knobloch syndrome (D2) and Norrie disease (D3) respectively, which were collected from different regions of Pakistan. Numbers are given in each pedigree only to the participating members.
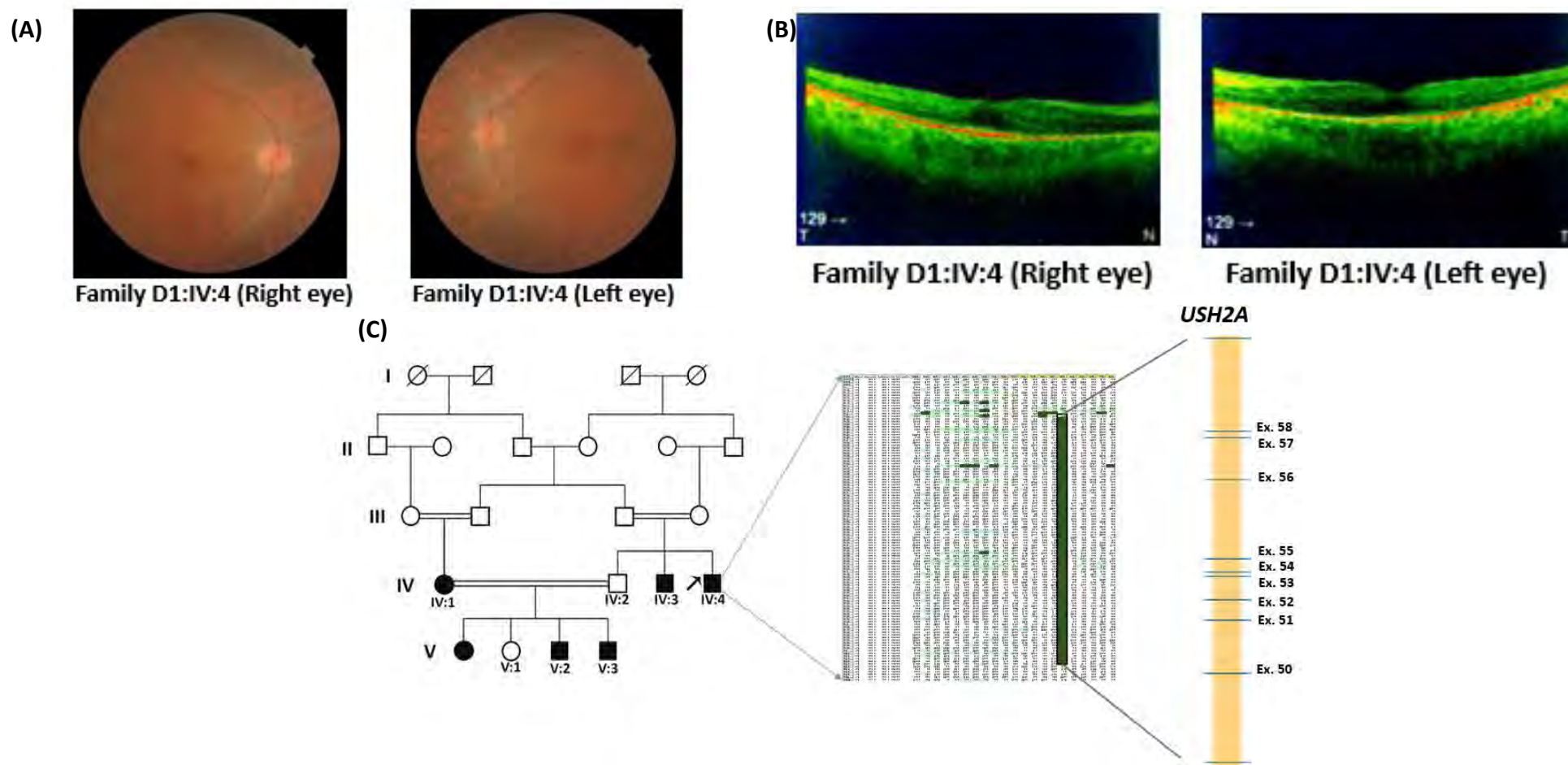
Figure 6.2: (A). Fundus images of both eyes of affected individual IV:4 from family D1 with Usher syndrome. Fundus clearly show pigment deposition mainly in the peripheral region. (B). Optical coherence tomography (OCT) images of both eyes of same individual (IV:4) show retinal layer degeneration. (C). Copy number variation (CNV) analysis based on the average coverage per run indicates homozygous deletion of smMIPs covering region of exon 49- exon 59 within *USH2A* gene in the panel sequencing data of proband (IV:4).
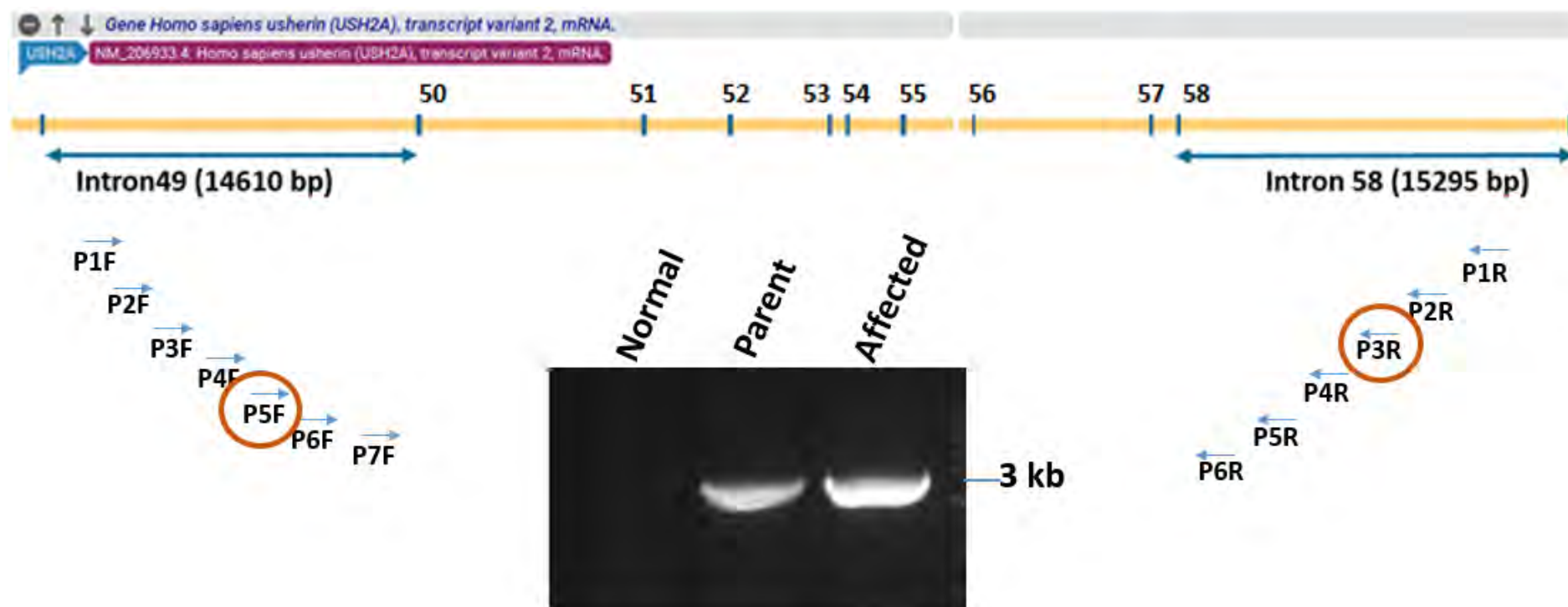
Figure 6.3: Deletion mapping of *USH2A* structural variant (SV) identified in D1 family. Upper panel is a schematic view of USH2A region containing exon49-exon 59. Below the arrows are the sizes of both intron 49 and intron 58, at right and left respectively. Seven forward primers designed within intron 49 are shown with arrows and six reverse primers designed within intron 58 are represented with arrows at the left. The gel image show absence of band in healthy control (normal), but band is present in individual heterozygous (Parent) and homozygous (Affected individual) for deletion. The product shown was approximately 3kb, amplified with the primers encircled.
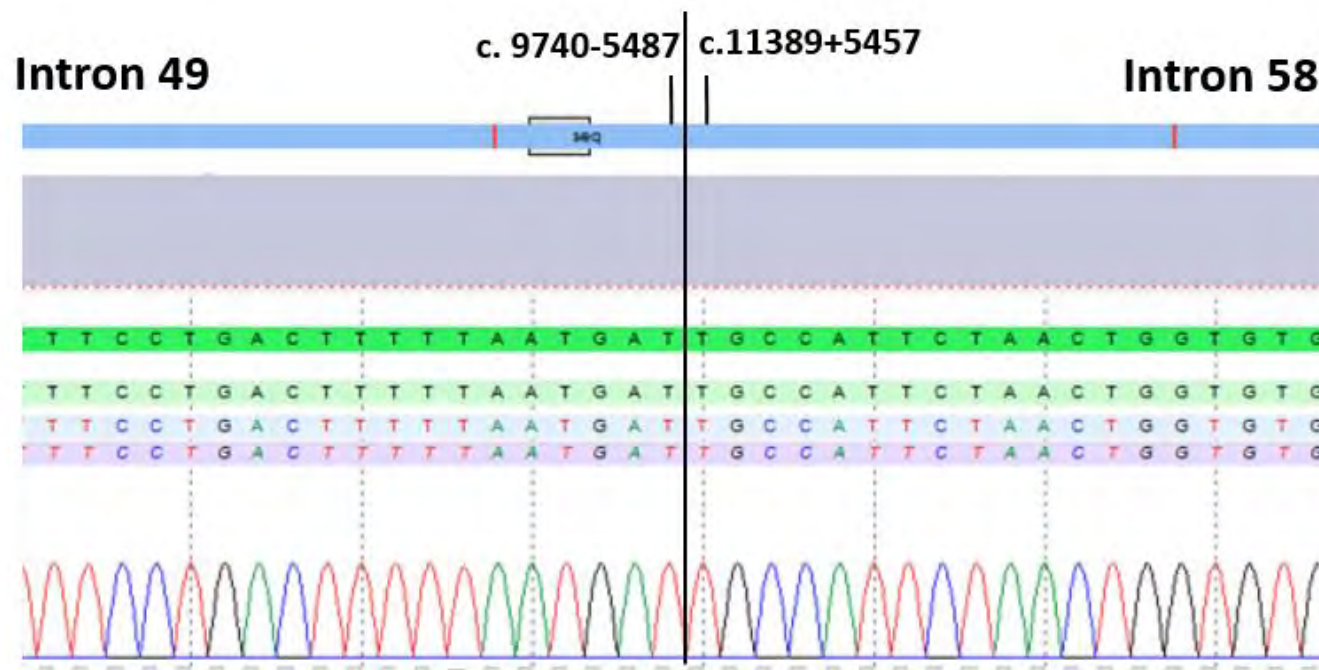
Figure 6.4: The chromatogram from PacBio long read sequencing show exact breakpoints of *USH2A* partial deletion. It is a deletion of 51.7kb (chr1:215977954_chr1:215926480del (hg19)) which most probably will result in an in-frame deletion p.(Glu3248_Gly3797del) in USH2A protein.
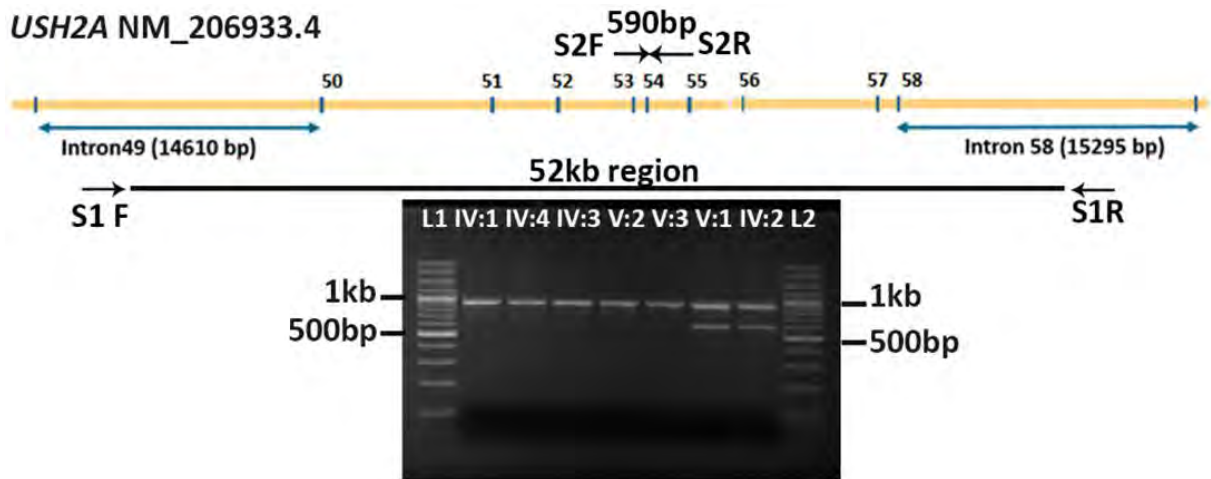
Figure 6.5: Segregation analysis of *USH2A* in family D1. Schematic representation of the *USH2A* region (exon 48-exon 59) is given above and the primer pairs (S1 and S2) location is indicated with the arrows. Expected product sizes from normal individual are mentioned between the indicated primers. The product obtained from pair S1 in affected or carrier is 889bp. The affected individuals showed absence of product (590bp) from primer S2 (amplifying region of exon 54 within the deleted region).
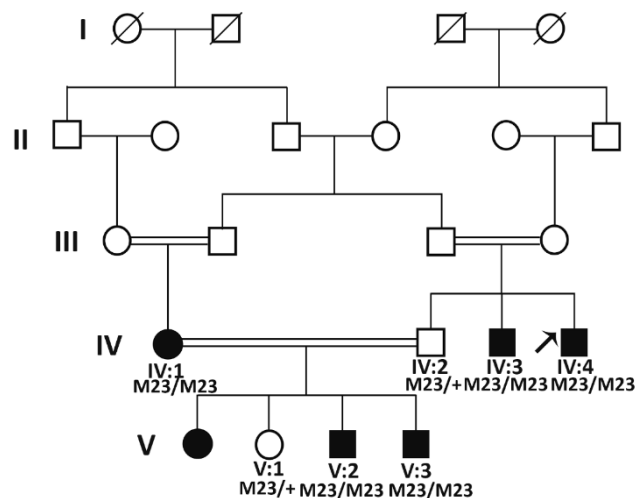
Figure 6.6: Pedigree of Family D1 where arrow is indicating the proband and below each participating member is shown the segregation results of structural variant (SV), M23= deletion of 51.7kb region (chr1:215977954_chr1:215926480del (hg19)) in *USH2A* gene.

(A)

(B) M24 = c.1785_1786delinsG; p.(Pro597Leufs*127)

WT:GACCACCAGGCCCCCCTGGGCCCCCT
MT:GACCACCAGGG-CCCCTGGGCCCCCT
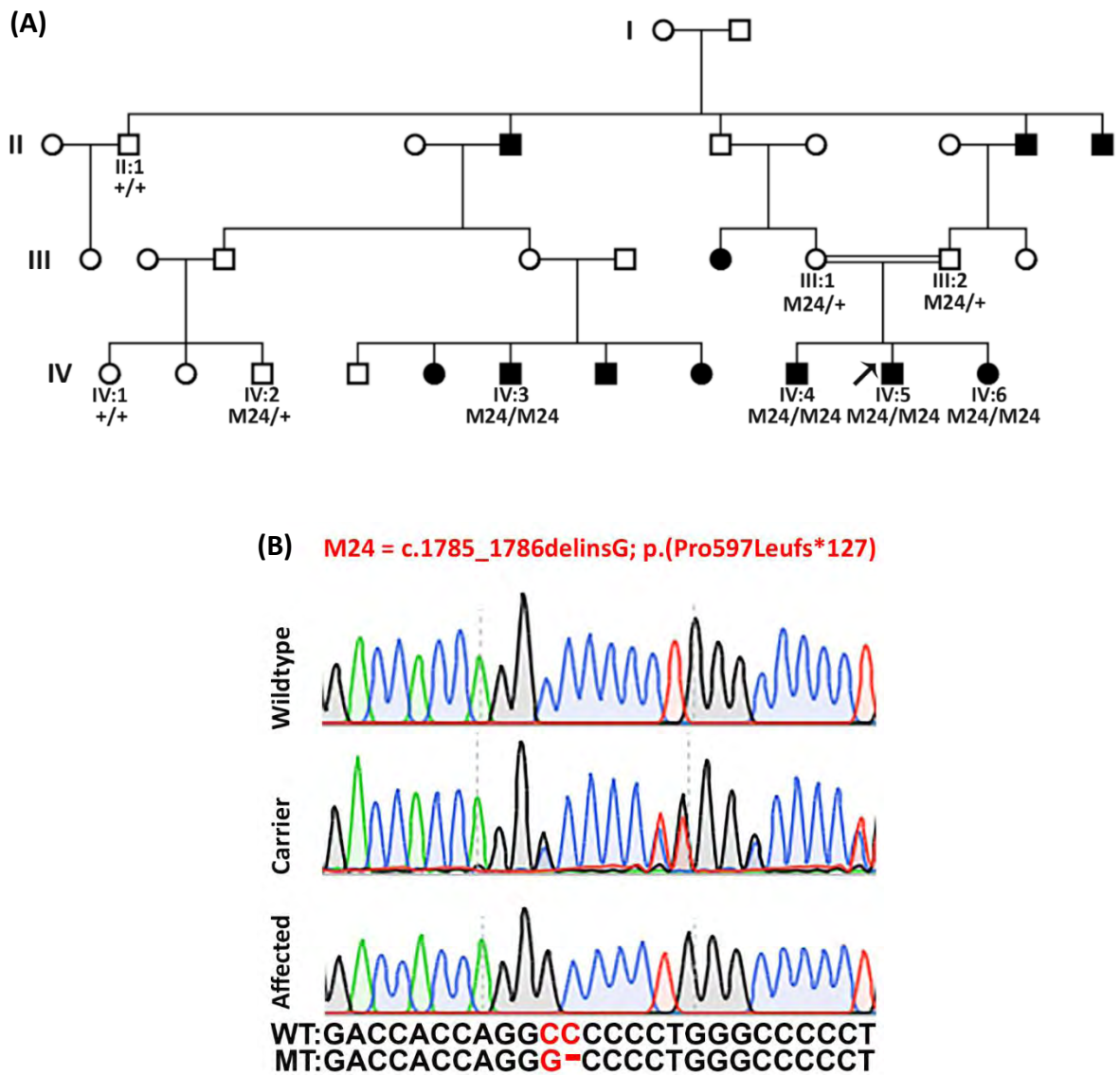
Figure 6.7: Pedigree of family D2 where arrow is indicating the proband and below each participating member is shown the segregation results. (B). Chromatogram of the variant M24 (c.1785_1786delinsG; p.(Pro596Argfs*16)) identified in *COL18A1* in wildtype, carrier and affected individuals.
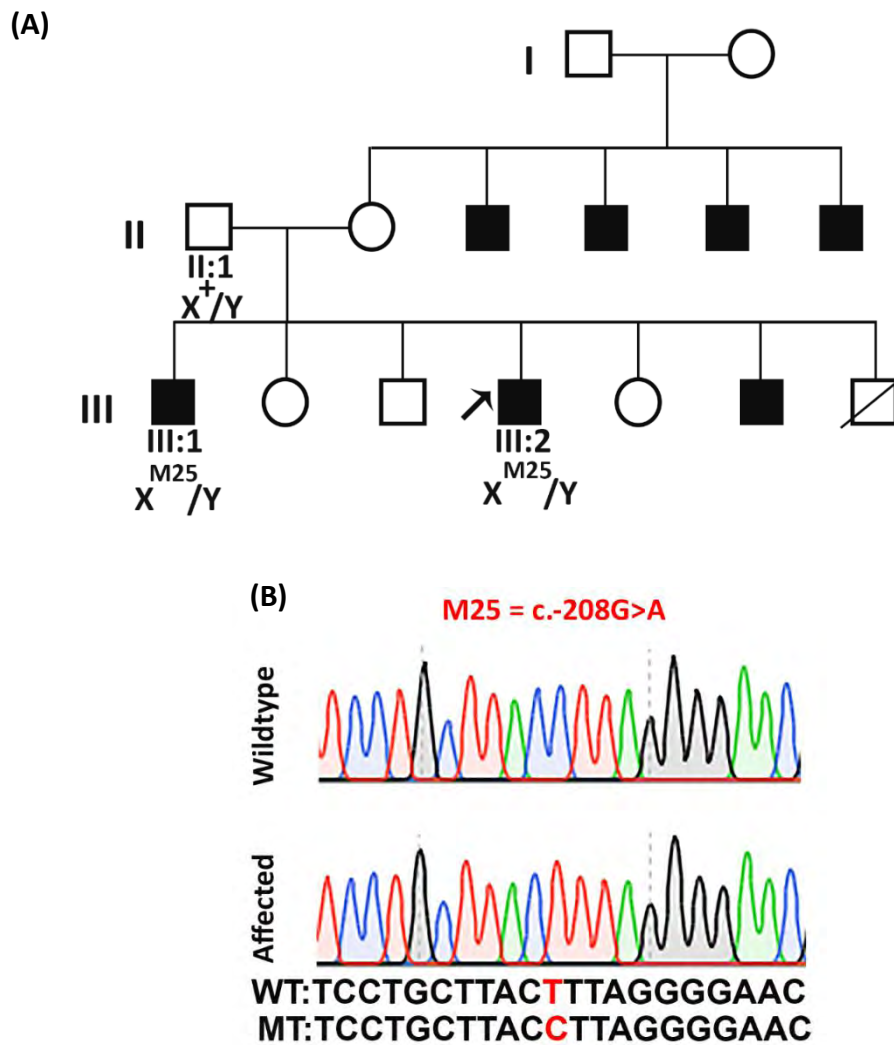
Figure 6.8: Pedigree of Family D3 where arrow is indicating the proband and below each participating member is shown the segregation results. (B). Chromatogram of the variant M25 (c.-208G>A) identified in *NDP* in wildtype and affected individuals.

Table 6.1: Clinical features of affected individuals from three families (D1-D3) affected with syndromic inherited retinal dystrophies.

Family ID	Inheritance Pattern	Phenotype	Patient ID	Gender	Age onset (age at the time of sampling)	Observation at the time of sampling			Nystagmus	Corneal haze	Photophobia	Additional features (if any)
						Night vision	Day vision	Color vision				
D1	AR	US	IV:1	F	1-2 yrs (52 yrs)	No	NPL	NA	-	-	-	Hearing loss
			IV:3	M	1-2 yrs (32 yrs)	No	NPL	NA	-	-	-	Hearing loss
			IV:4	M	1-2 yrs (29 yrs)	No	20/80	Normal	-	-	-	Hearing loss
			V:2	M	1-2 yrs (30 yrs)	No	NPL	NA	-	-	-	Hearing loss, Mild ID
			V:3	M	1-2 yrs (26 yrs)	No	20/80	Normal	-	-	-	Hearing loss, Mild ID
D2	AR	KS	IV:3	M	By birth (18 yrs)	No	PL	NA	+	LE	-	Flat nasal bridge
			IV:4	M	3-4 yrs (7 yrs)	No	20/100	Normal	-	-	-	Flat nasal bridge
			IV:5	M	3-4 yrs (9 yrs)	No	20/120	Normal	-	-	-	Flat nasal bridge
			IV:6	F	3-4 yrs (10 yrs)	No	20/120	Normal	+	-	-	Flat nasal bridge
D3	XLR	ND	III:1	M	By birth (36 yrs)	No	NPL	NA	-	+	-	Microcornea
			III:2	M	By birth (31 yrs)	No	NPL	NA	-	+	-	Microcornea

AR= Autosomal recessive, F= Female, ID= Intellectual disability, KS= Knobloch syndrome, LE= Left eye, M= Male, NA= Not applicable, ND= Norrie disease, NPL= No perception of light, PL= perception of light, US= Usher syndrome, XLR= X-linked recessive, yrs= years, += Present, - = Absent.

Table 6.2: *In silico* predictions for potential disease-causing variants identified in three families (D1-D3) affected with syndromic inherited retinal dystrophies.

Family ID	Gene	cDNA	Protein	gnomAD.G.AF	CADD-PHRED	Grantham	PhyloP	REVEL	ACMG classification	Reference
D1	*USH2A*	c.9740-5487_11389+5457del	p.(Glu3248_Gly3797del)	Not found	NA	NA	NA	NA	Pathogenic	This study
D2	*COL18A1*	c.1785_1786delinsG	p.(Pro597Leufs*127)	Not found	NA	NA	NA	NA	Likely pathogenic	This study
D3	*NDP*	c.-208G>A	NA	Not found	24.2	NA	5.4	NA	VUS	This study

gnomAD.G.AF= Allele frequency in genomes of gnomAD database, NA= Not applicable, VUS= Variant of uncertain significance.

7.0.CONCLUSION

The advancements in the sequencing technologies has revolutionized the genetic diagnosis. The genome sequencing costs have been reduced from $2.7 billion to $1000 now (Schloss 2008). With the combination of other omics approaches like transcriptomics, epigenomics, proteomics and metabolomics, the recognition of regulatory and non-coding elements in disease involvement have also broadened the horizon of genetics. Panel based sequencing has provided a solution for early diagnosis of already known variants and novel variants within the genes with known association to disease. Several eye-disorder related panels have been used in different studies for this purpose. The underdeveloped countries like Pakistan requires the use of panel based genetic testing which can provide a cost-effective and efficient genetic diagnosis. For this purpose, inclusion of already associated genes and regions specifically from our population is of huge importance. In this study we attempted to screen 28 Pakistani families affected with inherited eye disorders for the identification of genetic cause. We used several different approaches to identify the potential pathogenic variants in each family. These approaches provide successful solve rate with the identification of several known and novel disease-causing variants in genes related to eye disorders in Pakistan. Identification of already known variants with a different phenotype is increased the phenotypic spectrum as exemplified in case of *CNGB1* variant associated with RP (Maranhao et al. 2015; Saqib et al. 2015) is detected in CSNB in our cohort. Similarly, identification of novel variants in the already known genes has increased the genotypic landscape of the disease.

Targeted Sanger sequencing solved 7 families (25% of the solved families), though applied only on PCG and A/M families. Panel sequencing applied on non-syndromic and syndromic IRDs solved 10 families (37% of the solved families), while exome sequencing solved 3 (11% of the solved families) and genome sequencing solved 7 (25% of the solved families) families. We confirmed that *CYP1B1* and *FOXE3* variants as the prevalent cause of PCG and A/M in Pakistani population respectively. Therefore, targeted Sanger sequencing of *CYP1B1* gene in PCG patients and *FOXE3* gene in A/M patients in Pakistani cohort is cost-effective and is recommended prior to any NGS testing (chapter 3 and 4).

If considered alone, panel based sequencing solved 10 families out of 14 screened families (71%). The families which remained unsolved from the diagnostic panels were mis-diagnosed during initial clinical diagnosis. Two panels (RP-LCA and MD) successfully identified variants in specific clinical groups except an LCA family for which 1-bp deletion was identified in *ATOH7*. The patients harboring homozygous 1-bp deletion were presented with congenital blindness and therefore confused with LCA (considering early onset of retinal degeneration). This implies that the genetic testing can be helpful in situations where clinical diagnostic including OCT, fundoscopy and ERG is not available and patients themselves cannot move due to poor logistics in the region.

We also demonstrated the importance of panel sequencing in the identification of probable a 51.7 kb structural variant in *USH2A* gene in a family with usher syndrome. The identification of deep intronic variant and its involvement in altering the normal splicing lead to pseudoexon activation in the mature transcript and emphasizes the importance of screening non-coding regions in unsolved cases. This is possible with GS which is an expensive technique and not affordable for the patients residing in the low economic countries like Pakistan. This situation can be dealt, by initially increasing the mutational landscape of inherited eye disorders in Pakistan and then later designing our population based panels which captures the coding regions of the known genes and also non-coding regions with known disease causing variants.

In totality by the stepwise application of TSS, PS, ES and GS we obtained the genetic diagnostic yield of 96% in families affected with different eye disorders and the identification of 11 novel variants (10 SNVs and 1 SV) in this study. All the identified variants were present in the genes already known to be associated with the particular phenotype. The identification of 11 novel variants in a relatively small cohort of 28 families expanded the genetic landscape of eye disorders in our population. The identification of variants in already associated genes emphasizes utilization of time and cost effective screening panels for rapid diagnosis. Nevertheless, the homozygous deep intronic variant identified in A/M family also highlights the role of non-coding variants. Thus, initial screenings through several NGS techniques are required in our and other similar populations, to establish a well-defined panel for screening of inherited eye

disorders. The genetic diagnosis will eventually help us moving towards personalized medicine, for the patients affected with different inherited eye disorders.

8.0. REFERENCES

Abdolrahimzadeh S, Fameli V, Mollo R, Contestabile MT, Perdicchi A, Recupero SM (2015) Rare Diseases Leading to Childhood Glaucoma: Epidemiology, Pathophysiogenesis, and Management. Biomed Res Int 2015: 781294. doi: 10.1155/2015/781294

Aboobakar IF, Wiggs JL (2022) The genetics of glaucoma: Disease associations, personalised risk assessment and therapeutic opportunities-A review. Clin Exp Ophthalmol 50: 143-162. doi: 10.1111/ceo.14035

Abouzeid H, Youssef MA, Bayoumi N, ElShakankiri N, Marzouk I, Hauser P, Schorderet DF (2012) RAX and anophthalmia in humans: evidence of brain anomalies. Mol Vis 18: 1449-56.

Abu-Amero KK, Edward DP (1993) Primary Congenital Glaucoma. In: Adam MP, Mirzaa GM, Pagon RA, Wallace SE, Bean LJH, Gripp KW, Amemiya A (eds) GeneReviews((R)), Seattle (WA)

Abu-Amero KK, Osman EA, Mousa A, Wheeler J, Whigham B, Allingham RR, Hauser MA, Al-Obeidan SA (2011) Screening of CYP1B1 and LTBP2 genes in Saudi families with primary congenital glaucoma: genotype-phenotype correlation. Mol Vis 17: 2911-9.

Adhi MIA, Jamshed (2002) Frequency and clinical presentation of retinal dystrophies-A hospital based study. Pak. J. Ophthalmol 18: 4.

Adzhubei IA, Schmidt S, Peshkin L, Ramensky VE, Gerasimova A, Bork P, Kondrashov AS, Sunyaev SR (2010) A method and server for predicting damaging missense mutations. Nat Methods 7: 248-9. doi: 10.1038/nmeth0410-248

Ahmed AN, Tahir R, Khan N, Ahmad M, Dawood M, Basit A, Yasin M, Nowshid M, Marwan M, Sultan K, Saleha S (2021) USH2A gene variants cause Keratoconus and Usher syndrome phenotypes in Pakistani families. BMC Ophthalmol 21: 191. doi: 10.1186/s12886-021-01957-9

Aijaz S, Clark BJ, Williamson K, van Heyningen V, Morrison D, Fitzpatrick D, Collin R, Ragge N, Christoforou A, Brown A, Hanson I (2004) Absence of SIX6 mutations in microphthalmia, anophthalmia, and coloboma. Invest Ophthalmol Vis Sci 45: 3871-6. doi: 10.1167/iovs.04-0641

Ajmal M, Khan MI, Micheal S, Ahmed W, Shah A, Venselaar H, Bokhari H, Azam A, Waheed NK, Collin RW, den Hollander AI, Qamar R, Cremers FP (2012) Identification of recurrent and novel mutations in TULP1 in Pakistani families with early-onset retinitis pigmentosa. Mol Vis 18: 1226-37.

Ali M, Buentello-Volante B, McKibbin M, Rocha-Medina JA, Fernandez-Fuentes N, Koga-Nakamura W, Ashiq A, Khan K, Booth AP, Williams G, Raashid Y, Jafri H, Rice A, Inglehearn CF, Zenteno JC (2010) Homozygous FOXE3 mutations cause non-syndromic, bilateral, total sclerocornea, aphakia, microphthalmia and optic disc coloboma. Mol Vis 16: 1162-8.

Ali M, McKibbin M, Booth A, Parry DA, Jain P, Riazuddin SA, Hejtmancik JF, Khan SN, Firasat S, Shires M, Gilmour DF, Towns K, Murphy AL, Azmanov D, Tournev I, Cherninkova S, Jafri H, Raashid Y, Toomes C, Craig J, Mackey DA, Kalaydjieva L, Riazuddin S, Inglehearn CF (2009) Null mutations in LTBP2 cause primary congenital glaucoma. Am J Hum Genet 84: 664-71. doi: 10.1016/j.ajhg.2009.03.017

Alkuraya FS (2010) Homozygosity mapping: one more tool in the clinical geneticist's toolbox. Genet Med 12: 236-9. doi: 10.1097/GIM.0b013e3181ceb95d

Alsaif HS, Khan AO, Patel N, Alkuraya H, Hashem M, Abdulwahab F, Ibrahim N, Aldahmesh MA, Alkuraya FS (2019) Congenital glaucoma and CYP1B1: an old story revisited. Hum Genet 138: 1043-1049. doi: 10.1007/s00439-018-1878-z

Ammar THA, Ismail S, Mansour OAA, El-Shafey MM, Doghish AS, Kamal AM, Abdel-Salam GMH (2017) Genetic analysis of SOX2 and VSX2 genes in 27 Egyptian families with anophthalmia and microphthalmia. Ophthalmic Genet 38: 498-500. doi: 10.1080/13816810.2017.1279184

Anjum I, Eiberg H, Baig SM, Tommerup N, Hansen L (2010) A mutation in the FOXE3 gene causes congenital primary aphakia in an autosomal recessive consanguineous Pakistani family. Mol Vis 16: 549-55.

Arshavsky VY, Lamb TD, Pugh EN, Jr. (2002) G proteins and phototransduction. Annu Rev Physiol 64: 153-87. doi: 10.1146/annurev.physiol.64.082701.102229

Astuti GD, Bertelsen M, Preising MN, Ajmal M, Lorenz B, Faradz SM, Qamar R, Collin RW, Rosenberg T, Cremers FP (2016) Comprehensive genotyping reveals RPE65 as the most frequently mutated gene in Leber congenital

amaurosis in Denmark. Eur J Hum Genet 24: 1071-9. doi: 10.1038/ejhg.2015.241

Atac D, Mohn L, Feil S, Maggi K, Haenni D, Seebauer B, Koller S, Berger W (2022) Functional Characterization of an In-Frame Deletion in the Basic Domain of the Retinal Transcription Factor ATOH7. Int J Mol Sci 23. doi: 10.3390/ijms23031053

Azmanov DN, Dimitrova S, Florez L, Cherninkova S, Draganov D, Morar B, Saat R, Juan M, Arostegui JI, Ganguly S, Soodyall H, Chakrabarti S, Padh H, Lopez-Nevot MA, Chernodrinska V, Anguelov B, Majumder P, Angelova L, Kaneva R, Mackey DA, Tournev I, Kalaydjieva L (2011) LTBP2 and CYP1B1 mutations and associated ocular phenotypes in the Roma/Gypsy founder population. Eur J Hum Genet 19: 326-33. doi: 10.1038/ejhg.2010.181

Ba-Abbad R, Holder GE, Robson AG, Neveu MM, Waseem N, Arno G, Webster AR (2019) Isolated rod dysfunction associated with a novel genotype of CNGB1. Am J Ophthalmol Case Rep 14: 83-86. doi: 10.1016/j.ajoc.2019.03.004

Bailey JN, Loomis SJ, Kang JH, Allingham RR, Gharahkhani P, Khor CC, Burdon KP, Aschard H, Chasman DI, Igo RP, Jr., Hysi PG, Glastonbury CA, Ashley-Koch A, Brilliant M, Brown AA, Budenz DL, Buil A, Cheng CY, Choi H, Christen WG, Curhan G, De Vivo I, Fingert JH, Foster PJ, Fuchs C, Gaasterland D, Gaasterland T, Hewitt AW, Hu F, Hunter DJ, Khawaja AP, Lee RK, Li Z, Lichter PR, Mackey DA, McGuffin P, Mitchell P, Moroi SE, Perera SA, Pepper KW, Qi Q, Realini T, Richards JE, Ridker PM, Rimm E, Ritch R, Ritchie M, Schuman JS, Scott WK, Singh K, Sit AJ, Song YE, Tamimi RM, Topouzis F, Viswanathan AC, Verma SS, Vollrath D, Wang JJ, Weisschuh N, Wissinger B, Wollstein G, Wong TY, Yaspan BL, Zack DJ, Zhang K, Study EN, Consortium A, Weinreb RN, Pericak-Vance MA, Small K, Hammond CJ, Aung T, Liu Y, Vithana EN, MacGregor S, Craig JE, Kraft P, Howell G, Hauser MA, Pasquale LR, Haines JL, Wiggs JL (2016) Genome-wide association analysis identifies TXNRD2, ATXN2 and FOXC1 as susceptibility loci for primary open-angle glaucoma. Nat Genet 48: 189-94. doi: 10.1038/ng.3482

Bashir R, Sanai M, Azeem A, Altaf I, Saleem F, Naz S (2014) Contribution of GLC3A locus to Primary Congenital Glaucoma in Pakistani population. Pak J Med Sci 30: 1341-5. doi: 10.12669/pjms.306.5771

Bean LJH, Funke B, Carlston CM, Gannon JL, Kantarci S, Krock BL, Zhang S, Bayrak-Toydemir P, Committee ALQA (2020) Diagnostic gene sequencing panels: from design to report-a technical standard of the American College of Medical Genetics and Genomics (ACMG). Genet Med 22: 453-461. doi: 10.1038/s41436-019-0666-z

Bejjani BA, Stockton DW, Lewis RA, Tomey KF, Dueker DK, Jabak M, Astle WF, Lupski JR (2000) Multiple CYP1B1 mutations and incomplete penetrance in an inbred population segregating primary congenital glaucoma suggest frequent de novo events and a dominant modifier locus. Hum Mol Genet 9: 367-74. doi: 10.1093/hmg/9.3.367

Berger F, Lau C, Dahlmann M, Ziegler M (2005) Subcellular compartmentation and differential catalytic properties of the three human nicotinamide mononucleotide adenylyltransferase isoforms. J Biol Chem 280: 36334-41. doi: 10.1074/jbc.M508660200

Biel M, Zong X, Hofmann F (1996) Cyclic nucleotide-gated cation channels molecular diversity, structure, and cellular functions. Trends Cardiovasc Med 6: 274-80. doi: 10.1016/S1050-1738(96)00105-3

Bleeker-Wagemakers LM, Friedrich U, Gal A, Wienker TF, Warburg M, Ropers HH (1985) Close linkage between Norrie disease, a cloned DNA sequence from the proximal short arm, and the centromere of the X chromosome. Hum Genet 71: 211-4. doi: 10.1007/BF00284575

Botstein D, Risch N (2003) Discovering genotypes underlying human phenotypes: past successes for mendelian disease, future approaches for complex disease. Nat Genet 33 Suppl: 228-37. doi: 10.1038/ng1090

Boyle EA, O'Roak BJ, Martin BK, Kumar A, Shendure J (2014) MIPgen: optimized modeling and design of molecular inversion probes for targeted resequencing. Bioinformatics 30: 2670-2. doi: 10.1093/bioinformatics/btu353

Busby A, Dolk H, Armstrong B (2005) Eye anomalies: seasonal variation and maternal viral infections. Epidemiology 16: 317-22. doi: 10.1097/01.ede.0000158817.43037.ab

Caberoy NB, Zhou Y, Li W (2010) Tubby and tubby-like protein 1 are new MerTK ligands for phagocytosis. EMBO J 29: 3898-910. doi: 10.1038/emboj.2010.265

Caglayan AO, Baranoski JF, Aktar F, Han W, Tuysuz B, Guzel A, Guclu B, Kaymakcalan H, Aktekin B, Akgumus GT, Murray PB, Erson-Omay EZ, Caglar C, Bakircioglu M, Sakalar YB, Guzel E, Demir N, Tuncer O, Senturk S, Ekici B, Minja FJ, Sestan N, Yasuno K, Bilguvar K, Caksen H, Gunel M (2014) Brain malformations associated with Knobloch syndrome--review of literature, expanding clinical spectrum, and identification of novel mutations. Pediatr Neurol 51: 806-813 e8. doi: 10.1016/j.pediatrneurol.2014.08.025

Campos-Mollo E, Lopez-Garrido MP, Blanco-Marchite C, Garcia-Feijoo J, Peralta J, Belmonte-Martinez J, Ayuso C, Escribano J (2009) CYP1B1 mutations in Spanish patients with primary congenital glaucoma: phenotypic and functional variability. Mol Vis 15: 417-31.

Carrera W, Ng C, Burckhard B, Ng J, McDonald HR, Agarwal A (2021) Non-syndromic retinitis pigmentosa with bilateral retinal neovascularization due to HGSNAT mutation. Retin Cases Brief Rep. doi: 10.1097/ICB.0000000000001193

Carss KJ, Arno G, Erwood M, Stephens J, Sanchis-Juan A, Hull S, Megy K, Grozeva D, Dewhurst E, Malka S, Plagnol V, Penkett C, Stirrups K, Rizzo R, Wright G, Josifova D, Bitner-Glindzicz M, Scott RH, Clement E, Allen L, Armstrong R, Brady AF, Carmichael J, Chitre M, Henderson RHH, Hurst J, MacLaren RE, Murphy E, Paterson J, Rosser E, Thompson DA, Wakeling E, Ouwehand WH, Michaelides M, Moore AT, Consortium NI-BRD, Webster AR, Raymond FL (2017) Comprehensive Rare Variant Analysis via Whole-Genome Sequencing to Determine the Molecular Pathology of Inherited Retinal Disease. Am J Hum Genet 100: 75-90. doi: 10.1016/j.ajhg.2016.12.003

Castiglione A, Moller C (2022) Usher Syndrome. Audiol Res 12: 42-65. doi: 10.3390/audiolres12010005

Chang T, Brookes J, Cavuoto K, Bitrian E, Grajewski A (2013) Primary congenital glaucoma and juvenile open-angle glaucoma. . Childhood Glaucoma, The 9th Consensus Report of the World Glaucoma Association. Amsterdam: Kugler

Chang X, Wang K (2012) wANNOVAR: annotating genetic variants for personal genomes via the web. J Med Genet 49: 433-6. doi: 10.1136/jmedgenet-2012-100918

Chassaing N, Causse A, Vigouroux A, Delahaye A, Alessandri JL, Boespflug-Tanguy O, Boute-Benejean O, Dollfus H, Duban-Bedu B, Gilbert-Dussardier B, Giuliano F, Gonzales M, Holder-Espinasse M, Isidor B, Jacquemont ML, Lacombe D, Martin-Coignard D, Mathieu-Dramard M, Odent S, Picone O, Pinson L, Quelin C, Sigaudy S, Toutain A, Thauvin-Robinet C, Kaplan J, Calvas P (2014) Molecular findings and clinical data in a cohort of 150 patients with anophthalmia/microphthalmia. Clin Genet 86: 326-34. doi: 10.1111/cge.12275

Chassaing N, Ragge N, Plaisancie J, Patat O, Genevieve D, Rivier F, Malrieu-Eliaou C, Hamel C, Kaplan J, Calvas P (2016) Confirmation of TENM3 involvement in autosomal recessive colobomatous microphthalmia. Am J Med Genet A 170: 1895-8. doi: 10.1002/ajmg.a.37667

Chatziralli IP, Kanonidou ED, Keryttopoulos P, Dimitriadis P, Papazisis LE (2012) The value of fundoscopy in general practice. Open Ophthalmol J 6: 4-5. doi: 10.2174/1874364101206010004

Chen X, Schulz-Trieglaff O, Shaw R, Barnes B, Schlesinger F, Kallberg M, Cox AJ, Kruglyak S, Saunders CT (2016) Manta: rapid detection of structural variants and indels for germline and cancer sequencing applications. Bioinformatics 32: 1220-2. doi: 10.1093/bioinformatics/btv710

Chen Y, Jiang D, Yu L, Katz B, Zhang K, Wan B, Sun X (2008) CYP1B1 and MYOC mutations in 116 Chinese patients with primary congenital glaucoma. Arch Ophthalmol 126: 1443-7. doi: 10.1001/archopht.126.10.1443

Chen Y, Zhang Q, Shen T, Xiao X, Li S, Guan L, Zhang J, Zhu Z, Yin Y, Wang P, Guo X, Wang J, Zhang Q (2013) Comprehensive mutation analysis by whole-exome sequencing in 41 Chinese families with Leber congenital amaurosis. Invest Ophthalmol Vis Sci 54: 4351-7. doi: 10.1167/iovs.13-11606

Chitsazian F, Tusi BK, Elahi E, Saroei HA, Sanati MH, Yazdani S, Pakravan M, Nilforooshan N, Eslami Y, Mehrjerdi MA, Zareei R, Jabbarvand M, Abdolahi A, Lasheyee AR, Etemadi A, Bayat B, Sadeghi M, Banoei MM, Ghafarzadeh B, Rohani MR, Rismanchian A, Thorstenson Y, Sarfarazi M (2007) CYP1B1 mutation profile of Iranian primary congenital glaucoma patients and associated haplotypes. J Mol Diagn 9: 382-93. doi: 10.2353/jmoldx.2007.060157

Chiu W, Lin TY, Chang YC, Isahwan-Ahmad Mulyadi Lai H, Lin SC, Ma C, Yarmishyn AA, Lin SC, Chang KJ, Chou YB, Hsu CC, Lin TC, Chen SJ, Chien Y, Yang YP, Hwang DK (2021) An Update on Gene Therapy for Inherited Retinal Dystrophy: Experience in Leber Congenital Amaurosis Clinical Trials. Int J Mol Sci 22. doi: 10.3390/ijms22094534

Choi M, Scholl UI, Ji W, Liu T, Tikhonova IR, Zumbo P, Nayir A, Bakkaloglu A, Ozen S, Sanjad S, Nelson-Williams C, Farhi A, Mane S, Lifton RP (2009) Genetic diagnosis by whole exome capture and massively parallel DNA sequencing. Proc Natl Acad Sci U S A 106: 19096-101. doi: 10.1073/pnas.0910672106

Choi Y, Chan AP (2015) PROVEAN web server: a tool to predict the functional effect of amino acid substitutions and indels. Bioinformatics 31: 2745-7. doi: 10.1093/bioinformatics/btv195

Choudhary D, Jansson I, Stoilov I, Sarfarazi M, Schenkman JB (2004) Metabolism of retinoids and arachidonic acid by human and mouse cytochrome P450 1b1. Drug Metab Dispos 32: 840-7. doi: 10.1124/dmd.32.8.840

Cideciyan AV, Jacobson SG, Drack AV, Ho AC, Charng J, Garafalo AV, Roman AJ, Sumaroka A, Han IC, Hochstedler MD, Pfeifer WL, Sohn EH, Taiel M, Schwartz MR, Biasutto P, Wit W, Cheetham ME, Adamson P, Rodman DM, Platenburg G, Tome MD, Balikova I, Nerinckx F, Zaeytijd J, Van Cauwenbergh C, Leroy BP, Russell SR (2019) Effect of an intravitreal antisense oligonucleotide on vision in Leber congenital amaurosis due to a photoreceptor cilium defect. Nat Med 25: 225-228. doi: 10.1038/s41591-018-0295-0

Comander J, Weigel-DiFranco C, Maher M, Place E, Wan A, Harper S, Sandberg MA, Navarro-Gomez D, Pierce EA (2017) The Genetic Basis of Pericentral Retinitis Pigmentosa-A Form of Mild Retinitis Pigmentosa. Genes (Basel) 8. doi: 10.3390/genes8100256

Conforti L, Janeckova L, Wagner D, Mazzola F, Cialabrini L, Di Stefano M, Orsomando G, Magni G, Bendotti C, Smyth N, Coleman M (2011) Reducing expression of NAD+ synthesizing enzyme NMNAT1 does not affect the rate of Wallerian degeneration. FEBS J 278: 2666-79. doi: 10.1111/j.1742-4658.2011.08193.x

Cooper D, Krawczak M, Antonorakis S (1995) The nature and mechanisms of human gene mutation, 7th Edition edn. McGraw-Hill, New York

Costa KA, Salles MV, Whitebirch C, Chiang J, Sallum JMF (2017) Gene panel sequencing in Brazilian patients with retinitis pigmentosa. Int J Retina Vitreous 3: 33. doi: 10.1186/s40942-017-0087-6

Curcio CA, Allen KA (1990) Topography of ganglion cells in human retina. J Comp Neurol 300: 5-25. doi: 10.1002/cne.903000103

de Bruijn SE, Rodenburg K, Corominas J, Ben-Yosef T, Reurink J, Kremer H, Whelan L, Plomp AS, Berger W, Farrar GJ, Ferenc Kovacs A, Fajardy I, Hitti-Malin RJ, Weisschuh N, Weener ME, Sharon D, Pennings RJE, Haer-Wigman L, Hoyng CB, Nelen MR, Vissers L, van den Born LI, Gilissen C, Cremers FPM, Hoischen A, Neveling K, Roosing S (2022) Optical genome mapping and revisiting short-read genome sequencing data reveal previously overlooked structural variants disrupting retinal disease-associated genes. Genet Med: 100345. doi: 10.1016/j.gim.2022.11.013

Deepthi A, Fakhoury O, Daher M, Gambarini A, El-Hayek S, Megarbane A (2021) SIX6-related anophthalmia/microphthalmia: second report on a deletion in a consanguineous family. Ophthalmic Genet 42: 88-91. doi: 10.1080/13816810.2020.1836660

DelMonte DW, Kim T (2011) Anatomy and physiology of the cornea. J Cataract Refract Surg 37: 588-98. doi: 10.1016/j.jcrs.2010.12.037

den Hollander AI, Roepman R, Koenekoop RK, Cremers FP (2008) Leber congenital amaurosis: genes, proteins and disease mechanisms. Prog Retin Eye Res 27: 391-419. doi: 10.1016/j.preteyeres.2008.05.003

den Hollander AI, van Lith-Verhoeven JJ, Arends ML, Strom TM, Cremers FP, Hoyng CB (2007) Novel compound heterozygous TULP1 mutations in a family with severe early-onset retinitis pigmentosa. Arch Ophthalmol 125: 932-5. doi: 10.1001/archopht.125.7.932

Deyle DR, Russell DW (2009) Adeno-associated virus vector integration. Curr Opin Mol Ther 11: 442-7.

El-Amraoui A, Petit C (2014) The retinal phenotype of Usher syndrome: pathophysiological insights from animal models. C R Biol 337: 167-77. doi: 10.1016/j.crvi.2013.12.004

Ellingford JM, Barton S, Bhaskar S, Williams SG, Sergouniotis PI, O'Sullivan J, Lamb JA, Perveen R, Hall G, Newman WG, Bishop PN, Roberts SA, Leach R, Tearle

R, Bayliss S, Ramsden SC, Nemeth AH, Black GC (2016) Whole Genome Sequencing Increases Molecular Diagnostic Yield Compared with Current Diagnostic Testing for Inherited Retinal Disease. Ophthalmology 123: 1143-50. doi: 10.1016/j.ophtha.2016.01.009

Esmailpour T, Riazifar H, Liu L, Donkervoort S, Huang VH, Madaan S, Shoucri BM, Busch A, Wu J, Towbin A, Chadwick RB, Sequeira A, Vawter MP, Sun G, Johnston JJ, Biesecker LG, Kawaguchi R, Sun H, Kimonis V, Huang T (2014) A splice donor mutation in NAA10 results in the dysregulation of the retinoic acid signalling pathway and causes Lenz microphthalmia syndrome. J Med Genet 51: 185-96. doi: 10.1136/jmedgenet-2013-101660

Fadaie Z, Whelan L, Dockery A, Li CHZ, van den Born LI, Hoyng CB, Gilissen C, Corominas J, Rowlands C, Megaw R, Lampe AK, Cremers FPM, Farrar GJ, Ellingford JM, Kenna PF, Roosing S (2022) BBS1 branchpoint variant is associated with non-syndromic retinitis pigmentosa. J Med Genet 59: 438-444. doi: 10.1136/jmedgenet-2020-107626

Falk MJ, Zhang Q, Nakamaru-Ogiso E, Kannabiran C, Fonseca-Kelly Z, Chakarova C, Audo I, Mackay DS, Zeitz C, Borman AD, Staniszewska M, Shukla R, Palavalli L, Mohand-Said S, Waseem NH, Jalali S, Perin JC, Place E, Ostrovsky J, Xiao R, Bhattacharya SS, Consugar M, Webster AR, Sahel JA, Moore AT, Berson EL, Liu Q, Gai X, Pierce EA (2012) NMNAT1 mutations cause Leber congenital amaurosis. Nat Genet 44: 1040-5. doi: 10.1038/ng.2361

Fares-Taie L, Gerber S, Chassaing N, Clayton-Smith J, Hanein S, Silva E, Serey M, Serre V, Gerard X, Baumann C, Plessis G, Demeer B, Bretillon L, Bole C, Nitschke P, Munnich A, Lyonnet S, Calvas P, Kaplan J, Ragge N, Rozet JM (2013) ALDH1A3 mutations cause recessive anophthalmia and microphthalmia. Am J Hum Genet 92: 265-70. doi: 10.1016/j.ajhg.2012.12.003

Fedele AO, Hopwood JJ (2010) Functional analysis of the HGSNAT gene in patients with mucopolysaccharidosis IIIC (Sanfilippo C Syndrome). Hum Mutat 31: E1574-86. doi: 10.1002/humu.21286

Feldhammer M, Durand S, Mrazova L, Boucher RM, Laframboise R, Steinfeld R, Wraith JE, Michelakakis H, van Diggelen OP, Hrebicek M, Kmoch S, Pshezhetsky AV (2009) Sanfilippo syndrome type C: mutation spectrum in the

heparan sulfate acetyl-CoA: alpha-glucosaminide N-acetyltransferase (HGSNAT) gene. Hum Mutat 30: 918-25. doi: 10.1002/humu.20986

Feng W, Yasumura D, Matthes MT, LaVail MM, Vollrath D (2002) Mertk triggers uptake of photoreceptor outer segments during phagocytosis by cultured retinal pigment epithelial cells. J Biol Chem 277: 17016-22. doi: 10.1074/jbc.M107876200

Fernandez-Vega Cueto A, Alvarez L, Garcia M, Alvarez-Barrios A, Artime E, Fernandez-Vega Cueto L, Coca-Prados M, Gonzalez-Iglesias H (2021) Candidate Glaucoma Biomarkers: From Proteins to Metabolites, and the Pitfalls to Clinical Applications. Biology (Basel) 10. doi: 10.3390/biology10080763

Ferrari S, Di Iorio E, Barbaro V, Ponzin D, Sorrentino FS, Parmeggiani F (2011) Retinitis pigmentosa: genes and disease mechanisms. Curr Genomics 12: 238-49. doi: 10.2174/138920211795860107

Ferreira CR, van Karnebeek CDM (2019) Inborn errors of metabolism. Handb Clin Neurol 162: 449-481. doi: 10.1016/B978-0-444-64029-1.00022-9

Fitzpatrick DR, van Heyningen V (2005) Developmental eye disorders. Curr Opin Genet Dev 15: 348-53. doi: 10.1016/j.gde.2005.04.013

Forsythe E, Beales PL (2013) Bardet-Biedl syndrome. Eur J Hum Genet 21: 8-13. doi: 10.1038/ejhg.2012.115

Fromer M, Moran JL, Chambert K, Banks E, Bergen SE, Ruderfer DM, Handsaker RE, McCarroll SA, O'Donovan MC, Owen MJ, Kirov G, Sullivan PF, Hultman CM, Sklar P, Purcell SM (2012) Discovery and statistical genotyping of copy-number variation from whole-exome sequencing depth. Am J Hum Genet 91: 597-607. doi: 10.1016/j.ajhg.2012.08.005

Fujinami K, Oishi A, Yang L, Arno G, Pontikos N, Yoshitake K, Fujinami-Yokokawa Y, Liu X, Hayashi T, Katagiri S, Mizobuchi K, Mizota A, Shinoda K, Nakamura N, Kurihara T, Tsubota K, Miyake Y, Iwata T, Tsujikawa A, Tsunoda K, Japan Eye Genetics Consortium study g (2020) Clinical and genetic characteristics of 10 Japanese patients with PROM1-associated retinal disorder: A report of the phenotype spectrum and a literature review in the Japanese population. Am J Med Genet C Semin Med Genet 184: 656-674. doi: 10.1002/ajmg.c.31826

Gencik A, Gencikova A, Ferak V (1982) Population genetical aspects of primary congenital glaucoma. I. Incidence, prevalence, gene frequency, and age of onset. Hum Genet 61: 193-7. doi: 10.1007/BF00296440

Genomes Project C, Auton A, Brooks LD, Durbin RM, Garrison EP, Kang HM, Korbel JO, Marchini JL, McCarthy S, McVean GA, Abecasis GR (2015) A global reference for human genetic variation. Nature 526: 68-74. doi: 10.1038/nature15393

Gerth-Kahlert C, Williamson K, Ansari M, Rainger JK, Hingst V, Zimmermann T, Tech S, Guthoff RF, van Heyningen V, Fitzpatrick DR (2013) Clinical and mutation analysis of 51 probands with anophthalmia and/or severe microphthalmia from a single center. Mol Genet Genomic Med 1: 15-31. doi: 10.1002/mgg3.2

Geyer O, Wolf A, Levinger E, Harari-Shacham A, Walton DS, Shochat C, Korem S, Bercovich D (2011) Genotype/phenotype correlation in primary congenital glaucoma patients from different ethnic groups of the Israeli population. Am J Ophthalmol 151: 263-71 e1. doi: 10.1016/j.ajo.2010.08.038

Ghiasvand NM, Shirzad E, Naghavi M, Vaez Mahdavi MR (1998) High incidence of autosomal recessive nonsyndromal congenital retinal nonattachment (NCRNA) in an Iranian founding population. Am J Med Genet 78: 226-32.

Ghofrani M, Yahyaei M, Brunner HG, Cremers FP, Movasat M, Imran Khan M, Keramatipour M (2017) Homozygosity Mapping and Targeted Sanger Sequencing Identifies Three Novel CRB1 (Crumbs homologue 1) Mutations in Iranian Retinal Degeneration Families. Iran Biomed J 21: 294-302. doi: 10.18869/acadpub.ibj.21.5.294

Gillespie RL, O'Sullivan J, Ashworth J, Bhaskar S, Williams S, Biswas S, Kehdi E, Ramsden SC, Clayton-Smith J, Black GC, Lloyd IC (2014) Personalized diagnosis and management of congenital cataract by next-generation sequencing. Ophthalmology 121: 2124-37 e1-2. doi: 10.1016/j.ophtha.2014.06.006

Gilmour DF (2015) Familial exudative vitreoretinopathy and related retinopathies. Eye (Lond) 29: 1-14. doi: 10.1038/eye.2014.70

Giuffre I (2011) Molecular analysis of Italian patients with congenital glaucoma. Ophthalmic Genet. doi: 10.3109/13816810.2011.596891

Glockle N, Kohl S, Mohr J, Scheurenbrand T, Sprecher A, Weisschuh N, Bernd A, Rudolph G, Schubach M, Poloschek C, Zrenner E, Biskup S, Berger W, Wissinger B, Neidhardt J (2014) Panel-based next generation sequencing as a reliable and efficient technique to detect mutations in unselected patients with retinal dystrophies. Eur J Hum Genet 22: 99-104. doi: 10.1038/ejhg.2013.72

Goodwin S, McPherson JD, McCombie WR (2016) Coming of age: ten years of next-generation sequencing technologies. Nat Rev Genet 17: 333-51. doi: 10.1038/nrg.2016.49

Grantham R (1974) Amino acid difference formula to help explain protein evolution. Science 185: 862-4. doi: 10.1126/science.185.4154.862

Graw J (2010) Eye development. Curr Top Dev Biol 90: 343-86. doi: 10.1016/S0070-2153(10)90010-0

Greenwald SH, Brown EE, Scandura MJ, Hennessey E, Farmer R, Pawlyk BS, Xiao R, Vandenberghe LH, Pierce EA (2020) Gene Therapy Preserves Retinal Structure and Function in a Mouse Model of NMNAT1-Associated Retinal Degeneration. Mol Ther Methods Clin Dev 18: 582-594. doi: 10.1016/j.omtm.2020.07.003

Gregory-Evans CY, Williams MJ, Halford S, Gregory-Evans K (2004) Ocular coloboma: a reassessment in the age of molecular neuroscience. J Med Genet 41: 881-91. doi: 10.1136/jmg.2004.025494

Haddad R, Font RL, Reeser F (1978) Persistent hyperplastic primary vitreous. A clinicopathologic study of 62 cases and review of the literature. Surv Ophthalmol 23: 123-34. doi: 10.1016/0039-6257(78)90091-7

Haer-Wigman L, Newman H, Leibu R, Bax NM, Baris HN, Rizel L, Banin E, Massarweh A, Roosing S, Lefeber DJ, Zonneveld-Vrieling MN, Isakov O, Shomron N, Sharon D, Den Hollander AI, Hoyng CB, Cremers FP, Ben-Yosef T (2015) Non-syndromic retinitis pigmentosa due to mutations in the mucopolysaccharidosis type IIIC gene, heparan-alpha-glucosaminide N-acetyltransferase (HGSNAT). Hum Mol Genet 24: 3742-51. doi: 10.1093/hmg/ddv118

Haer-Wigman L, van Zelst-Stams WA, Pfundt R, van den Born LI, Klaver CC, Verheij JB, Hoyng CB, Breuning MH, Boon CJ, Kievit AJ, Verhoeven VJ, Pott JW, Sallevelt SC, van Hagen JM, Plomp AS, Kroes HY, Lelieveld SH, Hehir-Kwa JY, Castelein S, Nelen M, Scheffer H, Lugtenberg D, Cremers FP, Hoefsloot L,

Yntema HG (2017) Diagnostic exome sequencing in 266 Dutch patients with visual impairment. Eur J Hum Genet 25: 591-599. doi: 10.1038/ejhg.2017.9

Hagstrom SA, Adamian M, Scimeca M, Pawlyk BS, Yue G, Li T (2001) A role for the Tubby-like protein 1 in rhodopsin transport. Invest Ophthalmol Vis Sci 42: 1955-62.

Haider NB, Cruz NM, Allocca M, Yuan J (2014) Pathobiology of the Outer Retina: Genetic and Nongenetic Causes of Disease. Pathobiology of Human Disease. ELSEVIER, pp 2084-2114

Haim M (1992) Prevalence of retinitis pigmentosa and allied disorders in Denmark. II. Systemic involvement and age at onset. Acta Ophthalmol (Copenh) 70: 417-26. doi: 10.1111/j.1755-3768.1992.tb02109.x

Hamel C (2006) Retinitis pigmentosa. Orphanet J Rare Dis 1: 40. doi: 10.1186/1750-1172-1-40

Hamel CP (2007) Cone rod dystrophies. Orphanet J Rare Dis 2: 7. doi: 10.1186/1750-1172-2-7

Hamel CP (2014) Gene discovery and prevalence in inherited retinal dystrophies. C R Biol 337: 160-6. doi: 10.1016/j.crvi.2013.12.001

Harding P, Gore S, Malka S, Rajkumar J, Oluonye N, Moosajee M (2022) Real-world clinical and molecular management of 50 prospective patients with microphthalmia, anophthalmia and/or ocular coloboma. Br J Ophthalmol. doi: 10.1136/bjo-2022-321991

Harding P, Moosajee M (2019) The Molecular Basis of Human Anophthalmia and Microphthalmia. J Dev Biol 7. doi: 10.3390/jdb7030016

Hassan B, Ahmed R, Li B, Noor A, Hassan ZU (2019) A comprehensive study capturing vision loss burden in Pakistan (1990-2025): Findings from the Global Burden of Disease (GBD) 2017 study. PLoS One 14: e0216492. doi: 10.1371/journal.pone.0216492

Hedergott A, Volk AE, Herkenrath P, Thiele H, Fricke J, Altmuller J, Nurnberg P, Kubisch C, Neugebauer A (2015) Clinical and genetic findings in a family with NMNAT1-associated Leber congenital amaurosis: case report and review of the literature. Graefes Arch Clin Exp Ophthalmol 253: 2239-46. doi: 10.1007/s00417-015-3174-0

Henderson RH (2019) Inherited retinal dystrophies. vol 30, Paediatrics and Child Health

Heng Li RD (2009) Fast and accurate short read alignment with Burrows–Wheeler transform. BIOINFORMATICS 25: 1754-1760. doi: doi:10.1093/bioinformatics/btp324

Hitti-Malin RJ, Dhaenens CM, Panneman DM, Corradi Z, Khan M, den Hollander AI, Farrar GJ, Gilissen C, Hoischen A, van de Vorst M, Bults F, Boonen EGM, Saunders P, Group MDS, Roosing S, Cremers FPM (2022) Using single molecule Molecular Inversion Probes as a cost-effective, high-throughput sequencing approach to target all genes and loci associated with macular diseases. Hum Mutat 43: 2234-2250. doi: 10.1002/humu.24489

Hope CI, Bundey S, Proops D, Fielder AR (1997) Usher syndrome in the city of Birmingham--prevalence and clinical classification. Br J Ophthalmol 81: 46-53. doi: 10.1136/bjo.81.1.46

Huang D, Swanson EA, Lin CP, Schuman JS, Stinson WG, Chang W, Hee MR, Flotte T, Gregory K, Puliafito CA, et al. (1991) Optical coherence tomography. Science 254: 1178-81. doi: 10.1126/science.1957169

Hughes MO (2004) A pictorial anatomy of the human eye/anophthalmic socket: A review for ocularists. journal of ophthalmic prosthetics 8: 25-25.

Hull S, Kiray G, Chiang JP, Vincent AL (2020) Molecular and phenotypic investigation of a New Zealand cohort of childhood-onset retinal dystrophy. Am J Med Genet C Semin Med Genet 184: 708-717. doi: 10.1002/ajmg.c.31836

Idrees S, Sridhar J, Kuriyan AE (2019) Proliferative Vitreoretinopathy: A Review. Int Ophthalmol Clin 59: 221-240. doi: 10.1097/IIO.0000000000000258

Iglesias AI, Springelkamp H, van der Linde H, Severijnen LA, Amin N, Oostra B, Kockx CE, van den Hout MC, van Ijcken WF, Hofman A, Uitterlinden AG, Verdijk RM, Klaver CC, Willemsen R, van Duijn CM (2014) Exome sequencing and functional analyses suggest that SIX6 is a gene involved in an altered proliferation-differentiation balance early in life and optic nerve degeneration at old age. Hum Mol Genet 23: 1320-32. doi: 10.1093/hmg/ddt522

Inoue M, Kamachi Y, Matsunami H, Imada K, Uchikawa M, Kondoh H (2007) PAX6 and SOX2-dependent regulation of the Sox2 enhancer N-3 involved in

embryonic visual system development. Genes Cells 12: 1049-61. doi: 10.1111/j.1365-2443.2007.01114.x

Ioannidis NM, Rothstein JH, Pejaver V, Middha S, McDonnell SK, Baheti S, Musolf A, Li Q, Holzinger E, Karyadi D, Cannon-Albright LA, Teerlink CC, Stanford JL, Isaacs WB, Xu J, Cooney KA, Lange EM, Schleutker J, Carpten JD, Powell IJ, Cussenot O, Cancel-Tassin G, Giles GG, MacInnis RJ, Maier C, Hsieh CL, Wiklund F, Catalona WJ, Foulkes WD, Mandal D, Eeles RA, Kote-Jarai Z, Bustamante CD, Schaid DJ, Hastie T, Ostrander EA, Bailey-Wilson JE, Radivojac P, Thibodeau SN, Whittemore AS, Sieh W (2016) REVEL: An Ensemble Method for Predicting the Pathogenicity of Rare Missense Variants. Am J Hum Genet 99: 877-885. doi: 10.1016/j.ajhg.2016.08.016

Iseri SU, Wyatt AW, Nurnberg G, Kluck C, Nurnberg P, Holder GE, Blair E, Salt A, Ragge NK (2010) Use of genome-wide SNP homozygosity mapping in small pedigrees to identify new mutations in VSX2 causing recessive microphthalmia and a semidominant inner retinal dystrophy. Hum Genet 128: 51-60. doi: 10.1007/s00439-010-0823-6

Islam F, Htun S, Lai LW, Krall M, Poranki M, Martin PM, Sobreira N, Wohler ES, Yu J, Moore AT, Slavotinek AM (2020) Exome sequencing in patients with microphthalmia, anophthalmia, and coloboma (MAC) from a consanguineous population. Clin Genet 98: 499-506. doi: 10.1111/cge.13830

Ito YA, Walter MA (2014) Genomics and anterior segment dysgenesis: a review. Clin Exp Ophthalmol 42: 13-24. doi: 10.1111/ceo.12152

Jackson D, Malka S, Harding P, Palma J, Dunbar H, Moosajee M (2020) Molecular diagnostic challenges for non-retinal developmental eye disorders in the United Kingdom. Am J Med Genet C Semin Med Genet 184: 578-589. doi: 10.1002/ajmg.c.31837

Jaganathan K, Kyriazopoulou Panagiotopoulou S, McRae JF, Darbandi SF, Knowles D, Li YI, Kosmicki JA, Arbelaez J, Cui W, Schwartz GB, Chow ED, Kanterakis E, Gao H, Kia A, Batzoglou S, Sanders SJ, Farh KK (2019) Predicting Splicing from Primary Sequence with Deep Learning. Cell 176: 535-548 e24. doi: 10.1016/j.cell.2018.12.015

Jia LY, Ma K (2021) Novel Norrie disease gene mutations in Chinese patients with familial exudative vitreoretinopathy. BMC Ophthalmol 21: 84. doi: 10.1186/s12886-021-01852-3

Joyce S, Tee L, Abid A, Khaliq S, Mehdi SQ, Maher ER (2010) Locus heterogeneity and Knobloch syndrome. Am J Med Genet A 152A: 2880-1. doi: 10.1002/ajmg.a.33619

Kabra M, Zhang W, Rathi S, Mandal AK, Senthil S, Pyatla G, Ramappa M, Banerjee S, Shekhar K, Marmamula S, Mettla AL, Kaur I, Khanna RC, Khanna H, Chakrabarti S (2017) Angiopoietin receptor TEK interacts with CYP1B1 in primary congenital glaucoma. Hum Genet 136: 941-949. doi: 10.1007/s00439-017-1823-6

Kalatzis V, Hamel CP, MacDonald IM, First International Choroideremia Research S (2013) Choroideremia: towards a therapy. Am J Ophthalmol 156: 433-437 e3. doi: 10.1016/j.ajo.2013.05.009

Karczewski KJ, Francioli LC, Tiao G, Cummings BB, Alfoldi J, Wang Q, Collins RL, Laricchia KM, Ganna A, Birnbaum DP, Gauthier LD, Brand H, Solomonson M, Watts NA, Rhodes D, Singer-Berk M, England EM, Seaby EG, Kosmicki JA, Walters RK, Tashman K, Farjoun Y, Banks E, Poterba T, Wang A, Seed C, Whiffin N, Chong JX, Samocha KE, Pierce-Hoffman E, Zappala Z, O'Donnell-Luria AH, Minikel EV, Weisburd B, Lek M, Ware JS, Vittal C, Armean IM, Bergelson L, Cibulskis K, Connolly KM, Covarrubias M, Donnelly S, Ferriera S, Gabriel S, Gentry J, Gupta N, Jeandet T, Kaplan D, Llanwarne C, Munshi R, Novod S, Petrillo N, Roazen D, Ruano-Rubio V, Saltzman A, Schleicher M, Soto J, Tibbetts K, Tolonen C, Wade G, Talkowski ME, Genome Aggregation Database C, Neale BM, Daly MJ, MacArthur DG (2020) The mutational constraint spectrum quantified from variation in 141,456 humans. Nature 581: 434-443. doi: 10.1038/s41586-020-2308-7

Karczewski KJ, Weisburd B, Thomas B, Solomonson M, Ruderfer DM, Kavanagh D, Hamamsy T, Lek M, Samocha KE, Cummings BB, Birnbaum D, The Exome Aggregation C, Daly MJ, MacArthur DG (2017) The ExAC browser: displaying reference data information from over 60 000 exomes. Nucleic Acids Res 45: D840-D845. doi: 10.1093/nar/gkw971

Kawakami K, Sato S, Ozaki H, Ikeda K (2000) Six family genes--structure and function as transcription factors and their roles in development. Bioessays 22: 616-26. doi: 10.1002/1521-1878(200007)22:7<616::AID-BIES4>3.0.CO;2-R

Kenyon JR, Craig IW (1999) Analysis of the 5' regulatory region of the human Norrie's disease gene: evidence that a non-translated CT dinucleotide repeat in exon one has a role in controlling expression. Gene 227: 181-8. doi: 10.1016/s0378-1119(98)00611-8

Keser V, Khan A, Siddiqui S, Lopez I, Ren H, Qamar R, Nadaf J, Majewski J, Chen R, Koenekoop RK (2017) The Genetic Causes of Nonsyndromic Congenital Retinal Detachment: A Genetic and Phenotypic Study of Pakistani Families. Invest Ophthalmol Vis Sci 58: 1028-1036. doi: 10.1167/iovs.16-20281

Kevany BM, Palczewski K (2010) Phagocytosis of retinal rod and cone photoreceptors. Physiology (Bethesda) 25: 8-15. doi: 10.1152/physiol.00038.2009

Khafagy MM, El-Guendy N, Tantawy MA, Eldaly MA, Elhilali HM, Abdel Wahab AHA (2019) Novel CYP1B1 mutations and a possible prognostic use for surgical management of congenital glaucoma. Int J Ophthalmol 12: 607-614. doi: 10.18240/ijo.2019.04.14

Khan AO, Aldahmesh MA, Noor J, Salem A, Alkuraya FS (2015) Lens subluxation and retinal dysfunction in a girl with homozygous VSX2 mutation. Ophthalmic Genet 36: 8-13. doi: 10.3109/13816810.2013.827217

Khan K, Logan CV, McKibbin M, Sheridan E, Elcioglu NH, Yenice O, Parry DA, Fernandez-Fuentes N, Abdelhamed ZI, Al-Maskari A, Poulter JA, Mohamed MD, Carr IM, Morgan JE, Jafri H, Raashid Y, Taylor GR, Johnson CA, Inglehearn CF, Toomes C, Ali M (2012) Next generation sequencing identifies mutations in Atonal homolog 7 (ATOH7) in families with global eye developmental defects. Hum Mol Genet 21: 776-83. doi: 10.1093/hmg/ddr509

Khan K, Rudkin A, Parry DA, Burdon KP, McKibbin M, Logan CV, Abdelhamed ZI, Muecke JS, Fernandez-Fuentes N, Laurie KJ, Shires M, Fogarty R, Carr IM, Poulter JA, Morgan JE, Mohamed MD, Jafri H, Raashid Y, Meng N, Piseth H, Toomes C, Casson RJ, Taylor GR, Hammerton M, Sheridan E, Johnson CA, Inglehearn CF, Craig JE, Ali M (2011) Homozygous mutations in PXDN cause congenital cataract, corneal opacity, and developmental glaucoma. Am J Hum Genet 89: 464-73. doi: 10.1016/j.ajhg.2011.08.005

Khan M, Cornelis SS, Khan MI, Elmelik D, Manders E, Bakker S, Derks R, Neveling K, van de Vorst M, Gilissen C, Meunier I, Defoort S, Puech B, Devos A, Schulz HL, Stohr H, Grassmann F, Weber BHF, Dhaenens CM, Cremers FPM (2019) Cost-effective molecular inversion probe-based ABCA4 sequencing reveals deep-intronic variants in Stargardt disease. Hum Mutat 40: 1749-1759. doi: 10.1002/humu.23787

Khan M, Cornelis SS, Pozo-Valero MD, Whelan L, Runhart EH, Mishra K, Bults F, AlSwaiti Y, AlTalbishi A, De Baere E, Banfi S, Banin E, Bauwens M, Ben-Yosef T, Boon CJF, van den Born LI, Defoort S, Devos A, Dockery A, Dudakova L, Fakin A, Farrar GJ, Sallum JMF, Fujinami K, Gilissen C, Glavac D, Gorin MB, Greenberg J, Hayashi T, Hettinga YM, Hoischen A, Hoyng CB, Hufendiek K, Jagle H, Kamakari S, Karali M, Kellner U, Klaver CCW, Kousal B, Lamey TM, MacDonald IM, Matynia A, McLaren TL, Mena MD, Meunier I, Miller R, Newman H, Ntozini B, Oldak M, Pieterse M, Podhajcer OL, Puech B, Ramesar R, Ruther K, Salameh M, Salles MV, Sharon D, Simonelli F, Spital G, Steehouwer M, Szaflik JP, Thompson JA, Thuillier C, Tracewska AM, van Zweeden M, Vincent AL, Zanlonghi X, Liskova P, Stohr H, Roach JN, Ayuso C, Roberts L, Weber BHF, Dhaenens CM, Cremers FPM (2020) Resolving the dark matter of ABCA4 for 1054 Stargardt disease probands through integrated genomics and transcriptomics. Genet Med 22: 1235-1246. doi: 10.1038/s41436-020-0787-4

Khan MI, Azam M, Ajmal M, Collin RW, den Hollander AI, Cremers FP, Qamar R (2014) The molecular basis of retinal dystrophies in pakistan. Genes (Basel) 5: 176-95. doi: 10.3390/genes5010176

Kim HM, Joo K, Han J, Woo SJ (2021a) Clinical and Genetic Characteristics of Korean Congenital Stationary Night Blindness Patients. Genes (Basel) 12. doi: 10.3390/genes12060789

Kim YN, Kim YJ, Seol CA, Seo EJ, Lee JY, Yoon YH (2021b) Genetic Profile and Associated Characteristics of 150 Korean Patients with Retinitis Pigmentosa. J Ophthalmol 2021: 5067271. doi: 10.1155/2021/5067271

Kircher M, Kelso J (2010) High-throughput DNA sequencing--concepts and limitations. Bioessays 32: 524-36. doi: 10.1002/bies.200900181

Kliemann SE, Waetge RT, Suzuki OT, Passos-Bueno MR, Rosemberg S (2003) Evidence of neuronal migration disorders in Knobloch syndrome: clinical and molecular analysis of two novel families. Am J Med Genet A 119A: 15-9. doi: 10.1002/ajmg.a.20070

Kniestedt C, Punjabi O, Lin S, Stamper RL (2008) Tonometry through the ages. Surv Ophthalmol 53: 568-91. doi: 10.1016/j.survophthal.2008.08.024

Ko F, Papadopoulos M, Khaw PT (2015) Primary congenital glaucoma. Prog Brain Res 221: 177-89. doi: 10.1016/bs.pbr.2015.06.005

Kolb H (1995) The organization of the retina and visual system. In: Kolb H, Fernandez E, Nelson R (eds) Webvision: The Organization of the Retina and Visual System, Salt Lake City (UT)

Kumaran N, Moore AT, Weleber RG, Michaelides M (2017) Leber congenital amaurosis/early-onset severe retinal dystrophy: clinical features, molecular genetics and therapeutic interventions. Br J Ophthalmol 101: 1147-1154. doi: 10.1136/bjophthalmol-2016-309975

Lammer EJ, Chen DT, Hoar RM, Agnish ND, Benke PJ, Braun JT, Curry CJ, Fernhoff PM, Grix AW, Jr., Lott IT, et al. (1985) Retinoic acid embryopathy. N Engl J Med 313: 837-41. doi: 10.1056/NEJM198510033131401

Landrum MJ, Lee JM, Benson M, Brown GR, Chao C, Chitipiralla S, Gu B, Hart J, Hoffman D, Jang W, Karapetyan K, Katz K, Liu C, Maddipatla Z, Malheiro A, McDaniel K, Ovetsky M, Riley G, Zhou G, Holmes JB, Kattman BL, Maglott DR (2018) ClinVar: improving access to variant interpretations and supporting evidence. Nucleic Acids Res 46: D1062-D1067. doi: 10.1093/nar/gkx1153

Lau C, Niere M, Ziegler M (2009) The NMN/NaMN adenylyltransferase (NMNAT) protein family. Front Biosci (Landmark Ed) 14: 410-31. doi: 10.2741/3252

Ledford J, K., Sanders V, N (2006) The Slit Lamp Primer. SLACK INCORPORATED

Lee AJ, Cai MX, Thomas PE, Conney AH, Zhu BT (2003) Characterization of the oxidative metabolites of 17beta-estradiol and estrone formed by 15 selectively expressed human cytochrome p450 isoforms. Endocrinology 144: 3382-98. doi: 10.1210/en.2003-0192

Li H, Handsaker B, Wysoker A, Fennell T, Ruan J, Homer N, Marth G, Abecasis G, Durbin R, Genome Project Data Processing S (2009a) The Sequence

Alignment/Map format and SAMtools. Bioinformatics 25: 2078-9. doi: 10.1093/bioinformatics/btp352

Li L, Chen Y, Jiao X, Jin C, Jiang D, Tanwar M, Ma Z, Huang L, Ma X, Sun W, Chen J, Ma Y, M'Hamdi O, Govindarajan G, Cabrera PE, Li J, Gupta N, Naeem MA, Khan SN, Riazuddin S, Akram J, Ayyagari R, Sieving PA, Riazuddin SA, Hejtmancik JF (2017) Homozygosity Mapping and Genetic Analysis of Autosomal Recessive Retinal Dystrophies in 144 Consanguineous Pakistani Families. Invest Ophthalmol Vis Sci 58: 2218-2238. doi: 10.1167/iovs.17-21424

Li N, Zhou Y, Du L, Wei M, Chen X (2011) Overview of Cytochrome P450 1B1 gene mutations in patients with primary congenital glaucoma. Exp Eye Res 93: 572-9. doi: 10.1016/j.exer.2011.07.009

Li S, Huang L, Xiao X, Jia X, Guo X, Zhang Q (2014) Identification of CNGA3 mutations in 46 families: common cause of achromatopsia and cone-rod dystrophies in Chinese patients. JAMA Ophthalmol 132: 1076-83. doi: 10.1001/jamaophthalmol.2014.1032

Li X, Perissi V, Liu F, Rose DW, Rosenfeld MG (2002) Tissue-specific regulation of retinal and pituitary precursor cell proliferation. Science 297: 1180-3. doi: 10.1126/science.1073263

Li Y, Wang H, Peng J, Gibbs RA, Lewis RA, Lupski JR, Mardon G, Chen R (2009b) Mutation survey of known LCA genes and loci in the Saudi Arabian population. Invest Ophthalmol Vis Sci 50: 1336-43. doi: 10.1167/iovs.08-2589

Lim TC, Chattopadhyay S, Acharya UR (2012) A survey and comparative study on the instruments for glaucoma detection. Med Eng Phys 34: 129-39. doi: 10.1016/j.medengphy.2011.07.030

Lin S, Harlalka GV, Hameed A, Reham HM, Yasin M, Muhammad N, Khan S, Baple EL, Crosby AH, Saleha S (2018) Novel mutations in ALDH1A3 associated with autosomal recessive anophthalmia/microphthalmia, and review of the literature. BMC Med Genet 19: 160. doi: 10.1186/s12881-018-0678-6

Lin WJ, Kuang HY (2014) Oxidative stress induces autophagy in response to multiple noxious stimuli in retinal ganglion cells. Autophagy 10: 1692-701. doi: 10.4161/auto.36076

Liu IS, Chen JD, Ploder L, Vidgen D, van der Kooy D, Kalnins VI, McInnes RR (1994) Developmental expression of a novel murine homeobox gene (Chx10): evidence for roles in determination of the neuroretina and inner nuclear layer. Neuron 13: 377-93. doi: 10.1016/0896-6273(94)90354-9

Liu Q, Lyubarsky A, Skalet JH, Pugh EN, Jr., Pierce EA (2003) RP1 is required for the correct stacking of outer segment discs. Invest Ophthalmol Vis Sci 44: 4171-83. doi: 10.1167/iovs.03-0410

Liu S, Rauhut R, Vornlocher HP, Luhrmann R (2006) The network of protein-protein interactions within the human U4/U6.U5 tri-snRNP. RNA 12: 1418-30. doi: 10.1261/rna.55406

Loewen CJ, Moritz OL, Molday RS (2001) Molecular characterization of peripherin-2 and rom-1 mutants responsible for digenic retinitis pigmentosa. J Biol Chem 276: 22388-96. doi: 10.1074/jbc.M011710200

Loosli F, Staub W, Finger-Baier KC, Ober EA, Verkade H, Wittbrodt J, Baier H (2003) Loss of eyes in zebrafish caused by mutation of chokh/rx3. EMBO Rep 4: 894-9. doi: 10.1038/sj.embor.embor919

Lopez-Garrido MP, Medina-Trillo C, Morales-Fernandez L, Garcia-Feijoo J, Martinez-de-la-Casa JM, Garcia-Anton M, Escribano J (2013) Null CYP1B1 genotypes in primary congenital and nondominant juvenile glaucoma. Ophthalmology 120: 716-23. doi: 10.1016/j.ophtha.2012.09.016

MacKinnon JR, Giubilato A, Elder JE, Craig JE, Mackey DA (2004) Primary infantile glaucoma in an Australian population. Clin Exp Ophthalmol 32: 14-8. doi: 10.1046/j.1442-9071.2004.00750.x

Majewski J, Schwartzentruber J, Lalonde E, Montpetit A, Jabado N (2011) What can exome sequencing do for you? J Med Genet 48: 580-9. doi: 10.1136/jmedgenet-2011-100223

Mann I (1953) The developmental basis of eye malformations. JB Lippincott, Philadelphia.

Maranhao B, Biswas P, Gottsch AD, Navani M, Naeem MA, Suk J, Chu J, Khan SN, Poleman R, Akram J, Riazuddin S, Lee P, Riazuddin SA, Hejtmancik JF, Ayyagari R (2015) Investigating the Molecular Basis of Retinal Degeneration in a Familial Cohort of Pakistani Decent by Exome Sequencing. PLoS One 10: e0136561. doi: 10.1371/journal.pone.0136561

Maria M, Ajmal M, Azam M, Waheed NK, Siddiqui SN, Mustafa B, Ayub H, Ali L, Ahmad S, Micheal S, Hussain A, Shah ST, Ali SH, Ahmed W, Khan YM, den Hollander AI, Haer-Wigman L, Collin RW, Khan MI, Qamar R, Cremers FP (2015) Homozygosity mapping and targeted sanger sequencing reveal genetic defects underlying inherited retinal disease in families from pakistan. PLoS One 10: e0119806. doi: 10.1371/journal.pone.0119806

Marshall JD, Maffei P, Collin GB, Naggert JK (2011) Alstrom syndrome: genetics and clinical overview. Curr Genomics 12: 225-35. doi: 10.2174/138920211795677912

Martin R (2018) Cornea and anterior eye assessment with slit lamp biomicroscopy, specular microscopy, confocal microscopy, and ultrasound biomicroscopy. Indian J Ophthalmol 66: 195-201. doi: 10.4103/ijo.IJO_649_17

Maw MA, Corbeil D, Koch J, Hellwig A, Wilson-Wheeler JC, Bridges RJ, Kumaramanickavel G, John S, Nancarrow D, Roper K, Weigmann A, Huttner WB, Denton MJ (2000) A frameshift mutation in prominin (mouse)-like 1 causes human retinal degeneration. Hum Mol Genet 9: 27-34. doi: 10.1093/hmg/9.1.27

Mayank N, Amita M (2023) Complex micropthalmia due to a homozygous novel varaint in SIX homeobox 6 gene. Dehli journal of ophthalmology 33: 45-49.

May-Simera H, Nagel-Wolfrum K, Wolfrum U (2017) Cilia - The sensory antennae in the eye. Prog Retin Eye Res 60: 144-180. doi: 10.1016/j.preteyeres.2017.05.001

McKenna A, Hanna M, Banks E, Sivachenko A, Cibulskis K, Kernytsky A, Garimella K, Altshuler D, Gabriel S, Daly M, DePristo MA (2010) The Genome Analysis Toolkit: a MapReduce framework for analyzing next-generation DNA sequencing data. Genome Res 20: 1297-303. doi: 10.1101/gr.107524.110

McKie AB, McHale JC, Keen TJ, Tarttelin EE, Goliath R, van Lith-Verhoeven JJ, Greenberg J, Ramesar RS, Hoyng CB, Cremers FP, Mackey DA, Bhattacharya SS, Bird AC, Markham AF, Inglehearn CF (2001) Mutations in the pre-mRNA splicing factor gene PRPC8 in autosomal dominant retinitis pigmentosa (RP13). Hum Mol Genet 10: 1555-62. doi: 10.1093/hmg/10.15.1555

Meienberg J, Bruggmann R, Oexle K, Matyas G (2016) Clinical sequencing: is WGS the better WES? Hum Genet 135: 359-62. doi: 10.1007/s00439-015-1631-9

Meindl A, Berger W, Meitinger T, van de Pol D, Achatz H, Dorner C, Haasemann M, Hellebrand H, Gal A, Cremers F, et al. (1992) Norrie disease is caused by mutations in an extracellular protein resembling C-terminal globular domain of mucins. Nat Genet 2: 139-43. doi: 10.1038/ng1092-139

Menzel O, Bekkeheien RC, Reymond A, Fukai N, Boye E, Kosztolanyi G, Aftimos S, Deutsch S, Scott HS, Olsen BR, Antonarakis SE, Guipponi M (2004) Knobloch syndrome: novel mutations in COL18A1, evidence for genetic heterogeneity, and a functionally impaired polymorphism in endostatin. Hum Mutat 23: 77-84. doi: 10.1002/humu.10284

Miller NA, Farrow EG, Gibson M, Willig LK, Twist G, Yoo B, Marrs T, Corder S, Krivohlavek L, Walter A, Petrikin JE, Saunders CJ, Thiffault I, Soden SE, Smith LD, Dinwiddie DL, Herd S, Cakici JA, Catreux S, Ruehle M, Kingsmore SF (2015) A 26-hour system of highly sensitive whole genome sequencing for emergency management of genetic diseases. Genome Med 7: 100. doi: 10.1186/s13073-015-0221-8

Miller NR, Walsh FB, Hoyt WF (2005) Walsh and Hoyt's clinical neuro-ophthalmology. Lippincott Williams & Wilkins

Miraglia S, Godfrey W, Yin AH, Atkins K, Warnke R, Holden JT, Bray RA, Waller EK, Buck DW (1997) A novel five-transmembrane hematopoietic stem cell antigen: isolation, characterization, and molecular cloning. Blood 90: 5013-21.

Miraldi Utz V, Pfeifer W, Longmuir SQ, Olson RJ, Wang K, Drack AV (2018) Presentation of TRPM1-Associated Congenital Stationary Night Blindness in Children. JAMA Ophthalmol 136: 389-398. doi: 10.1001/jamaophthalmol.2018.0185

Mockel A, Perdomo Y, Stutzmann F, Letsch J, Marion V, Dollfus H (2011) Retinal dystrophy in Bardet-Biedl syndrome and related syndromic ciliopathies. Prog Retin Eye Res 30: 258-74. doi: 10.1016/j.preteyeres.2011.03.001

Murray AR, Fliesler SJ, Al-Ubaidi MR (2009) Rhodopsin: the functional significance of asn-linked glycosylation and other post-translational modifications. Ophthalmic Genet 30: 109-20. doi: 10.1080/13816810902962405

Myers CE, Klein BE, Meuer SM, Swift MK, Chandler CS, Huang Y, Gangaputra S, Pak JW, Danis RP, Klein R (2015) Retinal thickness measured by spectral-domain optical coherence tomography in eyes without retinal abnormalities: the

Beaver Dam Eye Study. Am J Ophthalmol 159: 445-56 e1. doi: 10.1016/j.ajo.2014.11.025

Najmabadi H, Hu H, Garshasbi M, Zemojtel T, Abedini SS, Chen W, Hosseini M, Behjati F, Haas S, Jamali P, Zecha A, Mohseni M, Puttmann L, Vahid LN, Jensen C, Moheb LA, Bienek M, Larti F, Mueller I, Weissmann R, Darvish H, Wrogemann K, Hadavi V, Lipkowitz B, Esmaeeli-Nieh S, Wieczorek D, Kariminejad R, Firouzabadi SG, Cohen M, Fattahi Z, Rost I, Mojahedi F, Hertzberg C, Dehghan A, Rajab A, Banavandi MJ, Hoffer J, Falah M, Musante L, Kalscheuer V, Ullmann R, Kuss AW, Tzschach A, Kahrizi K, Ropers HH (2011) Deep sequencing reveals 50 novel genes for recessive cognitive disorders. Nature 478: 57-63. doi: 10.1038/nature10423

Narooie-Nejad M, Paylakhi SH, Shojaee S, Fazlali Z, Rezaei Kanavi M, Nilforushan N, Yazdani S, Babrzadeh F, Suri F, Ronaghi M, Elahi E, Paisan-Ruiz C (2009) Loss of function mutations in the gene encoding latent transforming growth factor beta binding protein 2, LTBP2, cause primary congenital glaucoma. Hum Mol Genet 18: 3969-77. doi: 10.1093/hmg/ddp338

Naz S (2022) Molecular genetic landscape of hereditary hearing loss in Pakistan. Hum Genet 141: 633-648. doi: 10.1007/s00439-021-02320-0

Ng PC, Henikoff S (2003) SIFT: Predicting amino acid changes that affect protein function. Nucleic Acids Res 31: 3812-4. doi: 10.1093/nar/gkg509

Nishimura DY, Swiderski RE, Alward WL, Searby CC, Patil SR, Bennet SR, Kanis AB, Gastier JM, Stone EM, Sheffield VC (1998) The forkhead transcription factor gene FKHL7 is responsible for glaucoma phenotypes which map to 6p25. Nat Genet 19: 140-7. doi: 10.1038/493

North MA, Naggert JK, Yan Y, Noben-Trauth K, Nishina PM (1997) Molecular characterization of TUB, TULP1, and TULP2, members of the novel tubby gene family and their possible relation to ocular diseases. Proc Natl Acad Sci U S A 94: 3128-33. doi: 10.1073/pnas.94.7.3128

Ohuchi H, Sato K, Habuta M, Fujita H, Bando T (2019) Congenital eye anomalies: More mosaic than thought? Congenit Anom (Kyoto) 59: 56-73. doi: 10.1111/cga.12304

Ordonez-Labastida V, Montes-Almanza L, Garcia-Martinez F, Zenteno JC (2022) Effectiveness of Whole-Exome Sequencing for the Identification of Causal

Mutations in Patients with Suspected Inherited Ocular Diseases. Rev Invest Clin 74: 219-226. doi: 10.24875/RIC.22000107

Otterstedde CR, Spandau U, Blankenagel A, Kimberling WJ, Reisser C (2001) A new clinical classification for Usher's syndrome based on a new subtype of Usher's syndrome type I. Laryngoscope 111: 84-6. doi: 10.1097/00005537-200101000-00014

Palczewski K (2014) Chemistry and biology of the initial steps in vision: the Friedenwald lecture. Invest Ophthalmol Vis Sci 55: 6651-72. doi: 10.1167/iovs.14-15502

Panagiotou ES, Fernandez-Fuentes N, Farraj LA, McKibbin M, Elcioglu NH, Jafri H, Cerman E, Parry DA, Logan CV, Johnson CA, Inglehearn CF, Toomes C, Ali M (2022) Novel SIX6 mutations cause recessively inherited congenital cataract, microcornea, and corneal opacification with or without coloboma and microphthalmia. Mol Vis 28: 57-69.

Panneman DM, Hitti-Malin RJ, Holtes LK, de Bruijn SE, Reurink J, Boonen EGM, Khan MI, Ali M, Andreasson S, De Baere E, Banfi S, Bauwens M, Ben-Yosef T, Bocquet B, De Bruyne M, de la Cerda B, Coppieters F, Farinelli P, Guignard T, Inglehearn CF, Karali M, Kjellstrom U, Koenekoop R, de Koning B, Leroy BP, McKibbin M, Meunier I, Nikopoulos K, Nishiguchi KM, Poulter JA, Rivolta C, Rodriguez de la Rua E, Saunders P, Simonelli F, Tatour Y, Testa F, Thiadens A, Toomes C, Tracewska AM, Tran HV, Ushida H, Vaclavik V, Verhoeven VJM, van de Vorst M, Gilissen C, Hoischen A, Cremers FPM, Roosing S (2023) Cost-effective sequence analysis of 113 genes in 1,192 probands with retinitis pigmentosa and Leber congenital amaurosis. Front Cell Dev Biol 11: 1112270. doi: 10.3389/fcell.2023.1112270

Parisi MA, Doherty D, Chance PF, Glass IA (2007) Joubert syndrome (and related disorders) (OMIM 213300). Eur J Hum Genet 15: 511-21. doi: 10.1038/sj.ejhg.5201648

Pascolini D, Mariotti SP (2012) Global estimates of visual impairment: 2010. Br J Ophthalmol 96: 614-8. doi: 10.1136/bjophthalmol-2011-300539

Pasutto F, Chavarria-Soley G, Mardin CY, Michels-Rautenstrauss K, Ingelman-Sundberg M, Fernandez-Martinez L, Weber BH, Rautenstrauss B, Reis A (2010) Heterozygous loss-of-function variants in CYP1B1 predispose to

primary open-angle glaucoma. Invest Ophthalmol Vis Sci 51: 249-54. doi: 10.1167/iovs.09-3880

Perea-Romero I, Gordo G, Iancu IF, Del Pozo-Valero M, Almoguera B, Blanco-Kelly F, Carreno E, Jimenez-Rolando B, Lopez-Rodriguez R, Lorda-Sanchez I, Martin-Merida I, Perez de Ayala L, Riveiro-Alvarez R, Rodriguez-Pinilla E, Tahsin-Swafiri S, Trujillo-Tiebas MJ, Group ES, Group ES, Associated Clinical Study G, Garcia-Sandoval B, Minguez P, Avila-Fernandez A, Corton M, Ayuso C (2021) Genetic landscape of 6089 inherited retinal dystrophies affected cases in Spain and their therapeutic and extended epidemiological implications. Sci Rep 11: 1526. doi: 10.1038/s41598-021-81093-y

Perlman I (1995) The Electroretinogram: ERG. In: Kolb H, Fernandez E, Nelson R (eds) Webvision: The Organization of the Retina and Visual System, Salt Lake City (UT)

Petriman NA, Lorentzen E (2020) Moving proteins along in the cilium. Elife 9. doi: 10.7554/eLife.55254

Plaisancie J, Ceroni F, Holt R, Zazo Seco C, Calvas P, Chassaing N, Ragge NK (2019) Genetics of anophthalmia and microphthalmia. Part 1: Non-syndromic anophthalmia/microphthalmia. Hum Genet 138: 799-830. doi: 10.1007/s00439-019-01977-y

Plasilova M, Stoilov I, Sarfarazi M, Kadasi L, Ferakova E, Ferak V (1999) Identification of a single ancestral CYP1B1 mutation in Slovak Gypsies (Roms) affected with primary congenital glaucoma. J Med Genet 36: 290-4.

Pollard KS, Hubisz MJ, Rosenbloom KR, Siepel A (2010) Detection of nonneutral substitution rates on mammalian phylogenies. Genome Res 20: 110-21. doi: 10.1101/gr.097857.109

Pruett RC (1975) The pleomorphism and complications of posterior hyperplastic primary vitreous. Am J Ophthalmol 80: 625-9. doi: 10.1016/0002-9394(75)90392-x

Qassim A, Siggs O, M. (2020) Predicting the genetic risk of glaucoma. The biochemist 42: 26-30.

Rashid M, Qasim M, Ishaq R, Bukhari SA, Sajid Z, Ashfaq UA, Haque A, Ahmed ZM (2020) Pathogenic variants of AIPL1, MERTK, GUCY2D, and FOXE3 in

Pakistani families with clinically heterogeneous eye diseases. PLoS One 15: e0239748. doi: 10.1371/journal.pone.0239748

Rashid M, Yousaf S, Sheikh SA, Sajid Z, Shabbir AS, Kausar T, Tariq N, Usman M, Shaikh RS, Ali M, Bukhari SA, Waryah AM, Qasim M, Riazuddin S, Ahmed ZM (2019) Identities and frequencies of variants in CYP1B1 causing primary congenital glaucoma in Pakistan. Mol Vis 25: 144-154.

Rauf B, Irum B, Kabir F, Firasat S, Naeem MA, Khan SN, Husnain T, Riazuddin S, Akram J, Riazuddin SA (2016) A spectrum of CYP1B1 mutations associated with primary congenital glaucoma in families of Pakistani descent. Hum Genome Var 3: 16021. doi: 10.1038/hgv.2016.21

Rauf B, Irum B, Khan SY, Kabir F, Naeem MA, Riazuddin S, Ayyagari R, Riazuddin SA (2020) Novel mutations in LTBP2 identified in familial cases of primary congenital glaucoma. Mol Vis 26: 14-25.

Reddy AB, Kaur K, Mandal AK, Panicker SG, Thomas R, Hasnain SE, Balasubramanian D, Chakrabarti S (2004) Mutation spectrum of the CYP1B1 gene in Indian primary congenital glaucoma patients. Mol Vis 10: 696-702.

Reddy AB, Panicker SG, Mandal AK, Hasnain SE, Balasubramanian D (2003) Identification of R368H as a predominant CYP1B1 allele causing primary congenital glaucoma in Indian patients. Invest Ophthalmol Vis Sci 44: 4200-3. doi: 10.1167/iovs.02-0945

Reese AB (1955) Persistent hyperplastic primary vitreous. Am J Ophthalmol 40: 317-31. doi: 10.1016/0002-9394(55)91866-3

Rehman AU, Santos-Cortez RL, Drummond MC, Shahzad M, Lee K, Morell RJ, Ansar M, Jan A, Wang X, Aziz A, Riazuddin S, Smith JD, Wang GT, Ahmed ZM, Gul K, Shearer AE, Smith RJ, Shendure J, Bamshad MJ, Nickerson DA, University of Washington Center for Mendelian G, Hinnant J, Khan SN, Fisher RA, Ahmad W, Friderici KH, Riazuddin S, Friedman TB, Wilch ES, Leal SM (2015) Challenges and solutions for gene identification in the presence of familial locus heterogeneity. Eur J Hum Genet 23: 1207-15. doi: 10.1038/ejhg.2014.266

Reis LM, Khan A, Kariminejad A, Ebadi F, Tyler RC, Semina EV (2011) VSX2 mutations in autosomal recessive microphthalmia. Mol Vis 17: 2527-32.

Reis LM, Tyler RC, Schneider A, Bardakjian T, Stoler JM, Melancon SB, Semina EV (2010) FOXE3 plays a significant role in autosomal recessive microphthalmia. Am J Med Genet A 152A: 582-90. doi: 10.1002/ajmg.a.33257

Reis LM, Tyler RC, Weh E, Hendee KE, Kariminejad A, Abdul-Rahman O, Ben-Omran T, Manning MA, Yesilyurt A, McCarty CA, Kitchner TE, Costakos D, Semina EV (2016) Analysis of CYP1B1 in pediatric and adult glaucoma and other ocular phenotypes. Mol Vis 22: 1229-1238.

Rentzsch P, Witten D, Cooper GM, Shendure J, Kircher M (2019) CADD: predicting the deleteriousness of variants throughout the human genome. Nucleic Acids Res 47: D886-D894. doi: 10.1093/nar/gky1016

Reuter P, Koeppen K, Ladewig T, Kohl S, Baumann B, Wissinger B, Achromatopsia Clinical Study G (2008) Mutations in CNGA3 impair trafficking or function of cone cyclic nucleotide-gated channels, resulting in achromatopsia. Hum Mutat 29: 1228-36. doi: 10.1002/humu.20790

Richard EM, Santos-Cortez RLP, Faridi R, Rehman AU, Lee K, Shahzad M, Acharya A, Khan AA, Imtiaz A, Chakchouk I, Takla C, Abbe I, Rafeeq M, Liaqat K, Chaudhry T, Bamshad MJ, Nickerson DA, University of Washington Center for Mendelian G, Schrauwen I, Khan SN, Morell RJ, Zafar S, Ansar M, Ahmed ZM, Ahmad W, Riazuddin S, Friedman TB, Leal SM, Riazuddin S (2019) Global genetic insight contributed by consanguineous Pakistani families segregating hearing loss. Hum Mutat 40: 53-72. doi: 10.1002/humu.23666

Richards S, Aziz N, Bale S, Bick D, Das S, Gastier-Foster J, Grody WW, Hegde M, Lyon E, Spector E, Voelkerding K, Rehm HL, Committee ALQA (2015) Standards and guidelines for the interpretation of sequence variants: a joint consensus recommendation of the American College of Medical Genetics and Genomics and the Association for Molecular Pathology. Genet Med 17: 405-24. doi: 10.1038/gim.2015.30

Rogers K (2011) The Eye: The Physiology of Human Perception. 34.

Roller E, Ivakhno S, Lee S, Royce T, Tanner S (2016) Canvas: versatile and scalable detection of copy number variants. Bioinformatics 32: 2375-7. doi: 10.1093/bioinformatics/btw163

Rosenberg T, Haim M, Hauch AM, Parving A (1997) The prevalence of Usher syndrome and other retinal dystrophy-hearing impairment associations. Clin Genet 51: 314-21. doi: 10.1111/j.1399-0004.1997.tb02480.x

Rulli E, Quaranta L, Riva I, Poli D, Hollander L, Galli F, Katsanos A, Oddone F, Torri V, Weinreb RN, Italian Study Group on Qo LiG (2018) Visual field loss and vision-related quality of life in the Italian Primary Open Angle Glaucoma Study. Sci Rep 8: 619. doi: 10.1038/s41598-017-19113-z

Salamanca Viloria J, Allega MF, Lambrughi M, Papaleo E (2017) An optimal distance cutoff for contact-based Protein Structure Networks using side-chain centers of mass. Sci Rep 7: 2838. doi: 10.1038/s41598-017-01498-6

Sankila EM, Pakarinen L, Kaariainen H, Aittomaki K, Karjalainen S, Sistonen P, de la Chapelle A (1995) Assignment of an Usher syndrome type III (USH3) gene to chromosome 3q. Hum Mol Genet 4: 93-8. doi: 10.1093/hmg/4.1.93

Saqib MA, Nikopoulos K, Ullah E, Sher Khan F, Iqbal J, Bibi R, Jarral A, Sajid S, Nishiguchi KM, Venturini G, Ansar M, Rivolta C (2015) Homozygosity mapping reveals novel and known mutations in Pakistani families with inherited retinal dystrophies. Sci Rep 5: 9965. doi: 10.1038/srep09965

Sawyer SL, Hartley T, Dyment DA, Beaulieu CL, Schwartzentruber J, Smith A, Bedford HM, Bernard G, Bernier FP, Brais B, Bulman DE, Warman Chardon J, Chitayat D, Deladoey J, Fernandez BA, Frosk P, Geraghty MT, Gerull B, Gibson W, Gow RM, Graham GE, Green JS, Heon E, Horvath G, Innes AM, Jabado N, Kim RH, Koenekoop RK, Khan A, Lehmann OJ, Mendoza-Londono R, Michaud JL, Nikkel SM, Penney LS, Polychronakos C, Richer J, Rouleau GA, Samuels ME, Siu VM, Suchowersky O, Tarnopolsky MA, Yoon G, Zahir FR, Consortium FC, Care4Rare Canada C, Majewski J, Boycott KM (2016) Utility of whole-exome sequencing for those near the end of the diagnostic odyssey: time to address gaps in care. Clin Genet 89: 275-84. doi: 10.1111/cge.12654

Schloss JA (2008) How to get genomes at one ten-thousandth the cost. Nat Biotechnol 26: 1113-5. doi: 10.1038/nbt1008-1113

Schwartz SD, Regillo CD, Lam BL, Eliott D, Rosenfeld PJ, Gregori NZ, Hubschman JP, Davis JL, Heilwell G, Spirn M, Maguire J, Gay R, Bateman J, Ostrick RM, Morris D, Vincent M, Anglade E, Del Priore LV, Lanza R (2015) Human

embryonic stem cell-derived retinal pigment epithelium in patients with age-related macular degeneration and Stargardt's macular dystrophy: follow-up of two open-label phase 1/2 studies. Lancet 385: 509-16. doi: 10.1016/S0140-6736(14)61376-3

Schwarz JM, Cooper DN, Schuelke M, Seelow D (2014) MutationTaster2: mutation prediction for the deep-sequencing age. Nat Methods 11: 361-2. doi: 10.1038/nmeth.2890

Searle A, Shetty P, Melov SJ, Alahakoon TI (2018) Prenatal diagnosis and implications of microphthalmia and anophthalmia with a review of current ultrasound guidelines: two case reports. J Med Case Rep 12: 250. doi: 10.1186/s13256-018-1746-4

Sertie AL, Sossi V, Camargo AA, Zatz M, Brahe C, Passos-Bueno MR (2000) Collagen XVIII, containing an endogenous inhibitor of angiogenesis and tumor growth, plays a critical role in the maintenance of retinal structure and in neural tube closure (Knobloch syndrome). Hum Mol Genet 9: 2051-8. doi: 10.1093/hmg/9.13.2051

Sfeir A, Symington LS (2015) Microhomology-Mediated End Joining: A Back-up Survival Mechanism or Dedicated Pathway? Trends Biochem Sci 40: 701-714. doi: 10.1016/j.tibs.2015.08.006

Shaikh RS, Reuter P, Sisk RA, Kausar T, Shahzad M, Maqsood MI, Yousif A, Ali M, Riazuddin S, Wissinger B, Ahmed ZM (2015) Homozygous missense variant in the human CNGA3 channel causes cone-rod dystrophy. Eur J Hum Genet 23: 473-80. doi: 10.1038/ejhg.2014.136

Shastry BS (2009) Persistent hyperplastic primary vitreous: congenital malformation of the eye. Clin Exp Ophthalmol 37: 884-90. doi: 10.1111/j.1442-9071.2009.02150.x

Sheikh SA, Waryah AM, Narsani AK, Shaikh H, Gilal IA, Shah K, Qasim M, Memon AI, Kewalramani P, Shaikh N (2014) Mutational spectrum of the CYP1B1 gene in Pakistani patients with primary congenital glaucoma: novel variants and genotype-phenotype correlations. Mol Vis 20: 991-1001.

Shin J, Chul, Yaguchi H, Shioiri S (2004) Change of Color Appearance in Photopic, Mesopic and Scotopic Vision. Optical Review 11: 265-271.

Sivadorai P, Cherninkova S, Bouwer S, Kamenarova K, Angelicheva D, Seeman P, Hollingsworth K, Mihaylova V, Oscar A, Dimitrova G, Kaneva R, Tournev I, Kalaydjieva L (2008) Genetic heterogeneity and minor CYP1B1 involvement in the molecular basis of primary congenital glaucoma in Gypsies. Clin Genet 74: 82-7. doi: 10.1111/j.1399-0004.2008.01024.x

Slatko BE, Gardner AF, Ausubel FM (2018) Overview of Next-Generation Sequencing Technologies. Curr Protoc Mol Biol 122: e59. doi: 10.1002/cpmb.59

Sloan LL (1951) Measurement of visual acuity; a critical review. AMA Arch Ophthalmol 45: 704-25. doi: 10.1001/archopht.1951.01700010719013

Smith RJ, Berlin CI, Hejtmancik JF, Keats BJ, Kimberling WJ, Lewis RA, Moller CG, Pelias MZ, Tranebjaerg L (1994) Clinical diagnosis of the Usher syndromes. Usher Syndrome Consortium. Am J Med Genet 50: 32-8. doi: 10.1002/ajmg.1320500107

Soden SE, Saunders CJ, Willig LK, Farrow EG, Smith LD, Petrikin JE, LePichon JB, Miller NA, Thiffault I, Dinwiddie DL, Twist G, Noll A, Heese BA, Zellmer L, Atherton AM, Abdelmoity AT, Safina N, Nyp SS, Zuccarelli B, Larson IA, Modrcin A, Herd S, Creed M, Ye Z, Yuan X, Brodsky RA, Kingsmore SF (2014) Effectiveness of exome and genome sequencing guided by acuity of illness for diagnosis of neurodevelopmental disorders. Sci Transl Med 6: 265ra168. doi: 10.1126/scitranslmed.3010076

Souma T, Tompson SW, Thomson BR, Siggs OM, Kizhatil K, Yamaguchi S, Feng L, Limviphuvadh V, Whisenhunt KN, Maurer-Stroh S, Yanovitch TL, Kalaydjieva L, Azmanov DN, Finzi S, Mauri L, Javadiyan S, Souzeau E, Zhou T, Hewitt AW, Kloss B, Burdon KP, Mackey DA, Allen KF, Ruddle JB, Lim SH, Rozen S, Tran-Viet KN, Liu X, John S, Wiggs JL, Pasutto F, Craig JE, Jin J, Quaggin SE, Young TL (2016) Angiopoietin receptor TEK mutations underlie primary congenital glaucoma with variable expressivity. J Clin Invest 126: 2575-87. doi: 10.1172/JCI85830

Stigloher C, Ninkovic J, Laplante M, Geling A, Tannhauser B, Topp S, Kikuta H, Becker TS, Houart C, Bally-Cuif L (2006) Segregation of telencephalic and eye-field identities inside the zebrafish forebrain territory is controlled by Rx3. Development 133: 2925-35. doi: 10.1242/dev.02450

Stingl K, Mayer AK, Llavona P, Mulahasanovic L, Rudolph G, Jacobson SG, Zrenner E, Kohl S, Wissinger B, Weisschuh N (2017) CDHR1 mutations in retinal dystrophies. Sci Rep 7: 6992. doi: 10.1038/s41598-017-07117-8

Stoilov I, Akarsu AN, Alozie I, Child A, Barsoum-Homsy M, Turacli ME, Or M, Lewis RA, Ozdemir N, Brice G, Aktan SG, Chevrette L, Coca-Prados M, Sarfarazi M (1998) Sequence analysis and homology modeling suggest that primary congenital glaucoma on 2p21 results from mutations disrupting either the hinge region or the conserved core structures of cytochrome P4501B1. Am J Hum Genet 62: 573-84. doi: 10.1086/301764

Stoilov IR, Costa VP, Vasconcellos JP, Melo MB, Betinjane AJ, Carani JC, Oltrogge EV, Sarfarazi M (2002) Molecular genetics of primary congenital glaucoma in Brazil. Invest Ophthalmol Vis Sci 43: 1820-7.

Stromland K (2004) Visual impairment and ocular abnormalities in children with fetal alcohol syndrome. Addict Biol 9: 153-7; discussion 159-60. doi: 10.1080/13556210410001717024

Stromland K, Miller MT (1993) Thalidomide embryopathy: revisited 27 years later. Acta Ophthalmol (Copenh) 71: 238-45. doi: 10.1111/j.1755-3768.1993.tb04997.x

Su BN, Shen RJ, Liu ZL, Li Y, Jin ZB (2022) Global spectrum of USH2A mutation in inherited retinal dystrophies: Prompt message for development of base editing therapy. Front Aging Neurosci 14: 948279. doi: 10.3389/fnagi.2022.948279

Su CC, Liu YF, Li SY, Yang JJ, Yen YC (2012) Mutations in the CYP1B1 gene may contribute to juvenile-onset open-angle glaucoma. Eye (Lond) 26: 1369-77. doi: 10.1038/eye.2012.159

Tamcelik N, Atalay E, Bolukbasi S, Capar O, Ozkok A (2014) Demographic features of subjects with congenital glaucoma. Indian J Ophthalmol 62: 565-9. doi: 10.4103/0301-4738.126988

Tatour Y, Ben-Yosef T (2020) Syndromic Inherited Retinal Diseases: Genetic, Clinical and Diagnostic Aspects. Diagnostics (Basel) 10. doi: 10.3390/diagnostics10100779

Te Paske I, Mensenkamp AR, Neveling K, Group E-GL-LW, Hoogerbrugge N, Ligtenberg MJL, De Voer RM (2022) Noncoding Aberrations in Mismatch Repair Genes Underlie a Substantial Part of the Missing Heritability in Lynch

Syndrome. Gastroenterology 163: 1691-1694 e7. doi: 10.1053/j.gastro.2022.08.041

Tham YC, Li X, Wong TY, Quigley HA, Aung T, Cheng CY (2014) Global prevalence of glaucoma and projections of glaucoma burden through 2040: a systematic review and meta-analysis. Ophthalmology 121: 2081-90. doi: 10.1016/j.ophtha.2014.05.013

Trapani I, Auricchio A (2018) Seeing the Light after 25 Years of Retinal Gene Therapy. Trends Mol Med 24: 669-681. doi: 10.1016/j.molmed.2018.06.006

Trapani I, Auricchio A (2019) Has retinal gene therapy come of age? From bench to bedside and back to bench. Hum Mol Genet 28: R108-R118. doi: 10.1093/hmg/ddz130

Tsang SH, Aycinena ARP, Sharma T (2018) Ciliopathy: Senior-Loken Syndrome. Adv Exp Med Biol 1085: 175-178. doi: 10.1007/978-3-319-95046-4_34

Tsang SH, Sharma T (2018) Leber Congenital Amaurosis. Adv Exp Med Biol 1085: 131-137. doi: 10.1007/978-3-319-95046-4_26

Tsilou ET, Rubin BI, Caruso RC, Reed GF, Pikus A, Hejtmancik JF, Iwata F, Redman JB, Kaiser-Kupfer MI (2002) Usher syndrome clinical types I and II: could ocular symptoms and signs differentiate between the two types? Acta Ophthalmol Scand 80: 196-201. doi: 10.1034/j.1600-0420.2002.800215.x

Ullah E, Nadeem Saqib MA, Sajid S, Shah N, Zubair M, Khan MA, Ahmed I, Ali G, Dutta AK, Danda S, Lao R, Ling-Fung Tang P, Kwok PY, Ansar M, Slavotinek A (2016) Genetic analysis of consanguineous families presenting with congenital ocular defects. Exp Eye Res 146: 163-171. doi: 10.1016/j.exer.2016.03.014

UniProt C (2023) UniProt: the Universal Protein Knowledgebase in 2023. Nucleic Acids Res 51: D523-D531. doi: 10.1093/nar/gkac1052

Vaidya P, Vadiya A (2015) Retinitis Pigmentosa: Disease Encumbrance in the Eurozone. International Journal of Ophthalmology and Clinical Research 2. doi: 10.23937/2378-346X/1410030

Valleix S, Niel F, Nedelec B, Algros MP, Schwartz C, Delbosc B, Delpech M, Kantelip B (2006) Homozygous nonsense mutation in the FOXE3 gene as a cause of congenital primary aphakia in humans. Am J Hum Genet 79: 358-64. doi: 10.1086/505654

Valstar MJ, Ruijter GJ, van Diggelen OP, Poorthuis BJ, Wijburg FA (2008) Sanfilippo syndrome: a mini-review. J Inherit Metab Dis 31: 240-52. doi: 10.1007/s10545-008-0838-5

Van der Auwera GA, Carneiro MO, Hartl C, Poplin R, Del Angel G, Levy-Moonshine A, Jordan T, Shakir K, Roazen D, Thibault J, Banks E, Garimella KV, Altshuler D, Gabriel S, DePristo MA (2013) From FastQ data to high confidence variant calls: the Genome Analysis Toolkit best practices pipeline. Curr Protoc Bioinformatics 43: 11 10 1-11 10 33. doi: 10.1002/0471250953.bi1110s43

Veltel S, Wittinghofer A (2009) RPGR and RP2: targets for the treatment of X-linked retinitis pigmentosa? Expert Opin Ther Targets 13: 1239-51. doi: 10.1517/14728220903225016

Verbakel SK, van Huet RAC, Boon CJF, den Hollander AI, Collin RWJ, Klaver CCW, Hoyng CB, Roepman R, Klevering BJ (2018) Non-syndromic retinitis pigmentosa. Prog Retin Eye Res 66: 157-186. doi: 10.1016/j.preteyeres.2018.03.005

Verma AS, Fitzpatrick DR (2007) Anophthalmia and microphthalmia. Orphanet J Rare Dis 2: 47. doi: 10.1186/1750-1172-2-47

Vincent A, Billingsley G, Priston M, Glaser T, Oliver E, Walter M, Ritch R, Levin A, Heon E (2006) Further support of the role of CYP1B1 in patients with Peters anomaly. Mol Vis 12: 506-10.

Vincent A, Billingsley G, Priston M, Williams-Lyn D, Sutherland J, Glaser T, Oliver E, Walter MA, Heathcote G, Levin A, Heon E (2001) Phenotypic heterogeneity of CYP1B1: mutations in a patient with Peters' anomaly. J Med Genet 38: 324-6. doi: 10.1136/jmg.38.5.324

Vincent AL, Billingsley G, Buys Y, Levin AV, Priston M, Trope G, Williams-Lyn D, Heon E (2002) Digenic inheritance of early-onset glaucoma: CYP1B1, a potential modifier gene. Am J Hum Genet 70: 448-60. doi: 10.1086/338709

VonGraefe A (1858) Exceptionelles Verhalten des Gesichtsfeldes bei Pigmententartung der Netzhaut. Archiv für Ophthalmologie 4: 250-253.

Wagenaar M, van Aarem A, Huygen P, Pieke-Dahl S, Kimberling W, Cremers C (1999) Hearing impairment related to age in Usher syndrome types 1B and 2A. Arch Otolaryngol Head Neck Surg 125: 441-5. doi: 10.1001/archotol.125.4.441

Wang A, Savas U, Stout CD, Johnson EF (2011) Structural characterization of the complex between alpha-naphthoflavone and human cytochrome P450 1B1. J Biol Chem 286: 5736-43. doi: 10.1074/jbc.M110.204420

Wang H, Wang X, Zou X, Xu S, Li H, Soens ZT, Wang K, Li Y, Dong F, Chen R, Sui R (2015) Comprehensive Molecular Diagnosis of a Large Chinese Leber Congenital Amaurosis Cohort. Invest Ophthalmol Vis Sci 56: 3642-55. doi: 10.1167/iovs.14-15972

Wang J, Xiao X, Li S, Jiang H, Sun W, Wang P, Zhang Q (2022) Landscape of pathogenic variants in six pre-mRNA processing factor genes for retinitis pigmentosa based on large in-house data sets and database comparisons. Acta Ophthalmol 100: e1412-e1425. doi: 10.1111/aos.15104

Wang L, Zhang J, Chen N, Wang L, Zhang F, Ma Z, Li G, Yang L (2018) Application of Whole Exome and Targeted Panel Sequencing in the Clinical Molecular Diagnosis of 319 Chinese Families with Inherited Retinal Dystrophy and Comparison Study. Genes (Basel) 9. doi: 10.3390/genes9070360

Wang N, Xie X, Yang D, Xian J, Li Y, Ren R, Peng X, Jonas JB, Weinreb RN (2012) Orbital cerebrospinal fluid space in glaucoma: the Beijing intracranial and intraocular pressure (iCOP) study. Ophthalmology 119: 2065-2073 e1. doi: 10.1016/j.ophtha.2012.03.054

Wang Q, Chen Q, Zhao K, Wang L, Wang L, Traboulsi EI (2001) Update on the molecular genetics of retinitis pigmentosa. Ophthalmic Genet 22: 133-54. doi: 10.1076/opge.22.3.133.2224

Wang R, Han S, Khan A, Zhang X (2017) Molecular Analysis of Twelve Pakistani Families with Nonsyndromic or Syndromic Hearing Loss. Genet Test Mol Biomarkers 21: 316-321. doi: 10.1089/gtmb.2016.0328

Warr A, Robert C, Hume D, Archibald A, Deeb N, Watson M (2015) Exome Sequencing: Current and Future Perspectives. G3 (Bethesda) 5: 1543-50. doi: 10.1534/g3.115.018564

Waryah AM, Ahmed ZM, Bhinder MA, Choo DI, Sisk RA, Shahzad M, Khan SN, Friedman TB, Riazuddin S, Riazuddin S (2011) Molecular and clinical studies of X-linked deafness among Pakistani families. J Hum Genet 56: 534-40. doi: 10.1038/jhg.2011.55

Waseem NH, Vaclavik V, Webster A, Jenkins SA, Bird AC, Bhattacharya SS (2007) Mutations in the gene coding for the pre-mRNA splicing factor, PRPF31, in patients with autosomal dominant retinitis pigmentosa. Invest Ophthalmol Vis Sci 48: 1330-4. doi: 10.1167/iovs.06-0963

Wawrocka A, Skorczyk-Werner A, Wicher K, Niedziela Z, Ploski R, Rydzanicz M, Sykulski M, Kociecki J, Weisschuh N, Kohl S, Biskup S, Wissinger B, Krawczynski MR (2018) Novel variants identified with next-generation sequencing in Polish patients with cone-rod dystrophy. Mol Vis 24: 326-339.

Weinreb RN, Aung T, Medeiros FA (2014) The pathophysiology and treatment of glaucoma: a review. JAMA 311: 1901-11. doi: 10.1001/jama.2014.3192

Weisschuh N, Wolf C, Wissinger B, Gramer E (2009) A clinical and molecular genetic study of German patients with primary congenital glaucoma. Am J Ophthalmol 147: 744-53. doi: 10.1016/j.ajo.2008.11.008

Wiggs JL, Pasquale LR (2017) Genetics of glaucoma. Hum Mol Genet 26: R21-R27. doi: 10.1093/hmg/ddx184

Willig LK, Petrikin JE, Smith LD, Saunders CJ, Thiffault I, Miller NA, Soden SE, Cakici JA, Herd SM, Twist G, Noll A, Creed M, Alba PM, Carpenter SL, Clements MA, Fischer RT, Hays JA, Kilbride H, McDonough RJ, Rosterman JL, Tsai SL, Zellmer L, Farrow EG, Kingsmore SF (2015) Whole-genome sequencing for identification of Mendelian disorders in critically ill infants: a retrospective analysis of diagnostic and clinical findings. Lancet Respir Med 3: 377-87. doi: 10.1016/S2213-2600(15)00139-3

Willoughby C, E., Ponzin D, Ferrari S, Lobo A, Landau K, Omidi Y (2010) Anatomy and physiology of the human eye: effects of mucopolysaccharidoses disease on structure and function – a review. Clinical & Experimental Ophthalmology 38: 2-11.

Winkler S, Loosli F, Henrich T, Wakamatsu Y, Wittbrodt J (2000) The conditional medaka mutation eyeless uncouples patterning and morphogenesis of the eye. Development 127: 1911-9. doi: 10.1242/dev.127.9.1911

Wissinger B, Gamer D, Jagle H, Giorda R, Marx T, Mayer S, Tippmann S, Broghammer M, Jurklies B, Rosenberg T, Jacobson SG, Sener EC, Tatlipinar S, Hoyng CB, Castellan C, Bitoun P, Andreasson S, Rudolph G, Kellner U, Lorenz B, Wolff G, Verellen-Dumoulin C, Schwartz M, Cremers FP,

Apfelstedt-Sylla E, Zrenner E, Salati R, Sharpe LT, Kohl S (2001) CNGA3 mutations in hereditary cone photoreceptor disorders. Am J Hum Genet 69: 722-37. doi: 10.1086/323613

Wiszniewski W, Lewis RA, Lupski JR (2007) Achromatopsia: the CNGB3 p.T383fsX mutation results from a founder effect and is responsible for the visual phenotype in the original report of uniparental disomy 14. Hum Genet 121: 433-9. doi: 10.1007/s00439-006-0314-y

Wojcik MH, Reuter CM, Marwaha S, Mahmoud M, Duyzend MH, Barseghyan H, Yuan B, Boone PM, Groopman EE, Delot EC, Jain D, Sanchis-Juan A, Genomics Research to Elucidate the Genetics of Rare Diseases C, Starita LM, Talkowski M, Montgomery SB, Bamshad MJ, Chong JX, Wheeler MT, Berger SI, O'Donnell-Luria A, Sedlazeck FJ, Miller DE (2023) Beyond the exome: What's next in diagnostic testing for Mendelian conditions. Am J Hum Genet 110: 1229-1248. doi: 10.1016/j.ajhg.2023.06.009

Xi Q, Pauer GJ, Marmorstein AD, Crabb JW, Hagstrom SA (2005) Tubby-like protein 1 (TULP1) interacts with F-actin in photoreceptor cells. Invest Ophthalmol Vis Sci 46: 4754-61. doi: 10.1167/iovs.05-0693

Yahya S, Watson CM, Carr I, McKibbin M, Crinnion LA, Taylor M, Bonin H, Fletcher T, El-Asrag ME, Ali M, Toomes C, Inglehearn CF (2023) Long-Read Nanopore Sequencing of RPGR ORF15 is Enhanced Following DNase I Treatment of MinION Flow Cells. Mol Diagn Ther 27: 525-535. doi: 10.1007/s40291-023-00656-z

Yamazaki S, Sato K, Suhara K, Sakaguchi M, Mihara K, Omura T (1993) Importance of the proline-rich region following signal-anchor sequence in the formation of correct conformation of microsomal cytochrome P-450s. J Biochem 114: 652-7. doi: 10.1093/oxfordjournals.jbchem.a124232

Yang C, Georgiou M, Atkinson R, Collin J, Al-Aama J, Nagaraja-Grellscheid S, Johnson C, Ali R, Armstrong L, Mozaffari-Jovin S, Lako M (2021) Pre-mRNA Processing Factors and Retinitis Pigmentosa: RNA Splicing and Beyond. Front Cell Dev Biol 9: 700276. doi: 10.3389/fcell.2021.700276

Yang M, Guo X, Liu X, Shen H, Jia X, Xiao X, Li S, Fang S, Zhang Q (2009) Investigation of CYP1B1 mutations in Chinese patients with primary congenital glaucoma. Mol Vis 15: 432-7.

Yannuzzi LA, Rohrer KT, Tindel LJ, Sobel RS, Costanza MA, Shields W, Zang E (1986) Fluorescein angiography complication survey. Ophthalmology 93: 611-7. doi: 10.1016/s0161-6420(86)33697-2

Ye X, Wang Y, Nathans J (2010) The Norrin/Frizzled4 signaling pathway in retinal vascular development and disease. Trends Mol Med 16: 417-25. doi: 10.1016/j.molmed.2010.07.003

Yu DY, Cringle SJ (2005) Retinal degeneration and local oxygen metabolism. Exp Eye Res 80: 745-51. doi: 10.1016/j.exer.2005.01.018

Zazo-Seco C, Plaisancie J, Bitoun P, Corton M, Arteche A, Ayuso C, Schneider A, Zafeiropoulou D, Gilissen C, Roche O, Fremont F, Calvas P, Slavotinek A, Ragge N, Chassaing N (2020) Novel PXDN biallelic variants in patients with microphthalmia and anterior segment dysgenesis. J Hum Genet 65: 487-491. doi: 10.1038/s10038-020-0726-x

Zeitz C, Robson AG, Audo I (2015) Congenital stationary night blindness: an analysis and update of genotype-phenotype correlations and pathogenic mechanisms. Prog Retin Eye Res 45: 58-110. doi: 10.1016/j.preteyeres.2014.09.001

Zhai RG, Cao Y, Hiesinger PR, Zhou Y, Mehta SQ, Schulze KL, Verstreken P, Bellen HJ (2006) Drosophila NMNAT maintains neural integrity independent of its NAD synthesis activity. PLoS Biol 4: e416. doi: 10.1371/journal.pbio.0040416

Zhang Q, Zulfiqar F, Xiao X, Riazuddin SA, Ahmad Z, Caruso R, MacDonald I, Sieving P, Riazuddin S, Hejtmancik JF (2007) Severe retinitis pigmentosa mapped to 4p15 and associated with a novel mutation in the PROM1 gene. Hum Genet 122: 293-9. doi: 10.1007/s00439-007-0395-2

Zhang XM, Hashimoto T, Tang R, Yang XJ (2018) Elevated expression of human bHLH factor ATOH7 accelerates cell cycle progression of progenitors and enhances production of avian retinal ganglion cells. Sci Rep 8: 6823. doi: 10.1038/s41598-018-25188-z

Zhao Y, Sorenson CM, Sheibani N (2015) Cytochrome P450 1B1 and Primary Congenital Glaucoma. J Ophthalmic Vis Res 10: 60-7. doi: 10.4103/2008-322X.156116

Zhu AY, Costain G, Cytrynbaum C, Weksberg R, Cohn RD, Ali A (2021) Novel heterozygous variants in PXDN cause different anterior segment dysgenesis

phenotypes in monozygotic twins. Ophthalmic Genet 42: 624-630. doi: 10.1080/13816810.2021.1925929

Zlotogora J, Harel T, Meiner V (2023) Explanations for the discrepancy between variant frequency and homozygous disease occurrence: Lessons from Ashkenazi Jewish data. Eur J Med Genet 66: 104765. doi: 10.1016/j.ejmg.2023.104765

Appendix I: Anophthalmia and microphthalmia-associated genes as listed in OMIM

Gene	OMIM	Gene	OMIM	Gene	OMIM	Gene	OMIM
ABCB6	605452	*ESCO2*	609353	*NF1*	613113	*SALL4*	607343
ALDH1A3	600463	*FAM111A*	615292	*NHS*	300457	*SCLT1*	611399
ALDH6A1	603178	*FANCA*	607139	*NUP188*	615587	*SEMA3E*	608166
ALX1	601527	*FANCD2*	613984	*OCLN*	602876	*SHH*	600725
ARHGAP6	300118	*FANCF*	613897	*OLFM2*	617492	*SIN3A*	607776
ATOH7	609875	*FANCL*	608111	*OTX2*	600037	*SIPA1L3*	616655
B3GALNT2	610194	*FKRP*	606596	*PAX2*	167409	*SIX3*	603714
BCOR	300485	*FKTN*	607440	*PAX6*	607108	*SIX6*	606326
BEST1	607854	*FNBP4*	615265	*PCYT1A*	123695	*SLC16A12*	611910
BMP4	112262	*FOXE3*	601094	*PDE6D*	602676	*SLC38A8*	615585
BRCA1	113705	*FREM1*	608944	*PITX3*	602669	*SMCHD1*	614982
BRCA2	600185	*FREM2*	608945	*PLK4*	605031	*SMG9*	613176
BRIP1	605882	*GDF3*	606522	*PNPT1*	610316	*SMOC1*	608488
C12orf57	615140	*GDF6*	601147	*POMGNT1*	606822	*SNX3*	605930
C2CD3	615944	*GJA1*	121014	*POMK*	615247	*SOX2*	184429
CAPN15	603267	*GJA8*	600897	*POMT1*	607423	*STRA6*	610745
CDKL5	300203	*GLI2*	165230	*POMT2*	607439	*TBC1D20*	611663
CENPF	600236	*GSC*	138890	*PQBP1*	300463	*TBC1D32*	615867
CEP120	613446	*GTF2H5*	608780	*PRMT7*	610087	*TBL1XR1*	608628
CHD7	608892	*HCCS*	300056	*PRR12*	616633	*TCTN2*	613846
CHUK	600664	*HDAC6*	300272	*PRSS56*	613858	*TENM3*	610083
CNTNAP1	602346	*HMGB3*	300193	*PTCH1*	601309	*TFAP2A*	107580
COL4A1	120130	*HMX1*	142992	*PUF60*	604819	*TKFC*	615844
COX14	614478	*HUWE1*	300697	*PXDN*	605158	*TMEM216*	613277
COX7B	300885	*INTS1*	611345	*RAB18*	602207	*TMTC3*	617218
CRPPA	614631	*INTU*	610621	*RAB3GAP1*	602536	*TMX3*	616102
CRYAA	123580	*KERA*	603288	*RAB3GAP2*	609275	*TOGARAM1*	617618
CRYBA4	123631	*KIF11*	148760	*RARB*	180220	*TUBB*	191130
CRYBB2	123620	*LMBRD2*	619490	*RAX*	601881	*TUBGCP4*	609610

DAG1	128239	*LRP5*	603506	*RBBP8*	604124	*VAX1*	604294
DOCK6	614194	*MAB21L2*	604357	*RBP4*	180250	*VCAN*	118661
DONSON	611428	*MAF*	177075	*RERE*	605226	*VSX2*	142993
DPYD	612779	*MAPRE2*	605789	*RHOA*	165390	*WDR37*	618586
ERCC1	126380	*MFRP*	606227	*RIPK4*	605706	*YAP1*	606608
ERCC3	133510	*MITF*	156845	*RPGRIP1L*	610937	*ZBTB20*	606025
ERCC5	133530	*NAA10*	300013	*RTTN*	610436	*ZEB2*	605802
ERCC6	609413	*NDUFB11*	300403	*RXYLT1*	605862		

Turnitin Originality Report

Identification of Genes in Pakistani Families with Inherited Eye Diseases   by Rabia
Basharat .

From PhD (PhD DRSML)

- Processed on 15-Sep-2023 08:17 PKT
- ID: 2166572998
- Word Count: 36950

Similarity Index
14%
Similarity by Source

Internet Sources:
 11%
Publications:
 9%
Student Papers:
 5%

Focal Person (Turnitin)
Quaid-i-Azam University
Islamabad

sources:

| 1 | 1% match (student papers from 19-Jan-2017)
Submitted to Higher Education Commission Pakistan on 2017-01-19 |

| 2 | 1% match (Internet from 31-Jul-2023)
https://www.frontiersin.org/articles/10.3389/fcell.2023.1112270/full |

| 3 | < 1% match (student papers from 25-Jun-2016)
Submitted to Higher Education Commission Pakistan on 2016-06-25 |

| 4 | < 1% match (student papers from 04-Jul-2014)
Submitted to Higher Education Commission Pakistan on 2014-07-04 |

| 5 | < 1% match (student papers from 01-Jul-2015)
Submitted to Higher Education Commission Pakistan on 2015-07-01 |

| 6 | < 1% match (student papers from 23-Apr-2017)
Submitted to Higher Education Commission Pakistan on 2017-04-23 |

| 7 | < 1% match (student papers from 04-Oct-2012)
Submitted to Higher Education Commission Pakistan on 2012-10-04 |

| 8 | < 1% match (student papers from 02-Feb-2021)
Submitted to Higher Education Commission Pakistan on 2021-02-02 |

| 9 | < 1% match (student papers from 15-Nov-2022)
Submitted to Higher Education Commission Pakistan on 2022-11-15 |

| 10 | < 1% match (student papers from 22-Dec-2012)
Submitted to Higher Education Commission Pakistan on 2012-12-22 |

| 11 | < 1% match (student papers from 09-Dec-2012)
Submitted to Higher Education Commission Pakistan on 2012-12-09 |

| 12 | < 1% match (student papers from 07-Dec-2012)
Submitted to Higher Education Commission Pakistan on 2012-12-07 |

| 13 | < 1% match (student papers from 29-May-2013)
Submitted to Higher Education Commission Pakistan on 2013-05-29 |

| 14 | < 1% match (student papers from 04-Jun-2010)
Submitted to Higher Education Commission Pakistan on 2010-06-04 |

Combined Single Gene Testing and Genome Sequencing as an Effective Diagnostic Approach for Anophthalmia and Microphthalmia Patients

Rabia Basharat [1,2] , Kim Rodenburg [2] , María Rodríguez-Hidalgo [2,3] , Afeefa Jarral [4] , Ehsan Ullah [1,5] , Jordi Corominas [2] , Christian Gilissen [2] , Syeda Tatheer Zehra [1] , Usman Hameed [1] , Muhammad Ansar [1] and Suzanne E. de Bruijn [2,*]

1 Department of Biochemistry, Quaid-i-Azam University, Islamabad 45320, Pakistan
2 Department of Human Genetics, Radboud University Medical Center, 6500 HB Nijmegen, The Netherlands
3 Department of Neuroscience, Biodonostia Health Research Institute, 20014 Donostia-San Sebastián, Spain
4 Department of Biotechnology, Mirpur University of Science and Technology (MUST), Mirpur 10250, AJK, Pakistan
5 Ophthalmic Genetics and Visual Function Branch, National Eye Institute, National Institutes of Health, Bethesda, MD 20892, USA
* Correspondence: suzanne.debruijn@radboudumc.nl; Tel.: +31-243668901

Abstract: Anophthalmia and microphthalmia (A/M) are among the most severe congenital developmental eye disorders. Despite the advancements in genome screening technologies, more than half of A/M patients do not receive a molecular diagnosis. We included seven consanguineous families affected with A/M from Pakistani cohort and an unknown molecular basis. Single gene testing of *FOXE3* was performed, followed by genome sequencing for unsolved probands in order to establish a genetic diagnosis for these families. All seven families were provided with a genetic diagnosis. The identified variants were all homozygous, classified as (likely) pathogenic and present in an A/M-associated gene. Targeted *FOXE3* sequencing revealed two previously reported pathogenic *FOXE3* variants in four families. In the remaining families, genome sequencing revealed a known pathogenic *PXDN* variant, a novel 13bp deletion in *VSX2*, and one novel deep intronic splice variant in *PXDN*. An in vitro splice assay was performed for the *PXDN* splice variant which revealed a severe splicing defect. Our study confirmed the utility of genome sequencing as a diagnostic tool for A/M-affected individuals. Furthermore, the identification of a novel deep intronic pathogenic variant in *PXDN* highlights the role of non-coding variants in A/M-disorders and the value of genome sequencing for the identification of this type of variants.

Keywords: anophthalmia; microphthalmia; deep intronic variant; genome sequencing; targeted gene sequencing

1. Introduction

The development of the eye is a complex process and comprises a coordinated set of events between cells that occurs at the embryonic level, starting from the fourth week of gestation. The major eye structure formation is completed by the seventh week in human embryos [1]. Many genes play a role and are either upregulated or downregulated during these developmental events. These processes are tightly regulated, and any disturbance may lead to malformations. Anophthalmia and microphthalmia (A/M) are ocular defects that could arise during the development of the eye. Microphthalmia is defined as small eyes with axial length <21 mm in adults and <14 mm in newborns [2]. Microphthalmia is mostly observed as a complex phenotype associated with other developmental ocular defects, such as anterior segment dysgenesis, corneal opacity, coloboma, or glaucoma [3]. In contrast, anophthalmia is the complete absence of any eye tissue or any remnant eye structures. The combined prevalence of A/M is 1 in 10,000 births [4].

ELSEVIER

Research article

Next-generation sequencing to genetically diagnose a diverse range of inherited eye disorders in 15 consanguineous families from Pakistan

Rabia Basharat [a, b], Suzanne E. de Bruijn [b], Muhammad Zahid [a], Kim Rodenburg [b], Rebekkah J. Hitti-Malin [b], María Rodríguez-Hidalgo [c, d], Erica G.M. Boonen [b], Afeefa Jarral [e], Arif Mahmood [a], Jordi Corominas [b], Sharqa Khalil [a], Jawaid Ahmed Zai [f], Ghazanfar Ali [g], Javier Ruiz-Ederra [c, d], Christian Gilissen [b], Frans P.M. Cremers [b], Muhammad Ansar [a], Daan M. Panneman [b], Susanne Roosing [b, *]

[a] Department of Biochemistry, Quaid-i-Azam University, Islamabad, Pakistan
[b] Department of Human Genetics, Radboud University Medical Center, Nijmegen, the Netherlands
[c] Department of Neuroscience, Biogipuzkoa Health Research Institute, Donostia-San Sebastián, Spain
[d] Department of Dermatology, Ophthalmology, and Otorhinolaryngology, University of the Basque Country (UPV/EHU), Donostia-San Sebastián, Spain
[e] Department of Biotechnology, Mirpur University of Science and Technology, Mirpur, (AJK), Pakistan
[f] Department of Physiology and MLT, University of Sindh, Jamshoro, Pakistan
[g] Department of Biotechnology, University of Azad Jammu and Kashmir, Muzaffarabad, Pakistan

ARTICLE INFO

ABSTRACT

Inherited retinal dystrophies (IRDs) are characterized by photoreceptor dysfunction or degeneration. Clinical and phenotypic overlap between IRDs makes the genetic diagnosis very challenging and comprehensive genomic approaches for accurate diagnosis are frequently required. While there are previous studies on IRDs in Pakistan, causative genes and variants are still unknown for a significant portion of patients. Therefore, there is a need to expand the knowledge of the genetic spectrum of IRDs in Pakistan. Here, we recruited 52 affected and 53 normal individuals from 15 consanguineous Pakistani families presenting non-syndromic and syndromic forms of IRDs. We employed single molecule Molecular Inversion Probes (smMIPs) based panel sequencing and whole genome sequencing to identify the probable disease-causing variants in these families. Using this approach, we obtained a 93% genetic solve rate and identified 16 (likely) causative variants in 14 families, of which seven novel variants were identified in *ATOH7, COL18A1, MERTK, NDP, PROM1, PRPF8* and *USH2A* while nine recurrent variants were identified in *CNGA3, CNGB1, HGSNAT, NMNAT1, SIX6* and *TULP1*. The novel *MERTK* variant and one recurrent *TULP1* variant explained the intra-familial locus heterogeneity in one of the screened families while two recurrent *CNGA3* variants explained compound heterozygosity in another family. The identification of variants in known disease-associated genes emphasizes the utilization of time and cost-effective screening approaches for rapid diagnosis. The timely genetic diagnosis will not only identify any associated systemic issues in case of syndromic IRDs, but will also aid in the acceleration of personalized medicine for patients affected with IRDs.

1. Introduction

Inherited retinal dystrophies (IRDs) are a heterogeneous group of rare eye disorders, collectively affecting approximately 1:2000 people worldwide (Berger et al., 2010). These disorders are characterized by dysfunction and/or cell death of various retinal cell types ultimately leading to both progressive or stationary forms of vision loss. IRDs are classified on the basis of disease progression and affected part of the retina (Moradi and Moore, 2007). The most prevalent IRD is retinitis pigmentosa (RP) (prevalence 1:4000) (Verbakel et al., 2018), which is characterized by night blindness and a progressive loss of peripheral vision and ultimately complete blindness. It is caused by dysfunction or cell death of rod photoreceptors and, eventually, cone photoreceptors (Pagon, 1988). Leber congenital amaurosis (LCA) (prevalence 1:80,000) (Tsang and Sharma, 2018) on the other hand is a more severe form of IRD, where both rod and cone photoreceptors and/or retinal

Note: Low-resolution images were used to create this PDF. The original images will be used in the final composition.